Synthesis of Cyclic Polymers by Ring Expansion and Ring Opening Metathesis Polymerization

Thesis by

Quan Gan

In Partial Fulfillment of the Requirements for the Degree of

Doctor of Philosophy

Caltech

CALIFORNIA INSTITUTE OF TECHNOLOGY

Pasadena, California

2023

(Defended March 22, 2023)

Quan Gan
ORCID: 0000-0001-5908-4163

ACKNOWLEDGEMENTS

First and foremost, I want to express my deep gratitude to Prof. Bob Grubbs for giving me the opportunity to join the Grubbs group. As a world-renowned scientist, he not only taught me to be creative and passionate in my research, but also exemplified humility and kindness as a person. His unwavering support made my time at Caltech truly enjoyable, and I will strive to follow his example throughout my life. Rest in peace, Bob.

After Bob's passing, Prof. Max Robb kindly accepted me into the Robb group and provided invaluable guidance to help me complete my graduate studies. Working with Max and the Robb group allowed me to expand my knowledge and skills in different aspects of chemistry. I am incredibly grateful for his support and mentorship.

I would also like to express my appreciation to my committee members, Profs. Dave Tirrell, Theo Agapie, and Sarah Reisman. Their insightful questions and feedback during committee meetings helped me to delve deeper into my research projects and proposals, and I learned a great deal from their expertise.

I am grateful for the opportunity to work alongside the talented individuals in the Grubbs and Robb groups. Dr. Jeong Hoon Ko (JK) has been like an older brother to me, always ready to offer help and advice both inside and outside of the lab. His energy and willingness to take on responsibilities inspired me to be more responsible myself. Dr. Yan Xu, with his exceptional knowledge of organic chemistry and experimental skills, has been an invaluable collaborator on the catalysis project. I could not have solved many difficult problems without his assistance. Dr. Ki-Young Yoon's productivity and organization were instrumental in our work on cyclic polymers, and I always enjoyed discussing research with him. Dr. Jianchun Wang's patience and friendliness helped me to learn more about chemistry and his contribution to the macrocycle separation project was

encouragement, and sacrifice have been essential in enabling me to pursue my dreams and achieve

my goals. I am forever grateful for their unconditional love and unwavering support.

ABSTRACT

Cyclic polymers are topologically interesting and envisioned as a lubricant material. However, scalable synthesis of pure cyclic polymers remains elusive. The most straightforward way is to recover a used catalyst after the synthesis of cyclic polymers and reuse it. Unfortunately, this is demanding because of the catalyst's vulnerability and inseparability from polymers, which reduce the practicality of the process. In Chapter 1 we describe a continuous circular process, where polymerization, polymer separation, and catalyst recovery happen in situ, to dispense a pure cyclic polymer after bulk ring-expansion metathesis polymerization of cyclopentene. This process is enabled by introducing silica-supported ruthenium catalysts and newly designed glassware. Different depolymerization kinetics of the cyclic polymer from its linear analogue are also discussed. This process minimizes manual labour, maximizes the security of vulnerable catalysts and guarantees the purity of cyclic polymers, thereby showcasing a prototype of a scalable access to cyclic polymers with increased turnovers ($\geq$415,000) of precious catalysts.

α-Oxygenated Z-olefins are ubiquitous in biologically active molecules and serve as versatile handles for organic synthesis, but their syntheses are often tedious and less selective. In Chapter 2 we report the efficient Z-selective metathesis of various terminal acrylates and allyl alcohols, which enables facile and selective construction of high value-added α-oxygenated Z-olefins from readily available feedstock chemicals. These challenging metathesis transformations are enabled by novel cyclometalated Ru-carbene-nitrate complexes bearing bulky-yet-flexible side arms, whose assembly was unlocked by new organometallic syntheses.

Efficient separation of macrocyclic polyolefins from reaction mixtures of ring-opening metathesis polymerization is crucial for their application in materials science, drug delivery, and for the mechanistic study of the reaction mechanism. In Chapter 3, we present a facile method for

obtaining topologically pure macrocyclic fractions by modifying chain ends using enyne metathesis chemistry and introducing polar functional groups into linear polymer chains through the addition of polar monomers. Nonpolar cyclic polyolefins are then readily separated using silica gel chromatography. The purity of the cyclic fractions was verified using multiple techniques, including gel permeation chromatography, nuclear magnetic resonance spectroscopy, and matrix-assisted laser desorption/ionization time-of-flight mass spectrometry. We investigate the reaction factors affecting the yield and molecular weight of macrocycles during ring-opening metathesis polymerization of cyclooctadiene and discuss macrocycle formation in the ring-opening metathesis polymerization of cyclooctene, cyclopentene, and norbornene. Our work offers crucial insights into the synthesis and separation of macrocycles.

PUBLISHED CONTENT AND CONTRIBUTIONS

The work in this thesis includes content from the following published articles or manuscripts in preparation. This thesis was enabled by the collaboration among all authors. For brevity, only contributions by Q.G. have been identified below.

Chapter 1

Yoon, K.-Y.; [+] Noh, J.; [+] **Gan, Q.**; [+] Edwards, J. P.; Tuba, R.; Choi, T.-L.; Grubbs, R. H. Scalable and Continuous Access to Pure Cyclic Polymers Enabled by 'Quarantined' Heterogeneous Catalysts. *Nature Chemistry* **2022**, *14* (11), 1242–1248. doi: 10.1038/s41557-022-01034-8. ([+]*Equal contributions*.)

> **Q.G.** performed some of the catalyst and polymer synthesis and characterization, analyzed some of the data, and provided edits to the manuscript.

Chapter 2

Xu, Y.; [+] **Gan, Q.**; [+] Samkian, A. E.; [+] Ko, J. H.; Grubbs, R. H. Bulky Cyclometalated Ruthenium Nitrates for Challenging Z-Selective Metathesis: Efficient One-Step Access to α-Oxygenated Z-Olefins from Acrylates and Allyl Alcohols. *Angewandte Chemie International Edition*, **2021**, 61, e202113089. doi: 10.1002/anie.202113089. ([+]*Equal contributions*.)

> **Q.G.** performed some of the catalyst and substrate synthesis and characterization, analyzed some of the data, and contributed to manuscript preparation.

Chapter 3

Gan, Q.; Yoon, K.-Y.; Xu, Y.; Wang, J.; Robb, M. J.; Grubbs, R. H. Synthesis and Separation of Macrocyclic Polyolefins through Polar Monomer Incorporation and Chain-End Modification. *In preparation*

> **Q.G.** contributed to the conception of the project (with all other authors), performed catalyst and polymer synthesis and characterization, analyzed data, and contributed to manuscript preparation.

TABLE OF CONTENTS

C h a p t e r   1

Scalable and Continuous Access to Pure Cyclic Polymers Enabled by 'Quarantined' Heterogeneous Catalysts

1.1 Introduction

The economy of lubrication is encumbered by a high replacement cost of lubricants in many applications[1,2]. One of its countermeasures is to increase the lifespan of lubricants, thereby decreasing the replacement frequency. The most common synthetic lubricant by far is polyalphaolefin[3-5], which gradually loses its viscosity due to permanent chain scissions over time[6]. Cyclic hydrocarbon polymers similar to polyalphaolefins or mineral oils (for example, polyethylene, polypropylene, polybutadiene, *etc.*)[7,8] are tribologically interesting because the initial chain scission of cyclic topology increases its viscosity by producing an opened linear topology with a higher chain volume[9-11]. This feature of cyclic polymers is envisioned as a viscosity-modifying additive to prolong the lubricant lifetime. Since our discovery of the ring expansion route to cyclic polymers in 2002[11], we[12-16] and other groups[17-26] have done exciting research on more functionalized cyclic polymers, which showed potential applications of semi-conducting materials or drug delivery[18,27,28].

One of the most important needs is the development of a practical synthetic process to produce pure cyclic polymers on a larger scale for testing in many applications. To date, all the reported synthetic protocols were operated on a milligram scale in solution by homogeneous catalysis, which was accompanied by rigorous *ex situ* processes for polymer purification without actual catalyst recovery (Fig. 1.1c)[24-26,29]. Nonetheless, the metal residue remained at a few hundred ppm level[12]; in this conventional process, it is difficult not only to obtain an uncontaminated polymer but also to recycle the precious metal carbene catalysts.
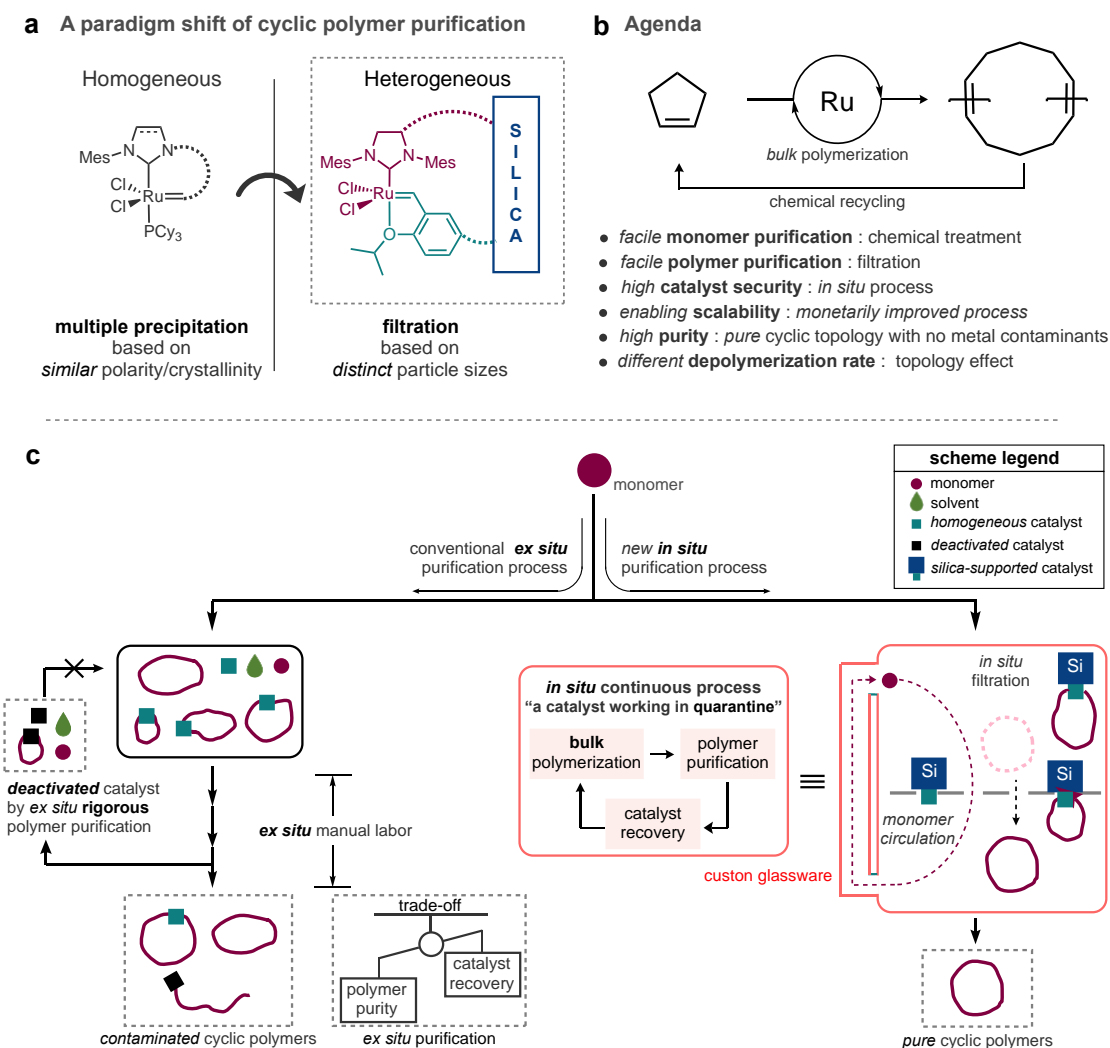
Figure 1.1. REMP and purification process for the preparation of cyclic polymers. a, Catalyst design strategy. **b**, Key points for REMP of cyclopentene in this work. **c**, Conventional ex situ purification processes and in situ continuous process in this work.

Here, we present a continuous process which is streamlined in a way that polymerization, polymer separation, and catalyst recovery simultaneously happen *in situ* in a closed loop to dispense a cyclic polymer synthesized by bulk ring-expansion metathesis polymerization (REMP) of cyclopentene (CP) (Fig. 1.1c). To avoid extensive purification, silica-supported catalysts are designed so that pure cyclic polymers can be segregated simply by filtration (Fig. 1.1a). Glassware that benefits most from the heterogeneous catalysts, namely a cyclic polymer dispenser, is

customized to allow bulk polymerization with a concomitant separation of cyclic polymers from the heterogeneous catalysts. A thimble containing the catalysts that is mounted as a cartridge on the dispenser is situated in the original place throughout the process. This *in situ* continuous process minimizes manual labor, quarantines the vulnerable catalytic species secured from any deactivating events that can occur otherwise upon *ex situ* purifications, and guarantees purity of cyclic polymers. Serendipitously, it is also found that the resulting cyclic polymer depolymerizes noticeably faster than its linear analogue. Overall, this report demonstrates a prototype of a scalable access to cyclic polymers with enlarged turnovers of precious catalysts.

1.2 REMP catalyst design for simple polymer separation: from homogeneity to heterogeneity

Previous REMP studies have adhered to a typical purification method conducted after ring-opening metathesis polymerization (ROMP), which is multiple polymer precipitation or crystallization in cold polar protic solvents[24-26,29]. The rigorous purification was inevitable because polarity and crystallinity of cyclic polymers were not sufficiently distinct from undesired polymeric metal complexes (*e.g.,* **P1** vs **H1** in Fig. 1.2b). While this purification is still suitable for the removal of metal which is already deactivated with a quencher in ROMP, it is in fact inappropriate from the aspect of catalyst *recovery* in REMP in which active ruthenium carbene catalysts are regenerated upon the release of cyclic polymers. Furthermore, all the polymeric ruthenium species generated *via* the side pathways are *de facto* active catalysts for REMP (Fig. 1.2b). Thus, the demanding post-synthetic purification likely decomposes the metal carbene catalysts by oxygen, moisture, or purification solvents[30], potentially followed by release of unwanted linear polymers or polymeric metal complexes, which are difficult to separate from the desired cyclic polymers, once generated (Fig. 1.1c).

Figure 1.2. REMP of CP with the immobilized ruthenium catalysts. a, The silica-supported ruthenium catalysts used in this study. **b**, Possible olefin metathesis pathways of cyclopentene ring opening.

Previous ruthenium-based catalysts for REMP shared a common structure of metallacycle where the N-heterocyclic carbene (NHC) and alkylidenes[11-13]/benzylidenes[17] were tethered by organic linkers in the cyclic form (Fig. 1.1c). By replacing the organic linker with the silica gel support, we envisioned a simpler and more guaranteed separation of the desired cyclic polymer from the rest by filtration — the cyclic polymer is the only product chemically unbound from the silica support unless linear chain-transfer agents are present in the system (Fig. 1.2b). The envisioned catalyst, **Het-D** (a silica-containing metallacycle), was synthesized with the longest linear steps of ten (Fig. 1.2a, see experimental section for the synthetic details). In addition, acyclic **Het-S** was prepared in fewer steps for comparison and found as effective (*vide infra*). These REMP catalysts consist of the chelating benzylidene structure, which are more stable in the air than the previous REMP catalysts. The amount of the ruthenium catalyst anchored onto silica support was determined from the Ru to Si ratio (4.0 µmol Ru/g silica for **Het-D**, 2.8 µmol Ru/g silica for **Het-S**) obtained by

the inductively coupled plasma mass spectrometry (ICP-MS) (Table A1). The degree of heterogeneity of the catalysts was confirmed with the hot filtration test[31,32] (Table A2).

1.3 Monomer selection and purification: "garbage in, garbage out"

Although known as a low-strain monomer that is challenging for exergonic ROMP/REMP[33-35], cyclopentene (CP) was selected as the monomer for initial studies. Given a typical molar mass range of polyalphaolefins used for lubrication (<50 kDa)[3], it is unnecessary to design higher-molar-mass cyclic polyCP/polyethylene for viscosity modifier purposes. In this respect, limited monomer conversion, even in bulk polymerization (*e.g.,* 84% at r.t.[33]), which was considered a problem in previous studies aiming to synthesize linear polyCP with higher molar masses (>100 kDa)[34,36,37], is no longer a drawback since the low boiling-point cyclopentene can play the dual role of monomer and solvent with no need of additional solvent. Furthermore, residual CP can be easily separated from polyCP by simple distillation or evaporation under ambient conditions (bp= 45 °C). Moreover, the resulting polyCP itself is interesting, as it is a chemically recyclable natural rubber analog, as well as a pre-hydrogenated polymer of unique polyethylene featuring odd-numbered CH_2 periodicity, which is otherwise hard to access[34].

Unfortunately, commercially available CP contained detectable amounts of acyclic olefin impurities (~2000 ppm)[37]. These impurities acting as chain transfer agents can not only decrease the molar mass of polyCP[37-39] but also deteriorate the purity of cyclic topology in the REMP process[16] (Fig. 1.3b). Previously, exhaustive fractional distillation was exploited to separate these impurities from CP because of the proximal boiling points between them[37]. We envisaged that this distillation method could be replaced with a simpler method, provided that a chemical treatment distinguishing acyclic olefins from CP would be found. We selected the cobalt-catalyzed olefin isomerization—selective hydroboration of terminal olefins developed by Chirik's group[40]; with only 0.001 mol% of

the cobalt catalyst based on CP, the acyclic olefin impurities were transformed into much heavier hydroborated products *via* isomerized terminal olefins. On the other hand, CP remained intact because the isomerization of CP never generates a terminal olefin (Fig. 1.3a) so that light CP could be separated by simple distillation (Fig. 1.3b and A1).
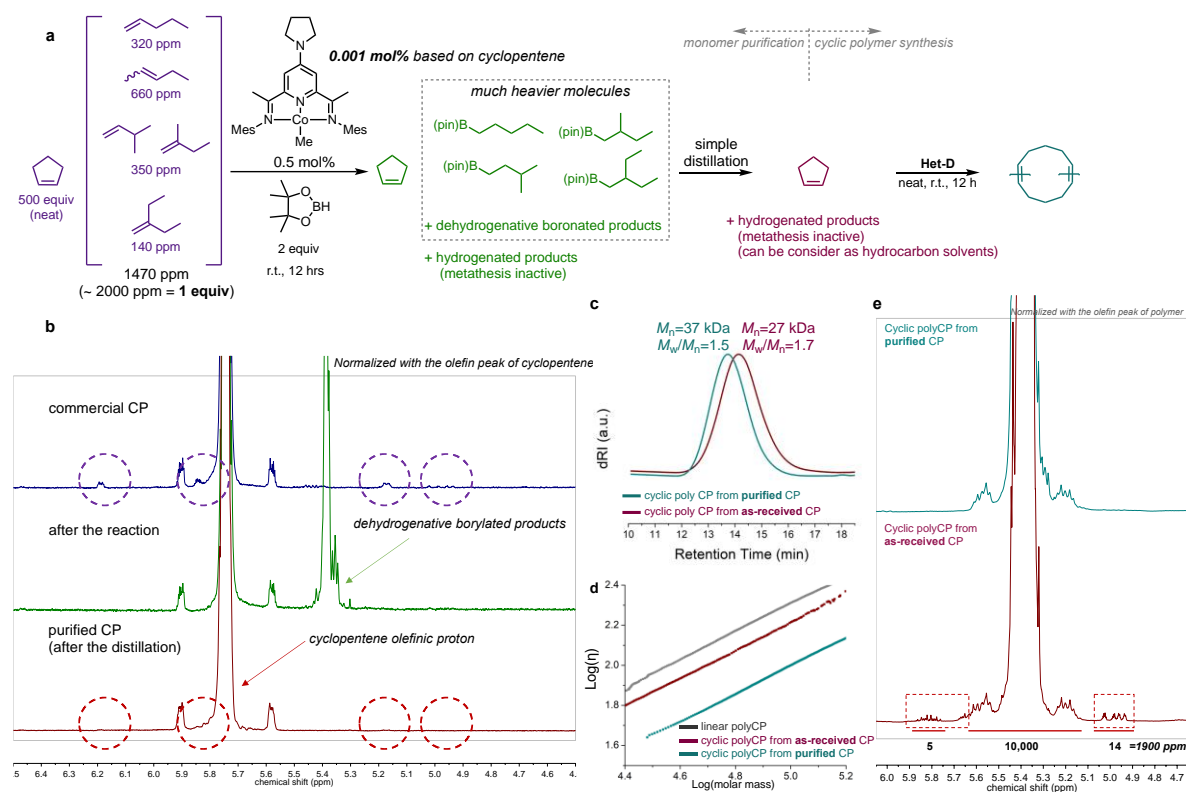

Figure 1.3. Importance of monomer purity for REMP. a, A chemical treatment to differentiate CP from linear olefin impurities. **b,** ^{1}H NMR spectra of olefinic regions before and after the hydroboration, as well as after simple distillation. comparison of cyclic polyCP made of the purified CP (M_n=37 kDa, M_w/M_n=1.5) vs cyclic polyCP made of commercial CP as received (M_n=27 kDa, M_w/M_n=1.5). **c,** SEC traces. **d,** Mark–Houwink–Sakurada plots **e,** ^{1}H NMR spectra.

We conducted bulk REMP of purified CP (vs commercial one) with 1.0 mL of CP (11.3 mmol) and 20 mg of **Het-D** (0.08 µmol) at room temperature in a 20-mL vial under an argon atmosphere. After filtration, the molar mass of the polymer made of commercial CP was found to be lower than that of the polymer from purified CP (Fig. 1.3c, see Fig. A2 for the similar result of the

corresponding ROMP). Also, the cyclic topology was clearly deteriorated when commercial CP was used. The intrinsic viscosities (η) of the two polyCPs over a range of molar masses, measured by size-exclusion chromatography (SEC) equipped with a differential viscometer, showed that the cyclic polyCP from purified CP ($<\eta>_{cyclic}/<\eta>_{linear}$=0.44) had a lower intrinsic viscosity than the one from commercial CP over the whole range ($<\eta>_{cyclic}/<\eta>_{linear}$=0.81), which indicated linear contaminants in the polymer from commercial CP (Fig. 1.3e, A3 and Table A3). The ^{1}H NMR spectrum of polyCP made of commercial CP shows minor olefinic proton signals around the major signal of polyCP, which were undetected from the cyclic polyCP made of purified CP (Fig. 1.3e). The integration of the minor signals was calculated to 1900 ppm, which is close to the amount of linear olefin impurities in commercial CP stock, implying the undesired chain transfer by the impurities. This negative effect on topology was also corroborated by DEPT 135 ^{13}C NMR spectroscopy, where ill-defined side signals were detected in the case of REMP of commercial CP (Fig. A3). These results highlighted that the use of a purer monomer is critical in REMP, where small changes of monomer purity make a big difference of topological purity.

1.4 A cyclic polymer dispenser: "monomer in, polymer out"

Despite the simplified separation, there remain practical challenges to catalyst recovery. Although the initiating catalyst is stabilized with the chelating benzylidene structure, ruthenium carbene catalysts regenerated after release of cyclic polyCP can result in vulnerable alkylidene structures[41] (Fig. A8); in the presence of such catalysts, the post-synthetic filtration requires anhydrous degassed washing solvents under inert conditions for the catalyst recovery. In addition, the required amount of solvent increases as the amount or molar-mass of polymer increases. This *ex situ* filtration endangers the catalysts and ultimately depreciates the practicality of the process.

Just as many synthetic chemists such as Dean, Stark, Schlenk, and Soxhlet did in the past, we anticipated that a well-designed glassware would be a game changer, which streamlines the process. Our initial attempt was to use a commercial solid-liquid extractor, known as the Soxhlet extractor, where **Het-D** was placed with a cellulose thimble as a cartridge in the extraction chamber, and then CP was refluxed in neat under an argon atmosphere. While CP was polymerized as a monomer inside of the thimble, unreacted CP as a solvent washed the released cyclic polyCP off the thimble, brought the filtered polymer to a collection flask, and was then freshly distilled back to the thimble. Since all the active catalytic species always remained in the thimble under the inert atmosphere, this *in situ* separation system provided the possible maximum level of the catalyst security.
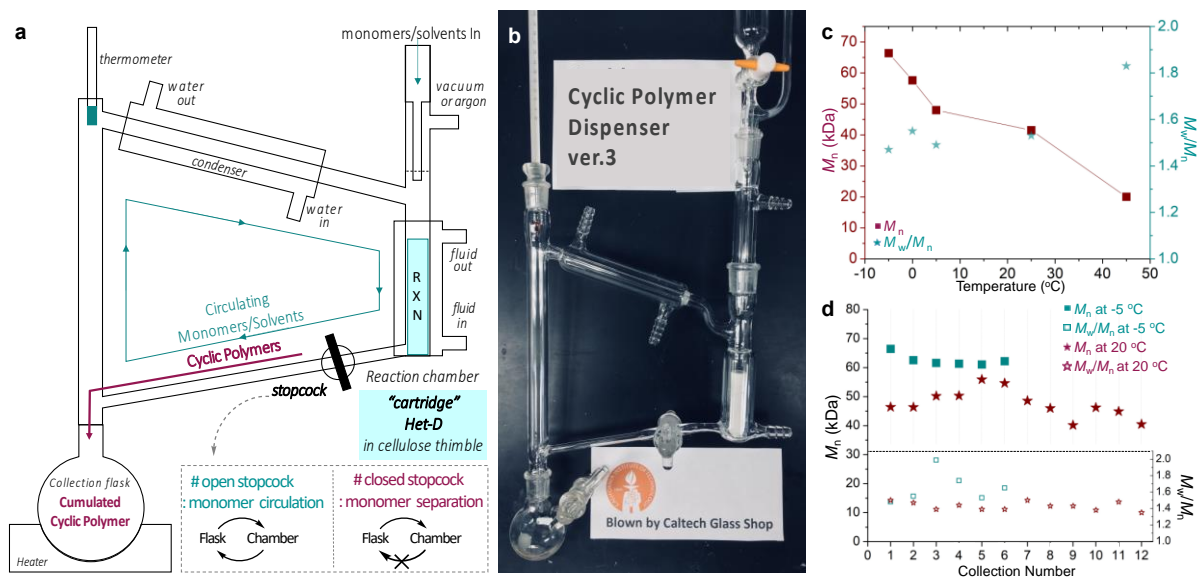

Figure 1.4. "Monomer in, Polymer out." a, Schematic illustration of the cyclic polymer extractor mechanism. **b**, Photo of the extractor. **c**, Temperature dependence of REMP of CP **d**, Multiple collection of duplicate cyclic polyCPs via the dispenser.

Nevertheless, two drawbacks were realized. One was that the reaction temperature was dictated by boiling points of refluxing monomer/solvent. This is a problem since in the REMP of CP, the ceiling temperature is low ($[M]_{eq}$=1.17 at 30 °C[42]). Indeed, the REMP of neat CP (bp=45 °C) in

a Soxhlet extractor afforded cyclic polyCP not exceeding the molar mass of 20 kDa. The other drawback was that the collection flask always contained a mixture of cyclic polyCP and CP, which required an additional step for CP recovery.

Accordingly, an apparatus that is a hybrid of the distillation apparatus and the Soxhlet extractor was customized with two intended features (Fig. 1.4b, see Fig. A4 for our initial drawing and preliminary versions). The custom glassware, namely a cyclic polymer dispenser, consists of a fluid jacket surrounding the reaction chamber so that the reaction temperature can be controlled by a recirculating chiller/heater (Fig. 1.4a). By decreasing the reaction temperature, increased molar masses of cyclic polyCP up to M_n= 66.4 kDa were observed, as a result of the improved monomer conversion (Fig. 1.4c)[35]. Another feature is to segregate the monomer and the polymer in the collection flask by closing a stopcock installed on the pathway between the reaction chamber and the collection flask (Fig. 1.4a). When the stopcock is closed, CP distilled from the flask into the reaction chamber cannot return to the flask, which leaves cyclic polyCP in the flask. Once the thermometer temperature drops (indicating the end of CP distillation), the flask filled with cyclic polyCP is rapidly switched to an empty flask under an increased argon pressure, and then the stopcock is reopened, which resumes CP circulation (and additional CP is added to maintain monomer levels).

After mounting a cartridge on the cyclic polymer dispenser—that is a cellulose thimble containing 100-mg **Het-D** (400 nmol Ru)—we began to operate the process by adding CP. The stopcock was closed whenever cyclic polyCP needed to be collected, and then reopened. After collecting cyclic polyCPs 12 times that were dispensed to collection flasks, we obtained 11.3 grams of combined cyclic polyCP in overall 73% yield based on recovered CP (415,000 catalytic turnovers). The amount of residual CP in the flasks, which was insufficient to be recovered by distillation, caused

the yield loss upon sample drying. Each collection offered a cyclic polyCP with similar molar masses (Fig. 1.4d). High purity of cyclic topology of each round was confirmed with SEC-viscometry and DEPT 135 ^{13}C NMR analysis (Fig. A5). The polymers were white with negligible sign of metal residue (< 10 ppb) (Table A1).

It is noted that the catalyst was kept on duty, "quarantined" safely in the cellulose cartridge under an argon atmosphere throughout the whole process. In many cases, regenerated catalysts are too vulnerable to recycle in a conventional way which includes an *ex situ step of off-duty* catalyst recovery. The use of the cyclic polymer dispenser showcases a new approach to preserve the reusability of precious REMP catalysts by quarantining them *in situ*, as demonstrated by constant activity over multiple collections with high total turnover number. In addition, it can be extended for the synthesis of cyclic polymers with higher molar masses by switching CP to higher ring-strain monomers such as cyclooctadiene (Fig. A6).

1.5 "Social distancing" effect of the immobilized catalyst

We came to realize a noncyclic catalyst in which only the benzylidene moiety is tethered to the silica (**Het-S** in Fig. 1.2a) can be as effective as **Het-D**, since only cyclic polymers can be released from the support by backbiting. If the ruthenium loading on silica gel is sufficiently low, "socially distancing" ruthenium centers may exclusively allow the desired backbiting pathway, physically disallowing the undesired interchain interaction pathway that would release linear polymeric ruthenium complexes unless the silica support holds both the NHC and benzylidene parts (Fig. 1.5a). On the other hand, if densely populated, the propagating ruthenium could undergo this undesired pathway to release linear defects because of chain proximity.
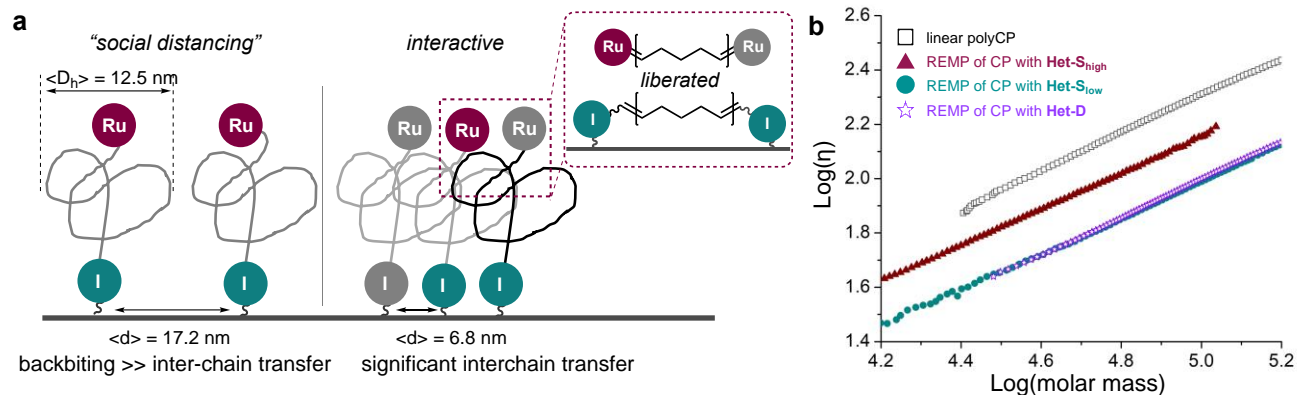
Figure 1.5. "Social distancing" effect. **a**, Schematic illustration of the propensity for the interchain interaction affected by ruthenium density on silica gel. **b**, Mark–Houwink–Sakurada plots of cyclic polyCP made with **Het-D**, **Het-S$_{low}$,** and **Het-S$_{high}$.**

To demonstrate the "social distancing" effect, densely populated **Het-S** (**Het-S$_{high}$**, 18 μmol Ru/1 g silica) and a low populated catalyst (**Het-S$_{low}$**, 2.8 μmol Ru/1 g silica) were prepared. Based on surface area of silica gel, the average ruthenium distance of **Het-S$_{low}$** was estimated to be 17.2 nm, which is larger than the hydrodynamic diameter (12.5 nm ± 0.6) of the isolated cyclic polyCP measured in CP at 22 °C by dynamic light scattering, whereas the ruthenium distance of **Het-S$_{high}$** was 6.8 nm, indicating more congested environment (Table A5).

All characterization data of two cyclic polyCPs obtained with **Het-D** and **Het-S$_{low}$**—molar masses, the Mark–Houwink–Sakurada plots, the conformation plots, ^{1}H NMR and DEPT 135 ^{13}C NMR spectra—are nearly identical (Fig. 1.5b&A7). In contrast, **Het-S$_{high}$** afforded polyCP with a higher intrinsic viscosity than **Het-S$_{low}$,** which implied more interchain transfer events. DEPT 135 ^{13}C NMR spectrum also manifested ill-defined side signals. ICP-MS detected 2000 times higher ruthenium content in the polymer made with **Het-S$_{high}$** (30,000 ppb vs 15 ppb) than one made with **Het-S$_{low}$** (Table A1). Each characterization consistently led us to a conclusion that **Het-S$_{low}$** provided cyclic polyCP with as pure topology as does **Het-D**, while "REMP" of CP with **Het-S$_{high}$** suffered

from the undesired side pathways. The discovery of the "social distancing" effect paves the way for potential manipulation of catalytic activity/selectivity of the catalysts by modifying the NHC[43]. In addition, noncyclic silica-supported catalysts are easier to prepare, which increases the practicality of the system.

1.6 Hydrogenation of cyclic polyCP to cyclic polyethylene

The isolated cyclic polyCP was hydrogenated to cyclic polyethylenes using the tosylhydrazine decomposition method[11]. The full conversion was confirmed by solid-state ^{13}C NMR analysis (Fig. A9). The cyclic polyethylene had a slightly lower melting point (T_m= 131 °C) and crystallization point (T_c= 113 °C) when compared with its linear analog (T_m= 133°C, T_c= 115°C) (Fig. A10), which is an opposite trend to our previous observation with higher-molar mass cyclic polyethylenes (T_m= 132 °C, T_c= 115°C vs for the cyclic one vs. T_m= 130 °C, T_c= 113°C for the linear one)[11]. This discrepancy as well as other properties of cyclic polyethylene are currently under thorough investigation.
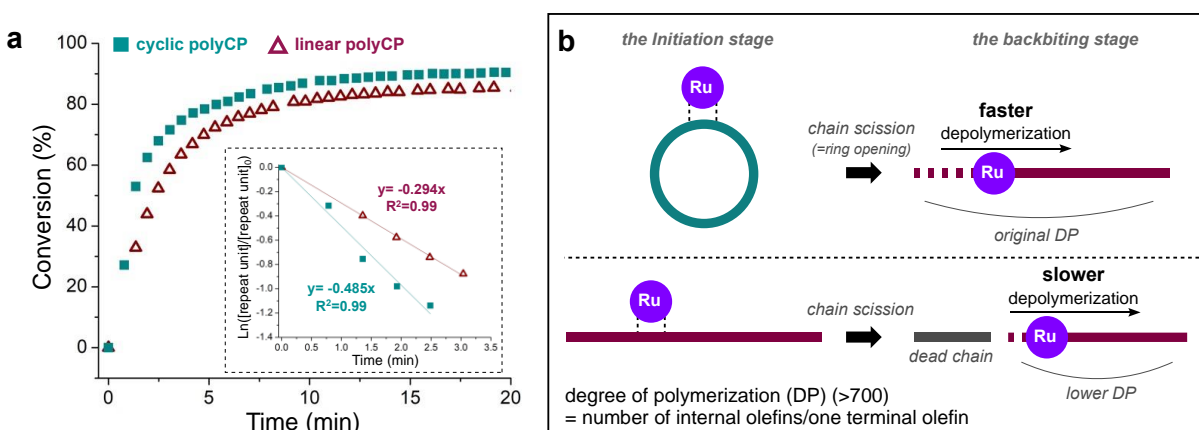

Figure 1.6. Topology dependence of depolymerization. a, Depolymerization conversions of cyclic polyCP (M_n=56.8 kDa, M_w/M_n=1.37) and linear polyCP (M_n=52.8 kDa, M_w/M_n=1.66). Depolymerization conditions: ^1H NMR, CDCl$_3$ (25 mM based on the repeat unit), 0.5 mol% Grubbs 1st generation catalyst, room temperature. **b**, A proposed rationale of the expedited polymerization rate of cyclic polyCP.

1.7 Depolymerization kinetics: cyclic polyCP vs linear polyCP

One of the merits of polyCP is its chemical recyclability to monomer in the presence of an olefin metathesis catalyst, which permits a circular polymer economy[44]. When cyclic and linear polyCPs with similar molar masses were treated respectively with the 1st generation Grubbs catalyst in chloroform, the cyclic polyCP was found to depolymerize 1.6 times faster than its linear analogue ($k_{depolymerization}$=-0.485 min^{-1} for cyclic polyCP vs -0.294 min^{-1} for linear polyCP in Fig. 1.6a&A11). Considering that the initiation process occurs dominantly by random chain cleavages of abundant internal olefins over terminal olefins (degree of polymerization (DP) >700), we tentatively believe that after the first metathesis turnover, the linear polyCP was bisected into two shorter linear polyCPs, one with an active ruthenium carbene and the other without it (Fig. 1.6b)[45,46]. On the other hand, cyclic polyCP would be always opened to active linear polyCP with the original DP without dead fragments[10], and this expedited depolymerization. Research on the detailed topology effect depending on other variables (molar mass, temperature, solvent, *etc.*) is ongoing.

1.8 Conclusions

A scalable process for the synthesis of cyclic polyCP has been developed by leveraging heterogeneity of the catalysts with the help of the customized glassware. Once the catalyst and the monomer were placed to the system, the circular loop of polymerization, polymer separation, and catalyst recovery operated on its own, and then dispensed cyclic polyCP. This continuous process not only resolved long-standing purification issues in homogeneous REMP systems but also unveiled a new concept of "quarantining" a heterogeneous catalyst in the compartmentalized system to maximize overall TONs of vulnerable REMP catalysts, thereby allowing affordable mass production of cyclic polymers. In addition, the effect of polymer topology on depolymerization rates

was discovered, with which we hope to give an intriguing insight to promote the circular polymer economy. Currently, preliminary tests of cyclic polymers as a lubricant additive are ongoing.

1.9 Experimental section

1.9.1 General materials information

The first generation Grubbs catalyst, the second generation Grubbs catalyst, and the second generation Hoveyda-Grubbs catalyst were generously provided by Umicore. The cobalt catalyst for the cyclopentene purification was prepared according to the reported procedure.[1] Cyclopentene and cyclooctadiene were purchased from Sigma Aldrich and degassed by the freeze-pump-thaw method or argon sparging before purification. For polymerization and catalyst synthesis, dichloromethane and toluene were distilled over drying agents under an argon atmosphere, degassed by the freeze-pump-thaw method, and then stored over activated molecular sieves in the glovebox. In other cases that dry solvents were needed, solvents were purified by passing through the solvent purification system (SPS). Deuterated solvents were purchased from Cambridge Isotopes Laboratories, Inc. and used as received. Synthesized polycyclopentenamer and polybutadiene were stabilized with butylated hydroxytoluene (BHT) before stored in the fridge to prevent polymers from cross-linking. Other compounds are synthesized as described in Section 1.9.15.

1.9.2 General experimental information

The standard Schlenk techniques were used for all reactions carried out under an argon atmosphere. The retention factor (Rf) of thin-layer chromatography (TLC) was recorded using E. Merck silica gel 60 F254 precoated plates (0.25 mm) and visualized by UV fluorescence quenching or potassium permanganate staining. Liquid ^{1}H and ^{13}C NMR spectra were recorded on either a

---

[1]Obligacion, J. V. & Chirik, P. J. Bis(imino)pyridine Cobalt-Catalyzed Alkene Isomerization–Hydroboration: A Strategy for Remote Hydrofunctionalization with Terminal Selectivity. *J. Am. Chem. Soc.* **135**, 19107–19110 (2013).

Bruker Ascend 400 spectrometer or a Varian Inova 500 MHz. Solid-state MAS ^{13}C NMR spectrum for the hydrogenated polycyclopentenamer was provided by the California Institute of Technology Solid State NMR Facility using Bruker DSX-500 MHz spectrometer, Bruker 4 mm magic angle spinning probe. High resolution mass spectra (HRMS) were provided by the California Institute of Technology Mass Spectrometry Facility using a JEOL JMS-600H High-Resolution Mass Spectrometer. THF Size exclusion chromatography (SEC) data were collected using two Agilent PLgel MIXED-B 300 × 7.5 mm columns with 10 μm beads, connected to an Agilent 1260 Series pump, a Wyatt 18-angle DAWN HELEOS light scattering detector, and an Optilab rEX differential refractive index detector. Also, another SEC setup was used with Waters high pressure liquid chromatography (HPLC) pump, Waters 2707 autosampler with a loop volume of 100 μL, and two Shodex gel permeation chromatography LF-804 size-exclusion columns maintained at 35 °C. Molar masses were determined from light scattering using dn/dc values calculated from batch mode measurements of polymer solutions at different concentrations. Intrinsic viscosity data were collected by Wyatt triple detector GPC (18-angle DAWN HELEOS light scattering detector–Viscostar II viscometer – Optilab rEX differential refractive index detector) using dn/dc values determined by representative samples. Five different concentrations of the polymers in THF were injected using Wyatt High-Pressure Injection Systems and the resulting RI signals were plotted as a function of concentration; gradient of a linear fit using ASTRA software provided actual $\underline{d}$n/dc values. Chloroform SEC analysis was carried out with the Waters system (a 515 pump and a 2707 autosampler with a loop volume of 100mL), Wyatt OptiLab T-rEx refractive index detector and Shodex SEC LF-804 column. The flow rate was 1.0 mL/min and the temperature of the column was maintained at 35 °C. Samples were filtered through a 0.20 mm PTFE filter before injection. Headspace GC-MS instrument was equipped with Gas Chromatographs (Trace 1300; Thermo

Fischer Sientific), GC/MS (TSQ Series; Thermo Fischer Scientific) and Autosampler (Triplus RSH; Thermo Fischer Scientific). The gas flow for the analysis using GC was 1.0mL/min and the inlet temperatures was 200 °C. The analysis was implemented in a 100:1 split ratio. TG-5MS (30 m X 0.25 mm X 0.25 μm) was used as GC column. Initial oven temperature was 35 °C for 10 min, then it was elevated by the rate of 50 °C/min and their temperature was maintained at 250 °C for 10 min. The analyzed peaks were the identified using Thermo Xcalibur Qual Browser. The samples were prepared as 500 ppm in N,N-dimethylacetamide (Alfa, anhydrous), and 3 mL of the sample was transferred to a headspace vial. Then, the sample was heated at an oven temperature of 35 °C for 10 min, elevated with the rate of 50 °C/min, and 250 °C for 10 min. Preprocessing condition for the samples was established using the Headspace-sampler with incubation temperature and time as 50 °C and 20 min, respectively. The ion source temperature of 230 °C and transfer line temperature of 250 °C. Injection volume was set as 1 mL. Bruker UltrafleXtreme MALDI-TOF MS was used for MALDI-TOF analysis. 0.2 mg of samples and 0.2 mg of additives (Na(TFA) or Ag(TFA)) were dissolved in 0.3 mL of matrix (anthracene or all-trans-retinoic acid) solution (40 mg/mL). A drop of the mixed solution was deposited onto the sample plate, dried under vacuum, then analyzed using flexAnalysis with Polytools software. Other instrumental details are described in corresponding sections with results.

1.9.3 ICP-MS experiment

Samples were analyzed using an **Agilent 8800 Triple Quadrupole ICP-MS**. The intensities of ruthenium isotopes 99, 100, 101, 102 and 104 were measured, and the intensity of pure 2% nitric acid was subtracted to give the net intensities. The net intensities were compared with that of ruthenium standard solutions obtained by diluting a ruthenium standard (99.60 ppm ruthenium in 2% HCl, purchased from VeriSpec) with 2% nitric acid. The numbers provided indicate the average concentration of the five isotopes measured.
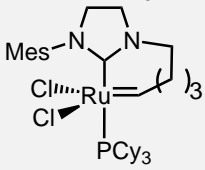
Catalyst digestion:

10 mg of supported molecular REMP catalysts (**Het-D**, **Het-S$_{low}$** and **Het-S$_{high}$**) were precisely weighed in plastic vials using a Sartorius BP110S balance, digested with 1 mL distilled 68% nitric acid at 20 °C for 20 hours on an IKA KS 260 shaker with a shaking speed of 100 motion/minute. After digestion, samples were diluted with 20 mL deionized water purified by Milli-Q system. Corresponding sample blanks were prepared using SiO_2 in an analogous manner.

Polymer digestion:

20 mg of the corresponding filtrate of polymer solution was concentrated under reduced pressure and then the organic residue was digested with 1 mL distilled 68% nitric acid at 20 °C for 20 hours on an IKA KS 260 shaker with a shaking speed of 100 motion/minute, and then sonicated using a Cole-Parmer 8851 Ultrasonic Cleaner for 2 hours at 0 °C. After digestion, samples were diluted with 20 mL deionized water purified by Milli-Q system.

Table A1. ICP-MS analysis data

	μmol Ru/1 g silica	*ppb*
Het-D	4.0	
Het-S (=HET-S$_{low}$)	2.8	
HET-S$_{high}$	18.4	
Cyclic polyCP made with **Het-D** (all iteration combined)		<10
Cyclic polyCP made with **Het-S$_{low}$**		<10
Cyclic polyCP made with **Het-S$_{high}$**		30,000
Cyclic polyCP made with the homogeneous REMP catalyst[2] (after 3 times precipitation in cold methanol)		10,000
Cyclic polybutadiene made with **Het-D**		10

1.9.4 The hot filtration test[3]
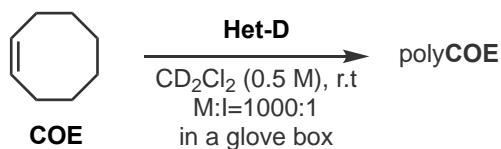
[Procedure]

In a glove box, 250 mg of **Het-D** (0.001 mmol) was weighed into an 8-mL vial. To this vial were added 2 ml of **CD$_2$Cl$_2$**, 10.0 mg of **1,3,5-trimethoxybenzene** (as internal standard) and 0.13 mL of **cyclooctene** (1 mmol). The reaction ran for 30 minutes at **room temperature**. Then, 1 ml of the reaction mixture was transferred using a syringe and filtered with a 0.45-micron PTFE syringe filter. The conversion of the filtrate was recorded with ^{1}H NMR. After 2.5 hours, the reaction mixture

[2]For the homogeneous catalyst synthesis, see: Boydston, A. J., Xia, Y., Kornfield, J. A., Gorodetskaya, I. A. & Grubbs, R. H. Cyclic Ruthenium-Alkylidene Catalysts for Ring-Expansion Metathesis Polymerization. *J. Am. Chem. Soc.* **130**, 12775–12782 (2008).

[3]Allen, D. P., Van Wingerden, M. M. & Grubbs, R. H. Well-Defined Silica-Supported Olefin Metathesis Catalysts. *Org. Lett.* **11**, 1261–1264 (2009).
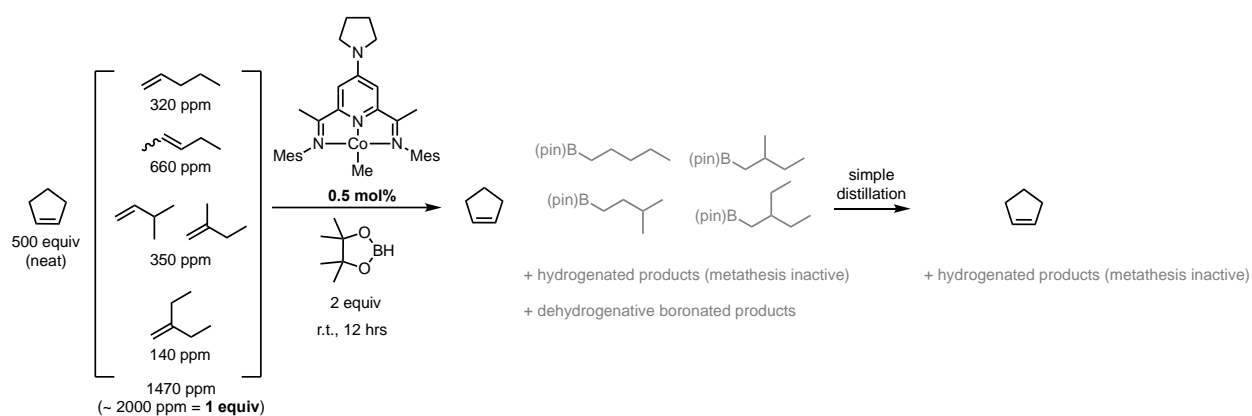
in the vial was filtered likewise, and the conversions of both samples were measured. ICP-MS detected less than 10 ppb of ruthenium from the filtrate.

Table A2. The hot filtration test

	Split Point (30 mins)	Original (3 h)	Filtrate (3 h)
COE conversion	20%	42%	20%

1.9.5 Monomer purification

(A) Cyclopentene purification

	Cyclopentene	impurities	pinacolborane	Chirik's catalyst
MW	68.12		127.98	540.64
d	0.771		0.882	
source	Aldrich 344508-100ML	Assume 2000 ppm	Aldrich 655856-5G	synthesized
state	colorless liquid		Colorless liquid	bluegreen solid
equiv	500	1	1.8	0.005
used	50 mL		0.30 mL	3.1 mg
mmol	565.91	1.132	2.04	0.0057

[Experimental Procedure]

Degassed cyclopentene was transferred into the glove box. A 100-mL oven-dried round-bottom flask (with a magnetic stir bar) was charged with cyclopentene, pinacolborane, and Chirik's cobalt precatalyst[1] in the glovebox — a group of linear olefin impurities[4] were considered limiting

---

[4] Mulhearn, W. D. & Register, R. A. Synthesis of Narrow-Distribution, High-Molecular-Weight ROMP Polycyclopentene via Suppression of Acyclic Metathesis Side Reactions. *ACS Macro Lett.* **6**, 112–116 (2017).

agents in this reaction. The flask was capped with a rubber septum (Fig. A1a) and the reaction mixture was stirred for 12 hours at room temperature (Fig. A1b). In the fume hood, the mixture was passed through a plug of silica gel (Fig. A1c) and then purified via simple distillation (Fig. A1d, Setup: mineral oil bath T = 55 °C, observed thermometer T = 45 °C).

*Note#1: When degassed, the solution stayed green, while the solution color changed from dark green to purple to red when not degassed.

*Note#2: The catalyst loading is 0.001 mol% based on cyclopentene. Given the green solution color after the 12-hour reaction, the catalyst loading could be even lower.

commerical CP (Aldrich)

	Apex RT	Start RT	End RT	Area	%Area	Height	%Height
2-pentene	1.69	1.62	1.74	13053271	0.61	4309099	0.34
cyclopentene	1.88	1.85	1.91	2.09E+09	97.88	1.22E+09	97.67
cyclopentane	1.94	1.92	1.97	32148527	1.51	24762309	1

Purified CP

	Apex RT	Start RT	End RT	Area	%Area	Height	%Height
cyclopentene	1.88	1.85	1.91	2.09E+09	99.86	1.22E+09	97.67
cyclopentane	1.94	1.92	1.97	32148527	0.14	24762309	1

Figure A1. Cyclopentene purification. a, 3 mins after adding the cobalt catalyst **b**, 12 hours after adding the cobalt catalyst (the same solution color, green). **c**, silica filtration. **d**, distillation. **e**,^{1}H NMR spectra of the purified cyclopentene and commercial one as received (upfield). **f**, Head-space GC-MS data of purified cyclopentene and commercial one as received.

*Note#3: As reported by Chirik (see ref.1 in page 14), dehydrogenative boronated products and hydrogenated products were generated as side products. The dehydrogenative boronated products were separated by the distillation step. Inseparable hydrogenated products were metathesis-inactive, which can be considered as hydrocarbon solvents. That was why the detected alkyl protons were different.

*Note#4: We did not perform GC calibration of the commercial CP with authentic impurities in order to convert %Area to %mol, because we think further efforts towards the commercial CP would be slightly off the point when the purified CP turned out to be sufficiently pure under GC sensitivity.

(B) Cyclooctadiene purification

Cyclooctadiene was purified by two previously reported methods[5,6] in a consecutive manner: Hoye's BH_3 treatment method[5], zeolite (molecular sieve) filtration[6], and then distillation. >99.99% Purity of cyclooctadiene was determined with gas chromatography (%Area). 4-vinylcyclohexene was not detected.

[5] Ji, S., Hoye, T. R. & Macosko, C. W. Controlled Synthesis of High Molecular Weight Telechelic Polybutadienes by Ring-Opening Metathesis Polymerization. *Macromolecules* **37**, 5485–5489 (2004).

[6] Kornfield, J. A., Davis, M. E., Wei, M.-H. & Jones, S. C. **2017**, patent No. WO2017112961.

1.9.6 Importance of monomer purity in ROMP and REMP

(A) ROMP of purified cyclopentene vs commercial cyclopentene
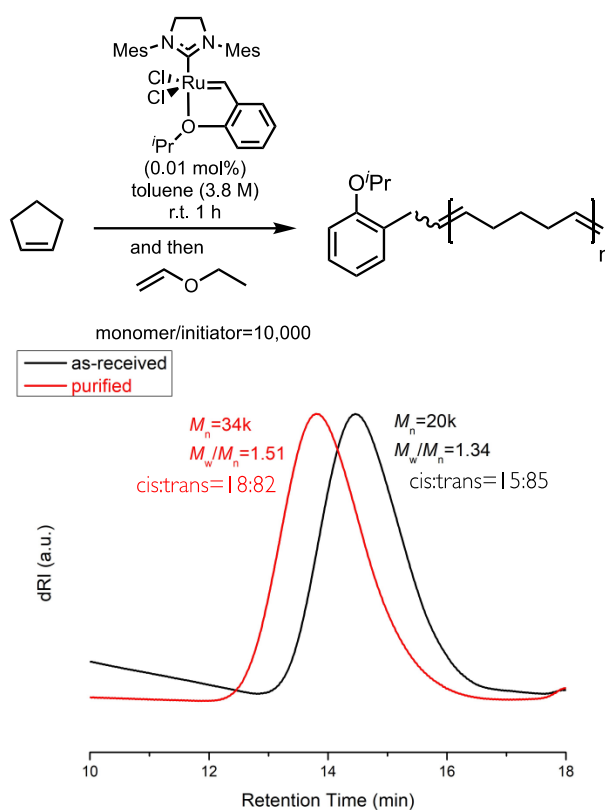
Figure A2. ROMP of cyclopentene. The purified cyclopentene (vs. commercial one) with the 2nd generation Hoveyda-Grubbs initiator and their THF SEC traces. The *cis*:*trans* ratio was obtained with ^{13}C NMR analysis.

[General Experimental Procedure][7]

In a flame-dried 5-mL vial was placed Hoveyda-Grubbs 2nd generation catalyst (0.01 mol%) or Grubbs 2nd generation catalyst (0.05 mol%). Degassed solvent (dichloromethane or toluene was added to the vial under an argon atmosphere. In another flame-dried vial were added cyclopentene and degassed solvent (dichloromethane (5.0 M) or toluene (3.8 M)). The catalyst solution was

---

[7]For the similar protocol, see: Mugemana, C. *et al.* Ring opening metathesis polymerization of cyclopentene using a ruthenium catalyst confined by a branched polymer architecture. *Polym. Chem.* **7**, 2923–2928 (2016).

quickly added to the vigorously stirring cyclopentene solution at r. t. or 0 °C. After 1-3 hours, the reaction was quenched with excess ethyl vinyl ether (~0.1 mL). The crude mixture was concentrated and precipitated in methanol multiple times, affording linear polyCP. The NMR spectra matched with the previous report.[7]

(B) REMP of purified cyclopentene vs commercial cyclopentene
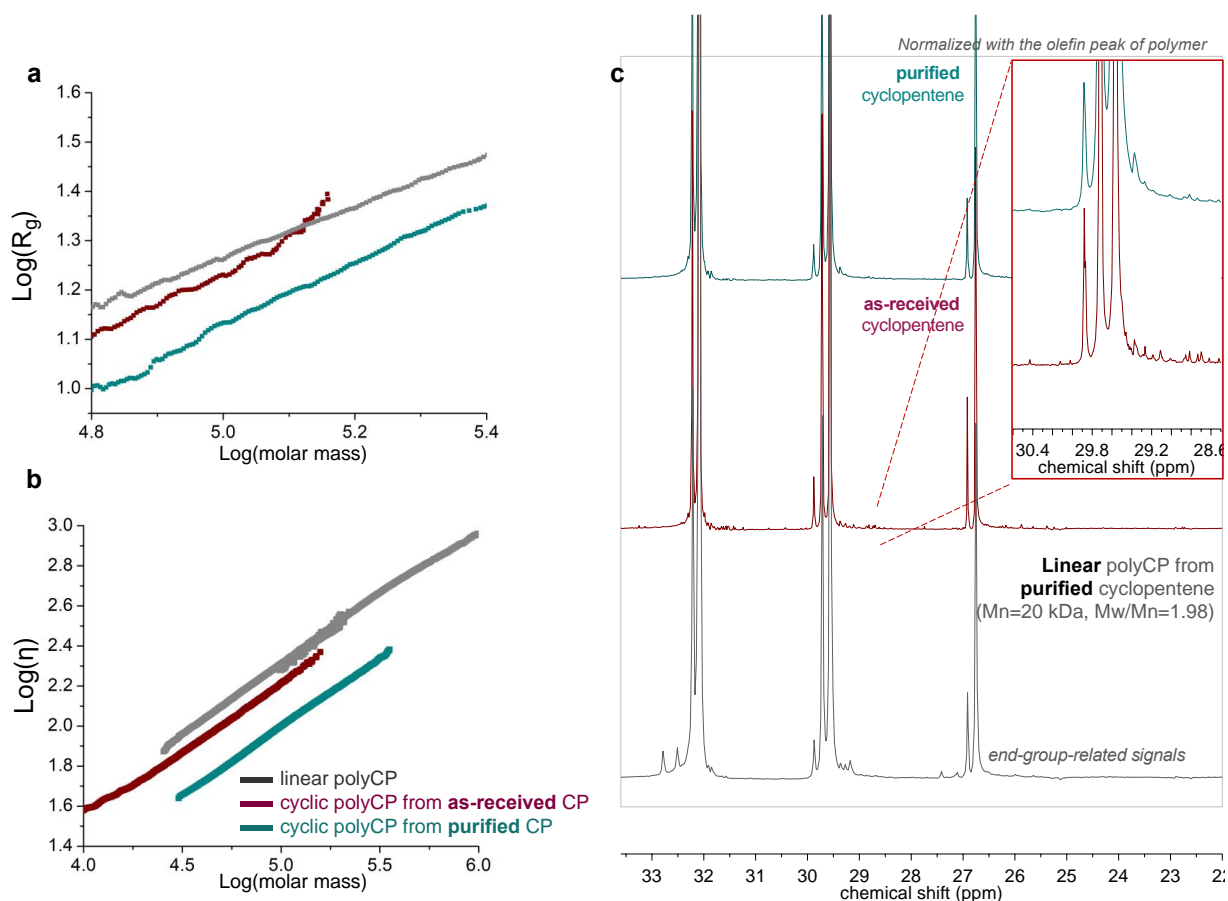
Figure A3. Importance of monomer purity. a, The conformation plot (Rg vs molar mass). b, Mark–Houwink–Sakurada plots (wide range). c, DEPT 135 13C NMR spectra (CDCl3, 100 MHz, 23 °C).

Table A3. Important parameters.

synthetic method	polymer	dn/dc	K (x10^{-2} mL/g)	a	$<\eta_{cyclic}>/<\eta_{linear}>$	$<R_{g,cyclic}>^2/<R_{g,linear}>^2$
ROMP of CP	linear polyCP	0.1318	7.06	0.69	1	1
REMP of purified CP	cyclic polyCP	0.0853	5.62	0.64	0.44	0.54
REMP of commercial CP	mixture	0.1166	6.79	0.68	0.81	0.81

K, a: Mark-Houwink-Sakurada constants.

Additional Discussion:

Cyclic polyCP was found to have a **lower specific refractive index increment (dn/dc)** than linear polyCP. This observation was coherent with Chen's recent report regarding acrylate-based cyclic polymers.[8] **The Mark-Houwink-Sakurada constant K** of linear polyCP was higher than that of cyclic polyCP. Presumably, linear polymers' higher chances of polymer entanglements which stem from the reptation of linear polymers are related to their higher sensitivity of the refractive index increment over the change of polymer concentration, as well as their higher sensitivity of the intrinsic viscosity over the molar mass.

The other Mark-Houwink-Sakurada constant a showed that these polymer chains were flexible random coils regardless of topology. **The ratio of the square radius of gyration** matched well with theoretical values in good solvents.[9] **The ratio of the intrinsic viscosity** was lower than many theoretical predictions or some experimental data[10]; however, this lower value is commonly shown by cyclic polymers produced by the ring-expansion method[11], the reason of which is still elusive.

[8] McGraw, M. L., Clarke, R. W. & Chen, E. Y. X. Synchronous Control of Chain Length/Sequence/Topology for Precision Synthesis of Cyclic Block Copolymers from Monomer Mixtures. *J. Am. Chem. Soc.* **143**, 3318–3322 (2021).

[9] Endo, K. in New Frontiers in Polymer Synthesis (ed. Kobayashi, S.) 121–183 (Springer Berlin Heidelberg, 2008).

[10] Jeong, Y., Jin, Y., Chang, T., Uhlik, F. & Roovers, J. Intrinsic Viscosity of Cyclic Polystyrene. *Macromolecules* **50**, 7770–7776 (2017).

[11] (a) Bielawski, C. W., Benitez, D. & Grubbs, R. H. An 'endless' route to cyclic polymers. *Science* **297**, 2041–2044 (2002). (b) Roland, C. D., Li, H., Abboud, K. A., Wagener, K. B. & Veige, A. S. Cyclic polymers from alkynes. *Nat. Chem.* **8**, 791–796 (2016). (c) Edwards, J. P., Wolf, W. J. & Grubbs, R. H. The synthesis of cyclic polymers by olefin metathesis: Achievements and challenges. *J. Polym. Sci. Poly. Chem.* **57**, 228–242 (2018).

1.9.7 Fabrication of the cyclic polymer dispenser

The glassware used for this research was blown by Mr. Nathan Hart of Caltech Glass shop (nhart@caltech.edu). The glassware has been upgraded based upon trials and errors of the research.
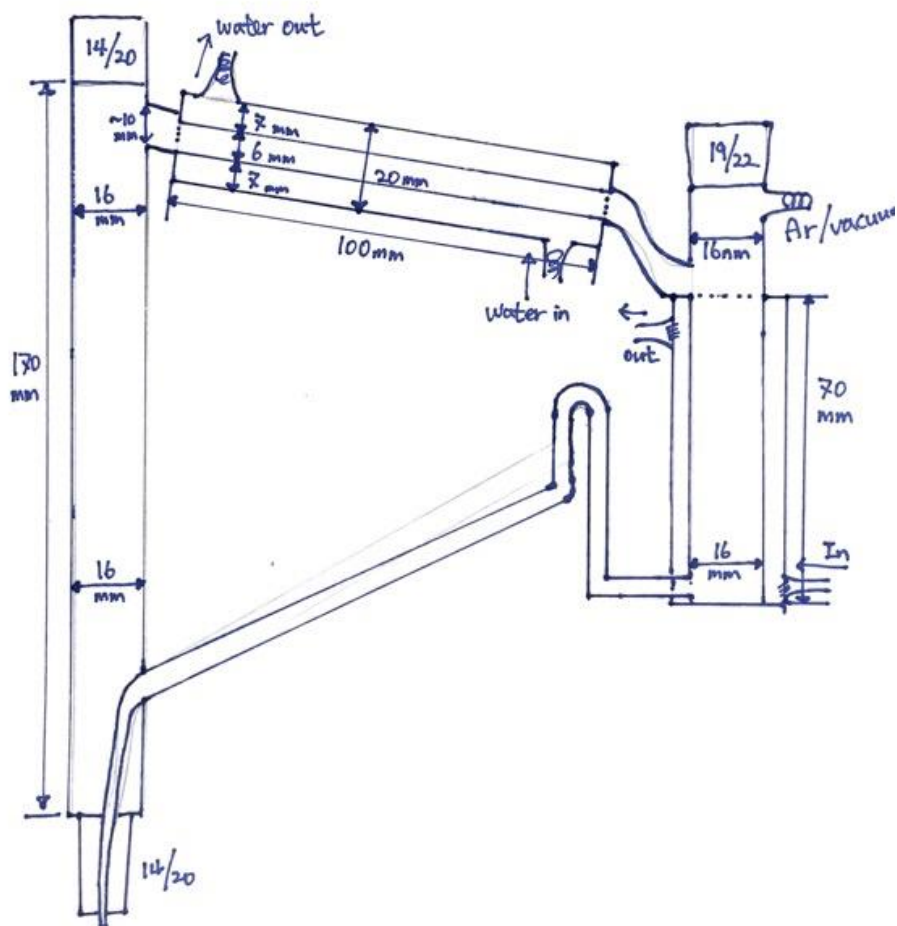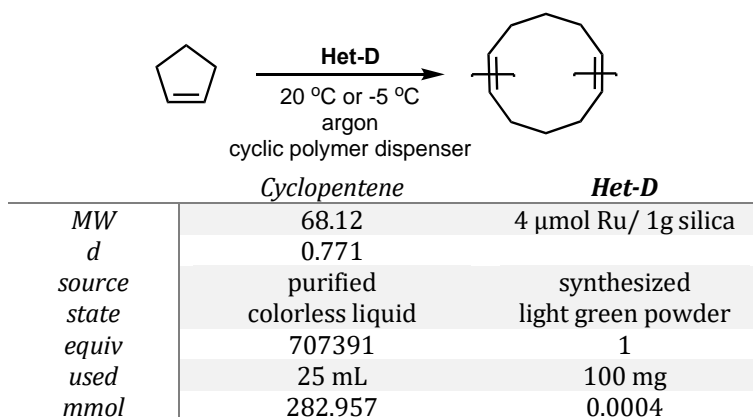

Figure A4. The design plan of the custom glassware and pictures of the modified versions.

1.9.8 REMP of CP in the cyclic polymer dispenser

	Cyclopentene	***Het-D***
MW	68.12	4 µmol Ru/ 1g silica
d	0.771	
source	purified	synthesized
state	colorless liquid	light green powder
equiv	707391	1
used	25 mL	100 mg
mmol	282.957	0.0004

[Experimental Procedure]

All glasses depicted in Fig.A5a were dried in a 165 °C oven prior to use. The cyclic polymer dispenser was connected to a thermometer, a 25-mL Schlenk flask containing a small amount of BHT (<5 mg), and a dropping funnel with the help of suitable joints (Fig. A5a). The upper cooling jacket was equipped with a water circulator, and the lower jacket was linked to a circulating chiller or heater, depending on the required reaction temperature (Fig. A5b). The catalyst (Het-D) was placed in a commercial cellulose thimble. The thimble containing the catalyst was transferred into the reaction chamber of the cyclic polymer dispenser (Fig. A5a&A5b). The whole glass system was charged with argon by vacuum and argon backfilling. Afterwards, CP was added to the reaction chamber via the dropping funnel (Fig. A5b). The distillation column part was wrapped with cotton and foils for heat insulation (Fig. A5b). The heater was set to 70 °C. For convenience, a heat block was used instead of an oil bath (Fig. A5b). Once the circulation of CP began, the thermometer turned to 44–45 °C (Fig. A5c). When the polymer needed to be collected, the stopcock of the dispenser was closed. After the thermometer temperature was dropped to room temperature, the argon pressure was increased, and then the filled flask was replaced with a new 25-mL Schlenk flask (Fig. A5d). The possible air contaminant was vented out of the system by quickly opening the valve of the new flask

(Fig. A5d). The argon pressure was reduced back to normal, and the stopcock was reopened, and then the CP circulation resumed. The product in the flask was a white solid (Fig A5e) and further dried by rotary evaporation. The procedure was iterated 11 times. After all the iterations (at 20 °C), 11.3 g of cyclic polyCP was obtained overall as a white solid and 4.9 mL of cyclopentene was recovered from the cyclic polymer dispenser (73% yield BRSM).

¹H NMR (400 MHz, CDCl3) δ 5.58 – 5.17 (m, 2H), 2.24 – 1.79 (m, 4H), 1.41 (p, J = 7.4 Hz, 2H). **¹³C NMR** (101 MHz, CDCl₃) δ 130.33, 129.82, 32.21, 32.08, 29.87, 29.72, 29.56, 26.91, 26.75. cis:trans=19:81

Table A4. Information of each collection

	1	2	3	4	5	6	7	8	9	10	11	12
collected Amount (mg)	110	200	690	950	2130	3850	670	710	330	510	420	750
M_n (kDa)	46.40	46.36	50.17	50.29	55.90	54.63	48.55	45.98	40.14	46.22	44.9	40.45
M_w/M_n	1.50	1.47	1.39	1.44	1.39	1.39	1.50	1.43	1.43	1.38	1.48	1.35
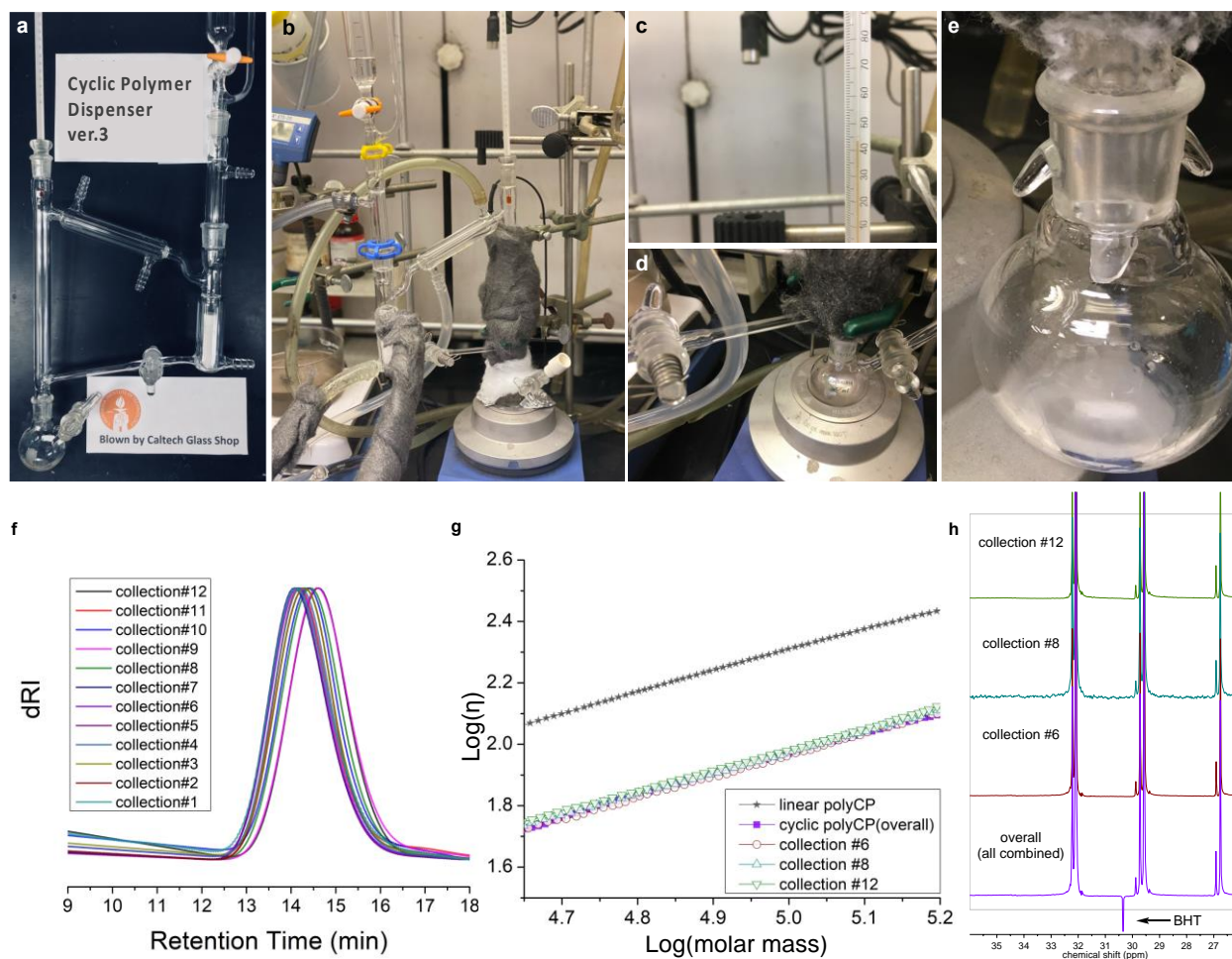
Figure A5. REMP of CP in the cyclic polymer dispenser. a, All required glasses. **b**, A real image of the reaction setup. **c**, The thermometer temperature when the monomer is circulating. **d**, The moment right after a filled flask was replaced with an empty one. **e**, The collected cyclic polyCP before evaporation. **f**, SEC traces of all collections. **g**, Mark-Hounwink-Sakurada plots of the representative collections. **h**, DEPT 135 ^{13}C NMR spectra of the representative collections.

1.9.9 REMP of cyclooctadiene

The use of the cyclic polymer dispenser was extended to REMP of cyclooctadiene (bp=150 °C); in this case, solvents such as dichloromethane or toluene (1–3 mL) were necessary under a reduced pressure (10 torr), because the high ring strain of the monomer results in full conversion of monomers. The solvent circulation in this system enabled formally high concentration

polymerization. Commercial cyclooctadiene was purified in the reported manner (See Section 1.9.5 in page 19).
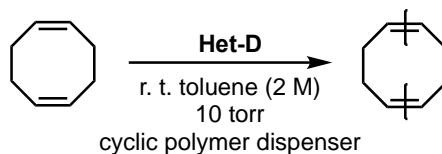
	Cyclooctadiene	Het-D	toluene
MW	108.18	4 µmol Ru/ 1g silica	
d	0.882		
source	purified	synthesized	distilled and degassed
state	colorless liquid	light green powder	
equiv	5000	1	
used	0.75 mL	300 mg	3.0 mL
mmol	6.0	0.0012	

[Experimental Procedure]

As described in Fig. A5 for the synthesis of cyclic polyCP, the whole glass system was used with 300 mg of Het-D in a cellulose thimble to prepare cyclic polybutadiene. The stopcock of the cyclic polymer dispenser was closed, and then cyclooctadiene and toluene were added to the reaction chamber. The reaction mixture remained still without the monomer/solvent circulation for an hour. After the temperature of the heater was set at 100 °C, the stopcock was opened. The pressure was decreased to 10 torr. Once the circulation of cyclooctadiene/toluene began, the thermometer turned to 60 °C. After 12 hours, the stopcock of the dispenser was closed. When the thermometer temperature was dropped to room temperature, the pump was off, and then the filled flask was collected. The product in the flask was further dried in vacuo. 500 mg of cyclic polybutadiene was obtained overall as a white solid (77% yield).

^{1}H NMR (400 MHz, CDCl$_3$) δ 5.45 – 5.19 (m, 4H), 2.26 – 1.73 (m, 8H). **^{13}C NMR** (101 MHz, CDCl$_3$) δ 130.11, 129.99, 129.60, 129.44, 32.72, 32.69, 27.43, 27.41. cis:trans=69:31
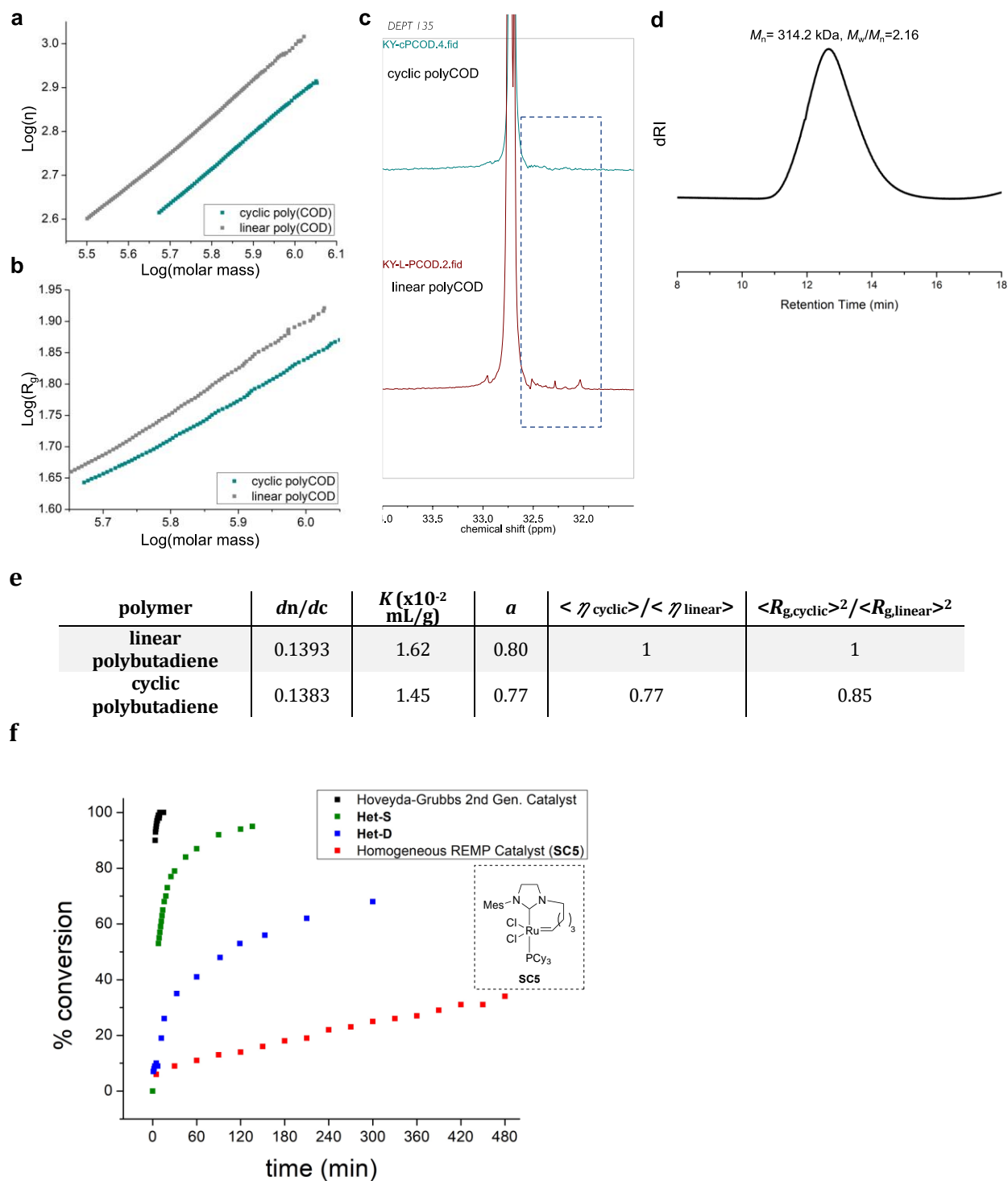
Figure A6. REMP of cyclooctadiene. a, Mark–Houwink–Sakurada plot. **b**, The conformation plot. **c,** DEPT 135 ^{13}C NMR spectra (CDCl$_3$, 100 MHz, 23 °C). **d**, THF SEC trace of cyclic polybutadiene. **e,** Important parameters. Linear polybutadiene presented in the plots: M_n= 220 kDa, M_w/M_n=1.71. **f,** Reaction rate comparison between homogeneous systems and heterogeneous systems.

*Note #1: Monomer kinetics

For kinetic experiments of the catalysts **Het-S** and **Het-D**, 0.001 mmol of catalyst was weighed in a 20 mL vial under nitrogen, followed by addition of 9 mL of C_6D_6 and a stir bar. 1 mL of 1 M cyclooctadiene solution was added under stirring, and the kinetic run was deemed to have started. Aliquots of 0.4 mL solution were retracted by syringe and filtered into NMR tubes to measure the monomer conversion. Conversions were calculated by comparing NMR peak integration of monomer (2.17 – 2.30 ppm) and polymer (1.86 – 2.17 ppm) at different time points. For kinetic experiments of Hoveyda-Grubbs 2nd generation catalyst and the homogeneous REMP catalyst **SC5**, the catalyst and COD monomer were dissolved separately in degassed C_6D_6 under nitrogen to afford 0.5 mM and 0.125 M solutions. 0.1 mL catalyst solution was transferred to an NMR tube, followed by addition of 0.4 mL of monomer solution. The NMR tube was inverted several times to ensure complete mixing before being inserted into the spectrometer. The kinetic run was deemed to have started upon addition of the monomer solution.

1.9.10 Calculation of ruthenium center distance

Based on the surface area information listed on the silica gel used for the silica supported catalysts (**Aldrich 60741**), average ruthenium center distances of **Het-S$_{low}$** and **Het-S$_{high}$** were calculated.

Table A5. Estimated Ru center distances.

(A)

Het-S$_{low}$		
Silica Surface Area (m^2/g)	470	530
Ru loading by ICP (mmol Ru/g silica)	0.0028	
mmol Ru/m^2 silica	5.9575 x 10^{-6}	5.28302 x 10^{-6}
Avogadro number (#/mmol)	6.022 x 10^{20}	
# of Ru/m^2 silica	3.5876x 10^{15}	3.1814 x 10^{15}
# of Ru/m silica	59,896,364.4	56,404,201.64
nm silica distance/Ru	16.69550414	17.72917568
<d> (nm)	17.2	

(B)

Het-S$_{high}$		
Silica Surface Area (m^2/g)	470	530
Ru loading by ICP (mmol Ru/g silica)	0.0180	
mmol Ru/m^2 silica	3.8298 x 10^{-5}	3.39623 x 10^{-5}
Avogadro number (#/mmol)	6.022 x 10^{20}	
# of Ru/m^2 silica	2.3063 x 10^{16}	2.04521x 10^{16}
# of Ru/m silica	151,865,002	143,010,753
nm silica distance/Ru	6.58479564	6.992481188
<d> (nm)	6.79	

1.9.11 Determination of hydrodynamic radius

Dynamic light scattering analysis was carried out with a **Malvern Zetasizer Nano-S**. The average hydrodynamic volume was obtained with 52 measurements using cyclic polyCP solution **at 22 °C** (5 mg/ml in cyclopentene, RI=1.423) in quartz glass cell (Hellma Analytics). The Mark-Houwink contant (*a*) of cyclic polyCP obtained from SEC analysis (Section 1.9.6 in page 22) was 0.64. This indicated a flexible random-coil polymer that can be considered a sphere to which Mie theory can apply.

	M_n (kDa)	Đ	$D_{h,v}$ (nm)
Cyclic PCP	49.7	1.74	12.48 ± 0.60
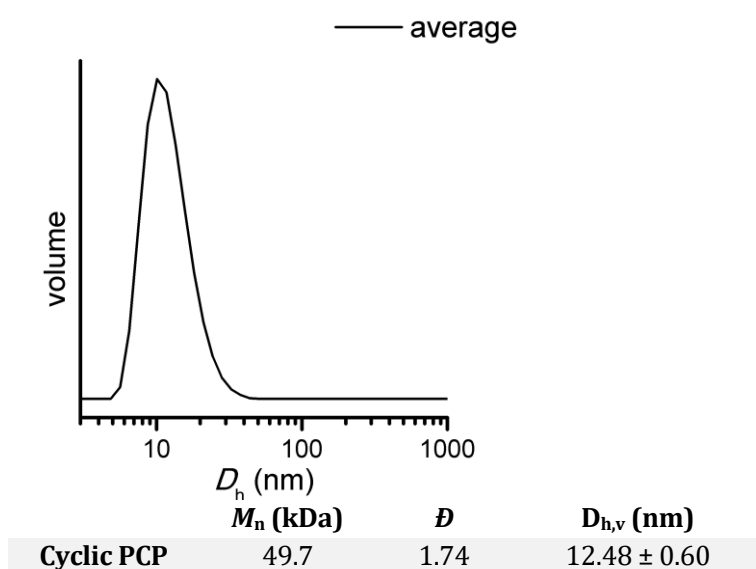
1.9.12 Difference between REMP of CP with Het-S$_{low}$ and Het-S$_{high}$
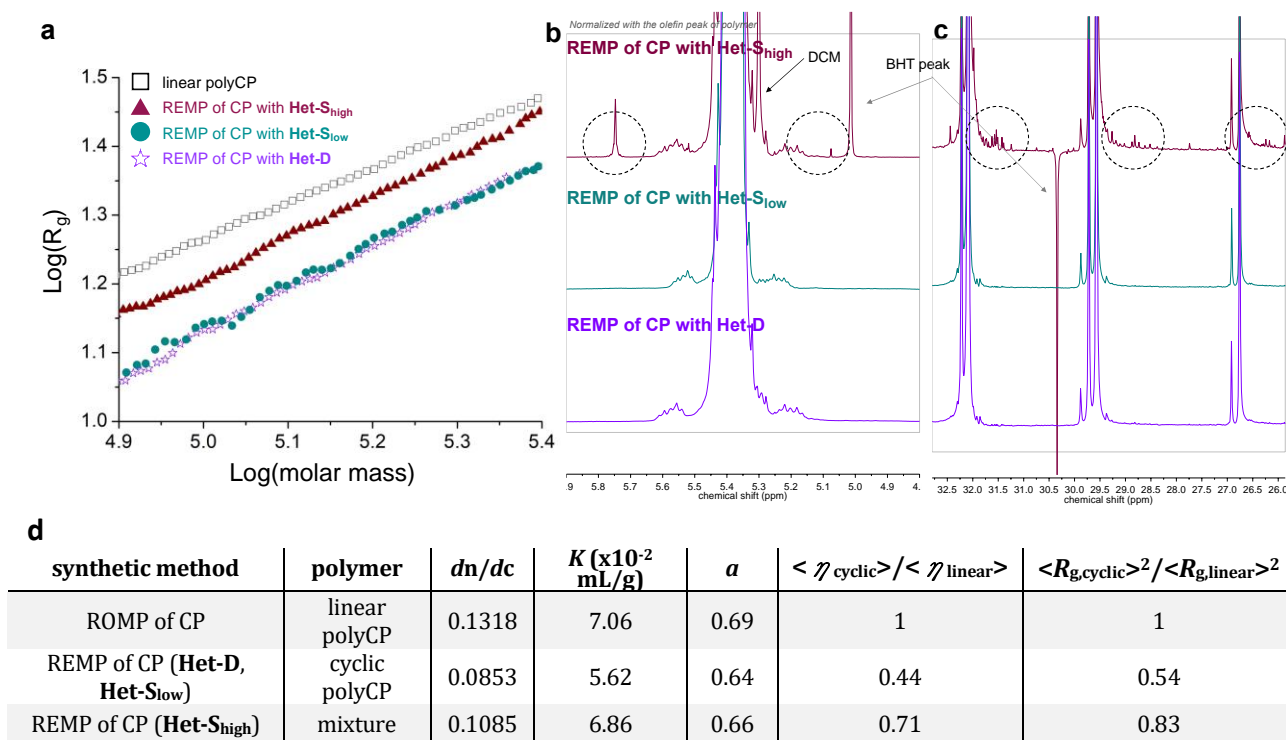
Figure A7. "Social distancing" effect. a, The conformation plot. **b**, ^{1}H NMR spectra of olefin ranges (CDCl$_3$, 400 MHz, 23 °C). **c,** DEPT 135 ^{13}C NMR spectra (CDCl$_3$, 100 MHz, 23 °C). **d**, Important parameters.

synthetic method	polymer	dn/dc	K (x10^{-2} mL/g)	a	$<\eta_{cyclic}>/<\eta_{linear}>$	$<R_{g,cyclic}>^2/<R_{g,linear}>^2$
ROMP of CP	linear polyCP	0.1318	7.06	0.69	1	1
REMP of CP (**Het-D**, **Het-S$_{low}$**)	cyclic polyCP	0.0853	5.62	0.64	0.44	0.54
REMP of CP (**Het-S$_{high}$**)	mixture	0.1085	6.86	0.66	0.71	0.83

1.9.13 Attempt to understand the backbiting process during REMP

[Catalyst cleavage reaction]

In the glovebox, **Het-S** (260 mg) was mixed with DCM (2 mL) and cyclopentene (0.5 mL). The reaction mixture was taken out of the glove box and was stirred for 3.5 hours at 40 °C. The reaction was quenched with 0.2 mL of ethyl vinyl ether. The catalyst was retained by filtration (DCM washing), resulting in quantitative mass of Het-S'.

50 mg of Het-S' added by 5 mL of TBAF solution (1 M in THF), stirred for 36 hours at 50 °C. After removal of residual solvent at reduced pressure, the product was isolated by filtration with a short silica pad, and characterized by NMR, MALDI-TOF, LC-MS, and SEC.

Figure A8. a, ^{1}H NMR of the crude product after the intentional cleavage reaction. **b**, MALDI-TOF spectrum of the crude product.

[Discussion]

^{1}H NMR showed oligomeric cyclopentene signals. With the assumption of the aromatic signals purely coming from the initiating benzilydene moiety, the average DP of the oligomer was five. Although SEC analysis provided no meaningful signal about this, MALDI-TOF exhibited some repetitive signals which can be assigned as the oligomeric species. A tentative conclusion was made that the backbiting process would occur at 5th olefin from the initial styrenyl olefin on average, thereby generating the oligomeric Ru alkylidene catalyst as below.
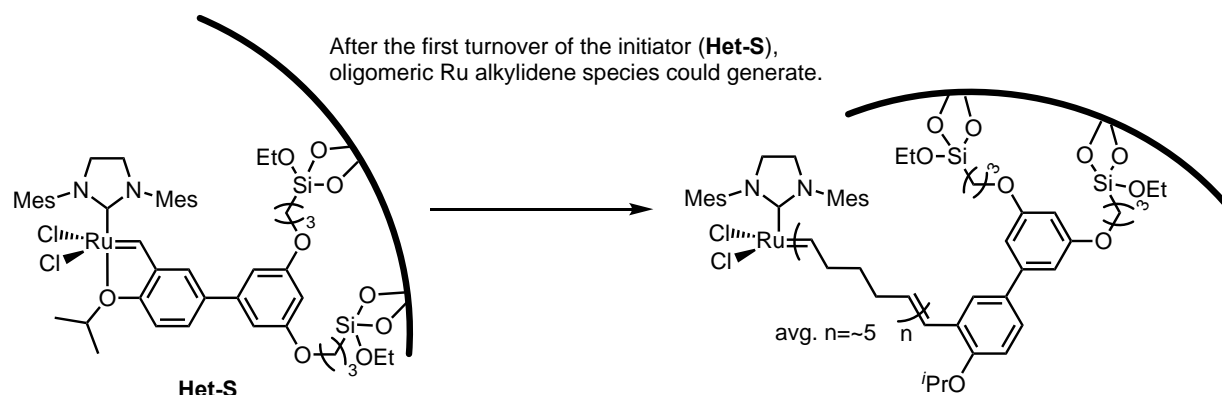
1.9.14 Hydrogenation of cyclic polyCP
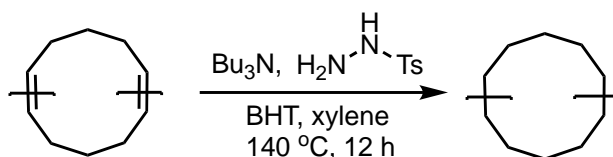
	polyCP	tributylamine	BHT	p-toluenesulfonhydrazide	Xylene
MW	68.12 cyclopentene MW	185.35	220.35	186.23	
d		0.778 (25 °C)			
source	Synthesized	Aldrich 90781-10ML	Aldrich 47168	Aldrich 132004-100	Fisher certified ACS
state	white polymer	colorless liquid	white crystal	white solid	bp=140 °C
equiv	double bond equiv 1	3.5	little	3.1258	
used	770 mg	9.5 mL	5 mg	6.58 g	50 mL
mmol	11.3	39.6		35.3	

[Experimental Procedure]

In a 100 mL round-bottom flask equipped with a reflux condenser was added cyclic polyCP, BHT, and xylene. Upon complete dissolution, *p*-toluenesulfonhydrazide and tributylamine were added. The mixture was stirred at 140 °C for 12 hours, and then the hot mixture was poured into stirring cold methanol (300 mL). The precipitate was filtered and dried in vacuo. Cyclic polyethylene was obtained as a white solid (quant., 792 mg).

#Note#1: The azide and the amine must be added after the polymer is fully dissolved. Otherwise, the conversion of double bonds is incomplete.

RHG21.12.fid
13C CPMAS
p15=1.0 ms, ns= 1k
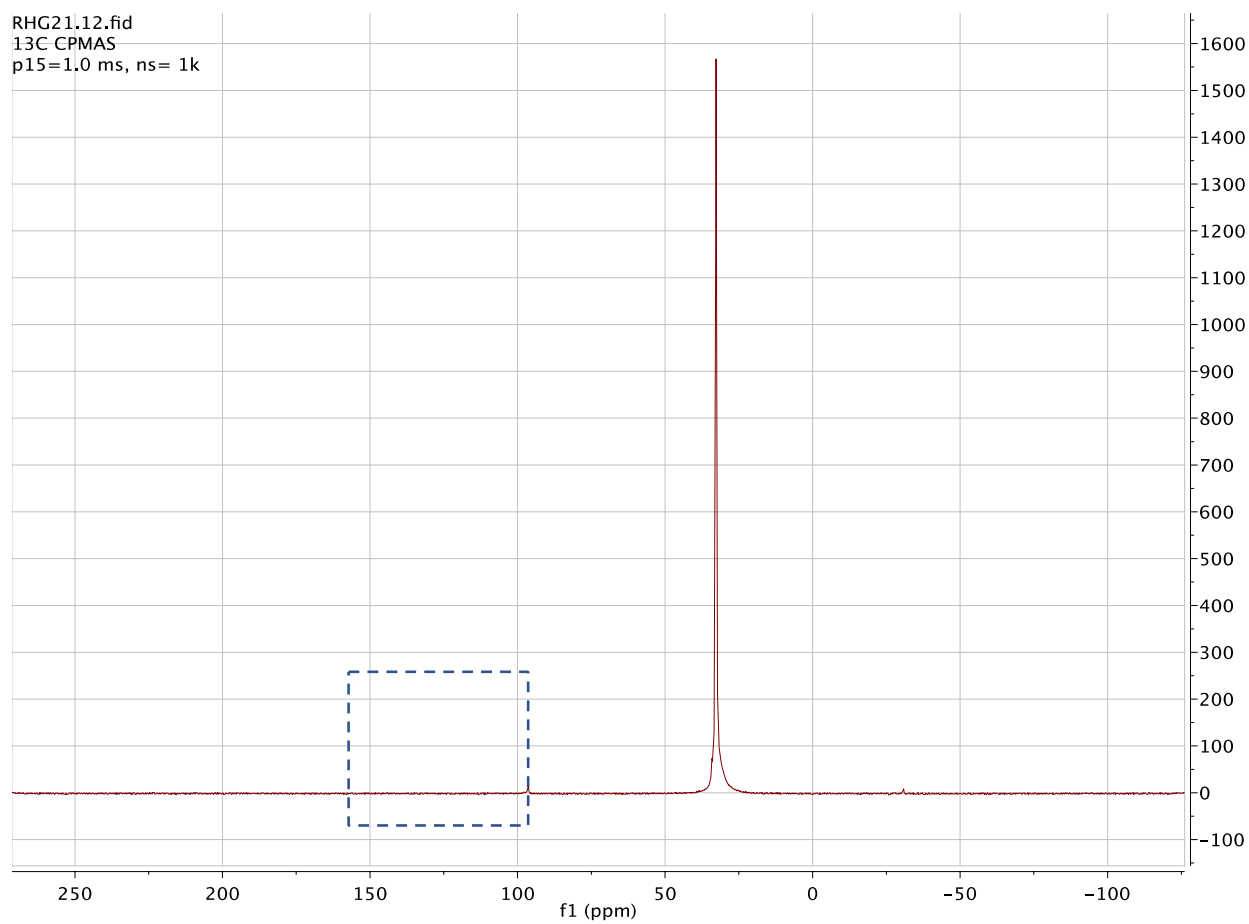
Figure A9. CP/MAS solid-state ^{13}C NMR after the hydrogenation of cyclic polyCP.

1.9.15 DSC analysis of polyethylenes (hydrogenated polyCPs)

Table A6. Differential scanning calorimetry (DSC) data

Samples	Melting point (°C)	Crystallization point(°C)
Cyclic Polyethylene	131.00	113.26
Linear Polyethylene	132.97	114.81
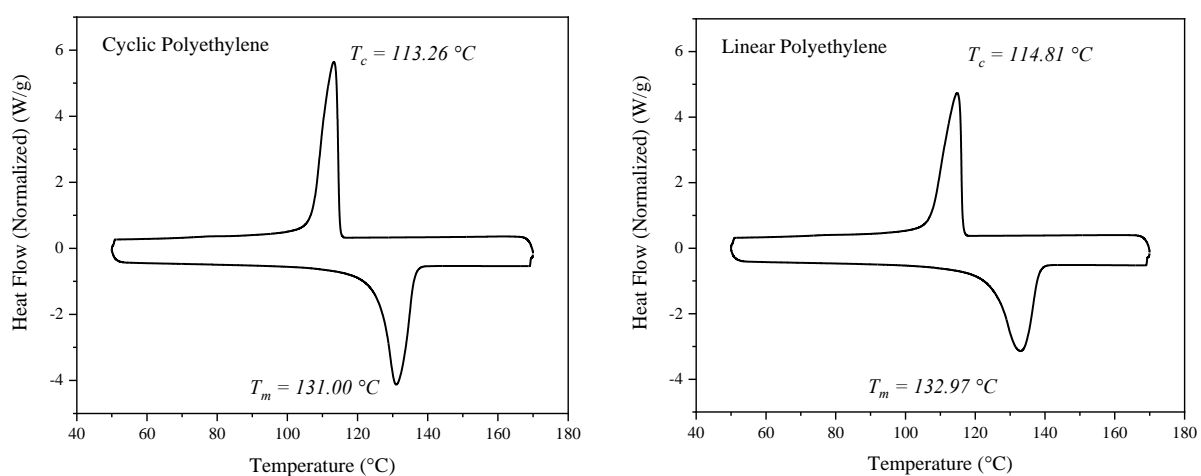
Figure A10. DSC curves for cyclic polyethylene synthesized from cyclic polyCP (M_n=40 kDa, M_w/M_n=1.5) and linear polyethylene synthesized from linear polyCP (M_n=32 kDa, M_w/M_n=1.7).

1.9.16 Depolymerization study
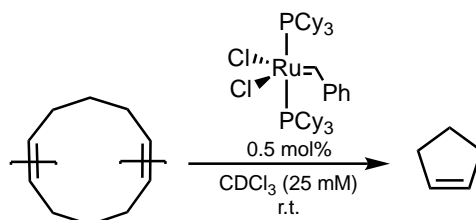
	polyCP	Grubbs 1st gen. cat	hexamethyldisilane	CDCl3
unit MW	68.12	822.96	146.38	
d			0.715	
source state	linear polyCP: M_n=52.8kDa, M_w/M_n=1.66 cyclic polyCP: M_n=56.8kDa, M_w/M_n=1.37	Umicore C823 purple solid	Aldrich 217069-5G colorless liquid	
equiv	1 (based on the repeating unit)	0.005		25 mM
used	0.75 mg	Stock solution	3 μL	0.44 mL
mmol	0.011	0.000055		

[Experimental Procedure] – NMR Study

PolyCP was placed in a flame-dried 5-mL vial under an argon atmosphere, and then hexamethyldisilane was added as an internal standard. After CDCl3 (430 μL) was added to the vial, the solution was transferred to an NMR tube. The initial ratio between polyCP and the internal standard was measured. To another flame-dried 5 mL vial was placed Grubbs 1st generation catalyst (0.35 mg). CDCl3 was added to make a 5 mM catalyst stock solution. After a portion of the catalyst stock solution (10 μL, 0.055 μmol) was added to the NMR tube, the solution was mixed by shaking the NMR tube for five seconds, and then ^{1}H NMR was recorded over time. The $k_{depolymerization}$ values were estimated based on the approximation of the 1st order reaction rate ($-d$[polyCP]/dt = $k_{depolymerization}$[polyCP]), where [polyCP] was calculated by the integration ratio of polyCP's olefinic protons (δ=5.39 ppm) compared to methyl protons of hexamethyldisilane.

[Experimental Procedure] – SEC Study

PolyCP (30 mg, 0.44 mmol of the repeating unit, 1.0 equiv) was placed in a flame-dried 20-mL vial under an argon atmosphere and dissolved with degassed CHCl$_3$ (13 mL, 33 mM). Grubbs 1st generation catalyst (0.36 mg, 0.1 mol%) in CHCl$_3$ was quickly added to the vigorously stirring polyCP solution. 0.7 mL of the aliquot was taken each time and transferred into a sealed 2-mL vial containing 30 μL of ethyl vinyl ether. The quenched polymer solution was directly injected to the CHCl$_3$ SEC to monitor the depolymerization.
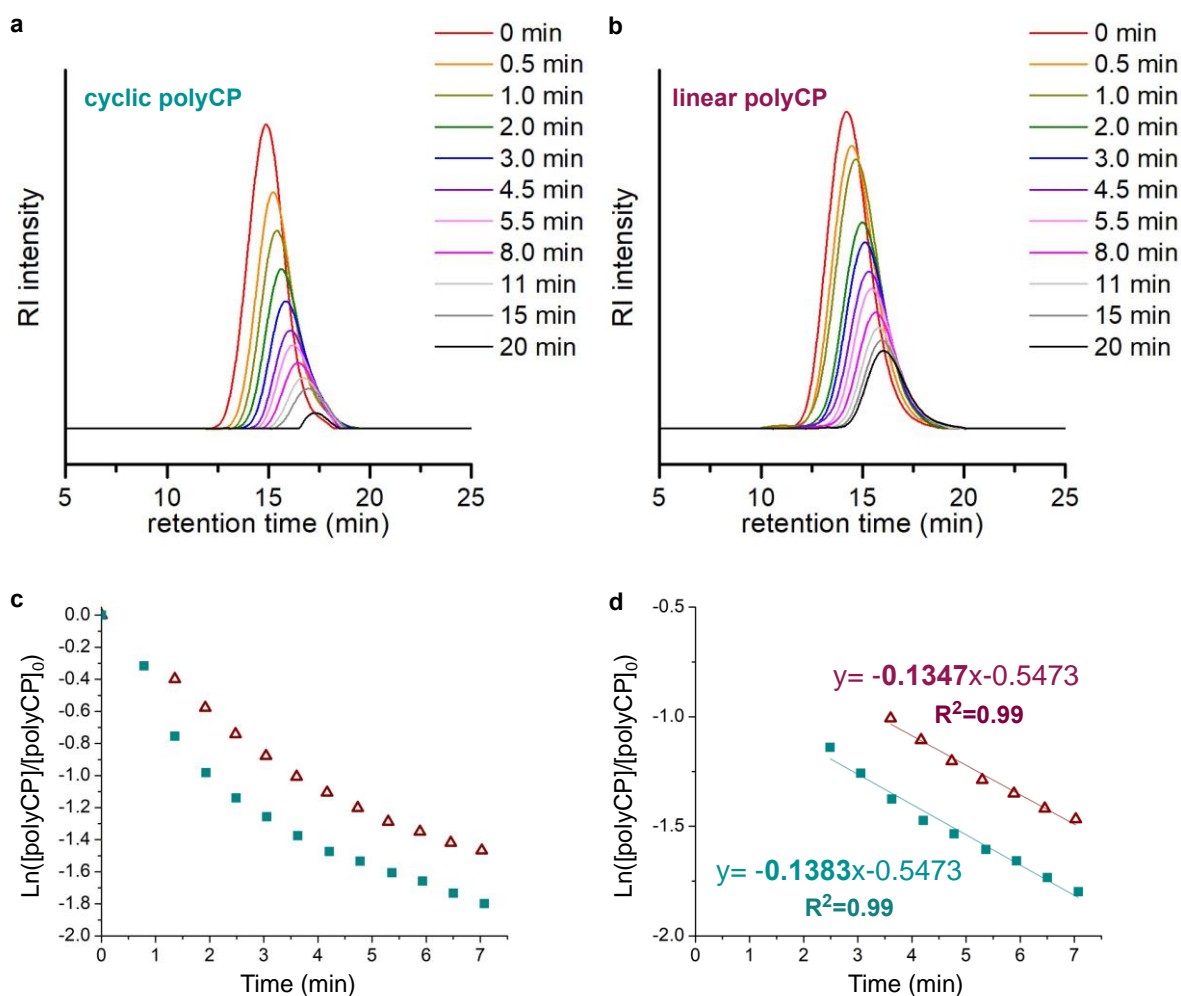
Figure A11. Depolymerization study. **a**, SEC traces of cyclic polyCP over time. **b**, SEC traces of linear polyCP over time. **c**, Depolymerization conversion of cyclic polyCP and linear polyCP. d, Similar depolymerization rate at the later stage.

1.9.17 Synthesis of catalysts

Scheme A1. Synthesis of the immobilized ruthenium catalysts **Het-S** and **Het-D**.
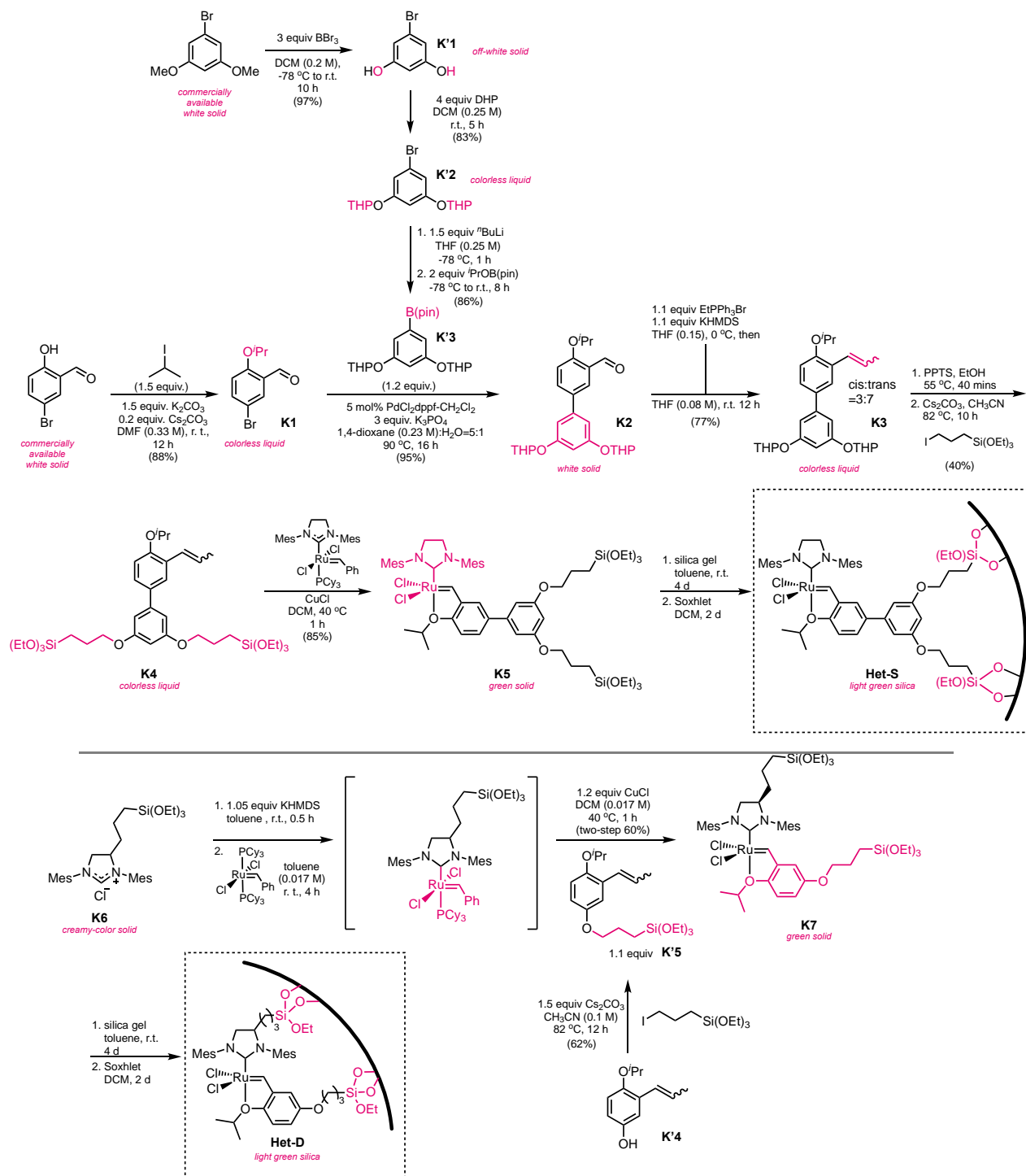
(A) Synthesis of Het-S

(i) Synthesis of K1: Nucleophilic substitution
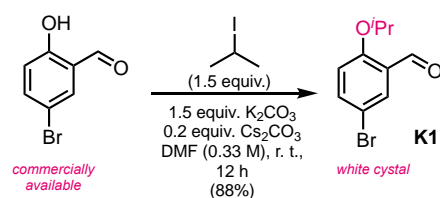
K1 was synthesized by the *modified* method from the previous literature.[12]

	5-bromosalicyladehyde	2-iodopropane	Cs$_2$CO$_3$	K$_2$CO$_3$	DMF
MW	201.02	169.99	325.82	138.21	
d		1.703			
source	Aldrich	Alfa Aesar	Aldrich	Aldrich	Aldrich
	137286-100G	A15066	441902-50G	791776-500G	227056-1L
state	white solid	colorless liquid	white solid	white solid	
equiv	1	1.5	0.2	1.5	0.33 M
used	2.0 g	1.5 mL	652 mg	2.07 g	30 mL
mmol	9.95	15	2.0	15	

[Experimental Procedure]

To 5-bromosalicyladehyde in 30-mL DMF in a 165 °C-oven-dried 100-mL round-bottom flask were added K$_2$CO$_3$ and Cs$_2$CO$_3$. The flask was capped with a white rubber septum, and the reaction mixture was stirred at room temperature for 10 mins. To the glowing yellow heterogeneous solution was slowly injected 2-iodopropane. The reaction mixture was further stirred at room temperature for 12 hours. Afterwards, the reaction mixture, the color of which was yale yellow with no glowing, was diluted with ether (120 mL) and washed with water (50 mL x 5) and brine (50 mL x 2). The organic layer was dried over MgSO$_4$ and concentrated *in vacuo*. The crude mixture was purified by flush silica column chromatography (Hexanes:EtOAc=20:1), affording the desired product as a colorless liquid which gradually turned into a white crystal over time (MW=243.10, 2.13 g, 8.78 mmol, 88%).

[12]Koç, F., Michalek, F., Rumi, L., Bannwarth, W. & Haag, R. Catalysts on Functionalized Polymer Chips (PC) as Recyclable Entities. *Synthesis* **2005**, 3362–3372 (2005).

Product R_f = 0.5 (hexanes:EtOAc=5:1) ^{1}H NMR (400 MHz, CDCl$_3$) δ 10.39 (s, 1H), 7.92 (d, J = 2.7 Hz, 1H), 7.59 (dd, J = 8.9, 2.7 Hz, 1H), 6.89 (d, J = 8.9 Hz, 1H), 4.65 (hept, J = 6.1 Hz, 1H), 1.40 (d, J = 6.1 Hz, 6H). ^{13}C NMR (101 MHz, CDCl$_3$) δ 188.71, 159.45, 138.13, 130.93, 126.98, 116.00, 113.12, 71.64, 21.90.

*Note#1: Proton and carbon NMR spectra matched those previously reported.[12]

*Note#2: We observed that this reaction worked similarly in up to 10-g scale.

*Note#3: Rf value of the starting material was 0.51 (hexanes:EtOAc=5:1), the spot of which was slightly higher but largely overlaps with that of the product on the TLC plate. However, they showed different fluorescence under longer wavelength UV light (365 nm, SM-green, product-blue), which can be rationalized by the excited-state intramolecular proton transfer process.[13]

---

[13]Jang, Y.-J., Hwang, S.-H. & Choi, T.-L. Iridium-Catalyzed Direct C−H Amidation Polymerization: Step-Growth Polymerization by C−N Bond Formation via C−H Activation to Give Fluorescent Polysulfonamides. *Angew. Chem. Int. Ed.* **56**, 14474–14478 (2017).

(ii) Synthesis of К'1: BBr₃-mediated Demethylation
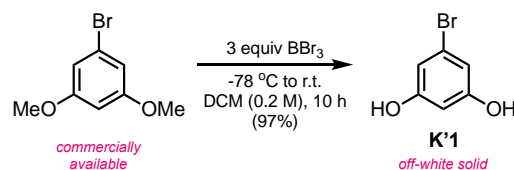
K'1 was synthesized by the modified method from the previous literature.[14]

	1-bromo-3,5-dimethoxybenzene	*1 M BBr₃ in DCM*	*DCM*
MW	217.06	250.52	
d		1.467	
source	Accela	Aldrich	SPS
	SY014454 100G	211222-100ML	
state	white solid	pale brownish liquid	
equiv	1	3	0.2 M
used	5.0 g	70 mL	50 mL
mmol	23.04	70	

[Experimental Procedure]

To 1-bromo-3,5-dimethoxybenzene in dry dichloromethane in a 165 °C-oven-dried 300-mL round-bottom flask capped with a white rubber septum was added a 1 M solution of boron tribromide (BBr₃) in methylene chloride at -78 °C under an argon atmosphere. The light brownish reaction solution was slowly warmed to room temperature and stirred for 10 hours, and then diluted with 100-mL ether. At 0 °C, water (30 mL) was carefully added, immediately forming water-soluble white solids. The organic layer was washed with water (100 mL x 2) — all the white solids were dissolved at this stage — and brine (100 mL), and then dried over anhydrous MgSO₄. After the solvent removal *in vacuo*, the liquid residue was digested with 10-mL chloroform and concentrated *in vacuo*. The solid residue was then vigorously stirred in 50-mL *n*-pentane for 15 mins, followed by decanting the supernatant, affording the desired product as an off-white solid (MW=189.01, 4.22 g, 22.3 mmol, 97%).

---

[14]Chaudhuri, D. *et al.* Metal-Free OLED Triplet Emitters by Side-Stepping Kasha's Rule. *Angew. Chem. Int. Ed.* **52**, 13449–13452 (2013).

^{1}H NMR (400 MHz, CD$_3$OD) δ 6.46 (d, J = 2.1 Hz, 2H), 6.22 (t, J = 2.1 Hz, 1H). ^{13}C NMR (101 MHz, CD$_3$OD) δ 160.52, 123.44, 111.04, 102.62.

*Note#1: The ^{13}C NMR chemical shift of C1 carbon (*C*-Br) in the referenced literature for this reaction was reported mistakenly.[14] Other values matched.

*Note#2: The 1 M solution of BBr$_3$ in methylene chloride must be handled extra-carefully in the fume hood, because it generates lots of white smoke, as soon as exposed to the air.

(iii) Synthesis of K'2: THP protection of K'1
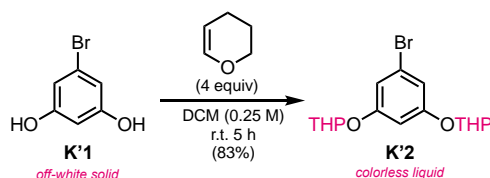
	K'1	3,4-dihydro-2H-pyran	PPTS	DCM
MW	189.01	84.12	251.30	
d		0.922		
source	handmade	TCI D0555 100mL	Alfa A15708-22	Fisher HPLC grade 4L
state	grayish solid	colorless liquid	white solid	
equiv	1	4	0.1	0.25 M
used	4.20 g	8.1 mL	558 mg	90 mL
mmol	22.2	88.8	2.22	

[Experimental Procedure]

To K'1 in 90-mL dichloromethane in a 250-mL round-bottom flask were added 3,4-dihydro-2H-pyran and pyridinium *p*-toluenesulfonate — K'1, insoluble in DCM, became fully soluble upon addition of DHP. The flask was capped with a brown rubber septum, and the brown reaction solution was stirred at room temperature for 5 hours (the air in the septum-closed system). Afterwards, the reaction mixture was diluted with DCM (100 mL) and washed with saturated NaHCO$_3$ (aq., 50 mL),

water (50 mL) and brine (50 mL). The organic layer was dried over $MgSO_4$ and concentrated *in vacuo*. The crude mixture was purified by silica column chromatography (Hexanes:EtOAc=15:1), affording the desired product as a colorless liquid (MW=357.24, 6.55 g, 18.3 mmol, 83%).

Product R_f = 0.5 (hexanes:EtOAc=6:1) ^{1}H NMR (500 MHz, CDCl$_3$) δ 6.86 (t, J = 2.5 Hz, 2H), 6.69 (d, J = 2.3 Hz, 1H), 5.36 (dt, J = 6.7, 3.2 Hz, 2H), 3.85 (td, J = 10.6, 3.0 Hz, 2H), 3.67 – 3.53 (m, 2H), 2.05 – 1.88 (m, 2H), 1.82 (dt, J = 7.8, 3.8 Hz, 4H), 1.75 – 1.43 (m, 6H). ^{13}C NMR (125 MHz, CDCl$_3$) δ 158.56, 158.51, 122.53, 122.49, 113.16, 113.11, 104.33, 104.14, 96.51, 96.36, 61.95, 61.91, 30.21, 30.19, 25.13, 18.59, 18.54. HRMS: Chemical formula ([M]): $C_{16}H_{21}BrO_4$, calcd. [M]$^+$ 356.0623 Found: 356.0625.

(iv) Synthesis of K'3: Borylation of K'2
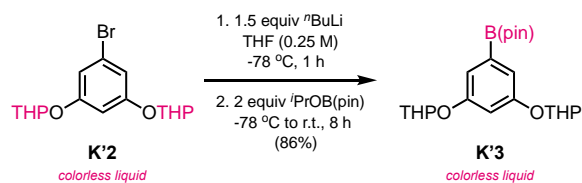
	K'2	2.5 M ^{n}BuLi in hexanes	^{i}PrOB(pin)	THF
MW	357.24		186.06	
d			0.912	
source	synthesized	Aldrich 230707-100 ML	Aldrich 417149-5ML	
state	colorless liquid		colorless liquid	
equiv	1	1.5	2	0.25 M
used	4.11 g	7.0 mL	4.8 mL	40 mL
mmol	11.5	17.25	23	

[Experimental Procedure]

To K'2 in tetrahydrofuran in a 100-mL round-bottom flask capped with a brown rubber septum was added dropwise 2.5 M nBuLi in hexanes at -78 °C under an argon atmosphere. The

reaction solution was stirred at -78 °C for 1 hour. Afterwards, 2-Isopropoxy-4,4,5,5-tetramethyl-1,3,2-dioxaborolane was added dropwise and then the reaction mixture was warmed to room temperature. After 8-hours, the crude mixture was diluted with DCM (120 mL) and washed with water (150 mL) and brine (50 mL x 2). The organic layer was dried over MgSO$_4$ and concentrated *in vacuo*. The crude mixture was purified by silica column chromatography (Hexanes:EtOAc=10:1), affording the desired product as a colorless liquid (MW=404.31, 3.98 g, 9.84 mmol, 86% yield). Although impurities were detected, we moved on to the next step without further purification, because K'3 was unstable.

Product R$_f$ = 0.5 (hexanes:EtOAc=5:1) ^{1}H NMR (400 MHz, CDCl$_3$) δ 7.12 (dd, J = 2.4, 1.7 Hz, 2H), 6.89 (q, J = 2.3 Hz, 1H), 5.47 (dt, J = 6.7, 3.1 Hz, 2H), 3.91 (m, 2H), 3.68 – 3.55 (m, 2H), 2.09 – 1.44 (m, 12H), 1.32 (s, 12H). ^{13}C NMR (101 MHz, CDCl$_3$) δ 157.67, 157.59, 115.67, 108.61, 108.37, 96.09, 95.88, 83.73, 61.76, 61.71, 30.33, 30.30, 25.28, 24.85, 18.61, 18.57. HRMS: Chemical formula ([M]): C$_{22}$H$_{33}$BO$_6$, calcd. [M]$^+$ 404.2370 Found: 404.2370.

(v) Synthesis of K2: Suzuki coupling of K1 and K'3
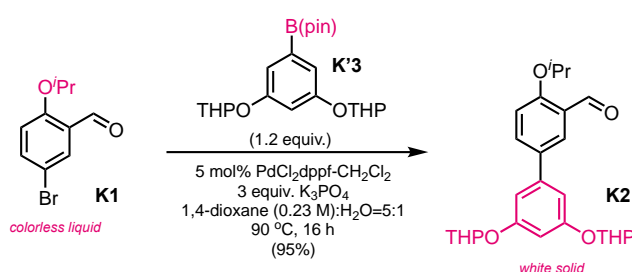
	K1	K'3	PdCl$_2$dppf-CH$_2$Cl$_2$	K$_3$PO$_4$	1,4-dioxane	H$_2$O
MW	243.10	404.31	251.30			
d		0.922				
source	synthesized	synthesized	Aldrich 379670-25G	Aldrich P5629-500G	Aldrich 34857-1L	degassed deionized water
state	white crystal	colorless liquid	dark red solid	white solid		

equiv	1	1.2	0.05	3	0.23 M	5:1
used	1.12 g	2.23 g	188 mg	3.00 g	20 mL	4 mL
mmol	4.61	5.52	0.230	13.8		

[Experimental Procedure]

In a 100-mL Schlenk flask, K1 and K'3 were dissolved in 20 mL of degassed 1,4-dioxane under an argon atmosphere. K_3PO_4 and degassed deionized water (4 mL) were added to the flask. To this solution, $PdCl_2dppf\text{-}CH_2Cl_2$ was quickly added, and then the reaction mixture was stirred at 90 °C (oil bath) for 16 hours. After cooling down to room temperature, the reaction mixture was diluted with ethyl acetate (100 mL), washed with water (50 x 2 mL) and brine (50 mL). The organic layer was dried with anhydrous Na_2SO_4 and concentrated in vacuo. The crude mixture was purified by silica column chromatography (Eluted with hexanes to hexanes:EtOAc=10:1 to hexanes:EtOAc=3:1), isolating the desired product as a white solid (MW=440.54, 1.92 g, 4.36 mmol, 95%).

Product R_f = 0.38 (hexanes:EtOAc=4:1). ^1H NMR (500 MHz, CD_2Cl_2) δ 10.50 (s, 1H), 8.00 (d, J = 2.5 Hz, 1H), 7.78 (dd, J = 8.7, 2.5 Hz, 1H), 7.09 (d, J = 8.7 Hz, 1H), 6.92 (s, 2H), 6.74 (t, J = 2.3 Hz, 1H), 5.47 (q, J = 3.6 Hz, 2H), 4.75 (hept, J = 6.1 Hz, 1H), 3.91 (ddd, J = 12.1, 9.3, 3.1 Hz, 2H), 3.68 – 3.57 (m, 2H), 2.09 – 1.95 (m, 2H), 1.94 – 1.80 (m, 4H), 1.79 – 1.65 (m, 4H), 1.61 (dd, J = 8.4, 4.2 Hz, 2H), 1.43 (d, J = 6.0 Hz, 6H). ^{13}C NMR (126 MHz, CD_2Cl_2) δ 189.73, 160.19, 158.54, 158.50, 141.43, 141.42, 134.13, 132.98, 126.12, 125.68, 114.50, 108.28, 108.22, 104.01, 103.92, 96.57, 96.48, 71.41, 62.07, 62.04, 30.36, 30.34, 25.24, 21.73, 18.83, 18.80. HRMS: Chemical formula ([M]): $C_{26}H_{32}O_6$, calcd. $[M]^+$ 440.2199 Found: 440.2182.

*Note#1: The fluorescence of the K1 at 365-nm UV was dark blue, whereas that of K2 was light blue.

*Note#2: The yellow transparent liquid was triturated with pentane after purification.

(vi) Synthesis of K3: Wittig olefination of K2
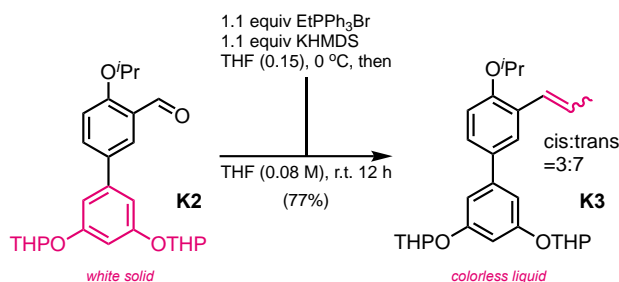
	K2	EtPPh₃Br	KHMDS	THF
MW	189.01	371.25	199.48	
d				
source	synthesized	Aldrich E50604-100G	Aldrich 324671-100G	SPS
state	white solid	white solid	White solid	
equiv	1	1.1	1.1	0.073 M
used	1.92 g	1.78 g	958 mg	60 mL
mmol	4.36	4.80	4.80	

[Experimental Procedure]

To a 15-mL THF solution of ethyltriphenylphosphonium bromide in a 50-mL round-bottom flask at 0 °C was slowly added another 15-mL THF solution of potassium bis(trimethylsilyl)amide. At 0 °C (an ice bath), this orange-color solution was transferred via a cannula to a 100-mL round-bottom flask containing K2 (1.92 g, 4.36 mmol) in 30-mL THF. The white heterogeneous reaction mixture was warmed up to room temperature, stirred for 12 hours. The reaction mixture was diluted with ethyl acetate (100 mL), washed with water (50 x 2 mL) and brine (50 mL). The organic layer was dried with anhydrous Na₂SO₄ and concentrated in vacuo. The crude mixture was purified by silica column chromatography (Eluted with hexanes to hexanes:EtOAc=10:1 to

hexanes:EtOAc=3:1), isolating the desired product as a colorless liquid (MW=452.59, 1.51 g, 3.34 mmol, 77%).

Product R_f = 0.5 (hexanes:EtOAc=4:1) ^{1}H NMR (500 MHz, C_6D_6) δ 7.95 (d, J = 1.8 Hz, 0.3H), 7.86 (d, J = 2.4 Hz, 0.7H), 7.56 (d, J = 8.2 Hz, 0.7H), 7.52 (dt, J = 8.7, 2.0 Hz, 0.3H), 7.39 (dd, J = 3.4, 2.3 Hz, 2H), 7.33 – 7.26 (m, 1H), 7.06 (dd, J = 15.9, 1.9 Hz, 0.3H), 6.88 (d, J = 11.6 Hz, 0.7H), 6.70 (d, J = 8.5 Hz, 0.7H), 6.67 (d, J = 8.5 Hz, 0.3H), 6.23 – 6.09 (m, 0.3H), 5.84 – 5.70 (m, 0.7H), 5.45 (ddt, J = 20.9, 13.9, 3.1 Hz, 2H), 4.27 – 4.13 (m, 1H), 3.97 – 3.78 (m, 2H), 3.51 – 3.38 (m, 2H), 1.97 – 1.82 (m, 2H), 1.82 – 1.68 (m, 5H), 1.62 – 1.50 (m, 2H), 1.46 – 1.23 (m, 4H), 1.23 – 1.15 (m, 2H), 1.13 (dd, J = 6.0, 3.1 Hz, 6H). ^{13}C NMR (125 MHz, CD_2Cl_2) δ 158.44, 158.42, 158.40, 158.38, 155.29, 154.36, 142.85, 142.84, 142.83, 142.81, 133.12, 133.10, 132.52, 128.83, 128.19, 127.64, 126.46, 126.33, 126.31, 126.21, 125.83, 125.61, 125.02, 114.15, 113.93, 108.41, 108.40, 108.34, 108.33, 103.54, 103.53, 103.46, 103.45, 96.75, 96.66, 96.63, 96.55, 70.79, 70.73, 62.21, 62.18, 62.12, 62.09, 53.97, 53.70, 53.43, 53.16, 52.89, 30.43, 30.41, 30.39, 25.27, 25.25, 21.93, 18.99, 18.96, 18.91, 18.89, 18.69, 14.63. HRMS: Chemical formula ([M]): $C_{28}H_{36}O_5$, calcd. $[M]^+$ 452.2563, Found: 452.2575.

Note#1: ^{13}C NMR spectrum obtain in CD_2Cl_2 gave a better signal-to-noise ratio than that obtained in C_6D_6.

(vii) Synthesis of K4: THP deprotection, followed by nucleophilic substitution
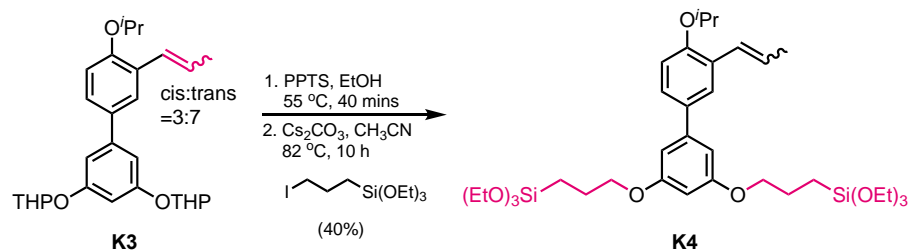
	K3	*PPTS*	*ethanol*	*Cs$_2$CO$_3$*	I⌇⌇Si(OEt)$_3$	*acetonitrile*
MW	452.59	251.30		325.82	332.25	
d						
source	synthesized	Alfa A15708-22		Aldrich 441902-50G	synthesized	Aldrich 45851-1L
state	colorless liquid	white solid		white solid	yellow liquid	
equiv	1	0.4	0.04 M	3.5	3.5	0.04 M
used	1.68 g	373 mg	100 mL	4.23 g	4.32 g	100 mL
mmol	3.71	1.48		13.0	13.0	

[Experimental Procedure]

To a 100-mL ethanol solution of K3 in a 250-mL round-bottom flask was added pyridinium p-toluenesulfonate. After the flask was capped with a rubber septum, the solution was stirred at 55 °C for 40 mins. After cooling down, the reaction mixture was diluted with ethyl acetate (100 mL) and washed with brine (50 mL). The organic layer was dried over anhydrous MgSO$_4$, filtered to a 250-mL Schlenk flask, and concentrated until approximately 5 mL of ethyl acetate remained. The product flask was immediately transferred into a glove box, where 100-mL acetonitrile was added. Afterwards, cesium carbonate and (3-iodopropyl)triethoxysilane[15] was sequentially added. The reaction mixture was stirred at 82 °C for 10 hours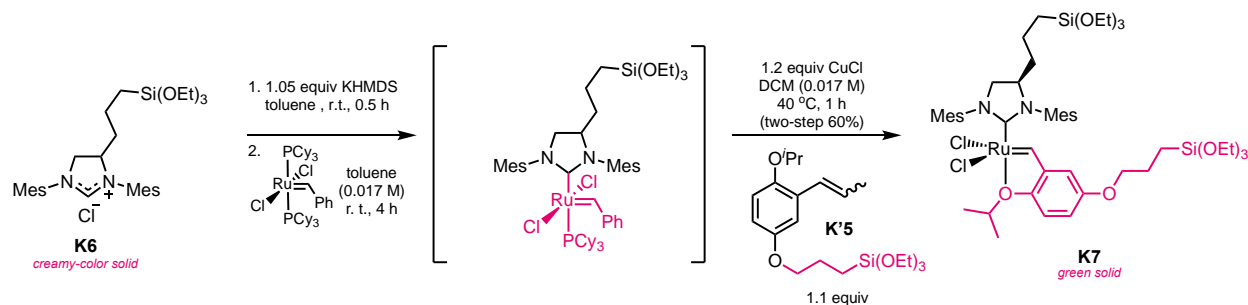. After cooling down, the reaction mixture was poured into ether:pentane=1:1 (150mL). The precipitate was filtered. The filtrate was concentrated

---

[15]For the synthesis of the alkyl iodide, see: Anyushin, A. V., Vanhaecht, S. & Parac-Vogt, T. N. A Bis-organosilyl-Functionalized Wells–Dawson Polyoxometalate as a Platform for Facile Amine Postfunctionalization. *Inorg. Chem.* **59**, 10146–10152 (2020).

and purified by silica column chromatography (eluted with hexanes to hexanes:EtOAc=30:1), isolating the desired product as a colorless liquid (MW=693.04, 1.03 g, 1.48 mmol, 40%).

Product R_f = 0.12 (hexanes:EtOAc=20:1) ^{1}H NMR (500 MHz, CDCl$_3$) δ 7.58 (d, J = 2.3 Hz, 0.3H), 7.45 (d, J = 2.4 Hz, 0.7H), 7.36 (dd, J = 8.5, 2.4 Hz, 0.7H), 7.32 (dd, J = 8.4, 2.3 Hz, 0.3H), 6.91 (d, J = 8.5 Hz, 0.7H), 6.88 (d, J = 8.6 Hz, 0.3H), 6.72 (dd, J = 15.9, 2.0 Hz, 0.3H), 6.68 – 6.60 (m, 2H), 6.55 (dd, J = 11.6, 2.1 Hz, 0.7H), 6.39 (q, J = 2.5 Hz, 1H), 6.26 (dt, J = 16.1, 6.7 Hz, 0.3H), 5.82 (dq, J = 11.6, 7.0 Hz, 0.7H), 4.59 – 4.46 (m, 1H), 3.96 (t, J = 6.7 Hz, 4H), 3.82 (q, J = 7.0 Hz, 12H), 2.00 – 1.82 (m, 7H), 1.36 (dd, J = 9.6, 6.0 Hz, 6H), 1.22 (t, J = 7.0 Hz, 18H), 0.84 – 0.71 (m, 4H). ^{13}C NMR (126 MHz, CD$_2$Cl$_2$) δ 160.57, 160.55, 160.54, 155.26, 155.16, 154.32, 142.97, 142.94, 133.38, 132.77, 128.82, 128.16, 127.61, 126.45, 126.30, 126.29, 126.17, 125.81, 125.61, 125.00, 114.10, 113.87, 105.34, 105.31, 99.56, 99.51, 70.76, 70.69, 70.01, 69.64, 63.64, 58.31, 22.84, 22.31, 21.92, 18.67, 18.14, 18.10, 18.05, 14.61, 14.09, 6.44, 6.23. HRMS: Chemical formula ([M]): C$_{36}$H$_{60}$O$_9$Si$_2$, calcd. [M]$^+$ 692.3776, Found: 692.3766.

*Note#1: The intermediate obtained after THP deprotection seemed to be unstable and quickly turned to a red solution especially when the solution was too concentrated. Probably, the electron-rich arene promoted an electrophilic aromatic substitution as a side reaction. Thus, we proceeded to the next step immediately after the work-up.

(viii) Synthesis of K5: Olefin metathesis of K4
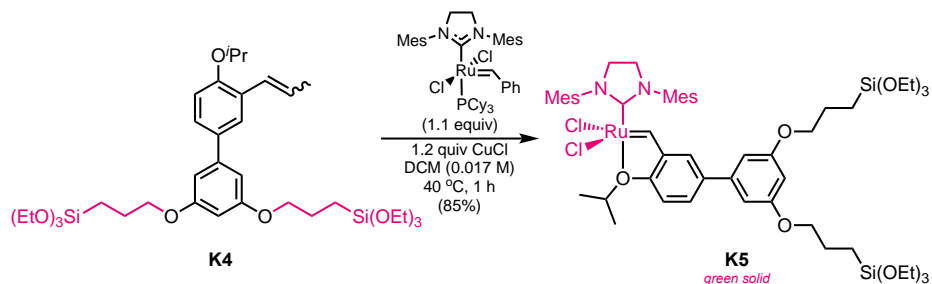
	K4	Grubbs catalyst	CuCl	DCM
MW	693.04	848.98	99.00	
d				
source state	synthesized light yellow liquid	Umicore C848 brown solid	Aldrich 229628-10G off-white solid	dried with CaH₂, distilled, and degassed by FPT
equiv	1	1.1	1.2	0.017 M
used	133 mg	179 mg	23 mg	11 mL
mmol	0.192	0.211	0.230	

[Experimental Procedure]

In the glove box, to a 7-mL DCM solution of the Grubbs 2nd generation catalyst and copper(I) chloride in a 165 °C-oven-dried 20-mL vial was added a 4-mL DCM solution of K4. The vial was sealed with a PTFE green cap, and the reaction mixture was stirred at 40 °C for 1 hour. The red-brownish solution turned green over a course of time. Brought out of the glove box, the reaction mixture was concentrated with a rotary evaporator. The crude product was purified by flush silica column chromatography (pentane:ether=9:1). The desired portion, an obvious green band, was collected, concentrated with a rotary evaporator, and further dried *in vacuo*. The desired product K5 was isolated as a green solid (MW=1143.41, 187 mg, 0.164 mmol, 85%) and stored in the glove box.

^{1}H NMR (500 MHz, CD$_2$Cl$_2$) δ 16.47 (s, 1H), 7.78 (dd, J = 8.6, 2.2 Hz, 1H), 7.15 (d, J = 2.2 Hz, 1H), 7.08 (s, 4H), 6.88 (d, J = 8.6 Hz, 1H), 6.61 (d, J = 2.2 Hz, 2H), 6.43 (s, 1H), 4.91 (hept, J = 6.1 Hz, 1H), 4.18 (s, 4H), 3.97 (t, J = 6.6 Hz, 4H), 3.83 (q, J = 7.0 Hz, 12H), 2.45 (s, 12H), 2.41 (s, 6H),

2.02 – 1.83 (m, 4H), 1.25 (d, J = 6.1 Hz, 6H), 1.22 (t, J = 7.0 Hz, 18H), 0.81 – 0.70 (m, 4H). ^{13}C

NMR (101 MHz, CD$_2$Cl$_2$) δ 295.00 (d) 210.91, 161.04, 152.01, 145.60, 142.06, 139.24, 135.86,

129.69, 128.18, 121.00, 113.46, 105.89, 100.56, 75.85, 70.51, 58.74, 58.70, 23.28, 21.31, 21.26,

18.55, 18.50, 6.90. HRMS: Chemical formula ([M]): C$_{55}$H$_{82}$Cl$_2$N$_2$O$_9$RuSi$_2$, calcd. [M]$^+$ 1142.3979,

Found: 1142.3998.

(B) Synthesis of Het-D

(i) Synthesis of K'5: Nucleophilic substitution of K'4
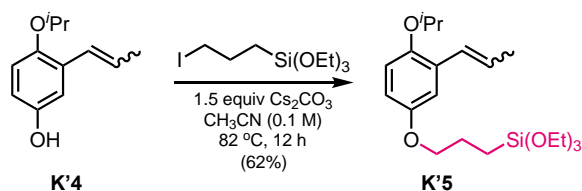
	K'4	*Cs$_2$CO$_3$*	I⌒⌒Si(OEt)$_3$	*acetonitrile*
MW	192.26	325.82	332.25	
d				
source	synthesized	Aldrich 441902-50G	synthesized	Aldrich 45851-1L
state	colorless liquid	white solid	yellow liquid	
equiv	1	1.5	1.5	0.24 M
used	1.374 g	3.49 g	3.56 g	30 mL
mmol	7.144	10.72	10.72	

[Experimental Procedure]

In a glove box, K'4[16] was dissolved in acetonitrile in a 40-mL vial. Afterwards, cesium

carbonate and (3-iodopropyl)triethoxysilane[15] was sequentially added. The reaction mixture was

stirred at 82 °C for 10 hours. After cooling down, the reaction mixture was poured into

---

[16]For the synthesis of **K'4**, see: a) Grudzień, K. & Barbasiewicz, M. Studies on synthesis of quinonylidene Hoveyda-type complexes. *Appl. Organometal. Chem.* **29**, 322–327 (2015). b) Allen, D. & Giardello, M. Supported olefin metathesis catalysts. U.S. Patent No. 9,427,731. (2016).

ether:pentane=1:1 (100mL). The precipitate was filtered out. The filtrate was concentrated and purified by silica column chromatography (eluted with hexanes to hexanes:EtOAc=10:1), isolating the desired product as a light yellow liquid (MW=396.60, 1.757 g, 4.429 mmol, 62%, cis:trans=1:1).

 Product R_f = 0.4 (hexanes:EtOAc=5:1)

^{1}H NMR (500 MHz, CDCl$_3$) (cis:trans=1:1) δ 6.96 (d, J = 3.0 Hz, 0.5H), 6.87 – 6.75 (m, 1.5H), 6.75 – 6.63 (m, 1.5H), 6.52 (dd, J = 11.7, 2.1 Hz, 0.5H), 6.19 (dq, J = 16.0, 6.6 Hz, 0.5H), 5.79 (dq, J = 11.9, 7.1 Hz, 0.5H), 4.41 – 4.26 (m, 1H), 3.90 (td, J = 6.7, 1.8 Hz, 2H), 3.83 (q, J = 7.0 Hz, 6H), 1.95 – 1.82 (m, 5H), 1.30 (dd, J = 11.4, 6.0 Hz, 6H), 1.24 (t, J = 7.0, 1.4 Hz, 9H), 0.84 – 0.72 (m, 2H).

^{13}C NMR (126 MHz, CDCl$_3$) δ 153.46, 152.80, 149.66, 148.75, 129.66, 129.25, 126.58, 126.01, 125.87, 125.70, 117.08, 116.84, 116.53, 113.63, 113.33, 111.99, 72.26, 72.21, 70.43, 70.40, 70.37, 58.46, 58.45, 58.40, 22.90, 22.89, 22.25, 22.19, 18.87, 18.31, 18.30, 14.77, 6.51. HRMS (FAB+): found 397.1765, calculated 397.1773.

(ii) Synthesis of K7: Ligand exchange, followed by olefin metathesis of K'5.

	K6	KHMDS	Grubbs catalyst	toluene	CuCl	K'5	DCM
MW d	515.25	199.48	822.97		99.00	396.60	
source state	Synthesized, creamy-color solid	Aldrich 324671-100G White solid	Umicore M700 brown solid purple solid	dried degassed	Aldrich 229628-10G off-white solid	synthesized, light yellow liquid	dried degassed
equiv	1	1.05	1.25	0.017 M	1.2	1.1	0.017 M
used	81.4 mg	34 mg	163 mg	10 mL	19 mg	69 mg	10 mL
mmol	0.158	0.166	0.198		0.190	0.174	

[Experimental Procedure]

K6[3,16b] was weighed into a 20 mL vial equipped with a stir bar in the glove box and then dissolved in toluene (5 mL). Solid potassium bis(trimethylsilyl)amide was added to the stirring solution. After 30 minutes, the amber solution was filtered through the celite plug and was collected to a 25-mL Schlenk flask containing Grubbs first generation catalyst. The original vial containing the NHC was washed with toluene (5 mL) which was then transferred similarly to the Schlenk flask via the vacuum filtration. After 4 hours, the reaction mixture was loaded directly onto silica gel for column chromatography (without concentration). The silica gel was untreated and the column was run in the fume hood. The crude reaction mixture was eluted through the silica column with 10:90=ether: pentane which easily separated the bright purple band (unreacted G1, eluted first), from the brown band (eluted second). This band was collected and concentrated via rotary evaporation. It was not 100% pure but directly used for the next step without further purification.

In a glove box, to a 5-mL dichloromethane solution of the Ru catalyst and copper(I) chloride in a 165 °C-oven-dried 40-mL vial was added 5-mL DCM solution of K'5. The vial was sealed with a PTFE green cap, and the reaction mixture was stirred at 40 °C for 3 h. Afterwards, the reaction mixture was concentrated in vacuo. The crude product was purified via flush silica column chromatography using pentane:ether (9:1 to 1:1). The obvious green band was collected, and the collected portion was concentrated via rotary evaporator, further dried in vacuo, and stored in the glove box. The desired product K7 was isolated as a green solid (MW=1051.31, 99.3 mg, 0.0945 mmol, 60%) and stored in the glove box.

^{1}H NMR (400 MHz, CD$_2$Cl$_2$) δ 16.37 (s, 1H), 7.23 – 7.03 (m, 5H), 6.75 (d, J = 8.9 Hz, 1H), 6.50 (t, J = 2.4 Hz, 1H), 4.81 (hept, J = 6.2 Hz, 1H), 4.51 (qd, J = 10.3, 3.4 Hz, 1H), 4.22 (t, J = 10.3 Hz, 1H), 3.89 (m, 9H), 3.78 (qd, J = 7.0, 1.8 Hz, 6H), 2.45 (br, 18H), 2.02 – 1.60 (m, 4H), 1.52 – 1.08 (m, 26H), 0.84 – 0.70 (m, 2H), 0.70 – 0.52 (m, 2H). ^{13}C NMR (101 MHz, CD$_2$Cl$_2$) δ 295.11, 211.70, 154.53, 145.94, 145.34, 140.07, 138.79, 138.61, 129.72, 129.43, 129.16, 115.48, 113.13, 107.11, 74.77, 70.82, 64.17, 58.35, 58.27, 57.71, 54.01, 53.74, 53.47, 53.20, 52.93, 36.95, 29.72, 22.87, 20.91, 20.84, 20.80, 19.83, 18.20, 18.14, 10.37, 6.44. HRMS: Chemical formula ([M]): C$_{49}$H$_{78}$N$_2$O$_8$Si$_2$Cl$_2$Ru, calcd. [M]$^+$ 1050.3712, Found: 1050.3712.

(C) General Procedure of Anchoring the Catalysts onto Silica Gel

[Experimental Procedure]

In the glove box, **the Ru catalyst (K5** or **K7)** was placed in a 165 °C-oven-dried **40-mL vial** and dissolved in **toluene (0.01 M)**. **Dry silica gel** was added to the vial—commercial silica gel (Aldrich 60741) was dried in a vacuum oven at 180 °C for 3 days before used. Extra toluene was added until the mixture could be smoothly stirred, and then the reaction mixture was stirred at **room temperature** for **4 days**. Afterwards, the vial was brought out from the glove box and centrifuged. After the supernatant was decanted (Fig. A10a), the remaining wet green silica was dried *in vacuo* until the powder was free-flowing (Fig. A10b). The powder was transferred to a glass thimble, washed with **dichloromethane** for **2 days** via the **Soxhlet** extractor (Fig. 10c), and then dried again *in vacuo* for a day. The actual catalyst loading on the silica was determined with the Ru-to-Si ratio using ICP-MS (see. Section 1.9.3 in page 17).
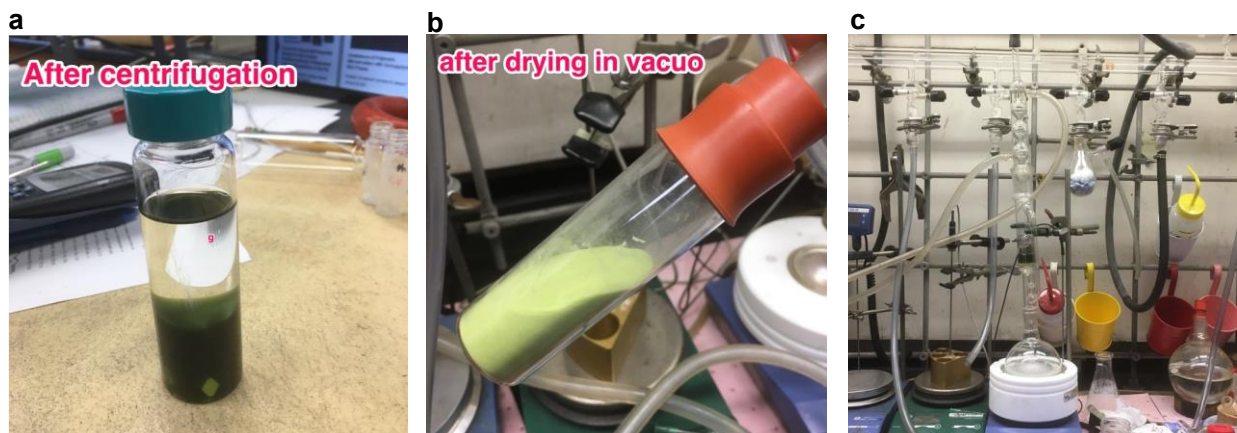
Figure A10. The catalyst anchoring process. a, The reaction mixture after the centrifugation. **b,** The supported catalyst after drying *in vacuo*. **c,** The Soxhlet setup.

*Note#1: The efficiency of the anchoring process was much lower when Ru complexes have one attachment point than when they have two attachment points (e.g., **K7** without the silyl tether of NHC/benzylidene). However, in terms of cyclic polymer generation *per se*, there was nothing special about having two attachment points. As long as the metal density on the surface is low, the complexes with one attachment point at either the NHC or the benzylidene generated cyclic polymers in the similar quality. Potentially, it would be more robust to have two attachment points against catalyst leaching although a noticeable metal leaching was not observed so far according to the ICP data. In this paper, the Ru complexes with two attachment points were used for the purpose that the number of tethers remains one of our control variables in the system.
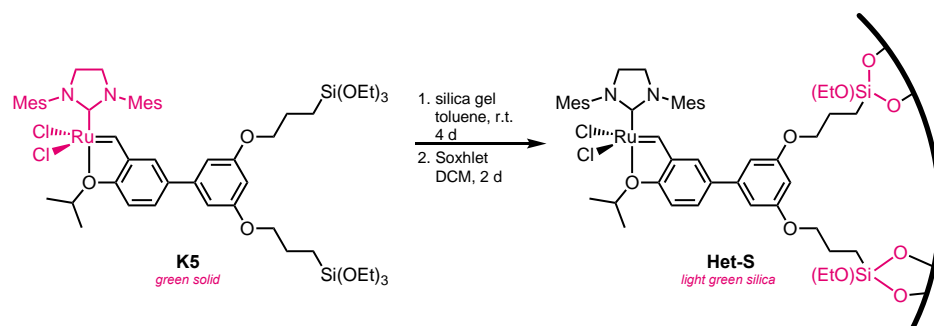
	K5	Silica	toluene	DCM (for Soxhlet)
MW	1143.41			
d				
source	synthesized		dried with Na, distilled and	SPS
state	green solid		degassed by FPT	
equiv	1	target loading 0.01 mmol Ru/1g Silica	0.01 M	
used	34.3 mg	3.0 g	3 mL + ~5 mL	200 mL
mmol	0.03			

*Note#1: For the preparation of **Het-S_high,** 200 mg of **Het-S_low** (instead of pure silica) was used as a starting material. The target loading was 0.1 mmol Ru/1g silica.
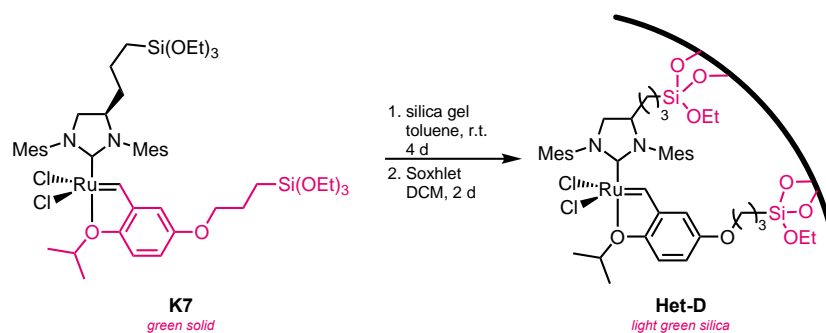
	K7	Silica	toluene	DCM (for Soxhlet)
MW	1051.31			
d				
source	synthesized		dried with Na, distilled and	SPS
state	green solid		degassed by FPT	
equiv	1	target loading 0.01 mmol Ru/1g Silica	0.01 M	
used	31.5 mg	3.0 g	3 mL + ~5 mL	200 mL
mmol	0.03			

1.10 References

(1) González-Reyes, G. A., Bayo-Besteiro, S., Vich Llobet, J. & Añel, J. A. Environmental and economic constraints on the use of lubricant oils for wind and hydropower generation: the case of NATURGY. *Sustainability* **12**, 4242 (2020).

(2) Wakiru, J., Pintelon, L., Muchiri, P. N., Chemweno, P. K. & Mburu, S. Towards an innovative lubricant condition monitoring strategy for maintenance of ageing multi-unit systems. *Reliab. Eng. Syst.* **204**, 107200 (2020).

(3) Zolper, T. *et al.* Lubrication properties of polyalphaolefin and polysiloxane lubricants: molecular structure–tribology relationships. *Tribol. Lett.* **48**, 355-365 (2012).

(4) Greaves, M. Pressure viscosity coefficients and traction properties of synthetic lubricants for wind turbine gear systems. *Lubr. Sci.* **24**, 75-83 (2012).

(5) Ray, S., Rao, P. V. C. & Choudary, N. V. Poly-α-olefin-based synthetic lubricants: a short review on various synthetic routes. *Lubr. Sci.* **24**, 23-44 (2012).

(6) Martini, A., Ramasamy, U. S. & Len, M. Review of viscosity modifier lubricant additives. *Tribol. Lett.* **66**, 58 (2018).

(7) Morgan, S., Ye, Z., Subramanian, R. & Zhu, S. Higher-molecular-weight hyperbranched polyethylenes containing crosslinking structures as lubricant viscosity-index improvers. *Polym. Eng. Sci.* **50**, 911-918 (2010).

(8) Ver Strate, G. & Struglinski, M. J. in *Polymers as rheology modifiers* Vol. 462 *ACS Symposium Series* Ch. 15, 256-272 (American Chemical Society, 1991).

(9) Peterson, G. I. & Choi, T.-L. The influence of polymer architecture in polymer mechanochemistry. *Chem. Commun.* **57**, 6465-6474 (2021).

(10) Lin, Y., Zhang, Y., Wang, Z. & Craig, S. L. Dynamic memory effects in the mechanochemistry of cyclic polymers. *J. Am. Chem. Soc.* **141**, 10943-10947 (2019).

(11) Bielawski, C. W., Benitez, D. & Grubbs, R. H. An "endless" route to cyclic polymers. *Science* **297**, 2041-2044 (2002).

(12) Xia, Y. *et al.* Ring-expansion metathesis polymerization: catalyst-dependent polymerization profiles. *J. Am. Chem. Soc.* **131**, 2670-2677 (2009).

(13) Boydston, A. J., Xia, Y., Kornfield, J. A., Gorodetskaya, I. A. & Grubbs, R. H. Cyclic ruthenium-alkylidene catalysts for ring-expansion metathesis polymerization. *J. Am. Chem. Soc.* **130**, 12775-12782 (2008).

(14) Xia, Y., Boydston, A. J. & Grubbs, R. H. Synthesis and direct imaging of ultrahigh molecular weight cyclic brush polymers. *Angew. Chem. Int. Ed.* **50**, 5882-5885 (2011).

(15) Boydston, A. J., Holcombe, T. W., Unruh, D. A., Fréchet, J. M. J. & Grubbs, R. H. A direct route to cyclic organic nanostructures via ring-expansion metathesis polymerization of a dendronized macromonomer. *J. Am. Chem. Soc.* **131**, 5388-5389 (2009).

(16) Bielawski, C. W., Benitez, D. & Grubbs, R. H. Synthesis of cyclic polybutadiene via ring-opening metathesis polymerization: the importance of removing trace linear contaminants. *J. Am. Chem. Soc.* **125**, 8424-8425 (2003).

(17) Wang, T.-W., Huang, P.-R., Chow, J. L., Kaminsky, W. & Golder, M. R. A cyclic ruthenium benzylidene initiator platform enhances reactivity for ring-expansion metathesis polymerization. *J. Am. Chem. Soc.* **143**, 7314-7319 (2021).

(18) Miao, Z. *et al.* Cyclic polyacetylene. *Nat. Chem.* **13**, 792-799 (2021).

(19) McGraw, M. L., Clarke, R. W. & Chen, E. Y. X. Synchronous control of chain length/sequence/topology for precision synthesis of cyclic block copolymers from monomer mixtures. *J. Am. Chem. Soc.* **143**, 3318-3322 (2021).

(20) Niu, W. *et al.* Polypropylene: now available without chain ends. *Chem* **5**, 237-244 (2019).

(21) Roland, C. D., Li, H., Abboud, K. A., Wagener, K. B. & Veige, A. S. Cyclic polymers from alkynes. *Nat. Chem.* **8**, 791-796 (2016).

(22) Lidster, B. J. *et al.* Macrocyclic poly(*p*-phenylenevinylene)s by ring expansion metathesis polymerisation and their characterisation by single-molecule spectroscopy. *Chem. Sci.* **9**, 2934-2941 (2018).

(23) Zhang, K., Lackey, M. A., Wu, Y. & Tew, G. N. Universal cyclic polymer templates. *J. Am. Chem. Soc.* **133**, 6906-6909 (2011).

(24) Edwards, J. P., Wolf, W. J. & Grubbs, R. H. The synthesis of cyclic polymers by olefin metathesis: achievements and challenges. *J. Polym. Sci. A Polym. Chem.* **57**, 228-242 (2018).

(25) Chang, Y. A. & Waymouth, R. M. Recent progress on the synthesis of cyclic polymers via ring-expansion strategies. *J. Polym. Sci. A Polym. Chem.* **55**, 2892-2902 (2017).

(26) Haque, F. M. & Grayson, S. M. The synthesis, properties and potential applications of cyclic polymers. *Nat. Chem.* **12**, 433-444 (2020).

(27) Golba, B., Benetti, E. M. & De Geest, B. G. Biomaterials applications of cyclic polymers. *Biomaterials* **267**, 120468 (2021).

(28) Miao, Z. *et al.* Semi-conducting cyclic copolymers of acetylene and propyne. *React. Funct. Polym.* **169**, 105088 (2021).

(29) Tuba, R. Synthesis of cyclopolyolefins via ruthenium catalyzed ring-expansion metathesis polymerization. *Pure Appl. Chem.* **86**, 1685-1693 (2014).

(30) Jawiczuk, M., Marczyk, A. & Trzaskowski, B. Decomposition of ruthenium olefin metathesis catalyst. *Catalysts* **10**, 887 (2020).

(31) Allen, D. P., Van Wingerden, M. M. & Grubbs, R. H. Well-defined silica-supported olefin metathesis catalysts. *Org. Lett.* **11**, 1261-1264 (2009).

(32) Dewaele, A., Van Berlo, B., Dijkmans, J., Jacobs, P. A. & Sels, B. F. Immobilized Grubbs catalysts on mesoporous silica materials: insight into support characteristics and their impact on catalytic activity and product selectivity. *Catal. Sci. Technol.* **6**, 2580-2597 (2016).

(33) Hejl, A., Scherman, O. A. & Grubbs, R. H. Ring-opening metathesis polymerization of functionalized low-strain monomers with ruthenium-based catalysts. *Macromolecules* **38**, 7214-7218 (2005).

(34) Neary, W. J. & Kennemur, J. G. Polypentenamer renaissance: challenges and opportunities. *ACS Macro Lett.* **8**, 46-56 (2019).

(35) Tuba, R. & Grubbs, R. H. Ruthenium catalyzed equilibrium ring-opening metathesis polymerization of cyclopentene. *Polym. Chem.* **4**, 3959-3962 (2013).

(36) Neary, W. J. & Kennemur, J. G. Variable temperature ROMP: leveraging low ring strain thermodynamics to achieve well-defined polypentenamers. *Macromolecules* **50**, 4935-4941 (2017).

(37) Mulhearn, W. D. & Register, R. A. Synthesis of narrow-distribution, high-molecular-weight ROMP polycyclopentene via suppression of acyclic metathesis side reactions. *ACS Macro Lett.* **6**, 112-116 (2017).

(38) Lee, L.-B. W. & Register, R. A. Acyclic metathesis during ring-opening metathesis polymerization of cyclopentene. *Polymer* **45**, 6479-6485 (2004).

(39) Ji, S., Hoye, T. R. & Macosko, C. W. Controlled synthesis of high molecular weight telechelic polybutadienes by ring-opening metathesis polymerization. *Macromolecules* **37**, 5485-5489 (2004).

(40) Obligacion, J. V. & Chirik, P. J. Bis(imino)pyridine cobalt-catalyzed alkene isomerization–hydroboration: a strategy for remote hydrofunctionalization with terminal selectivity. *J. Am. Chem. Soc.* **135**, 19107-19110 (2013).

(41) Ulman, M. & Grubbs, R. H. Ruthenium carbene-based olefin metathesis initiators: catalyst decomposition and longevity. *J. Org. Chem.* **64**, 7202-7207 (1999).

(42) Torre Iii, M., Mulhearn, W. D. & Register, R. A. Ring-opening metathesis copolymerization of cyclopentene above and below its equilibrium monomer concentration. *Macromol. Chem. Phys.* **219**, 1800030 (2018).

(43) Szczepaniak, G., Kosiński, K. & Grela, K. Towards "cleaner" olefin metathesis: tailoring the NHC ligand of second generation ruthenium catalysts to afford auxiliary traits. *Green Chem.* **16**, 4474-4492 (2014).

(44) Coates, G. W. & Getzler, Y. D. Y. L. Chemical recycling to monomer for an ideal, circular polymer economy. *Nat. Rev. Mater.* **5**, 501-516 (2020).

(45) Neary, W. J., Isais, T. A. & Kennemur, J. G. Depolymerization of bottlebrush polypentenamers and their macromolecular metamorphosis. *J. Am. Chem. Soc.* **141**, 14220-14229 (2019).

(46) Yuan, J., Giardino, G. J. & Niu, J. Metathesis cascade-triggered depolymerization of enyne self-immolative polymers. *Angew. Chem. Int. Ed.* **60**, 24800-24805 (2021).

Appendix 1. Spectra Relevant to Chapter 1

KY76.1.fid

10.39
10.39

7.91
7.91
7.90
7.59
7.57
7.56
6.90
6.89
6.87

4.69
4.67
4.66
4.64
4.63
4.61
4.60

1.40
1.39

O^{i}Pr

O

Br **K1**

0.94

0.92
0.96

1.00

0.99

6.00

^{1}H NMR spectrum of **K1** (400 MHz, CDCl$_3$)

KY76.2.fid

188.71

159.45

139.13
130.93
126.98

116.00
113.12

77.36 CDCl3
77.04 CDCl3
76.72 CDCl3
71.64

21.90

O^{i}Pr

O

Br **K1**

^{13}C NMR spectrum of **K1** (101 MHz, CDCl$_3$)

KY3-46rere.1.fid

6.46
6.45
6.23
6.22

—4.91 HDO

3.35 MeOD
3.34 MeOD
3.34 MeOD
3.34 MeOD
3.33 MeOD

Br

HO

OH

K'1

2.00
0.97

chemical shift (ppm)

^{1}H NMR spectrum of **K'1** (400 MHz, CD$_3$OD)

KY3-46rere.2.fid

—160.52

—123.44
—111.04
—102.62

Br

HO

OH

K'1

chemical shift (ppm)

^{13}C NMR spectrum of **K'1** (101 MHz, CD$_3$OD)

PROTON01 — KY-THPprotection1 —
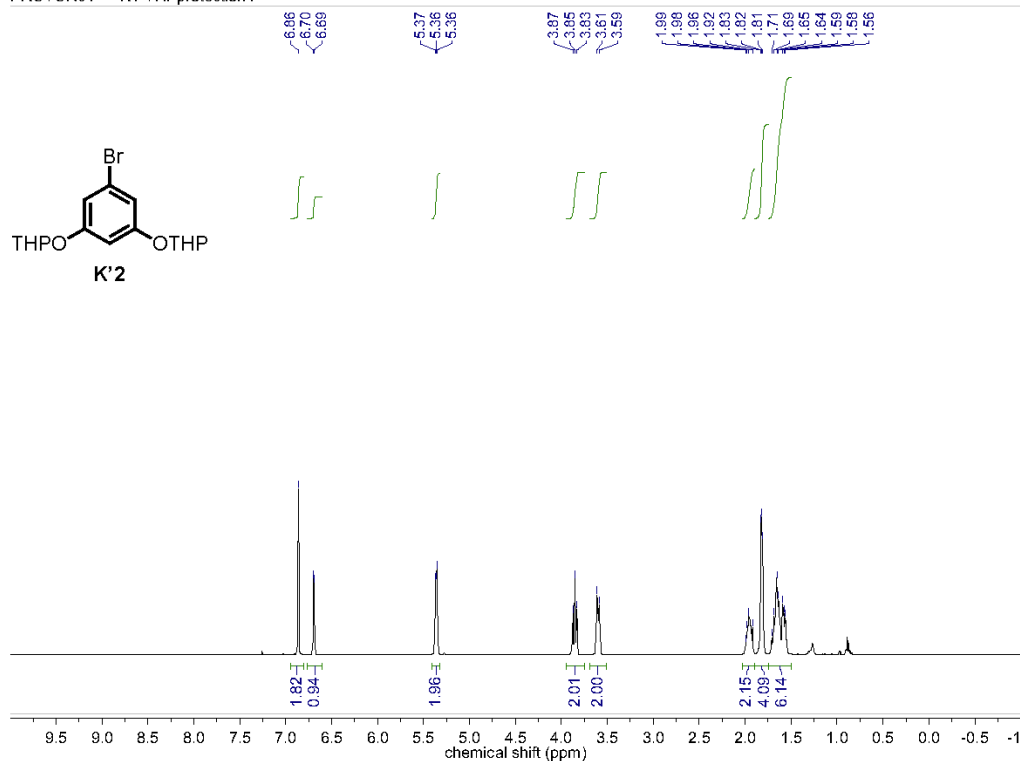
^{1}H NMR spectrum of **K'2** (500 MHz, CDCl$_3$)

KY-THPprotection1.1.fid —

^{13}C NMR spectrum of **K'2** (126 MHz, CDCl$_3$)

K'3

^{1}H NMR spectrum of **K'3** (400 MHz, CDCl$_3$)

K'3
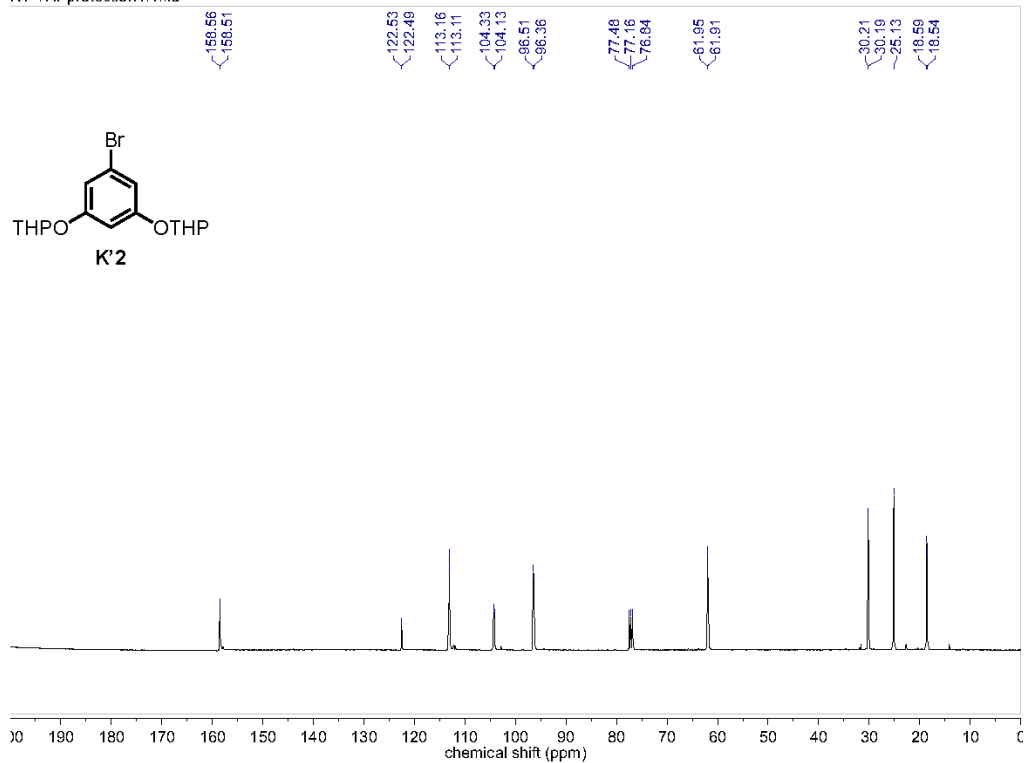
^{13}C NMR spectrum of **K'3** (101 MHz, CDCl$_3$)
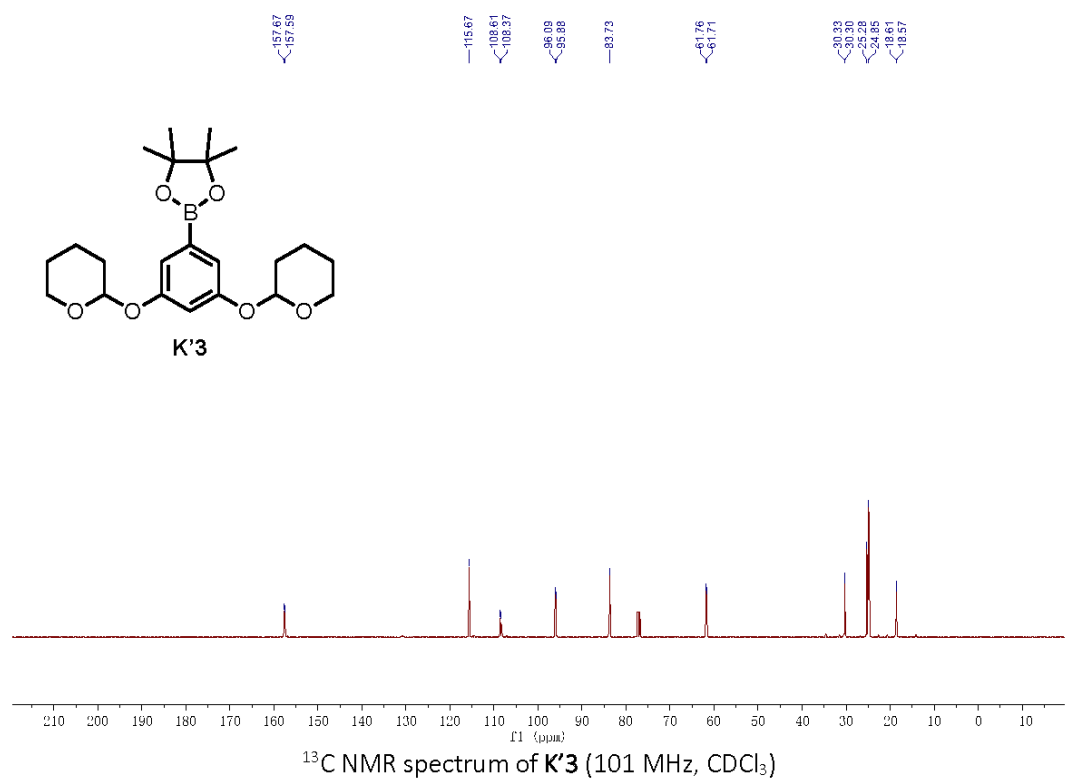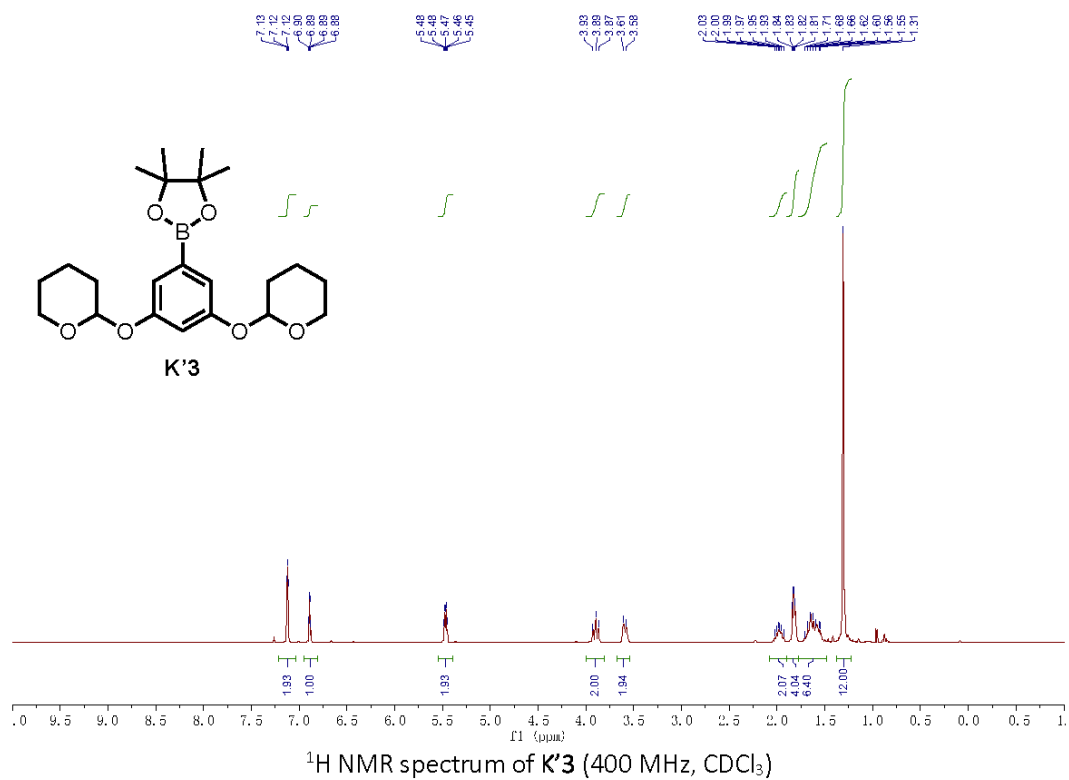
PROTON01 — KY-THP-Suzuki —
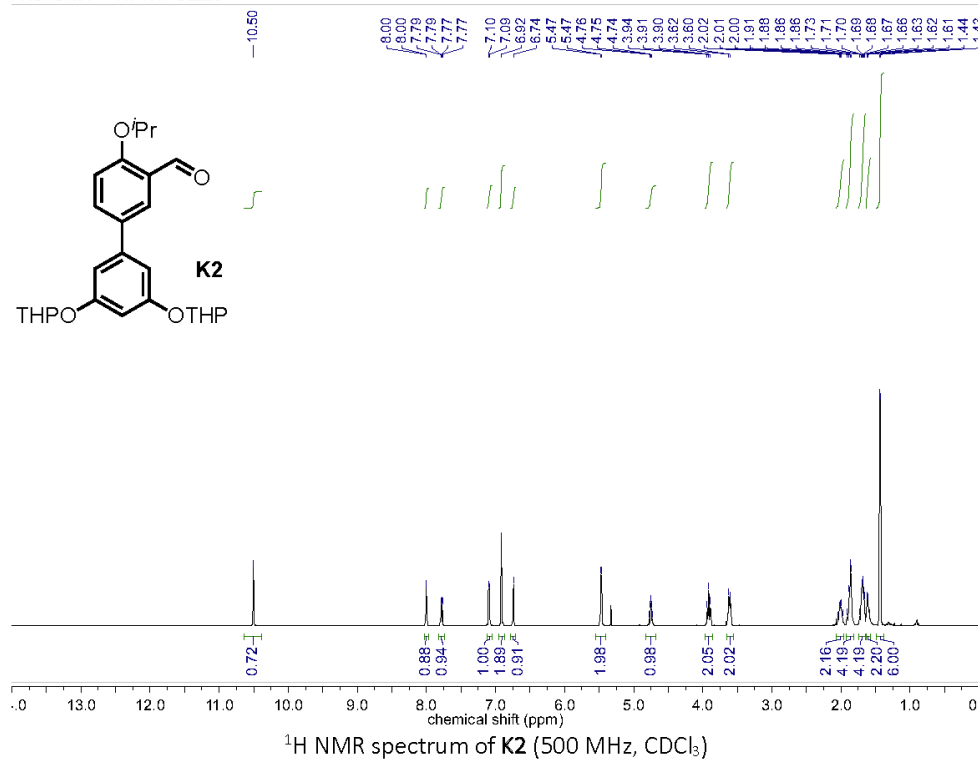
^{1}H NMR spectrum of **K2** (500 MHz, CDCl$_3$)

CARBON01 — KY-THP-Suzuki —

^{13}C NMR spectrum of **K2** (126 MHz, CDCl$_3$)

PROTON01 — KY4-methylstyrene-check —

^{1}H NMR spectrum of **K3** (500 MHz, C$_6$D$_6$)

KY-THP-Wittig.2.fid —

^{13}C NMR spectrum of **K3** (126 MHz, CD$_2$Cl$_2$)

PROTON01 — KY4-15recolumn —

^{1}H NMR spectrum of **K4** (500 MHz, CDCl$_3$)

CARBON02 — KY-sKY3-methylstyrene —

^{13}C NMR spectrum of **K4** (126 MHz, CD$_2$Cl$_2$)

PROTON01 — KY4-24_KY3precursor —

^{1}H NMR spectrum of **K5** (500 MHz, CD$_2$Cl$_2$)

KY4-24_sKY3precursor.1.fid —

^{13}C NMR spectrum of **K5** (126 MHz, CD$_2$Cl$_2$)

PROTON01 — KY-JC3-methylstyrene —

O^iPr

Si(OEt)₃

K'5

^{1}H NMR spectrum of **K'5** (500 MHz, CDCl₃)

CARBON01 — KY-JC3-methylstyrene —

O^iPr

Si(OEt)₃

K'5

^{13}C NMR spectrum of **K'5** (126 MHz, CDCl₃)

PROTON01 — KY-JC3-methylstyrene —

6.96, 6.95, 6.84, 6.84, 6.83, 6.81, 6.80, 6.78, 6.73, 6.72, 6.71, 6.70, 6.69, 6.68, 6.67, 6.53, 6.51

4.34, 3.92, 3.90, 3.89, 3.85, 3.84, 3.83, 3.81

1.90, 1.89, 1.85, 1.85, 1.31, 1.30, 1.28, 1.25, 1.23, 1.22, 0.79, 0.77, 0.76

O^{i}Pr

Si(OEt)$_3$

K'5

0.49, 1.61, 1.44, 0.55, 0.62, 0.60, 1.00, 2.05, 6.05, 5.12, 5.81, 9.12, 2.28

9.5 9.0 8.5 8.0 7.5 7.0 6.5 6.0 5.5 5.0 4.5 4.0 3.5 3.0 2.5 2.0 1.5 1.0 0.5 0.0 -0.5 -1
chemical shift (ppm)

^{1}H NMR spectrum of **K'5** (500 MHz, CDCl$_3$)

CARBON01 — KY-JC3-methylstyrene —

153.46, 152.80, 149.66, 148.75

129.66, 129.25, 126.58, 126.01, 125.87, 125.70, 117.08, 116.84, 116.53, 113.63, 113.33, 111.99

72.26, 72.21, 70.43, 70.37

58.40

22.90, 22.89, 22.25, 18.87, 18.31, 18.30, 14.77, 6.51

O^{i}Pr

Si(OEt)$_3$

K'5

00 190 180 170 160 150 140 130 120 110 100 90 80 70 60 50 40 30 20 10 0 -10
chemical shift (ppm)

^{13}C NMR spectrum of **K'5** (126 MHz, CDCl$_3$)

K7

^{1}H NMR spectrum of **K7** (400 MHz, CD$_2$Cl$_2$)

^{13}C NMR spectrum of **K7** (101 MHz, CD$_2$Cl$_2$)

^{1}H NMR spectrum of **the cobalt catalyst** (500 MHz, C$_6$H$_6$)

KY-PCP-pure.2.fid —

^{1}H NMR spectrum of **cyclic polyCP** (500 MHz, CDCl$_3$)

CARBON01 — KY3-16 —

7 peaks

● : (t,t) (c,t) (t,c) (c,c)
● : (t,t) (c,t)=(t,c) (c,c)
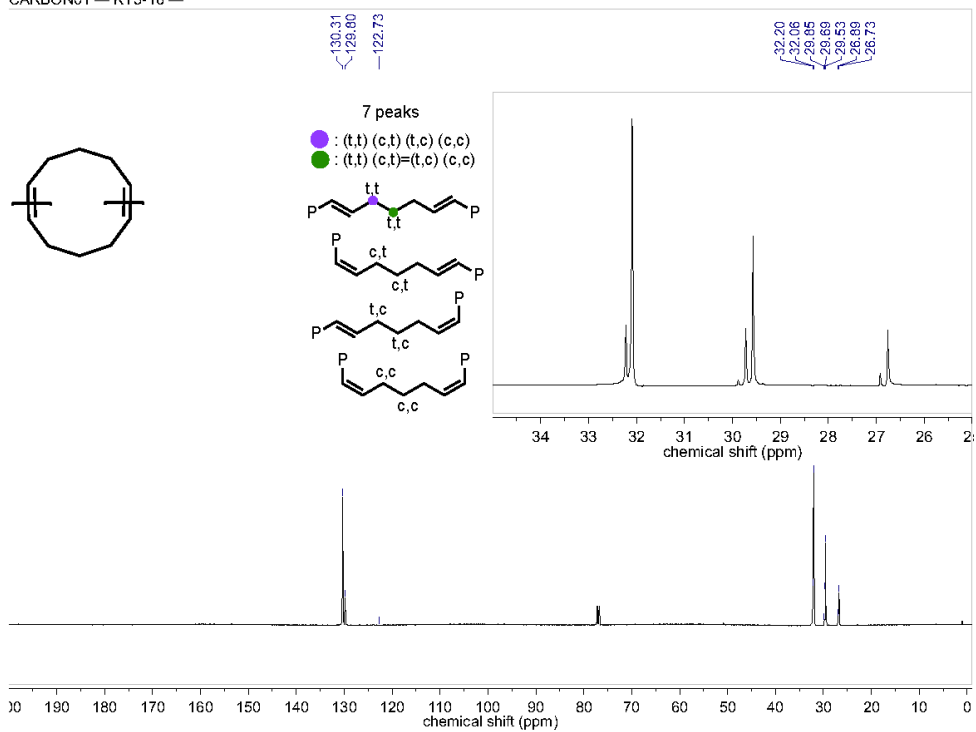
^{13}C NMR spectrum of **cyclic polyCP** (126 MHz, CDCl$_3$)

KY-cPCOD-Hoye.1.fid —

^{1}H NMR spectrum of **cyclic polycyclooctadiene** (500 MHz, CDCl$_3$)

KY-cPCOD-Hoye.2.fid —

^{13}C NMR spectrum of **cyclic polycyclooctadiene** (126 MHz, CDCl$_3$)
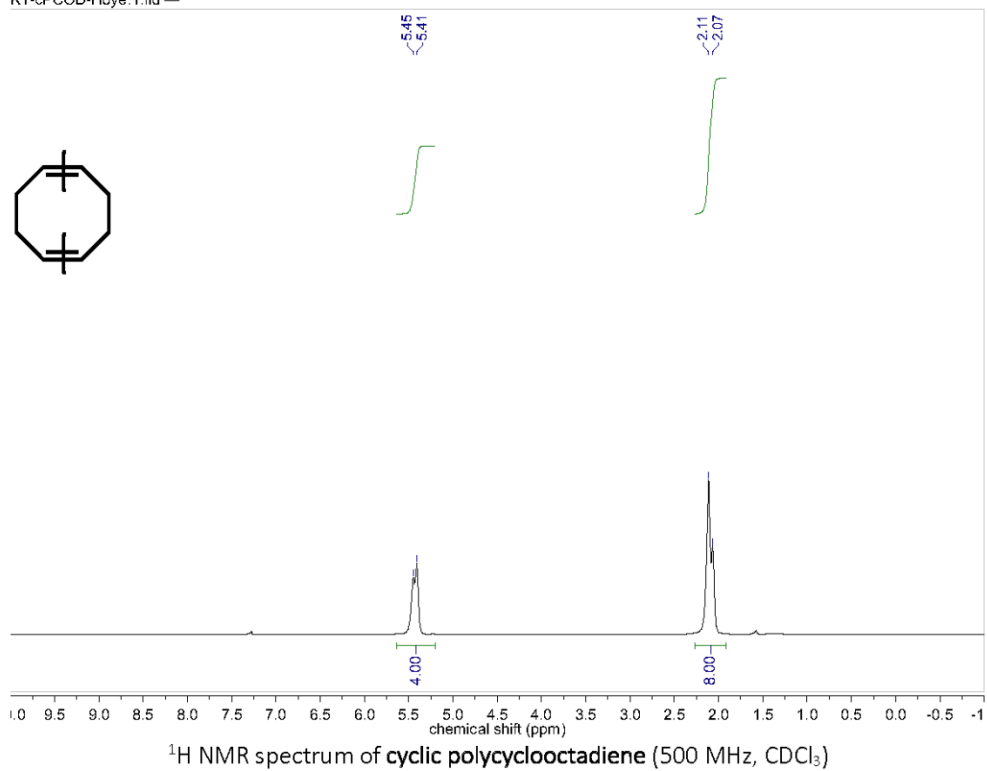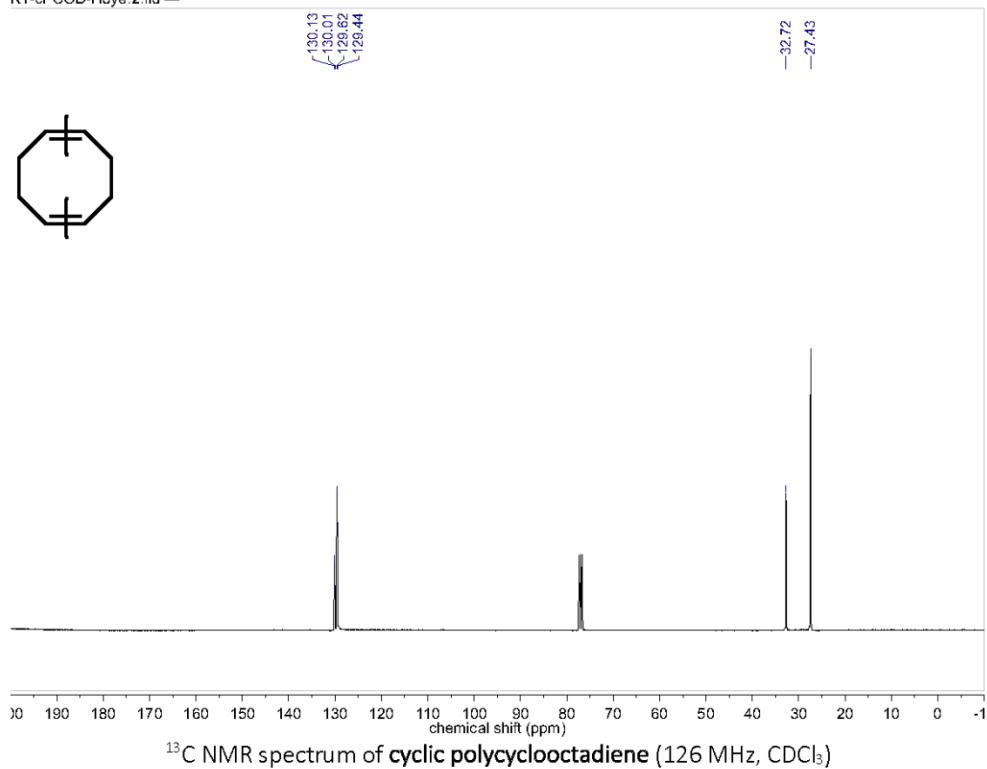
C h a p t e r   2

Bulky Cyclometalated Ruthenium Nitrates for Challenging Z-Selective Metathesis: Efficient One-Step Access to α-Oxygenated Z-Olefins from Acrylates and Allyl Alcohols

2.1 Introduction

The increasing demand for the timely assembly of biologically active molecules necessitates the development of new carbon-carbon bond-forming methods that construct challenging organic skeletons in a streamlined fashion.[1] Among these, Z-selective olefin metathesis showcases a precise and straightforward approach to important Z-configured C-C double bonds that are often thermodynamically less stable and non-trivial-to-access, and its practicality is further highlighted by the use of only terminal olefins as readily available and functional group-compatible handles.[2] A wide variety of terminal olefins have been investigated and found to be suitable for Z-selective metathesis catalyzed by Mo,[3] W,[4] or Ru-based catalysts;[5-6] however, a long-standing limitation of these transformations is the lack of *any* catalyst that could efficiently process diverse types of terminal acrylates and allyl alcohols. As a result, direct access to high value-added, α-oxygenated Z-olefins from these feedstock chemicals remains a much-desired yet unmet challenge, despite that enriched biological properties are often associated with molecules containing these structural motifs (Scheme 2.1A).[7] To date, the only reported Z-selective metathesis of this class is limited to bulky *t*-butyl acrylates, which is promoted by molybdenum monoaryloxide pyrrolide (MAP) complexes,[3d] and the use of terminal allyl alcohols remains elusive (Scheme 2.1B).[8]
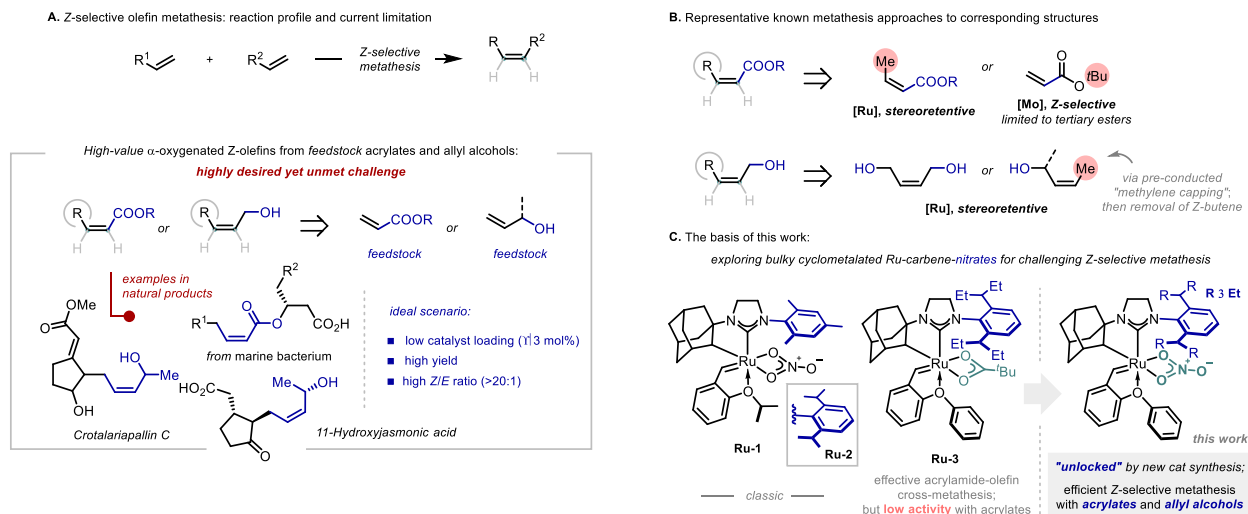
Scheme 2.1. Accessing high-value α-oxygenated *Z*-olefins *via* metathesis: current approaches and limitations.

Since the discovery of the cyclometalated Ru-based *Z*-selective metathesis catalysts in 2011,[5a] our group has observed that the sidearms of the N-heterocyclic carbene (NHC) ligand play an important role in influencing the catalyst activity and the level of stereo-control.[5] For example, catalysts bearing a 2,6-diisopropylphenyl (Dipp) group (e.g., **Ru-2**[5c]) in general displayed superior activity and *Z*-stereoselectivity when compared to their analogs with a smaller mesityl group (e.g., **Ru-1**[5b]). However, catalysts with even bulkier skeletons are challenging to access using conventional synthetic routes, as the C–H cyclometallation and its following steps are often rather sluggish and result in low-yielding mixtures due to the gradual decomposition of the cyclometalated Ru-carbene complexes.[13] Very recently, we successfully overcame the challenge in the C–H metalation step through a carefully optimized, "acid-base quenching"-driven approach, and introduced an even bulkier 2,6-diisopentylphenyl (Dipep) sidearm.[5e] The resulting ruthenium pivalate complex (**Ru-3**) readily promoted the acylamide-olefin cross-metathesis in a highly *Z*-selective fashion. However, **Ru-3** was found to be ineffective towards acrylate substrates (with a turnover number smaller than

5) and further derivatization of **Ru-3** (e.g., towards complexes bearing other anionic ligands)[14] remains elusive.[15]

2.2 "Acid-base quenching" approach to access new catalyst structures
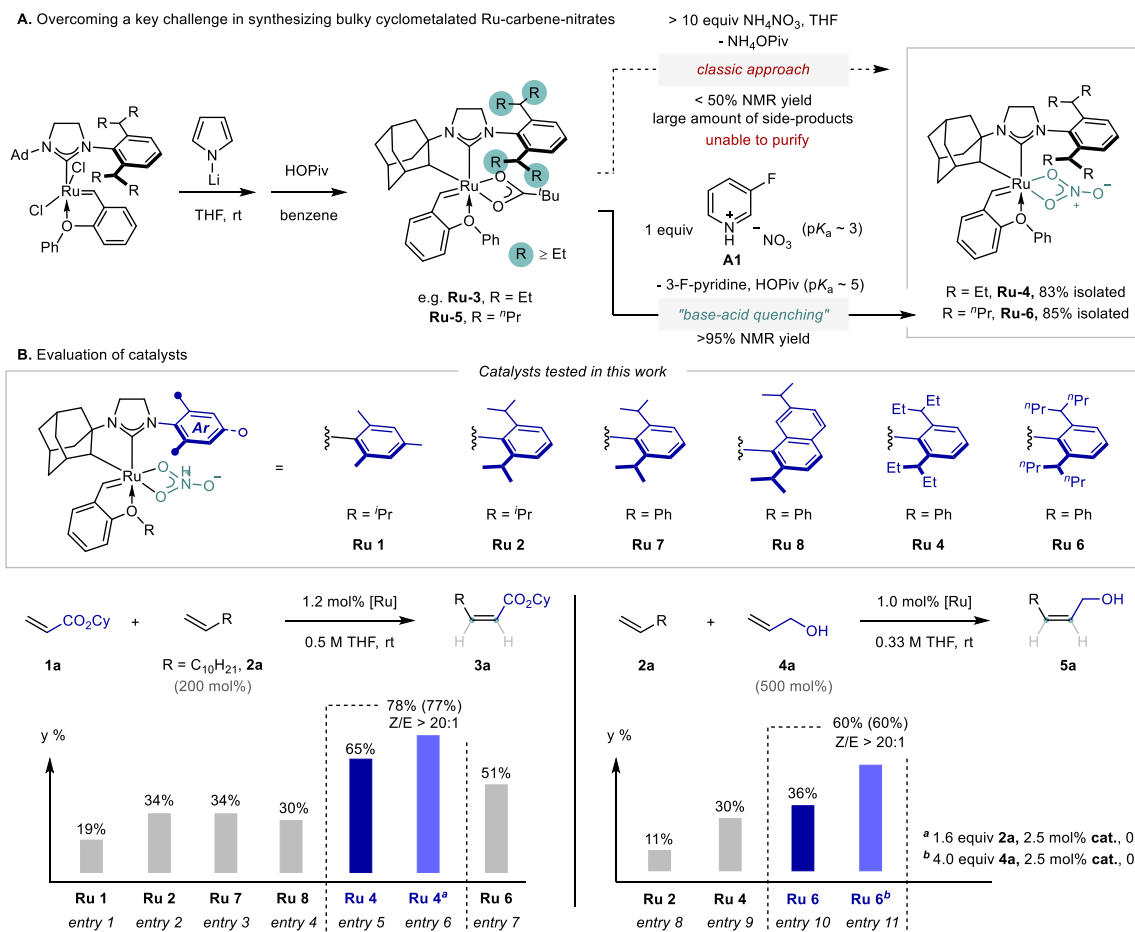
Scheme 2.2. Preparation and evaluation of cyclometalated Ru-nitrate catalysts.

A promising direction would be to prepare and investigate the less electron-rich nitrate analogs of **Ru-3** that are equipped with equally or even more sterically demanding sidearms.[5b] However, the seemingly easy-to-run anion exchange reaction quickly proved to be a formidable challenge in such a sterically encumbered environment. For example, under conventional conditions using a large excess of NH_4NO_3 in THF,[5b] the reaction not only failed to reach full conversion, but

also led to two unidentified Ru-carbene side-products. Significant catalyst decomposition also occurred concomitantly (see *Supporting Information* for details), making purification of the desired nitrate catalyst extremely difficult (Scheme 2.2A). To overcome this, we envisioned that a suitable nitrate source with a more acidic cation could potentially provide an additional driving force for this challenging anion exchange *via* another formal "acid-base quenching" process. Specifically, if the pivalate anion of the delicate cyclometalated ruthenium-carbene complexes could be exchanged and readily removed from the system *through* irreversible protonation, a much-simplified reaction system, e.g., with low equivalent of the nitrate reagent and short reaction period, might diminish or even eliminate the undesired side-pathways. Guided by this designing principle, we identified 3-fluoropyridinium nitrate (**A1**) as a suitable reagent. which is easily prepared and has a pK_a value approximately two units lower than that of pivalic acid. With only one equivalent added, **A1** fully "protonates" ruthenium-pivalates containing a Dipep or even a diisoheptylphenyl (Dihep) sidearm within 15 minutes at room temperature, with the release of *neutral* (instead of *ionic*) by-products, pivalic acid and 3-fluoropyridine. Upon workup, the corresponding bulky nitrate catalysts (**Ru-4** and **Ru-6**) were prepared in high yields and, more importantly, in high purity for the first time.

2.3 Substrate scope study for acrylates
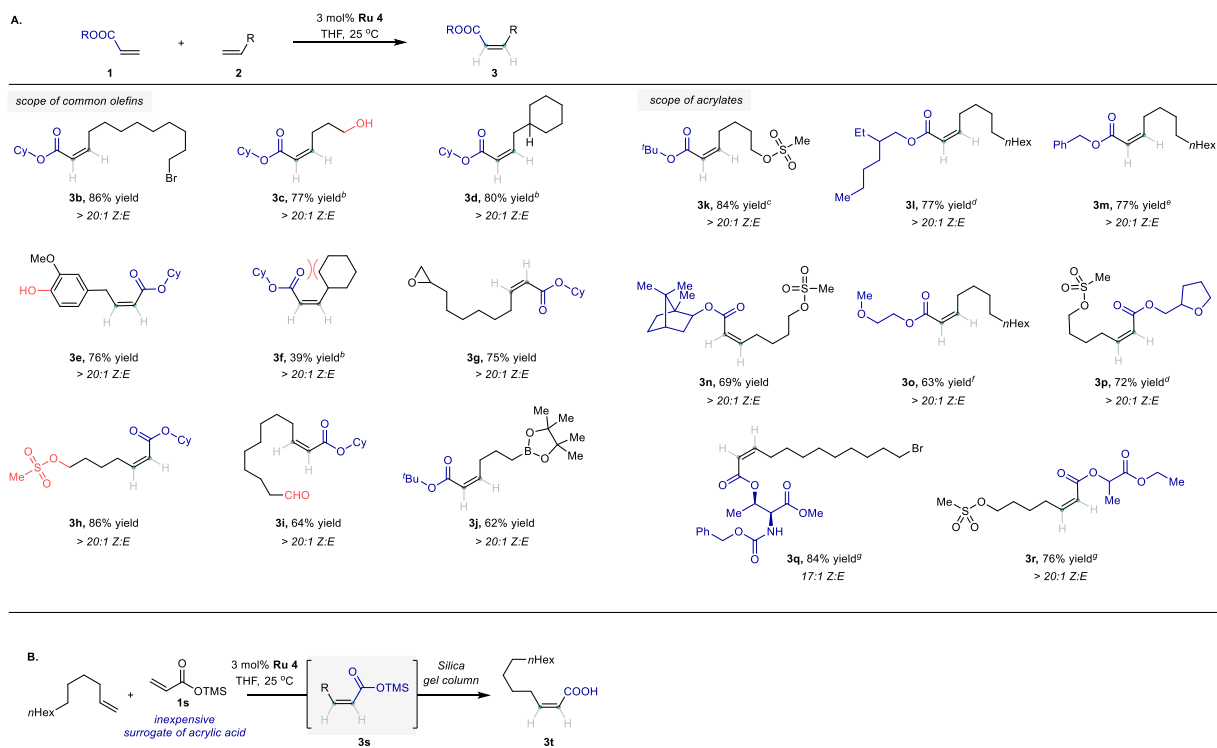
Scheme 2.3. Substrate scope with various acrylates and common olefins. [a] General reaction conditions: **1** (0.15 mmol), **2** (0.24 mmol), and **Ru-4** (0.0045 mmol) in THF, N$_2$, room temperature. All yields are isolated yields of the Z-products. The stereoselectivity was determined by ^{1}H NMR analysis of the crude reaction mixture. [b] **2** was used in 2 equiv. [c] **Ru-4** was used in 2 mol%. [d] **Ru-4** was used in 4 mol% and **2** was used in 2 equiv. [e] **Ru-4** was used in 5 mol% and **2** was used in 2 equiv. [f] **Ru-4** was used in 3.3 mol% and **2** was used in 2 equiv. [g] **Ru-4** was used in 5 mol%. For details, see SI.

The reaction scope was then investigated, first with various acrylates (Scheme 2.3A). Excellent Z-selectivity (>20:1) was obtained in nearly all cases under the standard or slightly modified conditions. The amino acid-derived substrate **3q** was the only exception where a slightly decreased, 17:1 Z/E ratio was observed. The desired products were generally isolated in pure Z-form with ease. Primary, secondary and tertiary acrylates were all suitable substrates, including acrylates bearing multiple heteroatoms (e.g., O and N) that may potentially coordinate with the catalyst (**3p**,

3q, and **3r**). Despite severe steric repulsion, (*Z*)-α,β-unsaturated esters bearing γ-substituents could be formed with high stereoselectivity, highlighting the robustness of the presented method (**3f**).[16] Both nucleophilic and electrophilic functional groups are well-tolerated, including bromides (**3b**), boronic esters (**3j**), epoxides (**3g**), sulfonates (**3h**), and aldehydes (**3i**). Efficient *Z*-selective metathesis was also observed in the presence of unprotected alcohols (**3c**) and phenols (**3e**), which are less likely to be tolerated in many conventional transformations that construct (*Z*)-α,β-unsaturated esters, such as Wittig-type reactions or esterification with *Z*-alkenyl acyl chlorides. Moreover, inexpensive trimethylsilyl acrylate (**1s**) could serve as a convenient surrogate for acrylic acid.[17] Using the standard metathesis condition followed by flash column chromatography over silica gel, *Z*-alkenyl acids (e.g., **3t**) could be readily isolated in good yield and high stereoselectivity (Scheme 2.3B).

2.4 Substrate scope study for allyl alcohols
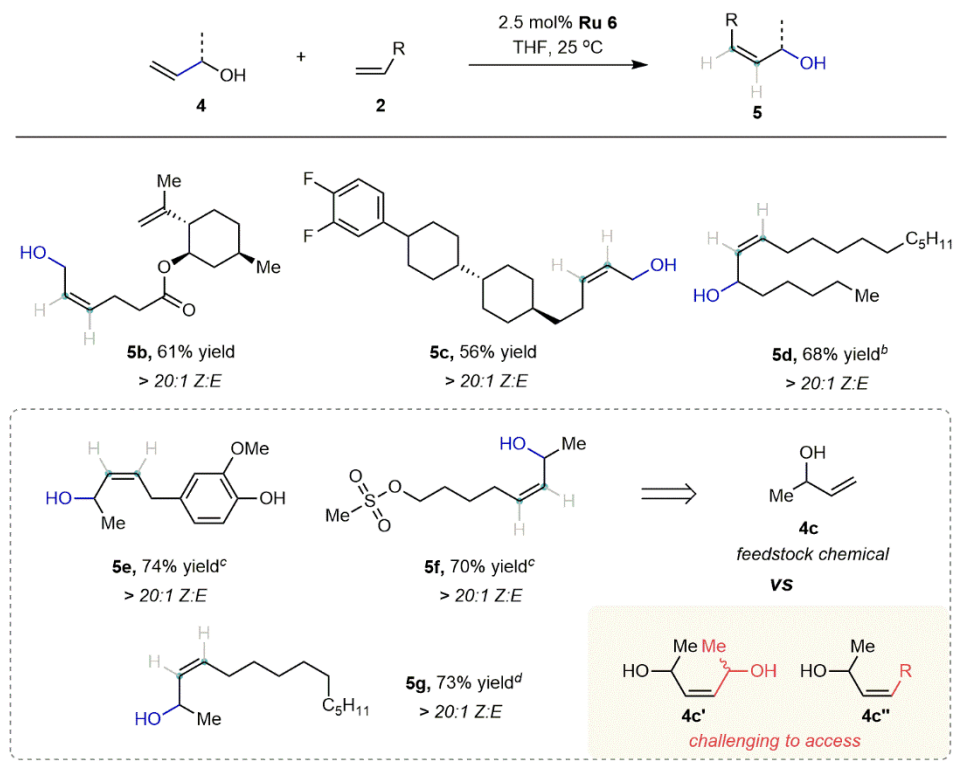
Scheme 2.4. Substrate scope with various allyl alcohols and common olefins. [a] General reaction conditions: **4** (0.6 mmol), **2** (0.15 mmol), and **Ru-6** (0.00375 mmol) in THF, N_2, room temperature. All yields are isolated yields of the *Z*-products. The stereoselectivity was determined by ^{1}H NMR analysis of the crude reaction mixture. [b] **4** was used in 1 equiv. and **2** was used in 8 equiv. [c] **4** was used in 8 equiv. and **Ru-6** was used in 4 mol%. [d] **4** was used in 8 equiv. and **Ru-6** was used in 5 mol%. For details, see SI.

Z-selective metathesis with various allyl alcohols was next investigated (Scheme 2.4). When feedstock allyl alcohols were used, olefin **2** was typically selected as the limiting reagent (e.g., **5b** and **5e**). Alternatively, **2** could also be added in excess, especially when heavy and valuable α-hydroxylated olefins were employed as the substrates (e.g., **5d**). Note that in a stereoretentive metathesis reaction, Z-configured olefins are often needed as the starting materials. While (*Z*)-but-

2-ene-1,4-diol is still commercially available as a surrogate for the simplest allyl alcohol,[9a] the corresponding "Z-dimer" of substituted allyl alcohols (e.g., **4c'**, "Z-dimer" of **4c**) are usually quite challenging to access. Therefore, the facile and direct incorporation of substituted allyl alcohols, such as in the cases of in **5e**, **5f**, and **5g,** showcases the unique benefit of this Z-selective approach. Moreover, enantio-enriched **4c** are also easily accessible, which are meaningful for the straightforward construction of chiral natural products bearing such Z-allyl alcohol motifs (c.f. Scheme 1A).[7a] Various functional groups are tolerated, and a 1,1-disubstituted olefin remains untouched (**5b**).[18] Again, > 20:1 Z-selectivity was observed in all the examined cases. Since substituted allyl alcohols are commonly used as a versatile synthetic handle, such a method may allow the rapid assemble of other challenging chemical structures through further derivatization.

2.5 Conclusions

In summary, we have described a type of novel approaches to α-oxygenated Z-olefins by efficient Z-selective metathesis using feedstock chemicals. These transformations are enabled by sterically congested cyclometalated ruthenium-nitrate complexes, whose synthesis are made possible by a new anion exchange method *via* "acid-base quenching." High stereoselectivity and good functional group compatibility were observed with various types of acrylates and allyl alcohols. Given the ubiquity of α-oxygenated Z-olefins in natural products and synthetic intermediates, such a method may find further application in streamlining the access to diverse organic molecules in a stereoselective fashion.

2.6 Experimental section

2.6.1 General consideration

All reactions were carried out in dry glassware under an argon atmosphere using standard Schlenk techniques or in a Vacuum Atmospheres Glovebox under a nitrogen atmosphere, unless otherwise specified. All solvents were purified by passing through solvent purification columns and further degassed by bubbling nitrogen. NMR solvents were dried over pre-baked 3 Å or 4 Å molecule sieves and subsequently degassed with bubbling nitrogen. $CDCl_3$ was used as received. Liquid olefin substrates purchased from commercial sources were filtered through a plug of neutral alumina prior to use. The retention factor (R_f) of thin-layer chromatography (TLC) was recorded by using E. Merck silica gel 60 F254 precoated plates (0.25 mm) and visualized by UV fluorescence quenching or potassium permanganate staining. ^{1}H and ^{13}C NMR spectra were recorded on either a Bruker Ascend 400 spectrometer (400 MHz and 101 MHz, respectively) or a Varian Inova 500 MHz (500 MHz and 126 MHz, respectively). For $CDCl_3$ solutions, the chemical shifts are reported as parts per million (ppm) referenced to residual protium or carbon of the solvents; $CHCl_3$ δ H (7.26 ppm) and $CDCl_3$ δ C (77.16 ppm). Coupling constants are reported in Hertz (Hz). Data for ^{1}H NMR spectra are reported as follows: chemical shift (ppm, referenced to protium: s = singlet, d = doublet, t = triplet, q = quartet, p = pentet (quintet), h = heptet, dd = doublet of doublets, td = triplet of doublets, ddd = doublet of doublet of doublets, m = multiplet, the coupling constant (Hz), and integration). High-resolution mass spectra (HRMS) were provided by the California Institute of Technology Mass Spectrometry Facility using a JEOL JMS-600H High-Resolution Mass Spectrometer. Infrared (IR) spectra were recorded on a Perkin Elmer Paragon 1000 spectrometer using neat samples on ATR diamond, and are reported in the frequency of absorption (cm^{-1}).

2.6.2 Catalyst synthesis

In Scheme B1, **Ru-1**[1]**, Ru-2**[2]**, Ru-7**[3]**,** and **Ru-8**[3] were synthesized according to the literature procedure (1, B. K. Keitz, K. Endo, P. R. Patel, M. B. Herbert, R. H. Grubbs, *J. Am. Chem. Soc.* **2012**, 134, 693–699. 2, L. E. Rosebrugh, M. B. Herbert, V. M. Marx, B. K. Keitz, R. H. Grubbs, *J. Am. Chem. Soc.* **2013**, 135, 1276–1279. 3, Y. Xu, J. J. Wong, A. E. Samkian, J. H. Ko, S. Chen, K. N. Houk, R. H. Grubbs, *J. Am. Chem. Soc.* **2020**, 142, 20987–20993.), and **Ru-4** and **Ru-6** were prepared according to the following procedure *(vide infra)*.

Scheme B1. Ru-carbene nitrate catalysts tested in this study.
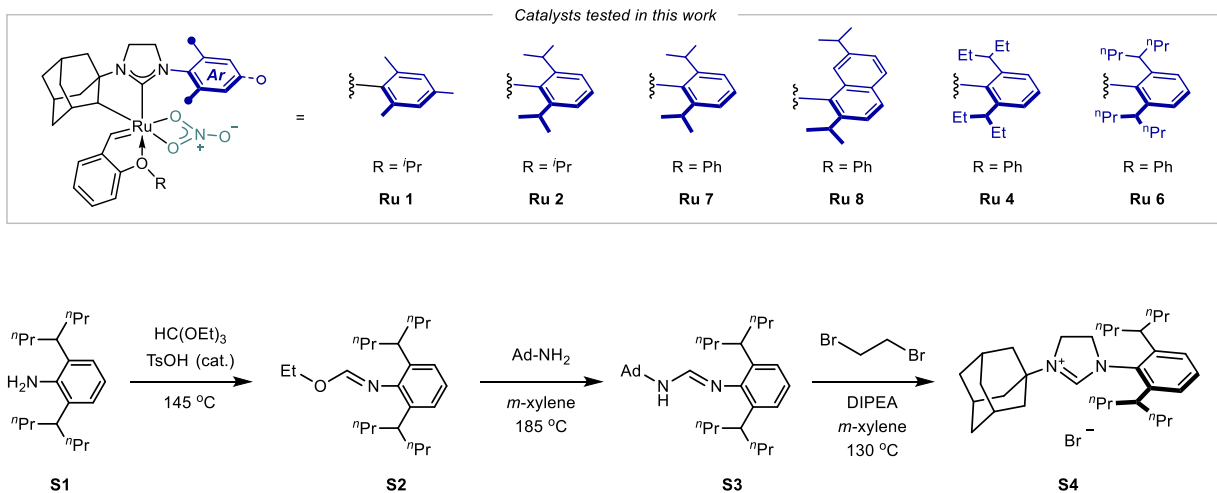
S2: S1 was prepared according to the literature procedure[4] (4, S. Meiries, G. L. Duc, A. Chartoire, A. Collado, K. Speck, K. S. A. Arachchige, A. M. Z. Slawin, S. P. Nolan, *Chemistry – A European Journal* **2013**, 19, 17358–17368.). A 100 mL round-bottom flask equipped with a short-path distillation apparatus was charged with **S1** (8.05 g, 27.8 mmol, 1 equiv), triethyl orthoformate (36 mL), and TsOH (70 mg) and connected to an argon bubbler. The round-bottom flask was heated in a metal block to 145 °C and stirred for 5 hours (the conversion of the reaction can be easily monitored by the volume of the EtOH collected in the receiving flask). Upon full conversion, the

majority of the remaining triethyl orthoformate was removed by reduced-pressure distillation. The residue was purified by flash column chromatography (pentane:Et$_2$O, 100:1 to 30:1) to give the crude **S2** as a colorless oil (6.45 g, 67% yield). R$_f$ = 0.75 (hexane/EtOAc = 10:1). A crude NMR spectrum is recorded for **S2**: ^{1}H NMR (400 MHz, C$_6$D$_6$) δ 7.47 (s, 1H), 7.12 (dd, J = 8.7, 6.3 Hz, 1H), 7.08 – 7.03 (m, 2H), 4.33 (q, J = 7.1 Hz, 2H), 2.99 (p, J = 7.3 Hz, 2H), 1.62 – 1.48 (m, 8H), 1.39 – 1.14 (m, 12H), 0.86 (t, J = 7.3 Hz, 12H). The crude **S2** was directly carried out to the next step without further purification.

S3: A 50 mL round-bottom flask equipped with a short-path distillation apparatus was charged with **S2** (6.28 g, 18.2 mmol, 1 equiv), 1-adamantylamine (4.1 g, 27 mmol, 1.48 equiv), TsOH (70 mg), and *m*-xylene (5 mL) and connected to an argon bubbler. The round-bottom flask was heated in a metal block to 185 °C and stirred for 48 hours. Upon cooled to room temperature, the reaction mixture was purified by flash column chromatography (hexane:Et$_2$O = 15:1 to pentane:acetone = 4:1) to give the crude **S3** as a colorless oil (6.85 g, ~90% purity). R$_f$ = 0.1 (hexane/EtOAc = 20:1). The crude **S3** was directly carried out to the next step without further purification.

S4: A 12 mL vial was charged with crude **S3** (720 mg, 1.6 mmol, 1 equiv), 1,2-dibromoethane (540 mg, 2.87 mmol, 1.8 equiv), DIPEA (415 mg, 3.2 mmol, 2 equiv), and *m*-xylene (0.8 mL) under a nitrogen atmosphere. The vial was stirred at 130 °C for 24 hours. Upon cooled to room temperature, the reaction mixture was diluted with 5 mL DCM and washed with water (8 mL × 5). The organic phase was then dried over Na$_2$SO$_4$, filtered, and concentrated *in vacuo*. The residue was triturated with Et$_2$O. The precipitate was collected by filtration and washed with Et$_2$O (2 mL × 2), leading to pure **S4** as a grey solid (640 mg, 72%). ^{1}H NMR (400 MHz, CDCl$_3$) δ 7.45 (s, 1H),

7.42 (t, J = 7.8 Hz, 1H), 7.15 (d, J = 7.8 Hz, 2H), 4.77 (t, J = 11.0 Hz, 2H), 4.37 (dd, J = 12.4, 9.5 Hz, 2H), 2.54 (td, J = 8.6, 4.3 Hz, 2H), 2.25 (s, 3H), 2.09 – 1.93 (m, 6H), 1.81 – 1.58 (m, 10H), 1.55 – 0.99 (m, 12H), 0.92 – 0.73 (m, 12H). ^{13}C NMR (101 MHz, CDCl$_3$) δ 153.7, 144.7, 132.9, 131.3, 125.2, 58.1, 54.1, 46.8, 41.4, 40.3, 40.2, 38.9, 35.4, 29.2, 21.6, 21.4, 14.6, 14.5. HRMS: calcd. 477.4209 [M]$^+$ (*for cation*) Found: 477.4212.
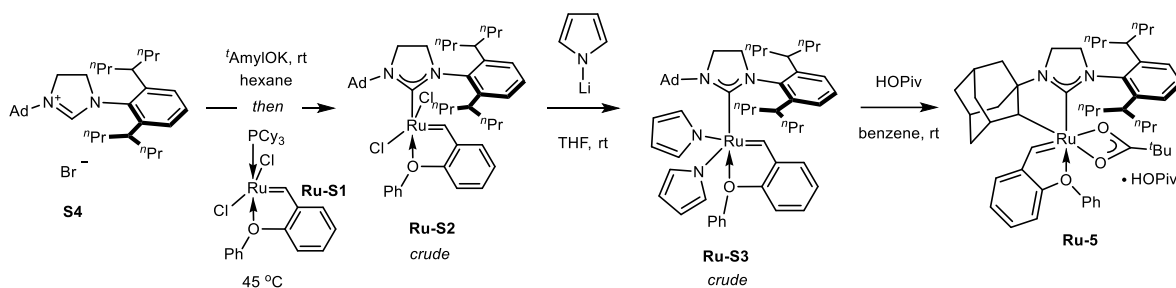
Ru-S2: In a N$_2$ glovebox, a 20 mL vial was charged with **S4** (640 mg, 1.15 mmol, 1 equiv) and hexane (17 mL). To this was added potassium *tert*-pentoxide (0.9 M solution in cyclohexane, 1.3 mL, 1.17 mmol, 1.02 equiv). The vial was sealed and stirred at room temperature for 2 hours. The reaction mixture was then filtered through a short plug of Celite into a 40 mL vial containing **Ru-S1**[3] (640 mg, 1.0 mmol, 0.87 equiv). The 40 mL vial was sealed and stirred at 45 °C for 50 hours. After cooled to room temperature, the reaction mixture was concentrated *in vacuo.* The residue was transferred onto a short Celite column and flushed with pentane to remove the impurity and then benzene to obtain the product as a dark green solution. Removal of the solvent furnished the crude **Ru-S2** as a green solid (580 mg, 70% yield, ~90% purity). The diagnostic chemical shift for the α-H of the Ru-alkylidene of **Ru-S2** is at 17.26 ppm (d, J = 1.0 Hz, 1H, C$_6$D$_6$). The crude **Ru-S2** was directly carried out to the next step without further purification.

Ru-S3: A 40 mL vial was charged with **Ru-S2** (558 mg, 0.67 mmol, 1 equiv) in THF (9 mL, *solution A*). A 20 mL vial was charged with lithium pyrrolate[3] (246 mg, 3.37 mmol, 5 equiv) in THF (8 mL, *solution B*). *Solution A* was chilled in a glovebox freezer for 2~3 minutes. *Solution A* was then taken out of the freezer, and *Solution B* was transferred into *solution A* using a syringe over one minute. The resulting mixture was stirred for 22 hours at room temperature, monitored by NMR to ensure full conversion, and then concentrated *in vacuo*. Benzene (6 mL) was added to the residue to dissolve most of the solid, resulting in a green suspension. Over a period of 3 minutes and with vigorous stirring, the suspension was dropwise added to a 60 mL vial pre-charged with pentane (45 mL), which led to a green solution and the generation of white precipitate. The white solid was removed through filtration and washed with a small amount of benzene. The filtrate was concentrated *in vacuo,* triturated with pentane, and concentrated *in vacuo* again. The residue was transferred onto a short Celite column. The column was flushed with hexamethyldisiloxane (2 mL × 2) and a mixed solution of hexamethyldisiloxane/pentane (1:1, 2 mL) to remove the impurity as a brown band. The Celite column was then flushed with a benzene/pentane solution (1:2, 12 mL × 3) to generate a green solution. Removal of the solvent furnished crude **Ru-S3** as a dark green solid (500 mg, 84% yield). A crude ^{1}H NMR spectrum was recorded for **Ru-S3**: ^{1}H NMR (400 MHz, Benzene-d_6) δ 16.72 (d, J = 1.1 Hz, 1H), 7.61 – 7.55 (m, 2H), 7.35 (dd, J = 8.1, 7.3 Hz, 1H), 7.20 – 7.17 (m, 2H), 7.01 – 6.92 (m, 2H), 6.90 – 6.82 (m, 3H), 6.80 – 6.73 (m, 1H), 6.71 (t, J = 1.8 Hz, 4H), 6.68 (dd, J = 7.4, 1.0 Hz, 1H), 6.44 (t, J = 1.8 Hz, 4H), 3.67 (dd, J = 10.1, 8.5 Hz, 2H), 3.39 (dd, J = 10.1, 8.5 Hz, 2H), 3.35 – 3.24 (m, 2H), 1.88 (s, 3H), 1.60 – 1.15 (m, 22H), 1.07 – 1.00 (m, 6H), 0.98 – 0.67 (m, 4H), 0.58 (t, J = 7.1 Hz, 6H), -0.27 (tdd, J = 12.2, 7.1, 4.3 Hz, 2H).

Ru-5: A 40 mL vial was charged with **Ru-S3** (470 mg, 0.53 mmol, 1 equiv). To this, a benzene (17 mL) solution of pivalic acid (250 mg, 2.45 mmol, 4.6 equiv.) was added at room temperature. The reaction mixture was stirred at room temperature for 36 hours, monitored by NMR to ensure full conversion, and then concentrated *in vacuo*. Pentane (5 mL) was added to the residue, and the resulting mixture was stirred at room temperature for 5 minutes before being concentrated *in vacuo* (*during this process, formation of a purple precipitate is expected --- if not, such a "trituration" procedure should be repeated*). The residue was transferred onto a short Celite column. The column was flushed with hexamethyldisiloxane (1 mL × 3) and pentane (1.5 mL) to remove the impurity as a brown band. The Celite column was then flushed with benzene (4.5 mL) to generate a purple solution. Removal of the solvent furnished **Ru-5** as a 1:1 HOPiv adduct (purple solid, 410 mg, 81% yield). The identity of the adduct was further elucidated by XRD analysis (*see below*).
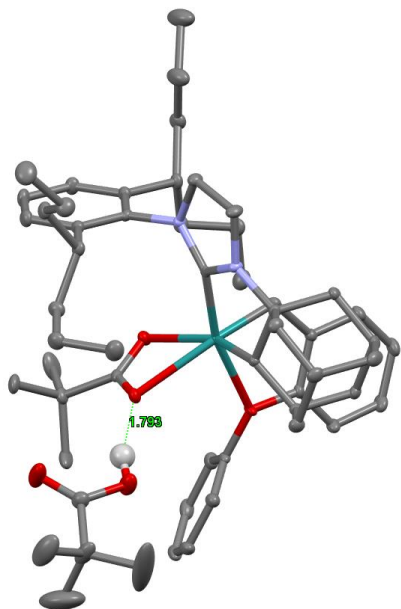
Characterization data of **Ru-5:** ^{1}H NMR (400 MHz, C_6D_6) δ 14.68 (s, 1H), 12.38 (s, 1H), 7.49 (dd, J = 7.6, 1.7 Hz, 1H), 7.31 (d, J = 8.0 Hz, 2H), 7.14 (d, J = 7.6 Hz, 1H), 7.09 (dd, J = 7.8, 1.7 Hz, 1H), 7.05 – 6.91 (m, 4H), 6.91 – 6.81 (m, 2H), 6.57 (d, J = 8.2 Hz, 1H), 4.14 (s, 1H), 4.11 – 3.95 (m, 1H), 3.74 – 3.62 (m, 2H), 3.55 (q, J = 10.4 Hz, 1H), 3.29 (ddd, J = 12.0, 9.6, 4.5 Hz, 1H), 2.91 – 2.79 (m, 1H), 2.45 (ddt, J = 13.1, 7.0, 3.6 Hz, 1H), 2.30 – 2.12 (m, 3H), 2.12 – 1.98 (m, 3H), 1.97 – 1.87 (m, 2H), 1.85 – 1.39 (m, 12H), 1.38 – 1.26 (m, 6H), 1.25 – 1.01 (m, 12H), 0.98 – 0.84 (m, 8H), 0.84 – 0.39 (m, 12H). ^{13}C NMR (101 MHz, C_6D_6) carbon signals were observed at δ 255.6, 255.4, 214.0, 157.4, 154.9, 147.7, 145.6, 142.7, 139.8, 129.8, 128.6, 125.9, 125.0, 125.0, 124.7, 124.4, 123.5, 121.9, 115.5, 68.3, 63.2, 55.8, 43.7, 41.2, 41.1, 40.8, 40.6, 39.8, 39.1, 38.4, 38.3, 36.6, 36.3, 33.7, 31.2, 30.2, 27.8 (br), 22.9, 22.2, 21.9, 21.9, 15.2, 15.1, 15.0, 14.6. HRMS: *Chemical formula* ([M]): $C_{51}H_{70}N_2O_3Ru$, calcd. $[M+H-H_2]^+$ 859.4352 Found: 859.4340.
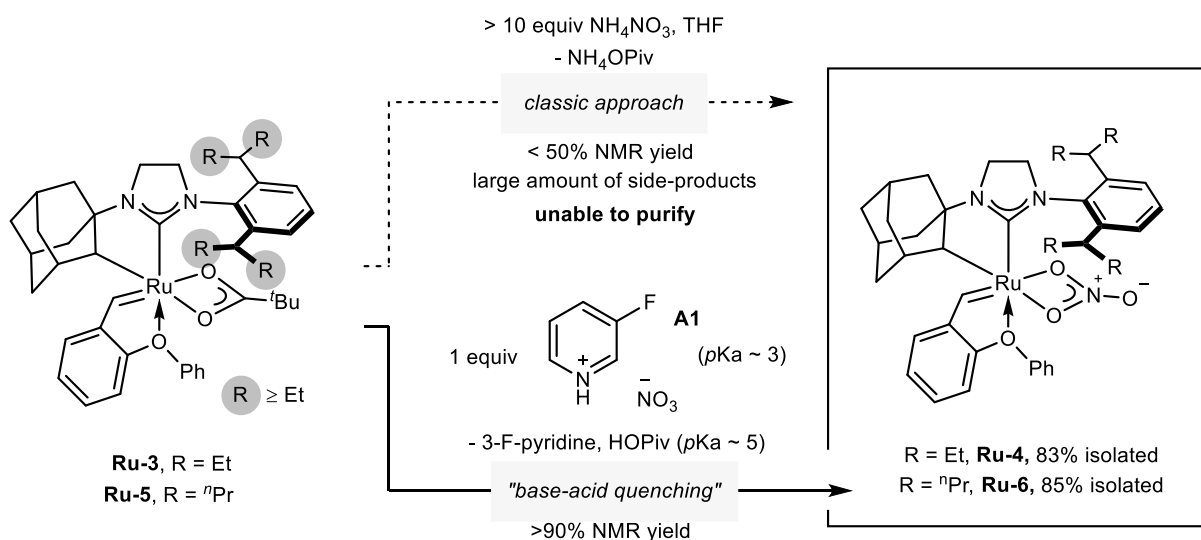
Ru-3 was synthesized according to the literature procedure.[3]

Ru-4:

An example of the classic approach: A 4 mL vial was charged with Ru-3 (30 mg, 0.0373 mmol, 1 equiv), NH_4NO_3 (60 mg, 0.75 mmol, 20 equiv), and THF (2 mL) in a N_2 glovebox. After stirring at room temperature for 16 hours, the reaction mixture reached a high conversion, and a crude ^{1}H NMR spectrum was recorded, indicating a 47% NMR yield of the desired Ru-4 and the generation of a significant amount of unidentifiable side products (Figure B1, *see below*). Note that elongating the reaction time led to lower NMR yields of the desired Ru-4. As Ru-4 is unstable against silica gel or aluminum oxide, purification was carried out mainly using filtration, wash, and/or recrystallization approaches. However, despite extensive trials, the complete purification of Ru-4 is hard to realize in our hands, and the best purity we could get is around 92%.
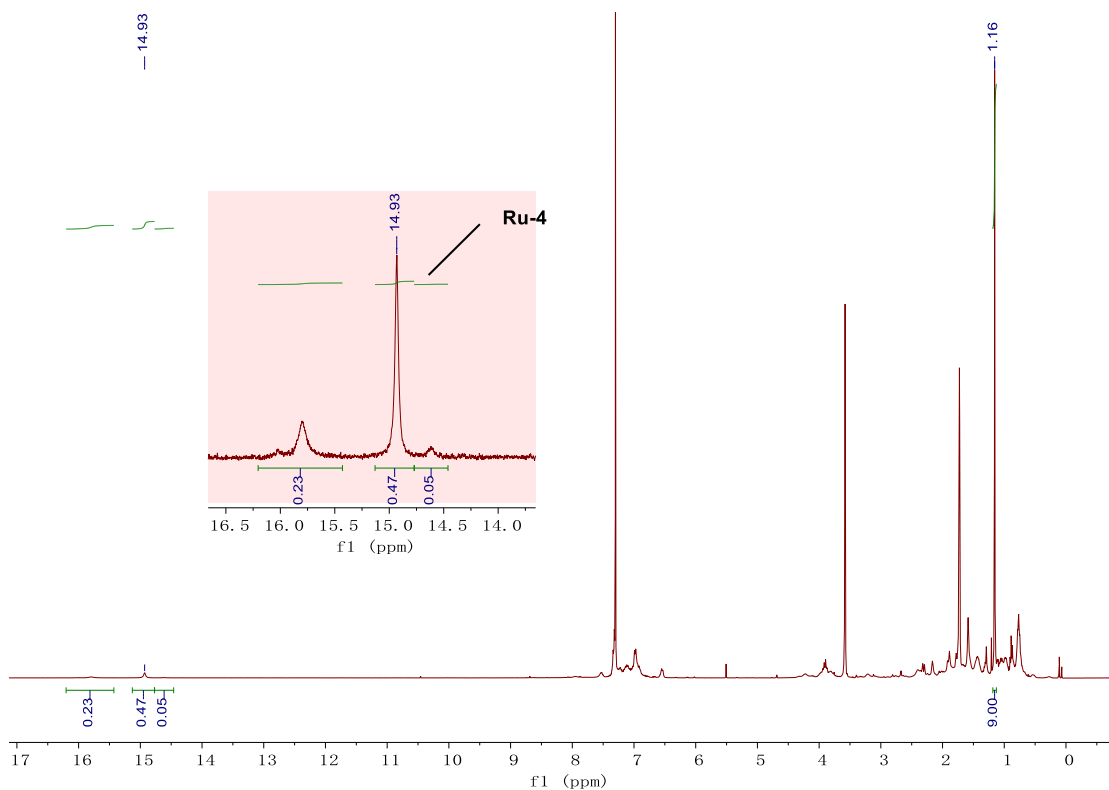
Figure B1. The crude ^{1}H NMR spectrum for the preparation of **Ru-4** using a classic approach.

The "base-acid quenching" approach: A 4 mL vial was charged with **Ru-3** (175 mg, 0.217 mmol, 1 equiv)**,** 3-fluoropyridinium nitrate (34.7 mg, 0.217 mmol, 1 equiv), and THF (3 mL) in a N$_2$ glovebox and stir at room temperature for 15 minutes. A crude ^{1}H NMR spectrum was recorded, showing a 91% NMR yield of the desired **Ru-4** (Figure B2, *see below*). The THF solution was then transferred to a 20 mL vial pre-charged with 5 mL of HMDSO, which was then concentrated *in vacuo.* The residue was triturated with pentane (1 mL) and concentrated again *in vacuo*. The residue was transferred onto a short Celite column and flushed with HMDSO (0.5 mL × 2) and pentane (1 mL × 3) to remove the impurity and then benzene (3~4 mL) to obtain the product as a purple solution. Removal of the solvent furnished **Ru-4** as a purple solid (137 mg, 83% yield).
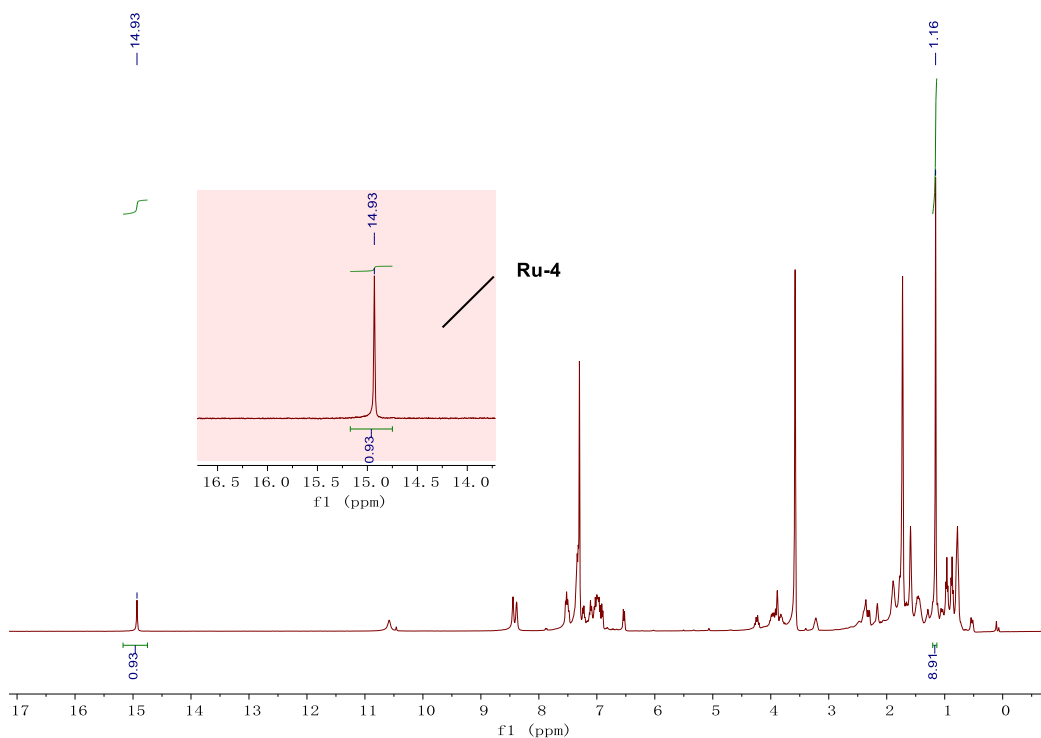
Figure B2. The crude 1H NMR spectrum for the preparation of Ru-4 using a "base-acid quenching" approach.

Characterization data of **Ru-4:** ^{1}H NMR (400 MHz, C$_6$D$_6$) δ 15.06 (s, 1H), 7.54 (dd, J = 7.5, 1.6 Hz, 1H), 7.20 (t, J = 7.7 Hz, 1H), 7.09 – 6.94 (m, 5H), 6.94 – 6.86 (m, 2H), 6.84 (td, J = 7.4, 1.0 Hz, 1H), 6.81 – 6.74 (m, 1H), 6.42 (dt, J = 8.3, 1.0 Hz, 1H), 4.17 (s, 1H), 3.87 (ddd, J = 11.7, 10.2, 9.3 Hz, 1H), 3.68 (td, J = 10.6, 6.4 Hz, 1H), 3.43 (dt, J = 10.8, 9.5 Hz, 1H), 3.32 – 3.16 (m, 2H), 2.60 (d, J = 3.9 Hz, 1H), 2.50 – 2.41 (m, 1H), 2.21 (dqd, J = 13.5, 7.5, 2.3 Hz, 1H), 2.15 – 2.02 (m, 2H), 1.97 – 1.74 (m, 5H), 1.73 – 1.37 (m, 9H), 1.27 (d, J = 12.2 Hz, 1H), 1.22 (t, J = 7.3 Hz, 3H), 1.16 (d, J = 11.4 Hz, 1H), 1.03 (t, J = 7.4 Hz, 3H), 0.83 – 0.67 (m, 7H). ^{13}C NMR (101 MHz, C$_6$D$_6$) δ 263.1, 212.8, 157.5, 154.1, 146.4, 145.5, 142.4, 137.9, 130.3, 128.7, 128.6, 126.6, 126.5, 125.9, 125.0, 124.6, 122.6, 122.2, 115.1, 67.3, 63.1, 54.7, 43.5, 42.6, 42.5, 41.6, 40.5, 38.1, 37.9, 37.1, 33.4, 30.9, 30.0, 28.9, 28.8, 28.1, 27.9, 14.3, 13.2, 12.6, 11.9. HRMS: calcd. 764.3002 [M+H-H$_2$]$^+$ Found: 764.3014.

Preparation of 3-fluoropyridinium nitrate (A1): To a 20 mL vial charged with 3-fluoropyridine (10 mmol, 970 mg, 1 equiv.) was added HNO$_3$ (70% w/w, 10 mmol, 900 mg, 1 equiv., dropwise over 5 minutes) at -20 °C. The reaction mixture was then allowed to warm to room temperature and stir for 10 minutes. The precipitate was collected by filtration and washed by a small amount of acetone and diethyl ether, giving the pyridinium salt **A1** as a white crystalline white solid (1.5 g, 94% yield). ^{1}H NMR (400 MHz, DMSO-d_6) δ 8.91 (t, J = 2.4 Hz, 1H), 8.67 (d, J = 5.2 Hz, 1H), 8.20 (td, J = 8.7, 2.9 Hz, 1H), 7.85 (dt, J = 9.7, 5.2 Hz, 1H), 5.48 (s, 1H). ^{13}C NMR (101 MHz, DMSO-d_6) δ 159.70 (d, J = 252.7 Hz), 142.72 (d, J = 4.0 Hz), 135.01 (d, J = 29.2 Hz), 128.96 (d, J = 18.1 Hz), 127.40 (d, J = 5.9 Hz).

Ru-6:

An example of the classic approach: A 4 mL vial was charged with **Ru-5** (as a 1:1 HOPiv adduct, 29 mg, 0.03 mmol, 1 equiv)**,** NH_4NO_3 (48 mg, 0.6 mmol, 20 equiv) and THF (0.65 mL) in a N_2 glovebox. After stirring at room temperature for 48 hours, the reaction mixture reached a high conversion, and a crude ^1H NMR spectrum was recorded, indicating a 40% NMR yield of the desired **Ru-6** and the generation of a significant amount of unidentifiable side products (Figure S3, *see below*). Note that elongating the reaction time led to lower NMR yields of the desired **Ru-6**. As **Ru-6** is unstable against silica gel or aluminum oxide, purification was carried out mainly using filtration, wash, and/or recrystallization approaches. However, despite extensive trials, the complete purification of **Ru-6** is hard to realize in our hands and the best purity we could get is less than 90%.
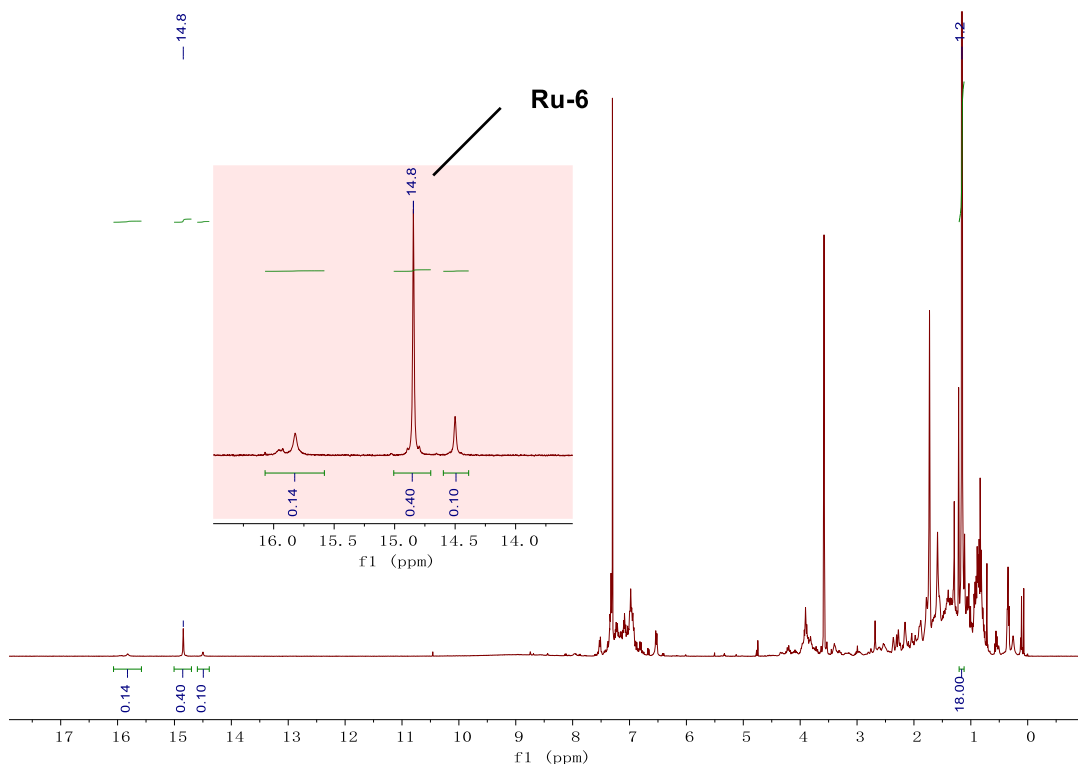
Figure B3. The crude ^1H NMR spectrum for the preparation of **Ru-6** using a classic approach.

The "base-acid quenching" approach: A 4 mL vial was charged with **Ru-5** (as a 1:1 HOPiv adduct, 96 mg, 0.1 mmol, 1 equiv)**,** 3-fluoropyridinium nitrate (16 mg, 0.1 mmol, 1 equiv) and THF (1.5 mL) in a N_2 glovebox and stir at room temperature for 15 minutes. A crude ^{1}H NMR spectrum was recorded, showing a 94% NMR yield of the desired **Ru-6** (Figure B4, *see below*). The THF solution was then transferred to a 20 mL vial pre-charged with 4 mL of HMDSO, which was then concentrated *in vacuo*. The residue was triturated with pentane (1 mL) and concentrated again *in vacuo*. The residue was transferred onto a short Celite column and flushed with HMDSO (0.25 mL × 2) and pentane (0.5 mL × 4) to remove the impurity and then benzene (1 mL) to obtain the product as a purple solution. Removal of the solvent furnished **Ru-6** as a purple solid (70 mg, 85% yield).
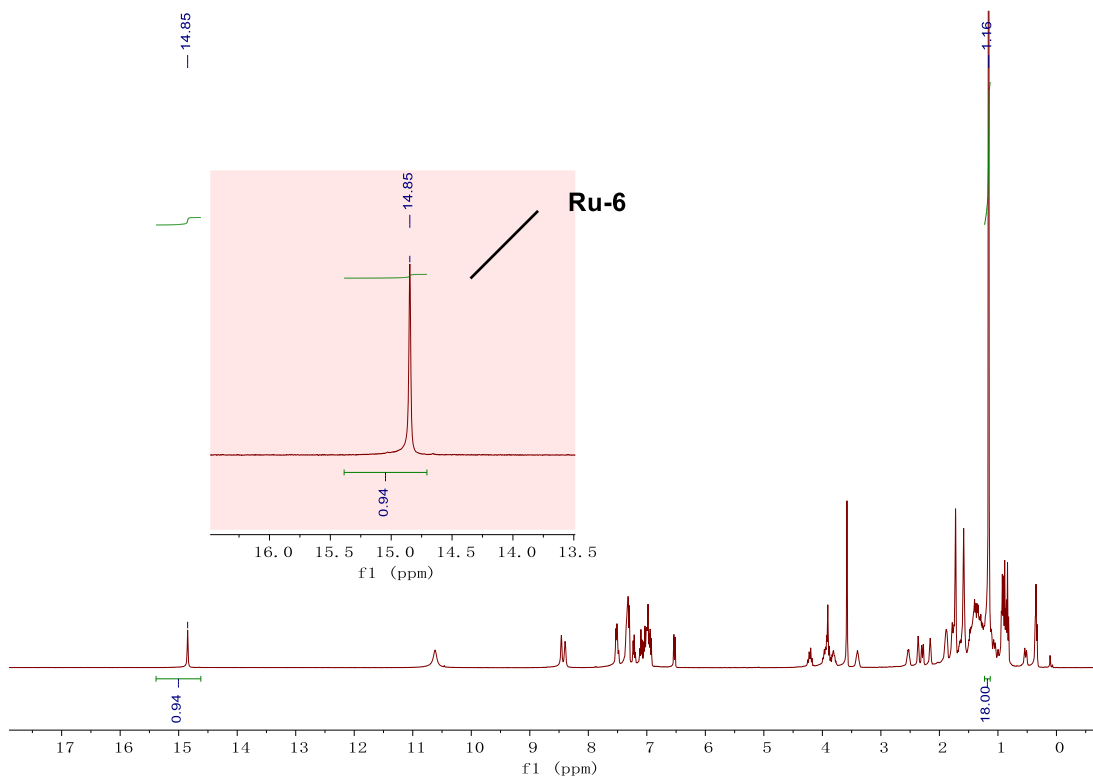
Figure B4. The crude ^{1}H NMR spectrum for the preparation of **Ru-6** using a "base-acid quenching" approach.

Characterization data of **Ru-6:**

^{1}H NMR (400 MHz, C$_6$D$_6$) δ 14.98 (s, 1H), 7.49 (dd, J = 7.6, 1.6 Hz, 1H), 7.22 (t, J = 7.7 Hz, 1H), 7.11 – 6.96 (m, 5H), 6.86 (dtd, J = 15.8, 7.6, 0.9 Hz, 3H), 6.80 – 6.73 (m, 1H), 6.44 (d, J = 8.3 Hz, 1H), 4.21 (s, 1H), 3.97 – 3.83 (m, 1H), 3.76 (td, J = 10.6, 6.4 Hz, 1H), 3.57 – 3.39 (m, 2H), 3.29 (ddd, J = 11.7, 9.6, 6.4 Hz, 1H), 2.70 – 2.52 (m, 2H), 2.20 – 1.96 (m, 4H), 1.92 (d, J = 10.7 Hz, 1H), 1.88 – 1.78 (m, 2H), 1.72 (s, 1H), 1.70 – 1.35 (m, 13H), 1.32 – 1.14 (m, 9H), 0.91 (t, J = 7.2 Hz, 3H), 0.81 (t, J = 7.3 Hz, 3H), 0.76 (d, J = 12.1 Hz, 1H), 0.61 (t, J = 6.7 Hz, 3H). ^{13}C NMR (101 MHz, C$_6$D$_6$) δ 262.5, 213.0, 157.6, 154.1, 146.9, 146.1, 142.4, 137.4, 130.3, 128.8, 128.6, 126.7, 126.4, 125.8, 125.0, 124.8, 122.5, 122.2, 115.1, 66.9, 63.2, 54.7, 43.5, 41.5, 40.7, 40.2, 39.6, 39.3, 39.0, 38.7, 38.2, 38.1, 38.0, 36.9, 33.4, 31.0, 30.0, 22.6, 21.8, 21.6, 21.4, 15.1, 15.0, 15.0, 14.6. HRMS: calcd. 820.3628 [M+H-H$_2$]$^+$ Found: 820.3615.

2.6.3 Catalyst screening

2.6.3.1 Catalyst screening with acrylates
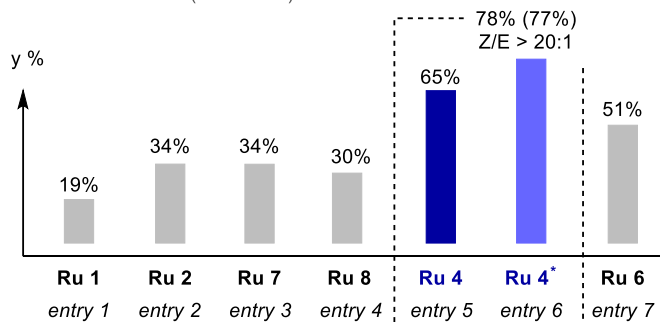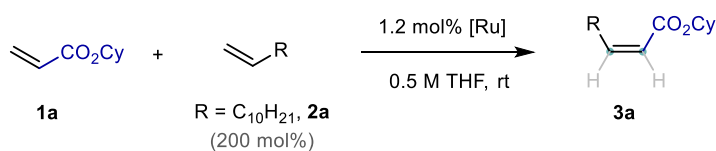
General procedure for entries 1-5 and 7:

A 4 mL vial was charged with a stir bar, **1a** (0.25 mmol, 1 equiv, 38.5 mg), **2a** (0.5 mmol, 2 equiv, 84 mg), and anthracene (*as the internal standard*) in a nitrogen glovebox. To this was added a stock solution of the ruthenium catalyst (0.003 mmol, 0.012 equiv) in d_8-THF (0.5 mL). The vial was loosely capped with a screw thread hole cap, and a 20-gauge needle was used to puncture the cap and left on. The reaction mixture was allowed to stir at room temperature in the glovebox for 12–48 hours until its color changed from purple to bright yellow (*which indicates the complete consumption of the catalyst*). The reaction can also be monitored by ^{1}H NMR to determine the quantity of the remaining ruthenium catalyst. Upon full consumption of the catalyst, the reaction was transferred to an NMR tube and removed from the glovebox. The yields and the *Z/E* ratio of the metathesis products were further determined by the ^{1}H NMR analysis of the crude reaction mixture.

<u>Note 1</u>: After 24 hours of reaction, a small amount of d_8-THF (0.1–0.2 mL) was added to compensate for the loss of the solvent (*due to slow evaporation*) if the reaction did not reach full catalyst consumption.

<u>Note 2</u>: A photo for the reaction setup can be found in the supporting information of a previous publication (*J. Am. Chem. Soc.* **2020**, *142*, 20987–20993, Figure B1).

Experiment procedure for entry 6:

A 4 mL vial was charged with a stir bar, **1a** (0.15 mmol, 1 equiv, 23.1 mg), **2a** (0.24 mmol, 1.6 equiv, 40.3 mg) and anthracene (*as the internal standard*) in a nitrogen glovebox. To this was added a stock solution of **Ru-4** (2.9 mg, 0.00375 mmol, 0.025 equiv) in THF (0.4 mL). The vial was loosely capped with a screw thread hole cap, and a 20-gauge needle was used to puncture the cap

and left on. The reaction mixture was allowed to stir at room temperature in the glovebox for 30 hours until its color changed from purple to bright yellow (*which indicates the complete consumption of the catalyst*). According to the ^{1}H NMR analysis of the crude reaction mixture, the NMR yield is 78% and the crude *Z:E* ratio is larger than 20:1.

The reaction was further purified by flash column chromatography over silica gel, furnishing pure *Z*-product **3a** in 77% isolated yield as a colorless oil (33.8 mg). Chromatography condition: hexane/acetone, 100:1. ^{1}H NMR (400 MHz, CDCl$_3$) δ 6.19 (dt, J = 11.5, 7.5 Hz, 1H), 5.73 (dt, J = 11.5, 1.7 Hz, 1H), 4.89 – 4.73 (m, 1H), 2.63 (qd, J = 7.5, 1.7 Hz, 2H), 1.94 – 1.81 (m, 2H), 1.78 – 1.68 (m, 2H), 1.62 – 1.19 (m, 22H), 0.88 (t, J = 6.8 Hz, 3H). ^{13}C NMR (101 MHz, CDCl$_3$) δ 166.2, 150.2, 120.3, 72.2, 32.1, 31.9, 29.7, 29.7, 29.6, 29.5, 29.5, 29.2, 29.2, 25.6, 24.0, 22.8, 14.3. IR: 2928.4, 2856.6, 1716.9, 1641.2, 1451.0, 1414.1, 1179.1, 1121.6 cm^{-1}. HRMS: *Chemical formula* ([M]): C$_{19}$H$_{34}$O$_2$, calcd. [M+H]$^+$ 295.2637 Found: 295.2618.

2.6.3.2 Catalyst screening with allyl alcohols
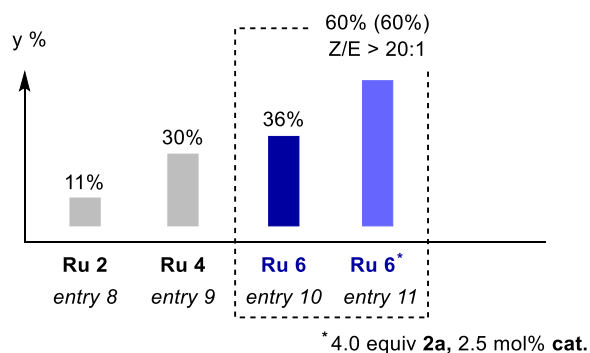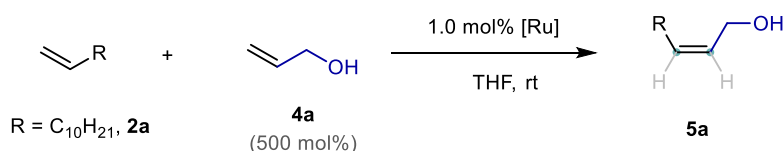
General procedure for entries 8-10:

A 4 mL vial was charged with a stir bar, **2a** (0.2 mmol, 1 equiv, 33.6 mg), **4a** (1 mmol, 5 equiv, 58 mg), and anthracene (as the internal standard) in a nitrogen glovebox. To this was added a stock solution of the ruthenium catalyst (0.002 mmol, 0.01 equiv) in THF (0.6 mL). The vial was loosely capped with a screw thread hole cap, and a 20-gauge needle was used to puncture the cap and left on. The reaction mixture was allowed to stir at room temperature in the glovebox for 24–48 hours until its color changed from purple to bright yellow (which indicates the complete consumption of the catalyst). An aliquot of the reaction was then diluted with CDCl3 and transferred to an NMR tube. The yields and the Z/E ratio of the metathesis products were further determined by 1H NMR analysis of the crude reaction mixture.

Note 1: After 24 hours of reaction, a small amount of THF (0.1-0.2 mL) was added to compensate for the loss of the solvent (due to slow evaporation) if the reaction did not reach full catalyst consumption.

Experiment procedure for entry 11:

A 4 mL vial was charged with a stir bar, **2a** (0.15 mmol, 1 equiv, 25.2 mg), **4a** (0.6 mmol, 4 equiv, 35 mg) and anthracene (*as the internal standard*) in a nitrogen glovebox. To this was added a stock solution of **Ru-6** (3.1 mg, 0.00375 mmol, 0.025 equiv) in THF (0.5 mL). The vial was loosely capped with a screw thread hole cap, and a 20-gauge needle was used to puncture the cap and left on. The reaction mixture was allowed to stir at room temperature in the glovebox for 20 hours until its color changed from purple to bright yellow (*which indicates the complete consumption of the*

catalyst). According to the ^{1}H NMR analysis of the crude reaction mixture, the NMR yield is 60%, and the crude *Z:E* ratio is larger than 20:1.

The reaction was further purified by flash column chromatography over silica gel, furnishing pure *Z*-product **5a** in 60% isolated yield as a colorless oil (17.8 mg). R_f = 0.29 (hexane/diethyl ether = 7:3). Chromatography condition: hexane/diethyl ether, 5:1. ^{1}H NMR (400 MHz, CDCl$_3$) δ 5.63 – 5.48 (m, 2H), 4.19 (d, J = 6.1 Hz, 2H), 2.06 (q, J = 7.0 Hz, 2H), 1.41 (s, 1H), 1.39 – 1.18 (m, 16H), 0.87 (t, J = 6.8 Hz, 3H). ^{13}C NMR (101 MHz, CDCl$_3$) δ 133.5, 128.4, 58.8, 32.0, 29.8, 29.6, 29.5, 29.4, 27.6, 22.8, 14.3. IR: 3326.4, 3011.9, 2920.6, 2852.7, 1658.7, 1470.4, 1377.2, 1280.1, 1264.6, 1115.1 cm^{-1}. HRMS: *Chemical formula* ([M]): C$_{13}$H$_{26}$O, calcd. [M+H-H$_2$]$^+$ 197.1905 Found: 197.1903.

Catalysts tested in this work

| R = ^{i}Pr | R = ^{i}Pr | R = Ph | R = Ph | R = Ph | R = Ph |
| Ru 1 | Ru 2 | Ru 7 | Ru 8 | Ru 4 | Ru 6 |
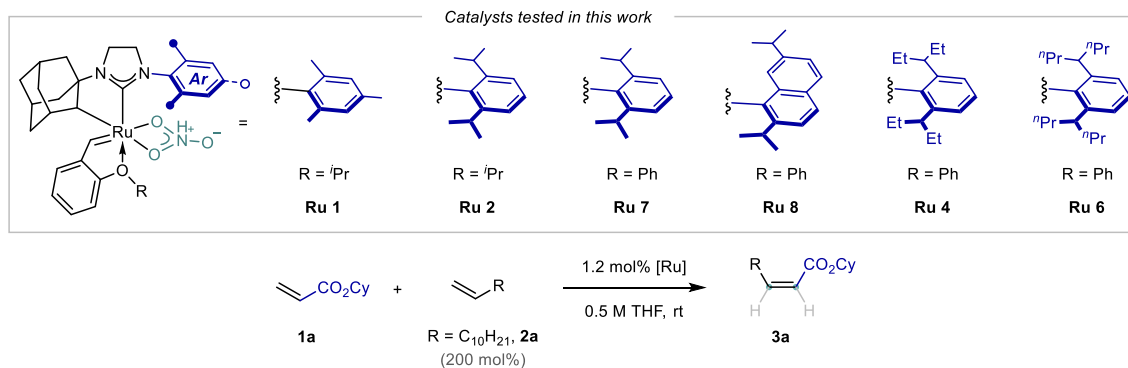
Entry in Scheme 2B	Catalyst	Yield of **3a** when Z/E ratio was measured	Z/E^a
1	**Ru-1**	19% (*full catalyst consumption*)	13:1
2	**Ru-2**	25%	21:1
		34% (*full catalyst consumption*)	19:1
3	**Ru-7**	34% (*full catalyst consumption*)	21:1
4	**Ru-8**	25%	16:1
		30% (*full catalyst consumption*)	14.5:1
5	**Ru-4**	36%	> 40:1

		50%	36:1
		65% (*full catalyst consumption*)	31:1
7	**Ru-6**	51%	30:1
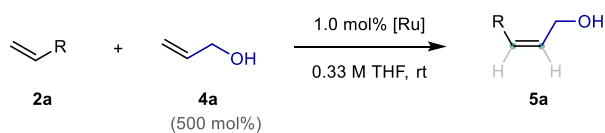
Entry in Scheme 2B	Catalyst	Yield of **3a** when Z/E ratio was measured	Z/E[a]
8	**Ru-2**	11% (*full catalyst consumption*)	>20:1
9	**Ru-4**	30% (*full catalyst consumption*)	>20:1
10	**Ru-6**	36% (*full catalyst consumption*)	>20:1

[a]*Z/E* ratio was determined based on ^{1}H NMR analysis of the crude reaction mixture.

2.6.4 Substrate scope study

2.6.4.1 Substrate synthesis

Most of the substrates in this study were commercially available. **2h**[3], **2r**[5], and **2t**[3] were synthesized according to the literature procedure (5, T. Poll, G. Helmchen, B. Bauer, *Tetrahedron Letters* **1984**, 25, 2191–2194) **2q** was synthesized according to the following procedure *(vide infra)*.
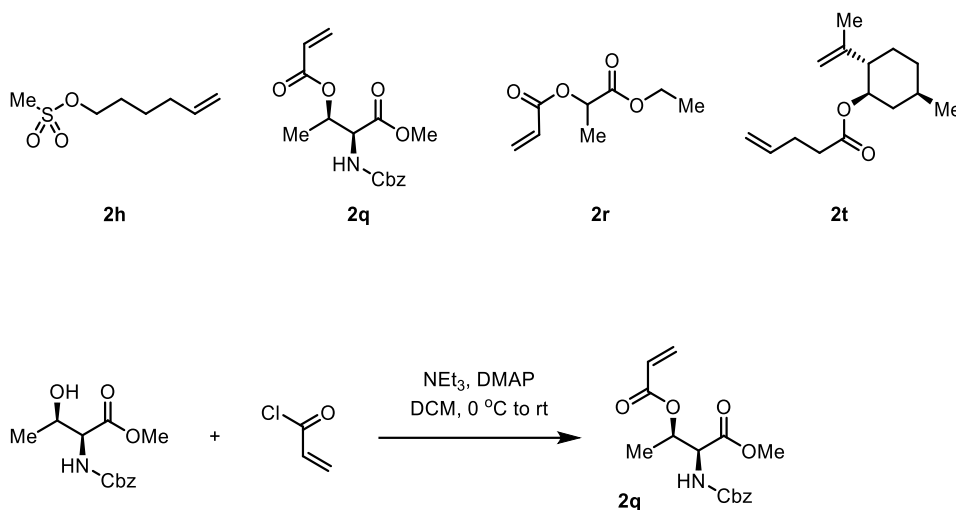
2q: A 40 mL vial was charged with *N*-carbobenzyloxy-L-threonine methyl ester (2.14 g, 8 mmol, 1 equiv), NEt$_3$ (2.2 mL, 16 mmol, 2.0 equiv), DMAP (48.8 mg, 0.4 mmol, 0.05 equiv), DCM (30 mL) and a stir bar. The vial was placed into an ice bath. Acryloyl chloride (0.643 mL, 8 mmol, 1 equiv) was added dropwise with stirring. The reaction was then stirred for 2 hours at room temperature. Upon full conversion, the reaction mixture was filtered, rinsed with DCM (50 mL), and the filtrate was concentrated under reduced pressure. The residue was further purified by column chromatography over silica gel (hexane/ethyl acetate = 4:1) to give **2q** as a colorless oil (900 mg, 35% yield). ^{1}H NMR (400 MHz, CDCl$_3$) δ 7.47 – 7.30 (m, 5H), 6.37 (dd, J = 17.3, 1.4 Hz, 1H), 6.04 (dd, J = 17.3, 10.4 Hz, 1H), 5.83 (dd, J = 10.4, 1.4 Hz, 1H), 5.53 – 5.37 (m, 2H), 5.14 (d, J = 3.0 Hz, 2H), 4.54 (dd, J = 9.7, 2.7 Hz, 1H), 3.73 (s, 3H), 1.35 (d, J = 6.4 Hz, 3H). ^{13}C NMR (101 MHz,

CDCl$_3$) δ 170.4, 164.9, 156.6, 136.1, 131.8, 128.7, 128.5, 128.3, 127.9, 70.8, 67.5, 57.7, 52.9, 17.1.

IR: 2957.8, 2928.2, 2860.9, 1729.7, 1692.0, 1640.9, 1441.6, 1258.4, 1239.6, 1064.5 cm^{-1}. HRMS:

Chemical formula ([M]): C$_{16}$H$_{19}$NO$_6$, calcd. [M+H]$^+$ 322.1291 Found: 322.1288.\

2.6.4.2 General procedure

General Procedure A for Z-selective metathesis with acrylates:
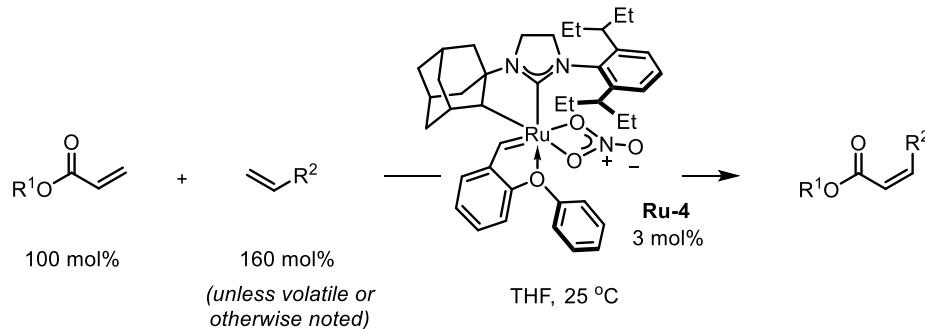
A 4 mL vial was charged with a stir bar, an acrylate substrate (0.15 mmol, 1 equiv), and an olefin substrate (0.24 mmol, 1.6 equiv) in a nitrogen glovebox. To this was added a stock solution of **Ru-4** (3.4 mg, 0.0045 mmol, 0.03 equiv) in THF (0.6 mL). The vial was loosely capped with a screw thread hole cap, and a 20-gauge needle was used to puncture the cap and left on (see Figure S1 in J. Am. Chem. Soc. **2020**, 142, 20987–20993). The reaction mixture was allowed to stir at room temperature in the glovebox for 24–48 hours until its color changed from purple to bright yellow (which indicates the complete consumption of the catalyst). Note that after 24 hours of reaction, a small amount of THF (0.2 – 0.3 mL) was usually added to the mixture to compensate for the loss of the solvent (due to slow evaporation) if the reaction did not reach full catalyst consumption. The reaction was then removed from the glovebox, concentrated, and further purified by flash column chromatography over silica. The reported yield was the isolated yield of the Z-metathesis product. Unless otherwise noted, the Z/E ratio of the metathesis product was determined by ^{1}H NMR analysis of the crude reaction mixture using $CDCl_3$ or CD_2Cl_2 as the NMR solvent.

General Procedure B for Z-selective metathesis with allyl alcohols:

THF, 25 °C
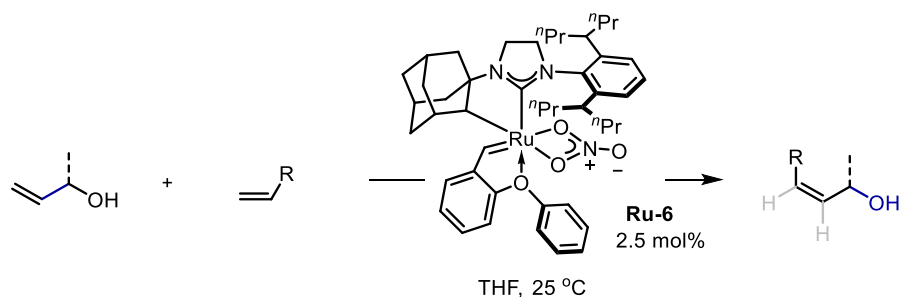
      Unless otherwise noted, a 4 mL vial was charged with a stir bar, a regular olefin substrate (0.15 mmol, 1 equiv), and an allyl alcohol substrate (0.6 mmol, 4 equiv) in a nitrogen glovebox. To this was added a stock solution of **Ru-6** (3.1 mg, 0.00375 mmol, 0.025 equiv) in THF (0.5 mL). The vial was loosely capped with a screw thread hole cap, and a 20-gauge needle was used to puncture the cap and left on (see Figure S1 in J. Am. Chem. Soc. **2020**, 142, 20987–20993). The reaction mixture was allowed to stir at room temperature in the glovebox for 24 hours until its color changed from purple to bright yellow (which indicates the complete consumption of the catalyst). The reaction was then removed from the glovebox, concentrated, and further purified by flash column chromatography over silica. The reported yield was the isolated yield of the Z-metathesis product, and the reported Z/E ratio was determined by ^{1}H NMR analysis of the crude reaction mixture using CDCl$_3$ or CD$_2$Cl$_2$ as the NMR solvent.
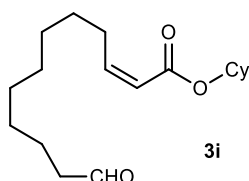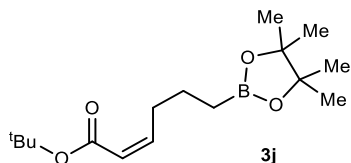
2.6.4.3 Product characterization

3b
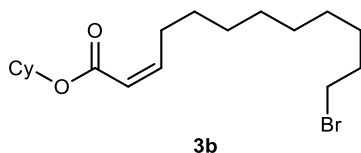
3b: Colorless oil (46.3 mg, 86% yield). Reaction time = 48 hours. *Z:E* ratio > 20:1 (determined by ^{1}H NMR analysis of the crude reaction mixture). R_f = 0.36 (hexane/acetone = 100:3). Chromatography condition: hexane/acetone, 200:1. ^{1}H NMR (400 MHz, CDCl$_3$) δ 6.18 (dt, *J* = 11.5, 7.5 Hz, 1H), 5.73 (dt, *J* = 11.5, 1.7 Hz, 1H), 4.88 – 4.72 (m, 1H), 3.39 (t, *J* = 6.8 Hz, 2H), 2.62 (qd, *J* = 7.5, 1.7 Hz, 2H), 1.92 – 1.79 (m, 4H), 1.77 – 1.66 (m, 2H), 1.60 – 1.49 (m, 1H), 1.46 – 1.25 (m, 17H). ^{13}C NMR (101 MHz, CDCl$_3$) δ 166.2, 150.1, 120.4, 72.2, 34.2, 32.9, 31.9, 29.5, 29.4, 29.4, 29.2, 29.1, 28.8, 28.3, 25.6, 23.9. IR: 2926.5, 2852.7, 1722.8, 1643.2, 1456.8, 1416.0, 1157.8, 1120.9 cm^{-1}. HRMS: Chemical formula ([M]): C$_{18}$H$_{31}$O$_2$Br, calcd. [M+H]$^+$ 359.1586 Found: 359.1581.

3c
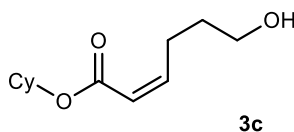
3c: Following a modified *General Procedure A*, the reaction was conducted using 2.0 equivalent (*instead of 1.6 equiv.*) of 4-penten-1-ol (b.p. = 134 ˚C, 25.8 mg). The titled compound was isolated as a colorless oil (24.4 mg, 77% yield). Reaction time = 48 hours. *Z:E* ratio > 20:1 (determined by ^{1}H NMR analysis of the crude reaction mixture). R_f = 0.25 (hexane/ethyl acetate = 3:1). Chromatography condition: hexane/ethyl acetate, 6:1. ^{1}H NMR (400 MHz, CDCl$_3$) δ 6.18 (dt, *J* = 11.4, 8.2 Hz, 1H), 5.83 (dd, *J* = 11.5, 1.7 Hz, 1H), 4.98 – 4.68 (m, 1H), 3.60 (t, *J* = 5.9 Hz, 2H), 2.71 (qd, *J* = 7.3, 6.9 Hz, 2H), 2.65 – 2.59 (s, 1H), 1.94 – 1.83 (m, 2H), 1.77 – 1.64 (m, 4H), 1.60 –

1.50 (m, 1H), 1.49 – 1.19 (m, 5H). ^{13}C NMR (101 MHz, CDCl$_3$) δ 166.8, 148.7, 121.5, 72.8, 61.0, 31.8, 31.1, 25.5, 25.0, 23.9. IR: 3485.6, 2922.6, 2854.6, 1716.9, 1641.2, 1454.8, 1412.1, 1173.3, 1130.6 cm^{-1}. HRMS: Chemical formula ([M]): C$_{12}$H$_{20}$O$_3$, calcd. [M+H]$^+$ 213.1491 Found: 213.1488.

3d
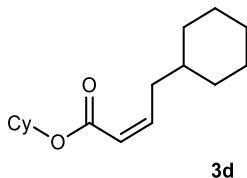
3d: Following a modified *General Procedure A*, the reaction was conducted using 2.0 equivalent (*instead of 1.6 equiv.*) of allylcyclohexane (b.p. = 150 ˚C, 37.3 mg). Th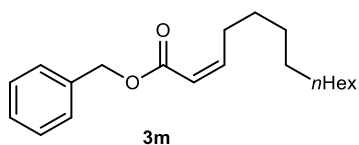e titled compound was isolated as a colorless oil (29.9 mg, 80% yield). Reaction time = 48 hours. *Z:E* ratio > 20:1 (determined by ^{1}H NMR analysis of the crude reaction mixture). R$_f$ = 0.12 (hexane/acetone = 100:1). Chromatography condition: hexane/acetone, 200:1. ^{1}H NMR (400 MHz, CDCl$_3$) δ 6.22 (dt, *J* = 11.6, 7.7 Hz, 1H), 5.77 (dt, *J* = 11.6, 1.7 Hz, 1H), 4.85 – 4.74 (m, 1H), 2.55 (td, *J* = 7.3, 1.7 Hz, 2H), 1.93 – 1.83 (m, 2H), 1.79 – 0.89 (m, 19H). ^{13}C NMR (101 MHz, CDCl$_3$) δ 166.3, 149.0, 120.9, 72.2, 38.3, 36.7, 33.2, 31.9, 26.6, 26.4, 25.6, 24.0. IR: 2924.5, 2852.7, 1715.0, 1643.2, 1447.1, 1414.1, 1175.2 cm^{-1}. HRMS: Chemical formula ([M]): C$_{16}$H$_{26}$O$_2$, calcd. [M+H]$^+$ 251.2011 Found: 251.2039.

3e
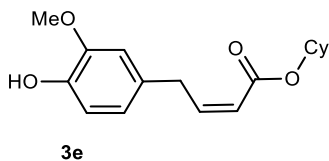
3e: Colorless oil (33.1 mg, 76% yield). Reaction time = 72 hours. *Z:E* ratio > 20:1 (determined by ^{1}H NMR analysis of the crude reaction mixture). R$_f$ = 0.19 (hexane/ethyl acetate =

10:1). Chromatography condition: hexane/ethyl acetate, 20:1. ^{1}H NMR (400 MHz, CD$_2$Cl$_2$) δ 6.80 (d, J = 8.0 Hz, 1H), 6.77 (d, J = 1.9 Hz, 1H), 6.73 – 6.69 (m, 1H), 6.30 (dt, J = 11.4, 7.6 Hz, 1H), 5.80 (dt, J = 11.4, 1.8 Hz, 1H), 5.56 (br, 1H), 4.89 – 4.78 (m, 1H), 3.91 (dd, J = 7.6, 1.8 Hz, 2H), 3.86 (s, 3H), 1.96 – 1.82 (m, 2H), 1.80 – 1.68 (m, 2H), 1.64 – 1.21 (m, 6H). ^{13}C NMR (101 MHz, CD$_2$Cl$_2$) δ 166.1, 147.9, 147.1, 144.5, 131.9, 121.5, 120.6, 114.5, 111.7, 72.7, 56.3, 35.1, 32.1, 25.8, 24.2. IR: 2922.6, 2856.6, 1716.9, 1647.0, 1515.0, 1458.7, 1417.9, 1177.2 cm^{-1}. HRMS: *Chemical formula* ([M]): C$_{17}$H$_{22}$O$_4$, calcd. [M+H]$^{+}$ 291.1596 Found: 291.1585.


3f
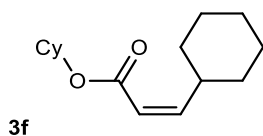
3f: Following a modified *General Procedure A*, the reaction was conducted using 2.0 equivalent (*instead of 1.6 equiv.*) of vinylcyclohexane (b.p. = 128 ˚C, 33.1 mg). The titled compound was isolated as a colorless oil (13.3 mg, 39% yield). Reaction time = 72 hours. *Z:E* ratio > 20:1 (determined by ^{1}H NMR analysis of the crude reaction mixture). R$_f$ = 0.47 (hexane/acetone = 100:3). Chromatography condition: hexane/acetone, 200:1. ^{1}H NMR (400 MHz, CDCl$_3$) δ 5.99 (dd, J = 11.5, 9.7 Hz, 1H), 5.63 (dd, J = 11.6, 1.1 Hz, 1H), 4.87 – 4.72 (m, 1H), 3.38 – 3.16 (m, 1H), 1.93 – 1.80 (m, 2H), 1.78 – 1.61 (m, 7H), 1.57 – 1.00 (m, 11H). ^{13}C NMR (101 MHz, CDCl$_3$) δ 166.3, 149.0, 120.9, 72.2, 38.3, 36.7, 33.2, 31.9, 26.6, 26.4, 25.6, 24.0. IR: 2926.5, 2856.6, 1715.0, 1641.2, 1452.9, 1414.1, 1361.6, 1262.6, 1173.3, 1122.8 cm^{-1}. HRMS: Chemical formula ([M]): C$_{15}$H$_{24}$O$_2$, calcd. [M+H]$^{+}$ 237.1855 Found: 237.1841.
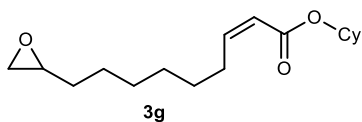
3g: Colorless oil (31.4 mg, 75% yield). Reaction time = 48 hours. *Z:E* ratio > 20:1 (determined by ^{1}H NMR analysis of the crude reaction mixture). R_f = 0.30 (hexane/ethyl acetate = 15:1). Chromatography condition: hexane/ethyl acetate, 30:1. ^{1}H NMR (400 MHz, CDCl$_3$) δ 6.18 (dt, *J* = 11.5, 7.5 Hz, 1H), 5.74 (dt, *J* = 11.6, 1.7 Hz, 1H), 4.83 – 4.75 (m, 1H), 2.94 – 2.85 (m, 1H), 2.74 (dd, *J* = 5.0, 3.9 Hz, 1H), 2.63 (qd, *J* = 7.4, 1.7 Hz, 2H), 2.45 (dd, *J* = 5.1, 2.7 Hz, 1H), 1.92 – 1.80 (m, 2H), 1.80 – 1.67 (m, 2H), 1.61 – 1.19 (m, 16H). ^{13}C NMR (101 MHz, CDCl$_3$) δ 166.2, 150.0, 120.5, 72.2, 52.5, 47.3, 32.6, 31.9, 29.4, 29.3, 29.1, 29.1, 26.0, 25.6, 24.0. IR: 2924.5, 2854.6, 1715.0, 1641.2, 1451.0, 1414.1, 1175.2 cm^{-1}. HRMS: Chemical formula ([M]): C$_{17}$H$_{28}$O$_3$, calcd. [M+H]$^+$ 281.2117 Found: 281.2129.
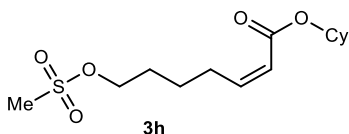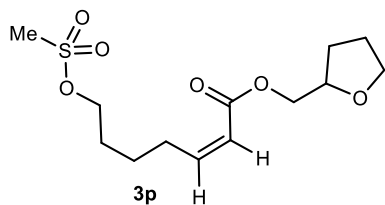

3h: Colorless oil (39.1 mg, 86% yield). Reaction time = 48 hours. *Z:E* ratio > 20:1 (determined by ^{1}H NMR analysis of the crude reaction mixture). R_f = 0.24 (hexane/ethyl acetate = 30:1). Chromatography condition: hexane/ethyl acetate, 60:1. ^{1}H NMR (400 MHz, CDCl$_3$) δ 6.15 (dt, *J* = 11.5, 7.6 Hz, 1H), 5.77 (dt, *J* = 11.5, 1.6 Hz, 1H), 4.87 – 4.68 (m, 1H), 4.23 (t, *J* = 6.4 Hz, 2H), 2.99 (s, 3H), 2.68 (qd, *J* = 7.6, 1.7 Hz, 2H), 1.94 – 1.67 (m, 6H), 1.62 – 1.21 (m, 8H). ^{13}C NMR (101 MHz, CDCl$_3$) δ 165.9, 148.6, 121.2, 72.4, 69.9, 37.4, 31.8, 28.7, 28.2, 25.5, 24.9, 23.9. IR:

2922.6, 2854.6, 1711.1, 1641.2, 1452.9, 1414.1, 1359.7, 1171.4, 1120.9 cm^{-1}. HRMS: Chemical

formula ([M]): $C_{14}H_{24}O_5S$, calcd. [M+H]$^+$ 305.1423 Found: 305.1407.

3i

3i: Colorless oil (28.3 mg, 64% yield). *The analysis of the ^1H NMR spectrum of the crude*

reaction mixture indicates a crude NMR yield of 86%, however, **3i** *appears to undergo partial*

oxidization during purification. Thus, proper precaution needs to be taken when handling this

chemical. Reaction time = 48 hours. *Z:E* ratio > 20:1 (determined by ^1H NMR analysis of the crude

reaction mixture). R_f = 0.09 (hexane/ethyl acetate = 30:1). Chromatography condition: hexane/ethyl

acetate, 30:1. ^1H NMR (400 MHz, CDCl$_3$) δ 9.75 (t, *J* = 1.8 Hz, 1H), 6.17 (dt, *J* = 11.5, 7.6 Hz, 1H),

5.73 (dt, *J* = 11.5, 1.7 Hz, 1H), 4.95 – 4.65 (m, 1H), 2.62 (qd, *J* = 7.5, 1.7 Hz, 2H), 2.40 (td, *J* = 7.4,

1.9 Hz, 2H), 1.96 – 1.79 (m, 2H), 1.78 – 1.66 (m, 2H), 1.66 – 1.16 (m, 18H). ^{13}C NMR (101 MHz,

CDCl$_3$) δ 203.1, 166.2, 150.1, 120.4, 72.2, 44.0, 31.9, 29.4, 29.3, 29.3, 29.2, 29.1, 29.1, 25.6, 23.9,

22.2. IR: 2933.6, 2858.2, 2723.5, 1721.6, 1643.6, 1278.0, 1261.1, 1185.7 cm^{-1}. HRMS: Chemical

formula ([M]): $C_{18}H_{30}O_3$, calcd. [M+H]$^+$ 295.2273 Found: 295.2262.

3j

3j: Colorless oil (27.6 mg, 62% yield). Reaction time = 48 hours. *Z:E* ratio > 20:1 (determined by ^{1}H NMR analysis of the crude reaction mixture). R_f = 0.15 (hexane/diethyl ether = 10:1). Chromatography condition: hexane/diethyl ether, 10:1. ^{1}H NMR (400 MHz, CD$_2$Cl$_2$) δ 6.11 (dt, *J* = 11.5, 7.5 Hz, 1H), 5.64 (dt, *J* = 11.6, 1.8 Hz, 1H), 2.57 (qd, *J* = 7.5, 1.8 Hz, 2H), 1.53 – 1.48 (m, 2H), 1.46 (s, 9H), 1.21 (s, 12H), 0.77 (t, *J* = 7.9 Hz, 2H). ^{13}C NMR (101 MHz, CD$_2$Cl$_2$) δ 166.1, 149.0, 121.9, 83.2, 80.1, 31.6, 28.3, 25.0, 24.0. IR: 2979.4, 2933.6, 2866.3, 1716.3, 1643.6, 1368.8, 1277.3, 1142.6 cm^{-1}. HRMS: Chemical formula ([M]): C$_{16}$H$_{29}$BO$_4$, calcd. [M+H]$^+$ 297.2237 Found: 297.2218.
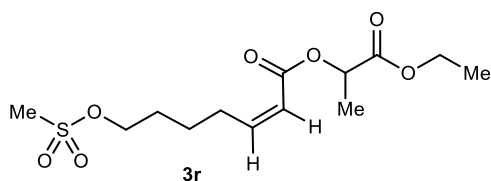

3k
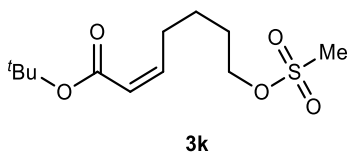
3k: Following a modified *General Procedure A*, the reaction was conducted using 0.02 equivalent (*instead of 0.03 equiv.*) of **Ru-4** (2.3 mg). The titled compound was isolated as a colorless oil (35.1 mg, 84% yield). Reaction time = 48 hours. *Z:E* ratio > 20:1 (determined by ^{1}H NMR analysis of the crude reaction mixture). R_f = 0.25 (hexane/ethyl acetate = 3:1). Chromatography condition: hexane/ethyl acetate, 6:1. ^{1}H NMR (400 MHz, CDCl$_3$) δ 6.07 (dt, *J* = 11.5, 7.5 Hz, 1H), 5.71 (dt, *J* = 11.5, 1.7 Hz, 1H), 4.24 (t, *J* = 6.4 Hz, 2H), 3.00 (s, 3H), 2.66 (qd, *J* = 7.5, 1.7 Hz, 2H), 1.84 – 1.73 (m, 2H), 1.62 – 1.50 (m, 2H), 1.47 (s, 9H). ^{13}C NMR (101 MHz, CDCl$_3$) δ 166.0, 147.6, 122.4, 80.3, 69.9, 37.4, 28.7, 28.3, 28.0, 25.0. IR: 2982.1, 2936.3, 2863.6, 1713.6, 1638.2, 1352.7, 1145.3 cm^{-1}. HRMS: *Chemical formula* ([M]): C$_{12}$H$_{22}$O$_5$S, calcd. [M+H]$^+$ 279.1266 Found: 279.1282.
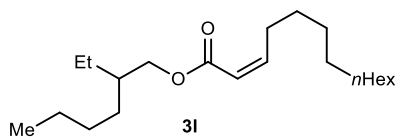
3l: Following a modified *General Procedure A*, the reaction was conducted using 2.0 equivalent (*instead of 1.6 equiv.*) of 1-dodecene (50.4 mg) and 0.04 equivalent (*instead of 0.03 equiv.*) of **Ru-4** (4.6 mg). The titled compound was isolated as a colorless oil (37.5 mg, 77% yield). Reaction time = 48 hours. *Z:E* ratio > 20:1 (determined by ^{1}H NMR analysis of the crude reaction mixture). R_f = 0.19 (hexane/acetone = 100:1). Chromatography condition: hexane/acetone, 200:1. ^{1}H NMR (400 MHz, CDCl$_3$) δ 6.20 (dt, *J* = 11.5, 7.5 Hz, 1H), 5.76 (dt, *J* = 11.5, 1.7 Hz, 1H), 4.13 – 3.96 (m, 2H), 2.63 (qd, *J* = 7.5, 1.7 Hz, 2H), 1.64 – 1.57 (m, 1H), 1.46 – 1.24 (m, 24H), 0.90 (dd, *J* = 8.6, 6.5 Hz, 9H). ^{13}C NMR (101 MHz, CDCl$_3$) δ 167.0, 150.5, 119.9, 66.4, 38.9, 32.1, 30.6, 29.9, 29.7, 29.6, 29.5, 29.5, 29.3, 29.3, 29.1, 24.0, 23.1, 22.8, 14.3, 14.2, 11.2. IR: 2924.5, 2854.6, 1720.8, 1645.1, 1458.7, 1412.1, 1171.4, 1122.8 cm^{-1}. HRMS: Chemical formula ([M]): C$_{21}$H$_{40}$O$_2$, calcd. [M+H]$^+$ 325.3107 Found: 325.3123.

3m: Following a modified *General Procedure A*, the reaction was conducted using 2.0 equivalent (*instead of 1.6 equiv.*) of 1-dodecene (50.4 mg) and 0.05 equivalent (*instead of 0.03 equiv.*) of **Ru-4** (5.7 mg). The titled compound was isolated as a colorless oil (34.8 mg, 77% yield). Reaction time = 48 hours. *Z:E* ratio > 20:1 (determined by ^{1}H NMR analysis of the crude reaction mixture).

R$_f$ = 0.23 (hexane/ethyl acetate = 30:1). Chromatography condition: hexane/ ethyl acetate, 60:1. ^{1}H NMR (400 MHz, CDCl$_3$) δ 7.42 – 7.29 (m, 5H), 6.26 (dt, J = 11.5, 7.5 Hz, 1H), 5.81 (dt, J = 11.5, 1.7 Hz, 1H), 5.16 (s, 2H), 2.66 (qd, J = 7.5, 1.8 Hz, 2H), 1.49 – 1.37 (m, 2H), 1.36 – 1.18 (m, 14H), 0.88 (t, J = 6.7 Hz, 3H). ^{13}C NMR (101 MHz, CDCl$_3$) δ 166.4, 151.6, 136.3, 128.7, 128.3, 128.3, 119.4, 65.8, 32.1, 29.7, 29.7, 29.6, 29.5, 29.5, 29.3, 29.2, 22.8, 14.3. IR: 2922.6, 2854.6, 1720.8, 1641.2, 1454.8, 1412.1, 1173.3, 1124.8 cm^{-1}. HRMS: Chemical formula ([M]): C$_{20}$H$_{30}$O$_2$, calcd. [M+H]$^+$ 303.2324 Found: 303.2340.
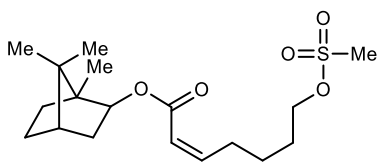
3n

3n: Colorless oil (36.9 mg, 69% yield). Reaction time = 72 hours. *Z:E* ratio > 20:1 (determined by ^{1}H NMR analysis of the crude reaction mixture). R$_f$ = 0.3 (hexane/ethyl acetate = 3:1). Chromatography condition: hexane/ethyl acetate, 6:1. ^{1}H NMR (400 MHz, CDCl$_3$) δ 6.15 (dt, J = 11.5, 7.6 Hz, 1H), 5.77 (dt, J = 11.5, 1.7 Hz, 1H), 4.68 (dd, J = 7.7, 3.6 Hz, 1H), 4.24 (t, J = 6.4 Hz, 2H), 3.00 (s, 3H), 2.70 (qd, J = 7.5, 1.7 Hz, 2H), 1.98 – 1.51 (m, 9H), 1.21 – 1.05 (m, 2H), 0.98 (s, 3H), 0.84 (s, 3H), 0.84 (s, 3H). ^{13}C NMR (101 MHz, CDCl$_3$) δ 166.1, 148.7, 121.1, 80.8, 69.9, 48.8, 47.1, 45.2, 39.1, 37.5, 34.0, 28.8, 28.2, 27.2, 25.0, 20.3, 20.1, 11.7. IR: 3006.3, 2952.5, 2874.4, 1713.6, 1643.6, 1352.7, 1172.2, 1056.4 cm^{-1}. HRMS: Chemical formula ([M]): C$_{18}$H$_{30}$O$_5$S, calcd. [M+H]$^+$ 359.1892 Found: 359.1877. The isolated **3n** contains 2~3% inseparable impurity, which is likely derived from the impurities in the commercial isobornyl acrylate.

3o
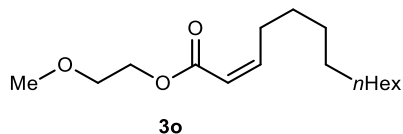
3o: Following a modified *General Procedure A*, the reaction was conducted using 2.0 equivalent (*instead of 1.6 equiv.*) of 1-dodecene (50.4 mg) and 0.033 equivalent (*instead of 0.03 equiv.*) of **Ru-4** (3.8 mg). The titled compound was isolated as a colorless oil (25.6 mg, 63% yield). Reaction time = 24 hours. *Z:E* ratio > 20:1 (determined by ^{1}H NMR analysis of the crude reaction mixture). R_f = 0.18 (hexane/ethyl acetate = 30:1). Chromatography condition: hexane/ethyl acetate, 60:1. ^{1}H NMR (400 MHz, CDCl$_3$) δ 6.24 (dt, *J* = 11.5, 7.5 Hz, 1H), 5.80 (dt, *J* = 11.5, 1.7 Hz, 1H), 4.33 – 4.15 (m, 2H), 3.69 – 3.59 (m, 2H), 3.39 (s, 3H), 2.64 (qd, *J* = 7.5, 1.7 Hz, 2H), 1.46 – 1.24 (m, 16H), 0.87 (t, *J* = 6.7 Hz, 3H). ^{13}C NMR (101 MHz, CDCl$_3$) δ 166.5, 151.6, 119.3, 70.7, 63.0, 59.1, 32.0, 29.7, 29.7, 29.6, 29.5, 29.2, 29.2, 22.8, 14.2. IR: 2922.6, 2854.6, 1720.8, 1643.2, 1456.8, 1417.9, 1175.2, 1126.7 cm^{-1}. HRMS: Chemical formula ([M]): C$_{16}$H$_{30}$O$_3$, calcd. [M+H]$^+$ 271.2273 Found: 271.2273.

3p

3p: Following a modified *General Procedure A*, the reaction was conducted using 2.0 equivalent (*instead of 1.6 equiv.*) of **2h** (hex-5-en-1-yl methanesulfonate, 53.5 mg) and 0.04 equivalent (*instead of 0.03 equiv.*) of **Ru-4** (4.6 mg). The titled compound was isolated as a colorless oil (33.0 mg, 72% yield). Reaction time = 48 hours. *Z:E* ratio > 20:1 (determined by ^{1}H NMR

analysis of the crude reaction mixture). $R_f = 0.20$ (hexane/diethyl ether = 1:2). Chromatography condition: hexane/diethyl ether, 1:1. ^{1}H NMR (400 MHz, CDCl$_3$) δ 6.21 (dt, $J = 11.5$, 7.6 Hz, 1H), 5.86 (dt, $J = 11.4$, 1.6 Hz, 1H), 4.24 (t, $J = 6.4$ Hz, 2H), 4.21 – 4.09 (m, 2H), 4.03 (dd, $J = 11.1$, 6.6 Hz, 1H), 3.89 (dt, $J = 8.4$, 6.7 Hz, 1H), 3.80 (ddd, $J = 8.3$, 7.2, 6.2 Hz, 1H), 3.00 (s, 3H), 2.71 (qd, $J = 7.6$, 1.7 Hz, 2H), 2.07 – 1.96 (m, 1H), 1.96 – 1.85 (m, 2H), 1.85 – 1.74 (m, 2H), 1.66 – 1.54 (m, 3H). ^{13}C NMR (101 MHz, CDCl$_3$) δ 166.3, 149.8, 120.4, 76.7, 69.8, 68.6, 66.2, 37.5, 28.7, 28.2, 28.2, 25.8, 24.9. IR: 2925.5, 1719.0, 1643.6, 1417.3, 1355.4, 1169.5, 1088.7 cm^{-1}. HRMS: Chemical formula ([M]): C$_{13}$H$_{22}$O$_6$S, calcd. [M+H]$^+$ 307.1215 Found: 307.1237.
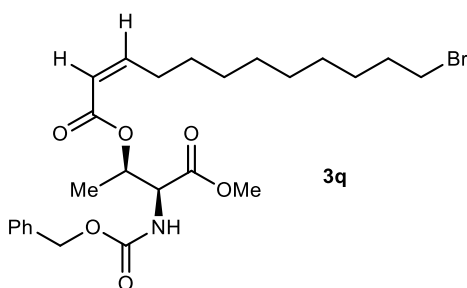
3q: Following a modified *General Procedure A*, the reaction was conducted using 0.05 equivalent (*instead of 0.03 equiv.*) of **Ru-4** (5.7 mg). The titled compound was isolated as a colorless oil (66.2 mg, 84% yield). Reaction time = 48 hours. *Z:E* ratio = 17:1 (determined by ^{1}H NMR analysis of the crude reaction mixture). $R_f = 0.25$ (hexane/ethyl acetate = 6:1). Chromatography condition: hexane/diethyl ether, 6:1. ^{1}H NMR (400 MHz, CDCl$_3$) δ 7.44 – 7.29 (m, 5H), 6.24 (dt, $J = 11.5$, 7.5 Hz, 1H), 5.67 (dt, $J = 11.5$, 1.7 Hz, 1H), 5.54 – 5.35 (m, 2H), 5.14 (d, $J = 2.3$ Hz, 2H), 4.51 (dd, $J = 9.7$, 2.5 Hz, 1H), 3.72 (s, 3H), 3.39 (t, $J = 6.9$ Hz, 2H), 2.59 (qd, $J = 7.4$, 1.7 Hz, 2H), 1.90 – 1.78 (m, 2H), 1.46 – 1.36 (m, 4H), 1.35 – 1.24 (m, 11H). ^{13}C NMR (101 MHz, CDCl$_3$) δ

170.5, 165.0, 156.6, 152.3, 136.2, 128.7, 128.4, 128.3, 118.8, 69.8, 67.5, 57.8, 52.9, 34.2, 32.9, 29.4, 29.4, 29.4, 29.4, 29.2, 29.0, 28.8, 28.3, 17.3. IR: 3426.5, 2928.2, 2852.8, 1751.3, 1724.3, 1517.0, 1266.5, 1161.5 cm^{-1}. HRMS: *Chemical formula* ([M]): C$_{25}$H$_{36}$BrNO$_6$, calcd. [M+H]$^+$ 526.1804 Found: 526.1807.

3r: Following a modified *General procedure*, the reaction was conducted using 0.05 equivalent (*instead of 0.03 equiv.*) of **Ru-4** (5.7 mg). The titled compound was isolated as a colorless oil (36.4 mg, 76% yield). Reaction time = 48 hours. *Z:E* ratio > 20:1 (determined by ^{1}H NMR analysis of the crude reaction mixture). R$_f$ = 0.14 (hexane/diethyl ether = 1:1). Chromatography condition: hexane/diethyl ether, 1:1. ^{1}H NMR (400 MHz, CDCl$_3$) δ 6.27 (dt, *J* = 11.5, 7.6 Hz, 1H), 5.89 (dt, *J* = 11.5, 1.6 Hz, 1H), 5.08 (q, *J* = 7.1 Hz, 1H), 4.28 – 4.12 (m, 4H), 3.00 (s, 3H), 2.70 (qd, *J* = 7.5, 1.7 Hz, 2H), 1.84 – 1.72 (m, 2H), 1.65 – 1.53 (m, 2H), 1.50 (d, *J* = 7.1 Hz, 3H), 1.27 (t, *J* = 7.2 Hz, 3H). ^{13}C NMR (101 MHz, CDCl$_3$) δ 171.0, 165.5, 150.6, 119.8, 69.8, 68.5, 61.5, 37.4, 28.7, 28.2, 24.8, 17.1, 14.2. IR: 3009.0, 2990.2, 2939.0, 1748.6, 1716.3, 1648.9, 1360.8, 1274.6, 1166.8 cm^{-1}. HRMS: *Chemical formula* ([M]): C$_{13}$H$_{22}$O$_7$S, calcd. [M+H]$^+$ 323.1164 Found: 323.1168.
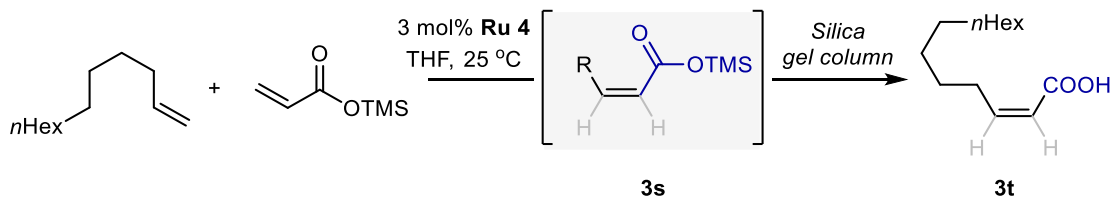
3t was prepared following *General Procedure A* using trimethylsilyl acrylate (21.6 mg, 0.15 mmol, 1 equiv) and 1-dodecene (40.3 mg, 0.24 mmol, 1.6 equiv). Reaction time = 48 hours. The trimethylsilyl tridec-2-enoate intermediate (**3s**) was unstable on column. Upon chromatography purification, **3t** was obtained as a yellow oil (20.1 mg, 63% yield). *Z:E* ratio > 20:1 (determined by ^{1}H NMR analysis of the crude reaction mixture). R_f = 0.32 (hexane/ethyl acetate = 5:1). Chromatography condition: hexane/ethyl acetate, 10:1. ^{1}H NMR (400 MHz, CDCl$_3$) δ 11.25 (br, 1H), 6.35 (dt, *J* = 11.5, 7.5 Hz, 1H), 5.78 (dt, *J* = 11.6, 1.7 Hz, 1H), 2.66 (qd, *J* = 7.5, 1.8 Hz, 2H), 1.51 – 1.39 (m, 2H), 1.39 – 1.19 (m, 14H), 0.92 – 0.83 (m, 3H). ^{13}C NMR (101 MHz, CDCl$_3$) δ 172.2, 153.8, 119.1, 32.1, 29.7, 29.7, 29.6, 29.5, 29.4, 29.4, 29.1, 22.8, 14.3. IR: 3060.2, 2960.5, 2928.2, 2850.1, 1694.7, 1640.8, 1438.9, 1239.6 cm^{-1}. HRMS: *Chemical formula* ([M]): C$_{13}$H$_{24}$O$_2$, calcd. [M+H]$^+$ 213.1855 Found: 213.1881.
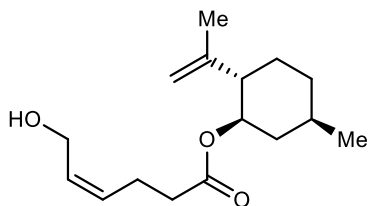
5b

5b: Colorless oil (24.4 mg, 61% yield). *Z:E* ratio > 20:1 (determined by ^{1}H NMR analysis of the crude reaction mixture). R_f = 0.2 (hexane/diethyl ether = 7:3). Chromatography condition: hexane/diethyl ether, 5:1. ^{1}H NMR (400 MHz, CDCl$_3$) δ 5.72 – 5.61 (m, 1H), 5.51 – 5.39 (m, 1H), 4.79 (td, *J* = 10.9, 4.4 Hz, 1H), 4.74 – 4.64 (m, 2H), 4.24 – 4.10 (m, 2H), 2.42 – 2.29 (m, 4H), 2.08 (ddd, *J* = 12.5, 10.7, 3.7 Hz, 1H), 2.03 – 1.91 (m, 2H), 1.73 – 1.65 (m, 2H), 1.64 (dd, *J* = 1.4, 0.9 Hz, 3H), 1.60 – 1.46 (m, 1H), 1.43 – 1.30 (m, 1H), 1.07 – 0.85 (m, 5H). ^{13}C NMR (101 MHz, CDCl$_3$) δ

172.8, 146.3, 131.0, 129.9, 111.9, 73.9, 58.3, 50.9, 40.6, 34.2, 34.0, 31.5, 30.4, 22.8, 22.1, 19.6. IR: 3389.2, 3072.9, 3007.6, 2950.2, 2926.6, 2869.2, 1728.4, 1647.4, 1451.6, 1380.5, 1275.7, 1257.9, 1170.9, 1129.4 cm^{-1}. HRMS: *Chemical formula* ([M]): $C_{16}H_{26}O_3$, calcd. [M+H]$^+$ 267.1960 Found: 267.1947.

5c
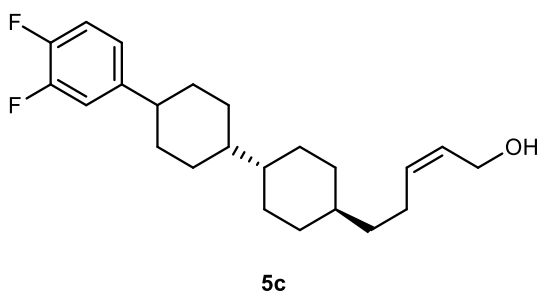
5c: Colorless wax (30.3 mg, 56% yield). *Z:E* ratio > 20:1 (determined by ^{1}H NMR analysis of the crude reaction mixture). R$_f$ = 0.20 (hexane/diethyl ether = 7:3). Chromatography condition: hexane/diethyl ether, 5:1. ^{1}H NMR (400 MHz, CDCl$_3$) δ 7.10 – 6.93 (m, 2H), 6.89 (ddd, *J* = 8.6, 4.2, 1.9 Hz, 1H), 5.71 – 5.42 (m, 2H), 4.23 – 4.17 (m, 2H), 2.40 (tt, *J* = 12.2, 3.4 Hz, 1H), 2.09 (dt, *J* = 8.3, 6.5 Hz, 2H), 1.94 – 1.69 (m, 8H), 1.43 – 1.29 (m, 2H), 1.29 – 0.80 (m, 12H). ^{13}C NMR (101 MHz, CDCl$_3$) carbon signals were observed at δ 151.6, 151.4, 149.9, 149.8, 149.1, 149.0, 147.5, 147.4, 145.0, 145.0, 145.0, 144.9, 133.7, 128.2, 122.7, 122.6, 122.6, 122.6, 117.0, 116.8, 115.6, 115.4, 58.8, 44.0, 43.4, 42.9, 37.6, 37.5, 37.4, 34.7, 33.5, 30.3, 30.1, 25.1. IR: 3279.8, 3006.1, 2916.8, 2846.9, 1606.3, 1517.0, 1451.0, 1435.4, 1276.2, 1210.2, 1198.6, 1115.1, 1018.0 cm^{-1}. HRMS: *Chemical formula* ([M]): $C_{23}H_{32}F_2O$, calcd. [M$^+$] 362.2416 Found: 362.2440.

5d
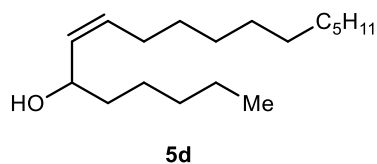
5d: The reaction was conducted following a modified *General Procedure B*, in which oct-1-en-3-ol was used as the limiting reagent (0.15 mmol, 1 equiv, 19.2 mg) and 1-dodecene was added in excess (1.2 mmol, 8 equiv, 202 mg). **5d** was isolated as a colorless oil (27.3 mg, 68% yield). *Z:E* ratio > 20:1 (determined by ^{1}H NMR analysis of the crude reaction mixture). R_f = 0.40 (hexane/diethyl ether = 7:3). Chromatography condition: hexane/diethyl ether, 10:1. ^{1}H NMR (400 MHz, CDCl$_3$) δ 5.48 (dtd, *J* = 10.9, 7.4, 0.9 Hz, 1H), 5.35 (ddt, *J* = 10.6, 8.8, 1.5 Hz, 1H), 4.42 (q, *J* = 7.5, 7.0 Hz, 1H), 2.15 – 2.01 (m, 2H), 1.61 – 1.51 (m, 1H), 1.44 – 1.23 (m, 24H), 0.92 – 0.84 (m, 6H). ^{13}C NMR (101 MHz, CDCl$_3$) δ 132.7, 132.5, 67.9, 37.6, 32.1, 32.0, 29.9, 29.8, 29.6, 29.5, 29.4, 27.9, 25.2, 22.8, 22.8, 14.3, 14.2. IR: 3330.3, 3010.0, 2955.6, 2926.5, 2854.6, 1466.5, 1379.1, 1278.2, 1264.6, 1124.8, 1060.7 cm^{-1}. HRMS: *Chemical formula* ([M]): C$_{18}$H$_{36}$O, calcd. [M+H-H$_2$]$^+$ 267.2688 Found: 267.2711.

5e
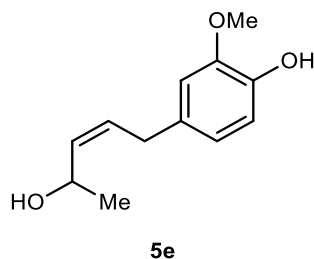
5e: Following a modified *General Procedure B*, the reaction was conducted at 0.1 mmol scale, using 0.10 mmol of eugenol (16.4 mg), 8.0 equivalent (*instead of 4.0 equiv.*) of 3-buten-2-ol (0.8 mmol, 57.6 mg) and 0.04 equivalent (*instead of 0.025 equiv.*) of **Ru-6** (3.3 mg). The titled

compound was isolated as a colorless oil (15.3 mg, 74% yield). *Z:E* ratio > 20:1 (determined by ^{1}H NMR analysis of the crude reaction mixture). R$_f$ = 0.24 (hexane/diethyl ether = 3:7). Chromatography condition: hexane/diethyl ether, 1:1. ^{1}H NMR (400 MHz, CDCl$_3$) δ 6.89 – 6.80 (m, 1H), 6.73 – 6.61 (m, 2H), 5.70 – 5.34 (m, 3H), 4.77 (tt, *J* = 9.2, 6.4 Hz, 1H), 3.87 (s, 3H), 3.50 – 3.32 (m, 2H), 1.49 (d, *J* = 3.3 Hz, 1H), 1.31 (d, *J* = 6.3 Hz, 3H). ^{13}C NMR (101 MHz, CDCl$_3$) δ 146.7, 144.1, 134.5, 132.3, 129.9, 120.9, 114.5, 111.0, 64.0, 56.0, 33.5, 23.9. IR: 3375.0, 3013.8, 2969.2, 2932.3, 2841.0, 1602.4, 1517.0, 1464.5, 1451.0, 1435.4, 1387.5, 1276.2, 1266.5, 1233.5, 1210.2, 1152.0, 1122.8, 1062.6, 1037.4 cm^{-1}. HRMS: *Chemical formula* ([M]): C$_{12}$H$_{16}$O$_3$, calcd. [M$^+$] 208.1094 Found: 208.1077.

5f
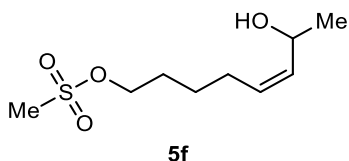
5f: Following a modified *General Procedure B*, the reaction was conducted at 0.1 mmol scale, using 0.10 mmol of **2h** (*hex-5-en-1-yl methanesulfonate*, 17.8 mg), 8.0 equivalent (*instead of 4.0 equiv.*) of 3-buten-2-ol (57.6 mg) and 0.04 equivalent (*instead of 0.025 equiv.*) of **Ru-6** (3.3 mg). The titled compound was isolated as a colorless oil (15.6 mg, 70% yield). *Z:E* ratio > 20:1 (determined by ^{1}H NMR analysis of the crude reaction mixture). R$_f$ = 0.19 (hexane/diethyl ether = 3:17). Chromatography condition: hexane/diethyl ether, 1:2. ^{1}H NMR (400 MHz, CDCl$_3$) δ δ 5.51 – 5.32 (m, 2H), 4.70 – 4.53 (m, 1H), 4.23 (t, *J* = 6.5 Hz, 2H), 3.00 (s, 3H), 2.24 – 2.05 (m, 2H), 1.83 – 1.71 (m, 2H), 1.62 (s, 1H), 1.55 – 1.44 (m, 2H), 1.25 (d, *J* = 6.3 Hz, 3H). ^{13}C NMR (101 MHz, CDCl$_3$) δ 134.8, 130.2, 69.9, 63.9, 37.5, 28.7, 26.9, 25.5, 23.8. IR: 3357.5, 3008.0, 2932.3, 2969.2,

2864.4, 1346.1, 1330.6, 1169.4, 1107.3, 1051.0 cm^{-1}. HRMS: *Chemical formula* ([M]): C$_9$H$_{18}$O$_4$S, calcd. [M+H-H$_2$]$^+$ 221.0848 Found: 221.0829.

5g
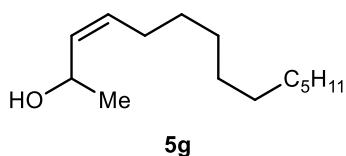
5g: Following a modified *General Procedure B*, the reaction was conducted at 0.1 mmol scale, using 0.10 mmol of 1-dodecene (16.8 mg), 8.0 equivalent (*instead of 4.0 equiv.*) of 3-buten-2-ol (57.6 mg) and 0.05 equivalent (*instead of 0.025 equiv.*) of **Ru-6** (4.1 mg). The titled compound was isolated as a colorless oil (15.5 mg, 73% yield). *Z:E* ratio > 20:1 (determined by ^{1}H NMR analysis of the crude reaction mixture). R$_f$ = 0.31 (hexane/diethyl ether = 7:3). Chromatography condition: hexane/diethyl ether, 5:1. ^{1}H NMR (400 MHz, CDCl$_3$) δ 5.47 – 5.36 (m, 2H), 4.70 – 4.58 (m, 1H), 2.13 – 2.01 (m, 2H), 1.45 – 1.16 (m, 20H), 0.96 – 0.82 (m, 3H). ^{13}C NMR (101 MHz, CDCl$_3$) δ 133.8, 131.6, 64.0, 32.0, 29.8, 29.8, 29.6, 29.5, 29.4, 27.7, 23.7, 22.8, 14.3. IR: 3334.2, 3011.9, 2955.6, 2922.6, 2852.7, 1458.7, 1367.5, 1276.2, 1111.2 cm^{-1}. HRMS: *Chemical formula* ([M]): C$_{14}$H$_{28}$O, calcd. [M+H-H$_2$]$^+$ 211.2062 Found: 211.2081.

2.7 References

(1) a) P. A. Wender, V. A. Verma, T. J. Paxton, T. H. Pillow, *Acc. Chem. Res.* **2008**, *41*, 40–49. b) Y. Hayashi, *Chem. Sci.* **2016**, *7*, 866–880. c) T. Newhouse, P. S. Baran, R. W. Hoffmann, *Chem.*

Soc. Rev. **2009**, *38*, 3010–3021. d) A. Borovika, J. Albrecht, J. Li, A. S. Wells, C. Briddell, B. R. Dillon, L. J. Diorazio, J. R. Gage, F. Gallou, S. G. Koenig, M. E. Kopach, D. K. Leahy, I. Martinez, M. Olbrich, J. L. Piper, F. Roschangar, E. C. Sherer, M. D. Eastgate, *Nat. Sustain.* **2019**, *2*, 1034–1040. e) D. S. Peters, C. R. Pitts, K. S. McClymont, T. P. Stratton, C. Bi, P. S. Baran, *Acc. Chem. Res.* **2021**, *54*, 605–617.

(2) For selected reviews, see: a) A. H. Hoveyda, R. K. M. Khan, S. Torker, S. J. Malcolmson, in *Handb. Metathesis*, John Wiley & Sons, Ltd, **2015**, pp. 503–562. b) M. B. Herbert, R. H. Grubbs, *Angew. Chem. Int. Ed.* **2015**, *54*, 5018–5024.

(3) For selected examples with molybdenum-based complexes, see: a) E. M. Townsend, R. R. Schrock, A. H. Hoveyda, *J. Am. Chem. Soc.* **2012**, *134*, 11334–11337. b) E. T. Kiesewetter, R. V. O'Brien, E. C. Yu, S. J. Meek, R. R. Schrock, A. H. Hoveyda, *J. Am. Chem. Soc.* **2013**, *135*, 6026–6029. c) H. Zhang, E. C. Yu, S. Torker, R. R. Schrock, A. H. Hoveyda, *J. Am. Chem. Soc.* **2014**, *136*, 16493–16496. d) E. C. Yu, B. M. Johnson, E. M. Townsend, R. R. Schrock, A. H. Hoveyda, *Angew. Chem. Int. Ed.* **2016**, *55*, 13210–13214.

(4) For selected examples with tungsten-based complexes, see: a) A. J. Jiang, Y. Zhao, R. R. Schrock, A. H. Hoveyda, *J. Am. Chem. Soc.* **2009**, *131*, 16630–16631. b) D. V. Peryshkov, R. R. Schrock, M. K. Takase, P. Müller, A. H. Hoveyda, *J. Am. Chem. Soc.* **2011**, *133*, 20754–20757.

(5) For selected examples with cyclometalated ruthenium complexes, see: a) K. Endo, R. H. Grubbs, *J. Am. Chem. Soc.* **2011**, *133*, 8525–8527. b) B. K. Keitz, K. Endo, P. R. Patel, M. B. Herbert, R. H. Grubbs, *J. Am. Chem. Soc.* **2012**, *134*, 693–699. c) L. E. Rosebrugh, M. B. Herbert, V. M. Marx, B. K. Keitz, R. H. Grubbs, *J. Am. Chem. Soc.* **2013**, *135*, 1276–1279. A related catalyst with an unsaturated NHC ligand: d) A. Dumas, R. Tarrieu, T. Vives, T. Roisnel, V. Dorcet, O.

Baslé, M. Mauduit, *ACS Catal.* **2018**, *8*, 3257–3262. e) Y. Xu, J. J. Wong, A. E. Samkian, J. H. Ko, S. Chen, K. N. Houk, R. H. Grubbs, *J. Am. Chem. Soc.* **2020**, *142*, 20987–20993.

(6) For selected examples with ruthenium monothiolate complexes, see: a) G. Occhipinti, F. R. Hansen, K. W. Törnroos, V. R. Jensen, *J. Am. Chem. Soc.* **2013**, *135*, 3331–3334. b) G. Occhipinti, K. W. Törnroos, V. R. Jensen, *Organometallics* **2017**, *36*, 3284–3292. c) W. Smit, J. B. Ekeli, G. Occhipinti, B. Woźniak, K. W. Törnroos, V. R. Jensen, *Organometallics* **2020**, *39*, 397–407.

(7) a) A. Lumbroso, M. L. Cooke, B. Breit, *Angew. Chem. Int. Ed.* **2013**, *52*, 1890–1932. b) D. K. Nomura, T. J. Maimone, in *Act.-Based Protein Profiling* (Eds.: B.F. Cravatt, K.-L. Hsu, E. Weerapana), Springer International Publishing, Cham, **2019**, pp. 351–374.

(8) In a recent report, an analog of **Ru-2** bearing an unsaturated NHC backbone was tested in the *Z*-selective cross-metathesis with an allyl alcohol substrate. A relatively low *Z*/*E* selectivity was reported (80:20 *Z*/*E* using a flow reactor and 65/35 *Z*/*E* in batch conditions), despite that much higher *Z*/*E* ratios were in general observed with common olefin substrates using this catalyst. For detail, see: J. Morvan, T. McBride, I. Curbet, S. Colombel-Rouen, T. Roisnel, C. Crévisy, D. L. Browne, M. Mauduit, *Angew. Chem. Int. Ed.* **2021**, *60*, 19685.

(9) a) M. J. Koh, R. K. M. Khan, S. Torker, M. Yu, M. S. Mikus, A. H. Hoveyda, *Nature* **2015**, *517*, 181–186. b) Z. Liu, C. Xu, J. del Pozo, S. Torker, A. H. Hoveyda, *J. Am. Chem. Soc.* **2019**, *141*, 7137–7146. c) C. Xu, X. Shen, A. H. Hoveyda, *J. Am. Chem. Soc.* **2017**, *139*, 10919–10928.

(10) For other examples with ruthenium-based stereoretentive catalysts, see: a) R. K. M. Khan, S. Torker, A. H. Hoveyda, *J. Am. Chem. Soc.* **2013**, *135*, 10258–10261. b) M. J. Koh, R. K. M. Khan, S. Torker, A. H. Hoveyda, *Angew. Chem. Int. Ed.* **2014**, *53*, 1968–1972. c) A. M. Johns, T. S. Ahmed, B. W. Jackson, R. H. Grubbs, R. L. Pederson, *Org. Lett.* **2016**, *18*, 772–775. d) T.

S. Ahmed, R. H. Grubbs, *J. Am. Chem. Soc.* **2017**, *139*, 1532–1537. For a review, see: e) T. P. Montgomery, T. S. Ahmed, R. H. Grubbs, *Angew. Chem. Int. Ed.* **2017**, *56*, 11024–11036.

(11) a) *Metathesis in Natural Product Synthesis: Strategies, Substrates, and Catalysis* (Eds.: J. Cossy, S. Arseniyadis, C. Meyer), Wiley-VCH, Weinheim, **2010**. b) "*Alkene Metathesis for Transformations of Renewables* in Organometallics for Green Catalysis": C. Bruneau, C. Fischmeister in *Topics in Organometallic Chemistry, Vol. 63* (Eds.: P. Dixneuf, J. F. Soulé), Springer, Heidelberg, **2018**.

(12) For selected examples of bulky-yet-flexible NHCs, see: a) G. Altenhoff, R. Goddard, C. W. Lehmann, F. Glorius, *J. Am. Chem. Soc.* **2004**, *126*, 15195–15201. b) X. Luan, R. Mariz, M. Gatti, C. Costabile, A. Poater, L. Cavallo, A. Linden, R. Dorta, *J. Am. Chem. Soc.* **2008**, *130*, 6848–6858. c) M. G. Organ, S. Çalimsiz, M. Sayah, K. H. Hoi, A. J. Lough, *Angew. Chem. Int. Ed.* **2009**, *48*, 2383–2387. d) S. Meiries, G. L. Duc, A. Chartoire, A. Collado, K. Speck, K. S. A. Arachchige, A. M. Z. Slawin, S. P. Nolan, *Chem. – Eur. J.* **2013**, *19*, 17358–17368.

(13) M. B. Herbert, Y. Lan, B. K. Keitz, P. Liu, K. Endo, M. W. Day, K. N. Houk, R. H. Grubbs, *J. Am. Chem. Soc.* **2012**, *134*, 7861–7866.

(14) S. Torker, R. K. M. Khan, A. H. Hoveyda, *J. Am. Chem. Soc.* **2014**, *136*, 3439–3455.

(15) For details, see Page S70 in reference 5e.

(16) For selected examples of bulky-yet-flexible NHCs, see: a) G. Altenhoff, R. Goddard, C. W. Lehmann, F. Glorius, *J. Am. Chem. Soc.* **2004**, *126*, 15195–15201. b) X. Luan, R. Mariz, M. Gatti, C. Costabile, A. Poater, L. Cavallo, A. Linden, R. Dorta, *J. Am. Chem. Soc.* **2008**, *130*, 6848–6858. c) M. G. Organ, S. Çalimsiz, M. Sayah, K. H. Hoi, A. J. Lough, *Angew. Chem. Int. Ed.* **2009**, *48*, 2383–2387. d) S. Meiries, G. L. Duc, A. Chartoire, A. Collado, K. Speck, K. S. A. Arachchige, A. M. Z. Slawin, S. P. Nolan, *Chem. – Eur. J.* **2013**, *19*, 17358–17368. For a

review, see: e) A. Gómez-Suárez, D. J. Nelson, S. P. Nolan, *Chem. Commun.* **2017**, *53*, 2650–2660.

(17) P. Liu, X. Xu, X. Dong, B. K. Keitz, M. B. Herbert, R. H. Grubbs, K. N. Houk, *J. Am. Chem. Soc.* **2012**, *134*, 1464–1467.

(18) B. L. Quigley, R. H. Grubbs, *Chem. Sci.* **2013**, *5*, 501–506.

(19) For a related traceless protection strategy, see: Y. Mu, T. T. Nguyen, F. W. van der Mei, R. R. Schrock, A. H. Hoveyda, *Angew. Chem. Int. Ed.* **2019**, *58*, 5365–5370.

(20) J. S. Cannon, R. H. Grubbs, *Angew. Chem. Int. Ed.* **2013**, *52*, 9001–9004.

Appendix 2. Spectra Relevant to Chapter 2

Figure B5. Crude ^{1}H NMR (400 MHz, CDCl$_3$) spectrum of **S2**.
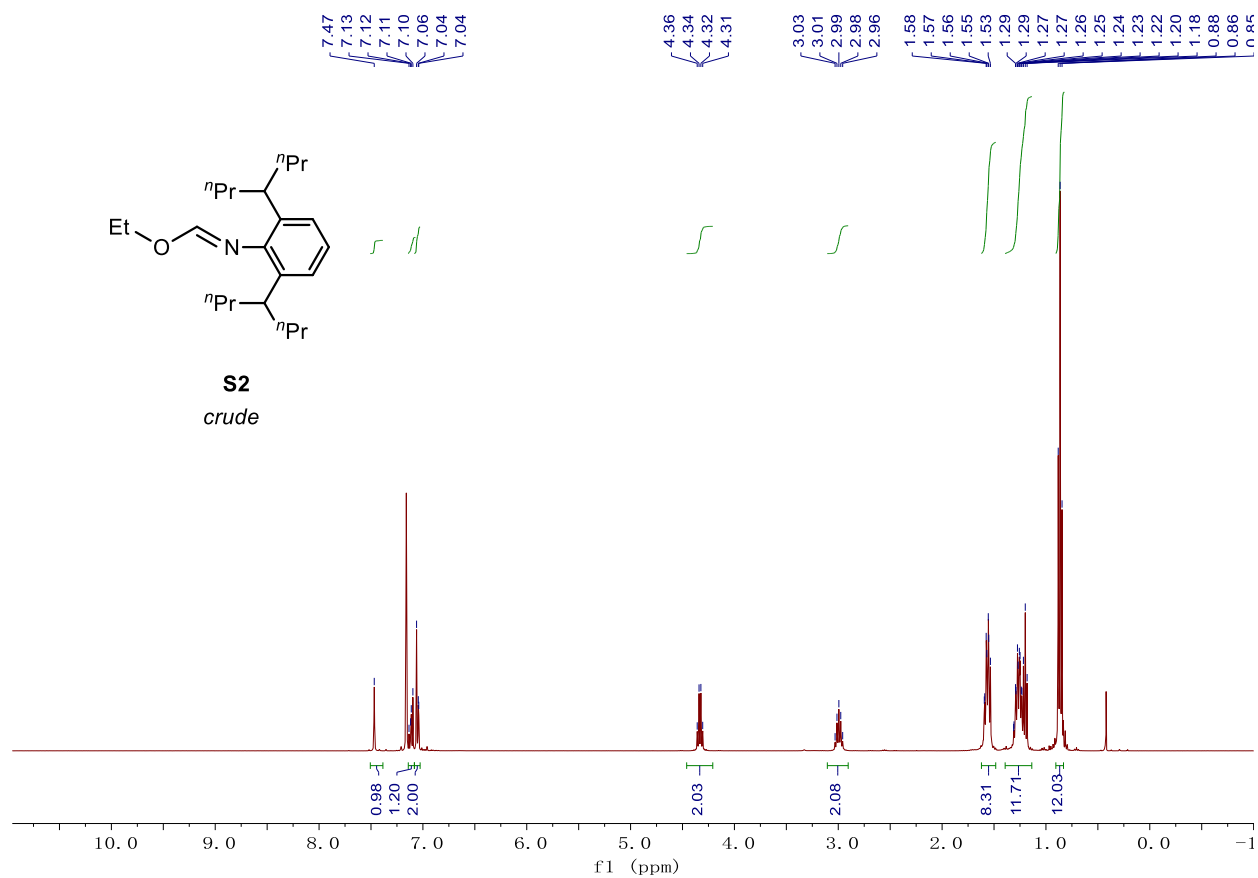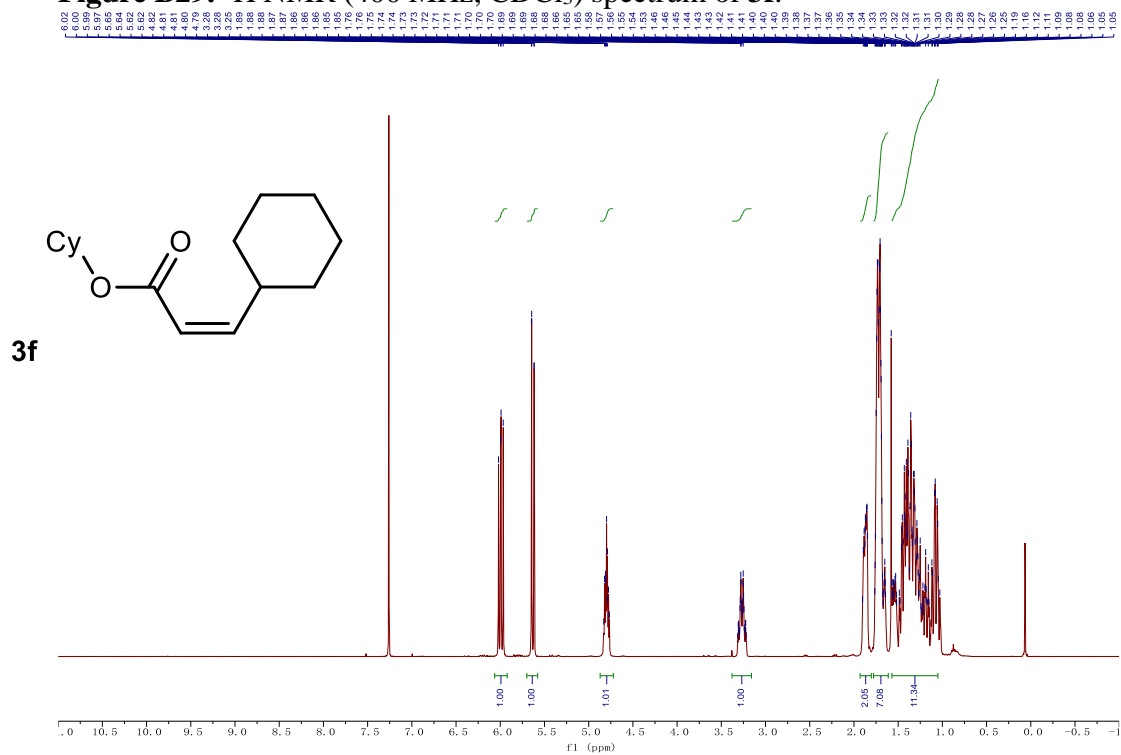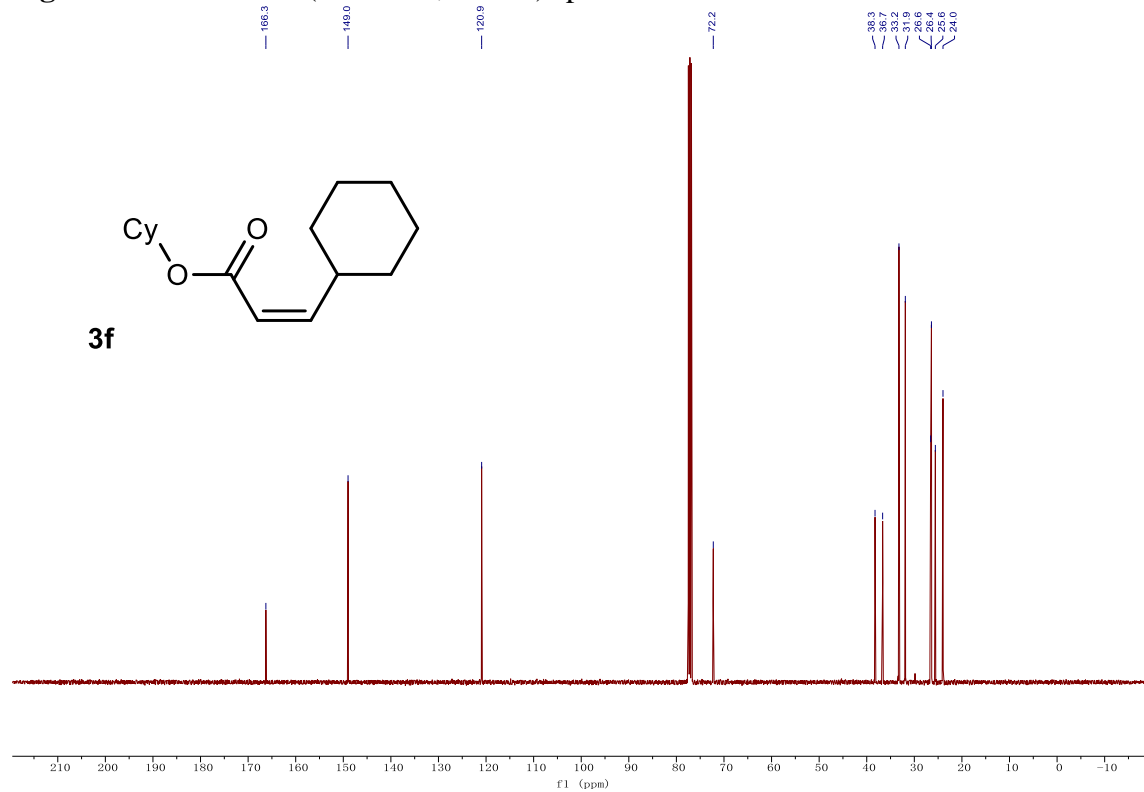
Figure B6. ^{1}H NMR (400 MHz, CDCl$_3$) spectrum of **S4**.
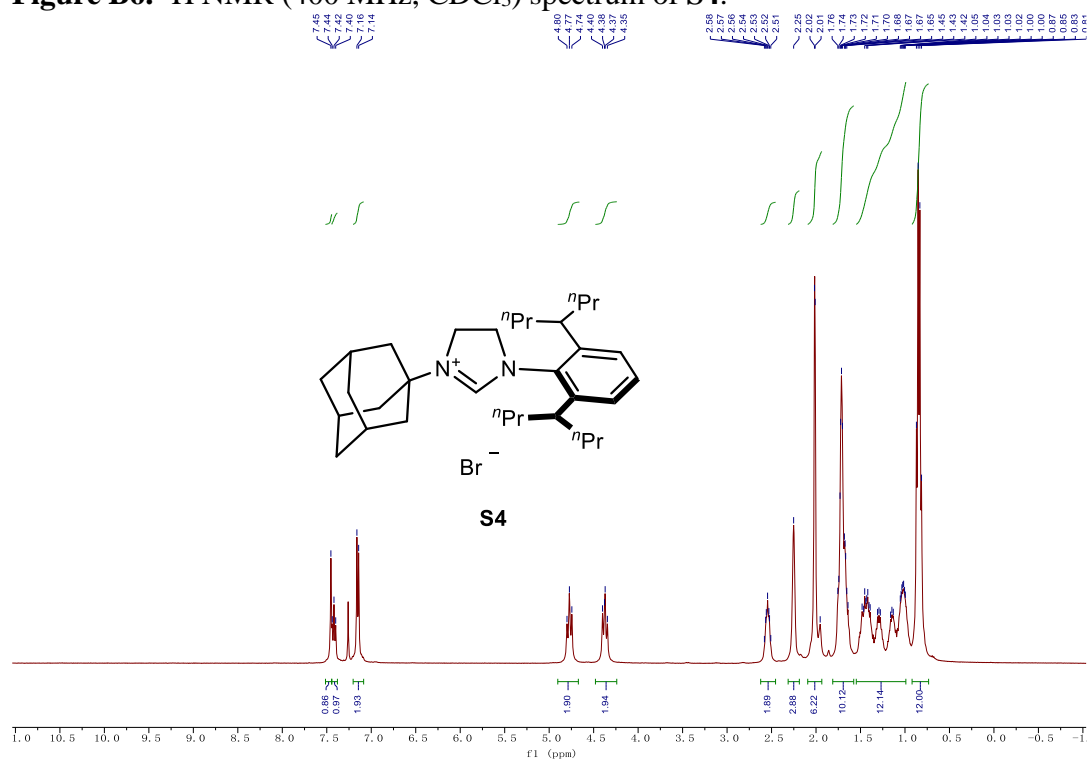
Figure B7. ^{13}C NMR (101 MHz, CDCl$_3$) spectrum of **S4**.
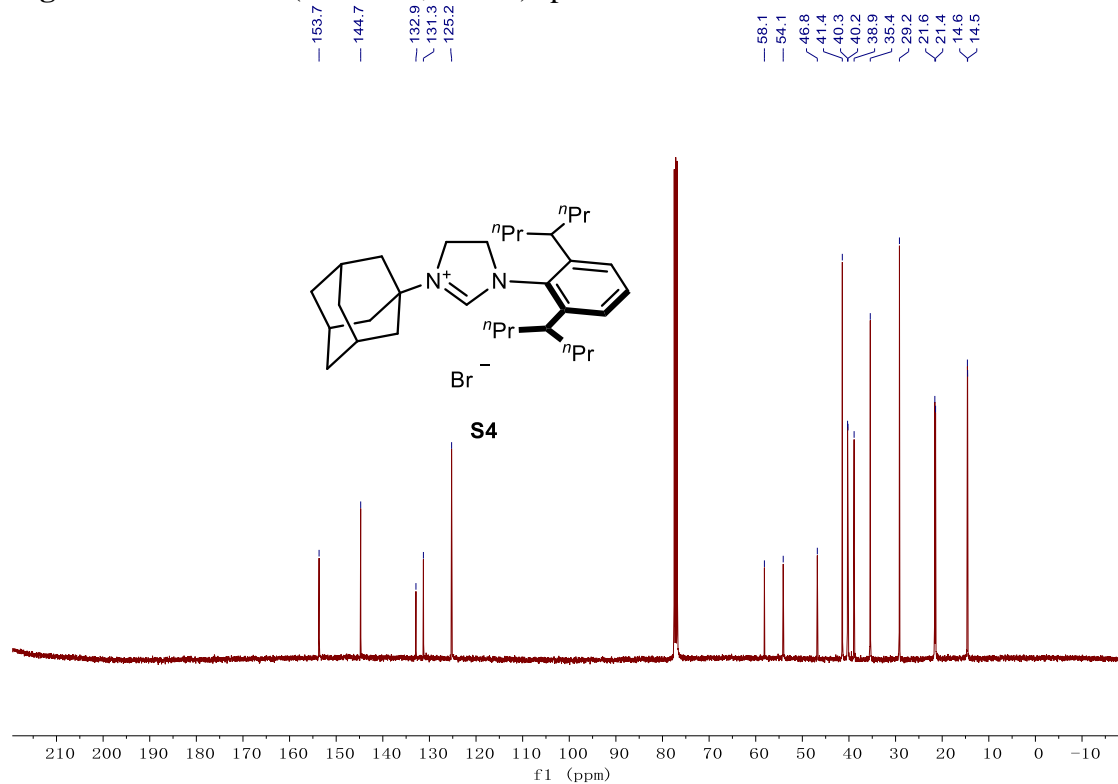
Figure B8. ^{1}H NMR (400 MHz, DMSO-d_6) spectrum of **A1**.
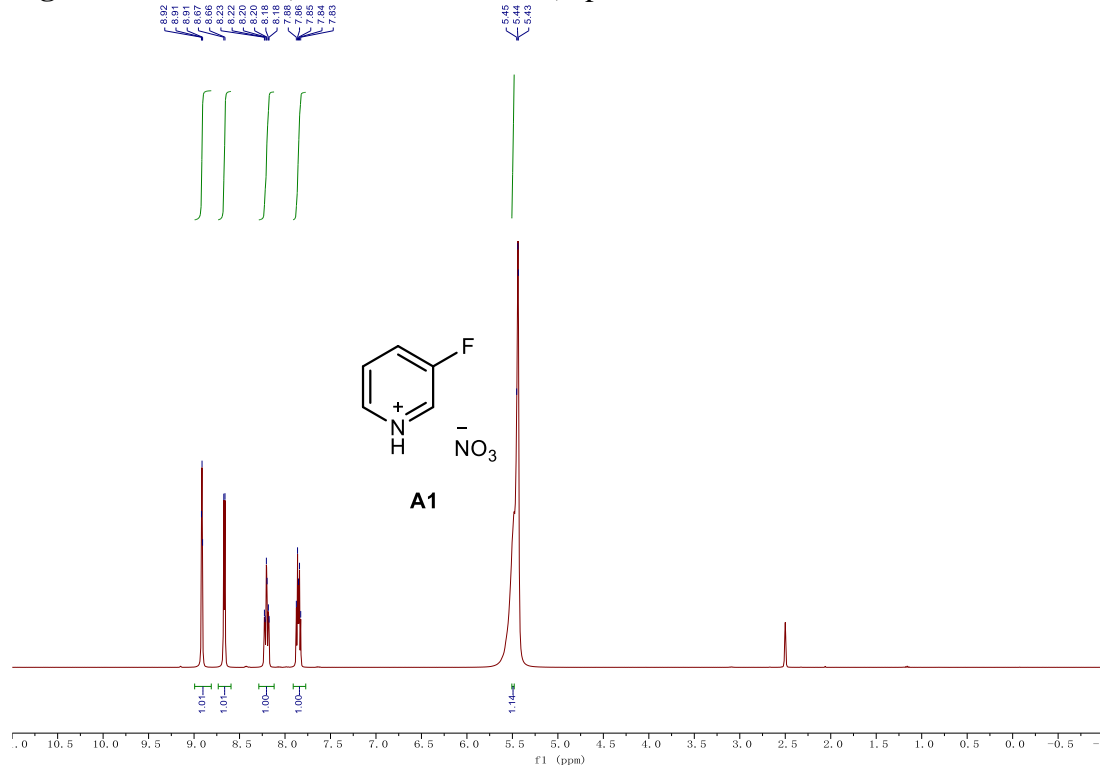
Figure B9. ^{13}C NMR (101 MHz, DMSO-d_6) spectrum of **A1**.
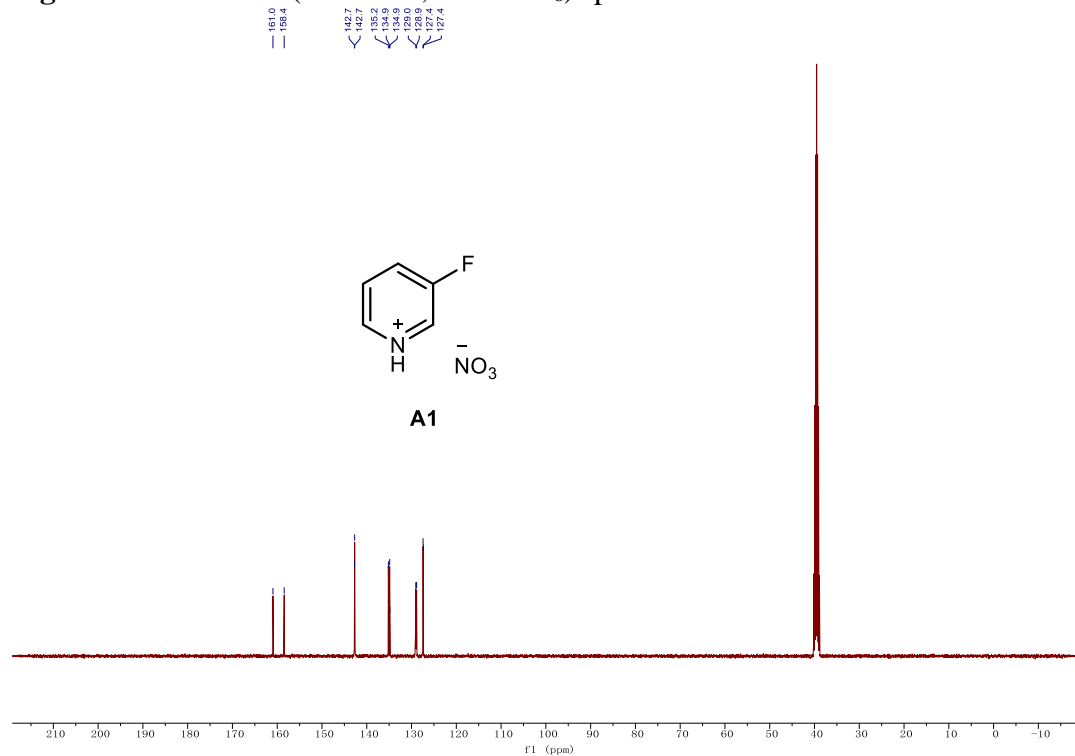
Figure B10. Crude ^{1}H NMR (400 MHz, C$_6$D$_6$) spectrum of **Ru-S3**.
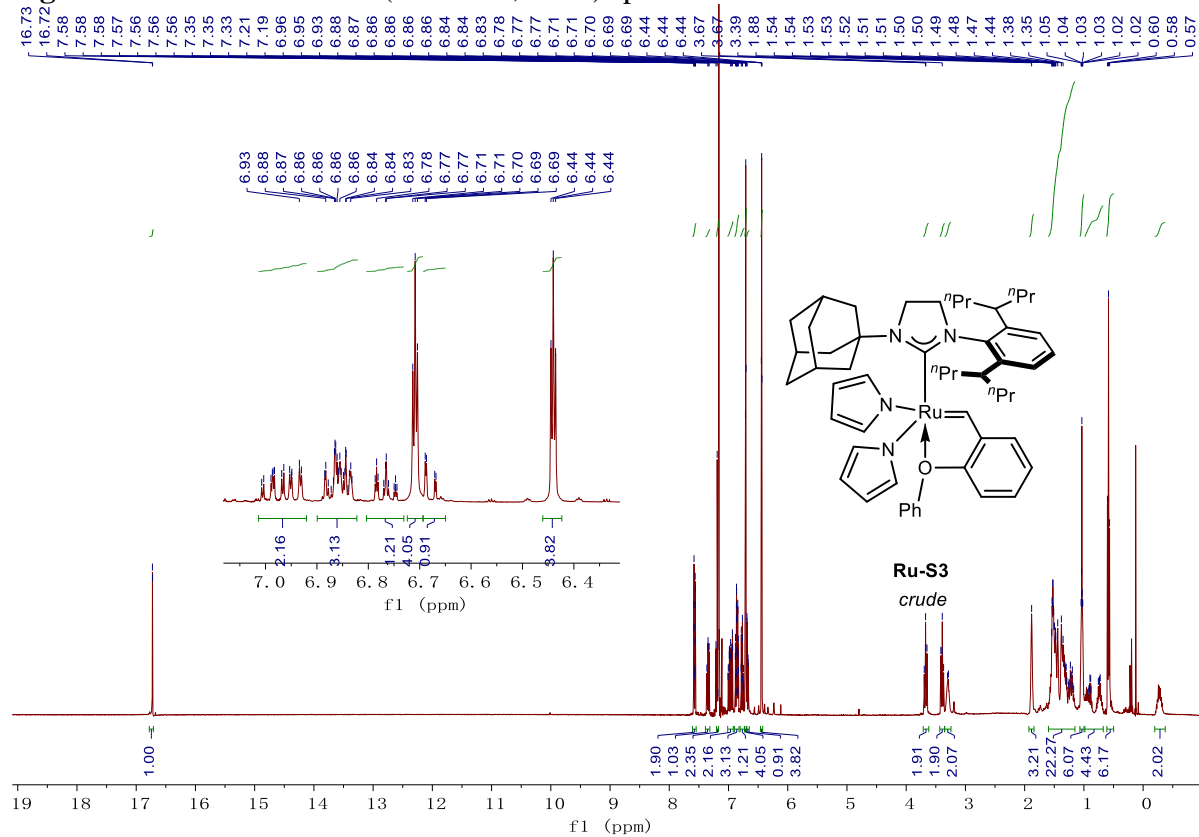
Figure B11. ^{1}H NMR (400 MHz, C$_6$D$_6$) spectrum of **Ru-5**.
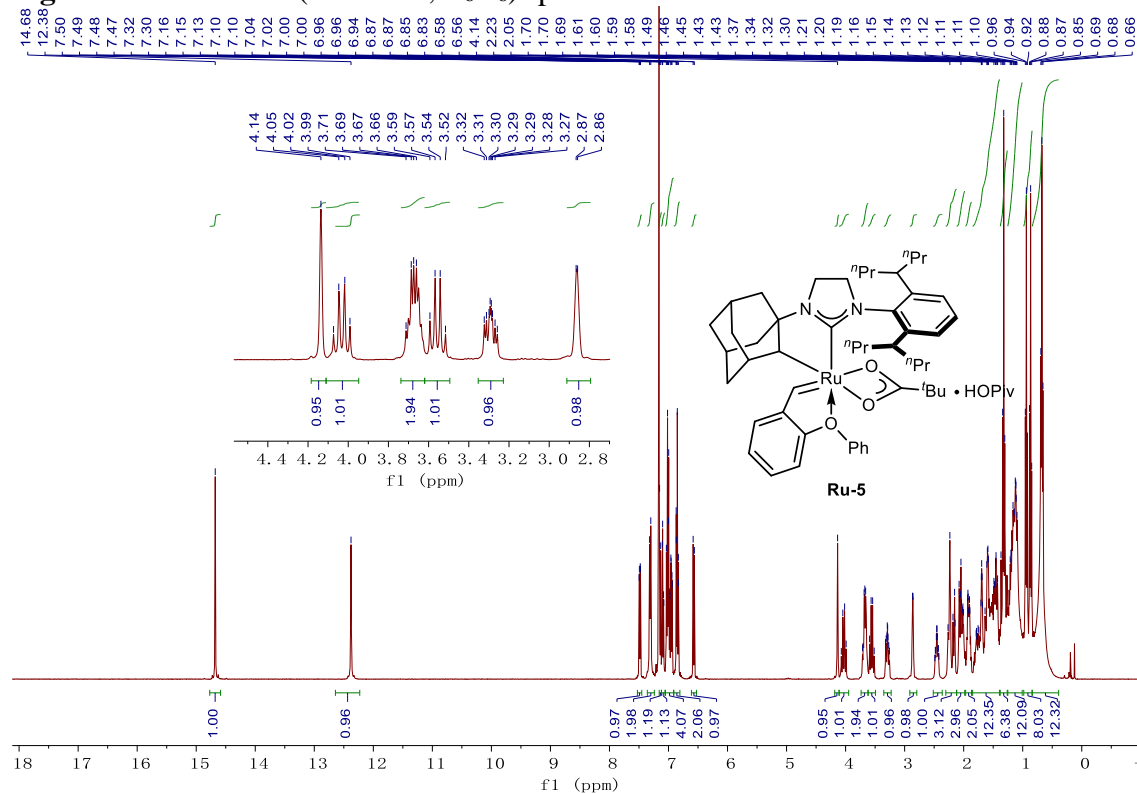
Figure B12. ^{13}C NMR (101 MHz, C$_6$D$_6$) spectrum of **Ru-5**.
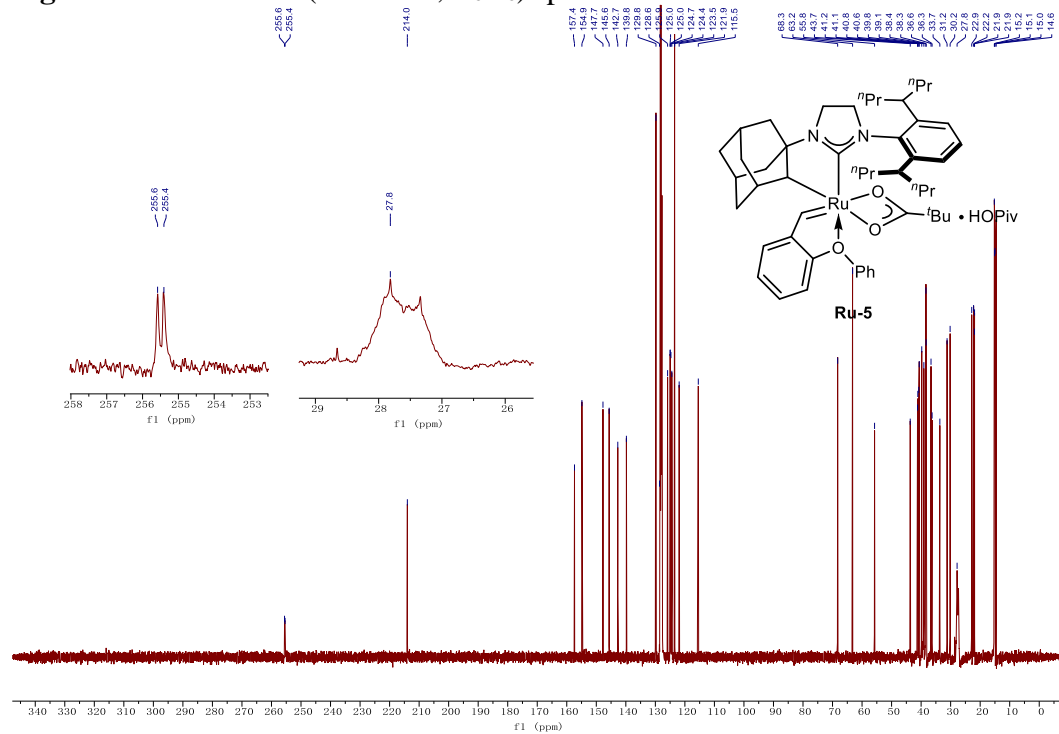
Figure B13. ^{1}H NMR (400 MHz, C$_6$D$_6$) spectrum of **Ru-4**.
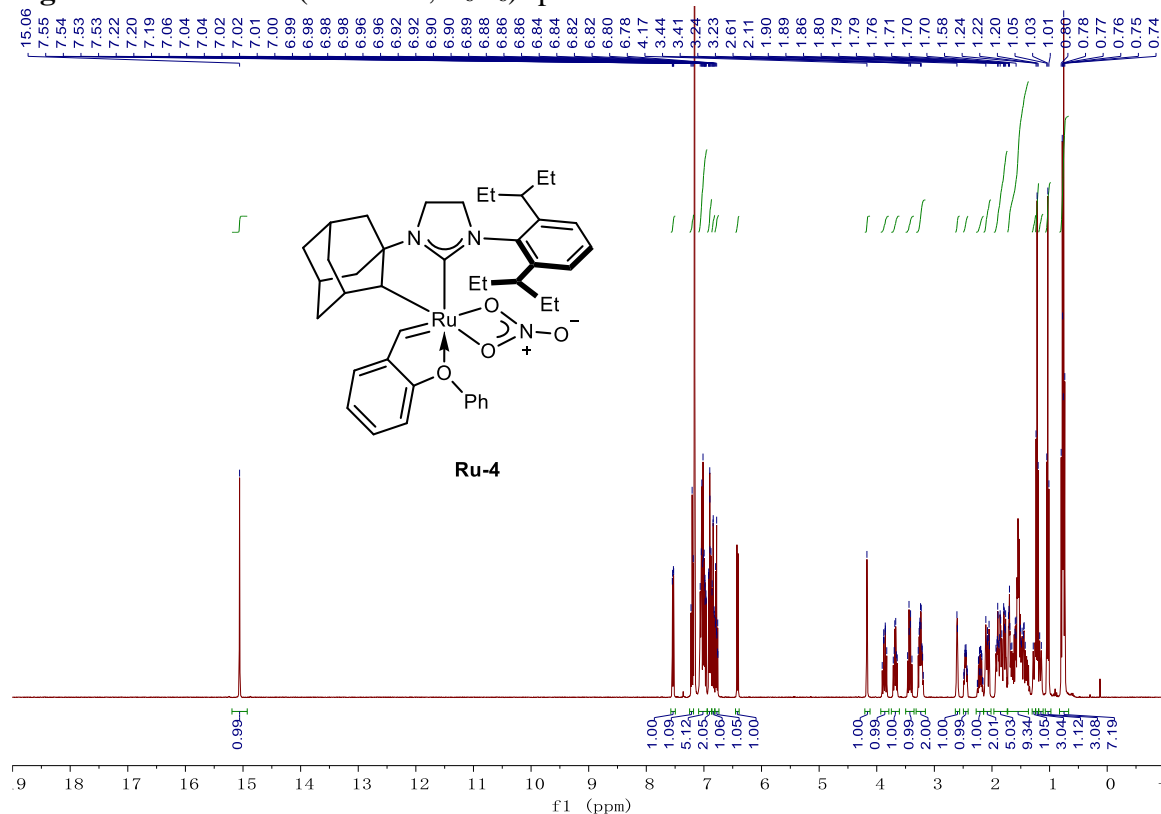
Figure B14. ^{13}C NMR (101 MHz, C$_6$D$_6$) spectrum of **Ru-4**.
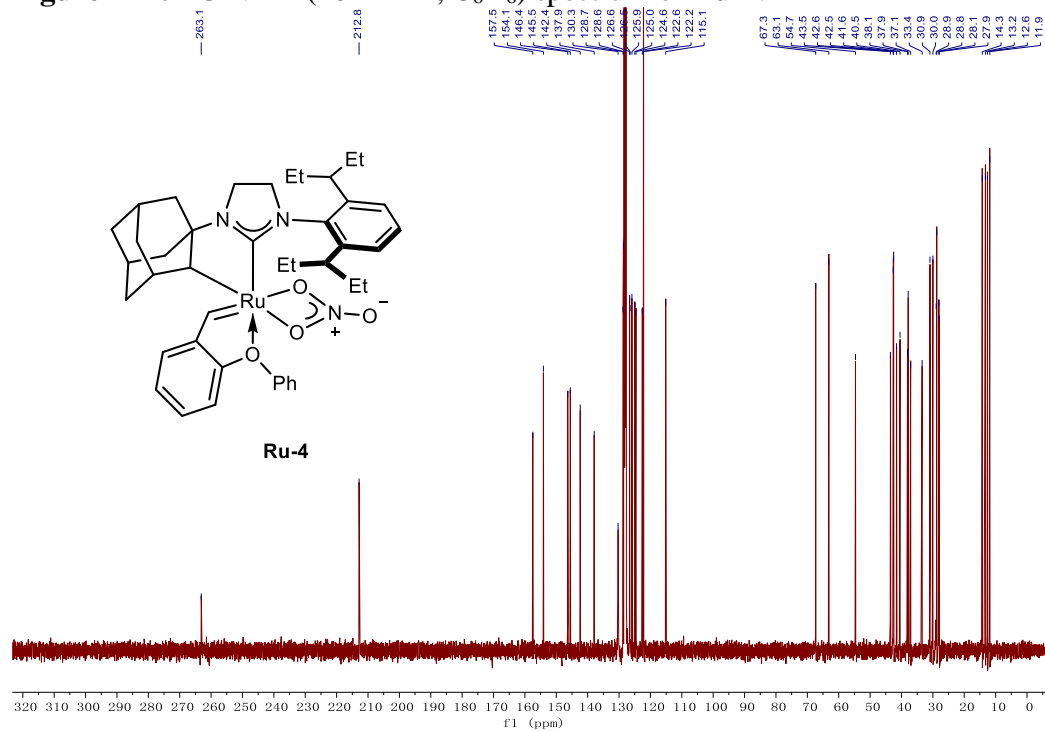
Figure B15. ^{1}H NMR (400 MHz, C$_6$D$_6$) spectrum of **Ru-6**.
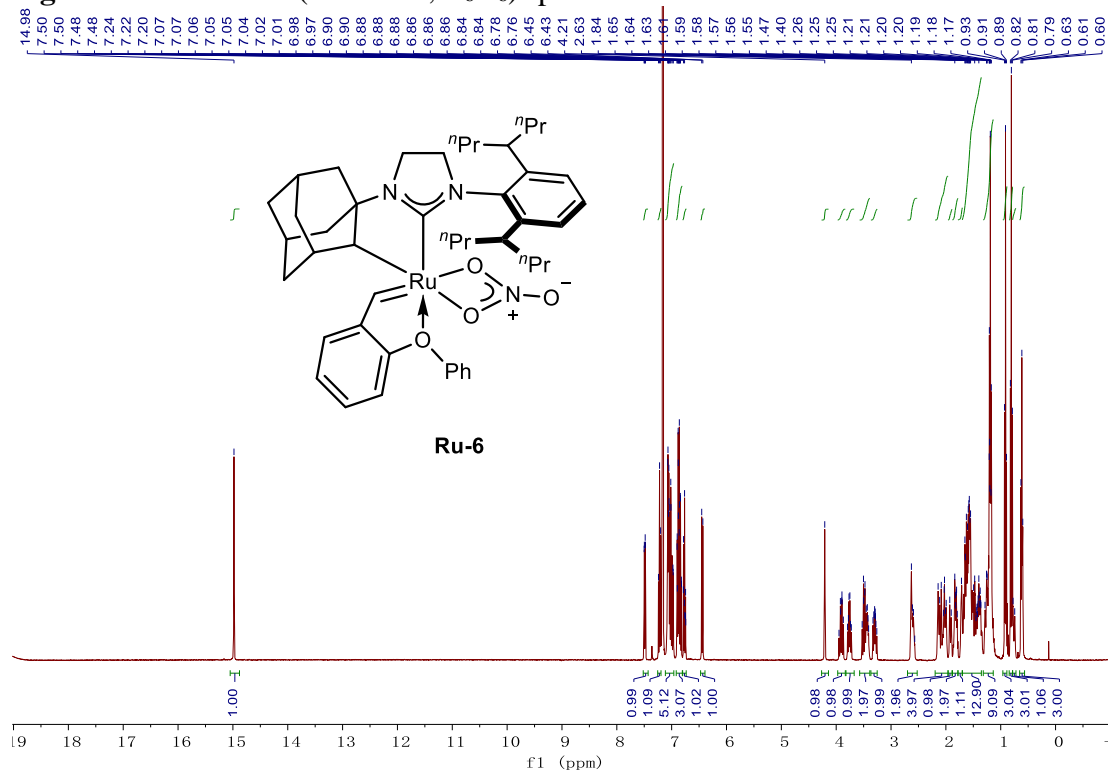
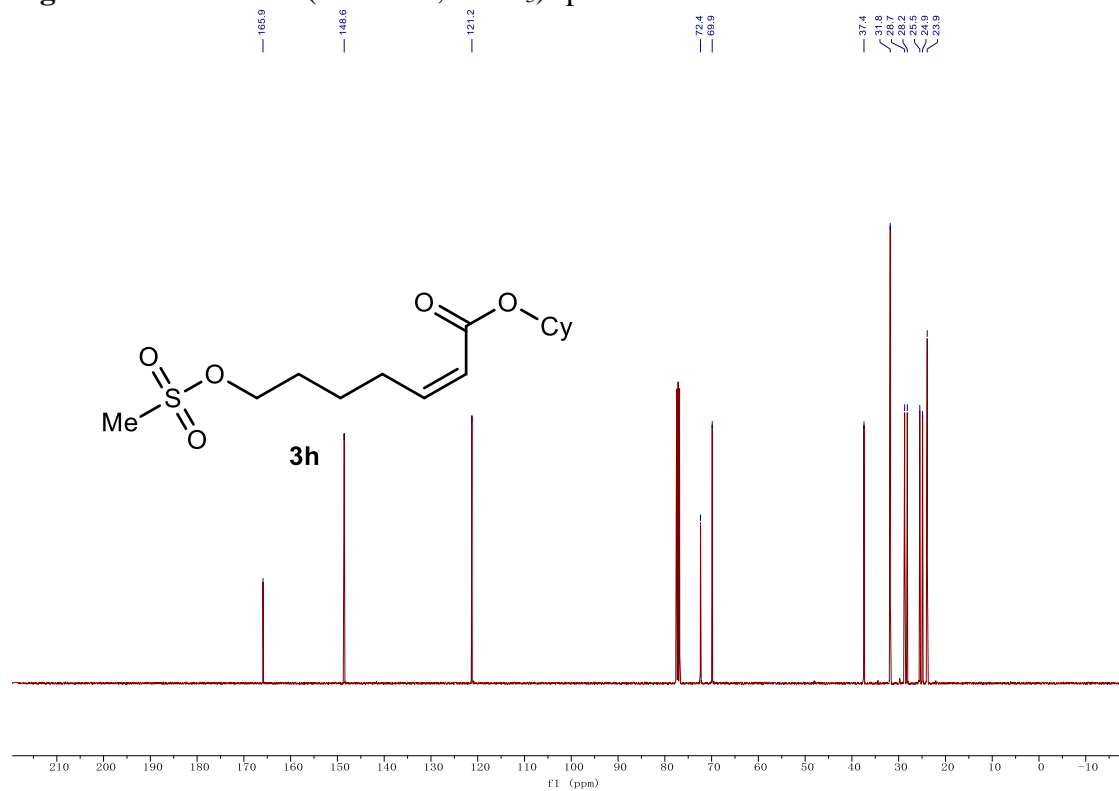**Figure B16.** ^{13}C NMR (101 MHz, C$_6$D$_6$) spectrum of **Ru-6**.
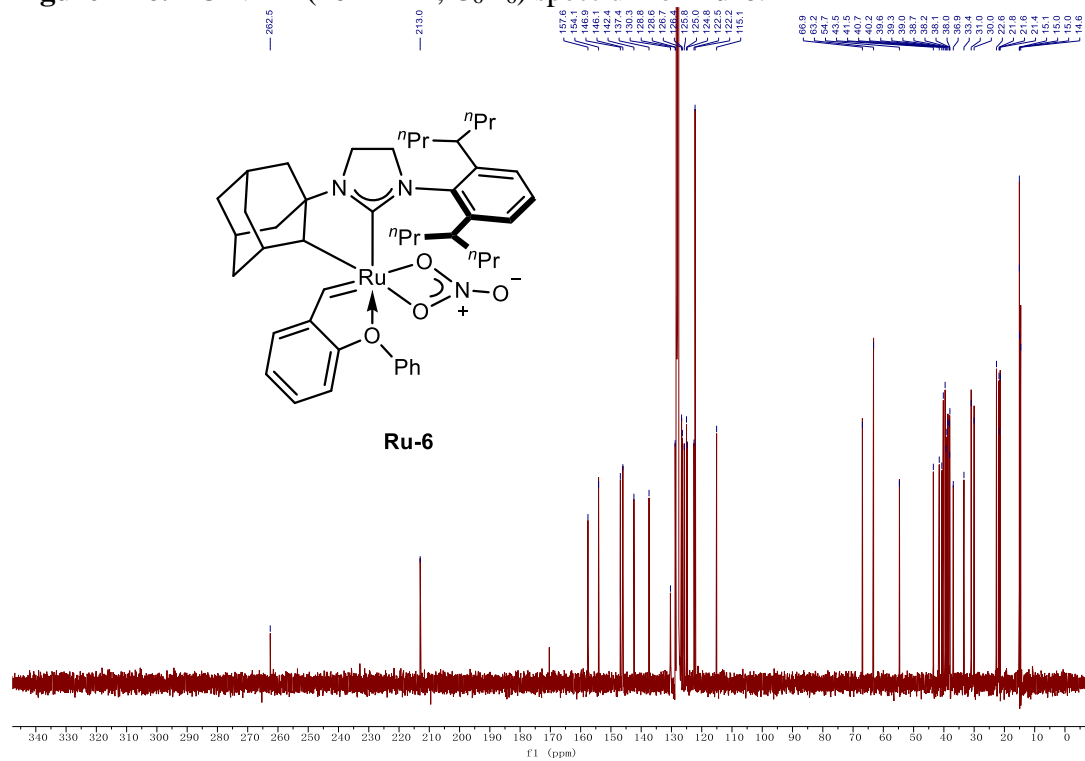
Figure B17. ^{1}H NMR (400 MHz, CDCl$_3$) spectrum of **2q**.
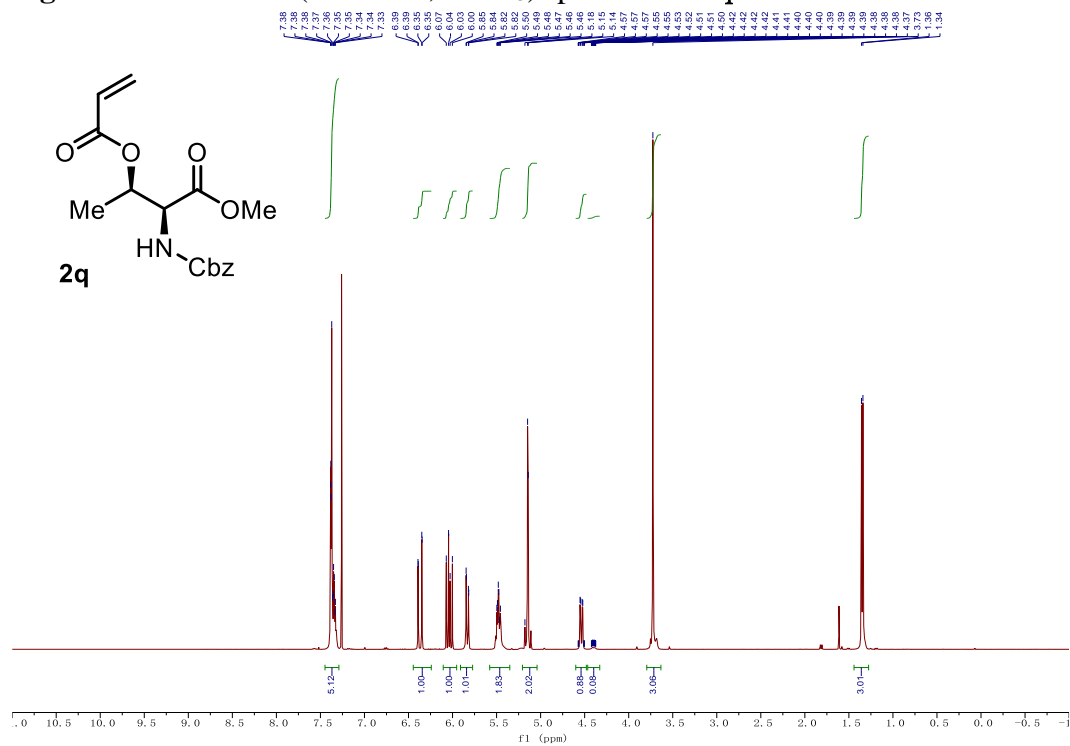
Figure B18. ^{13}C NMR (101 MHz, CDCl$_3$) spectrum of **2q**.
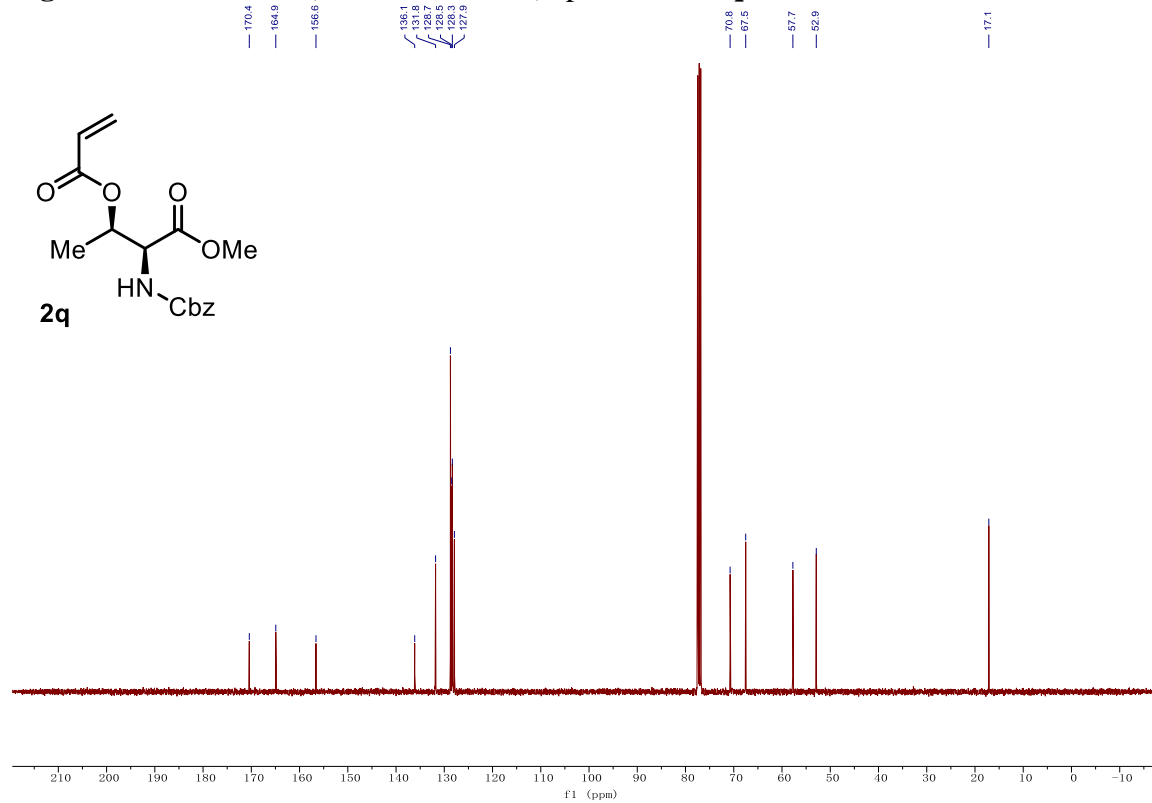
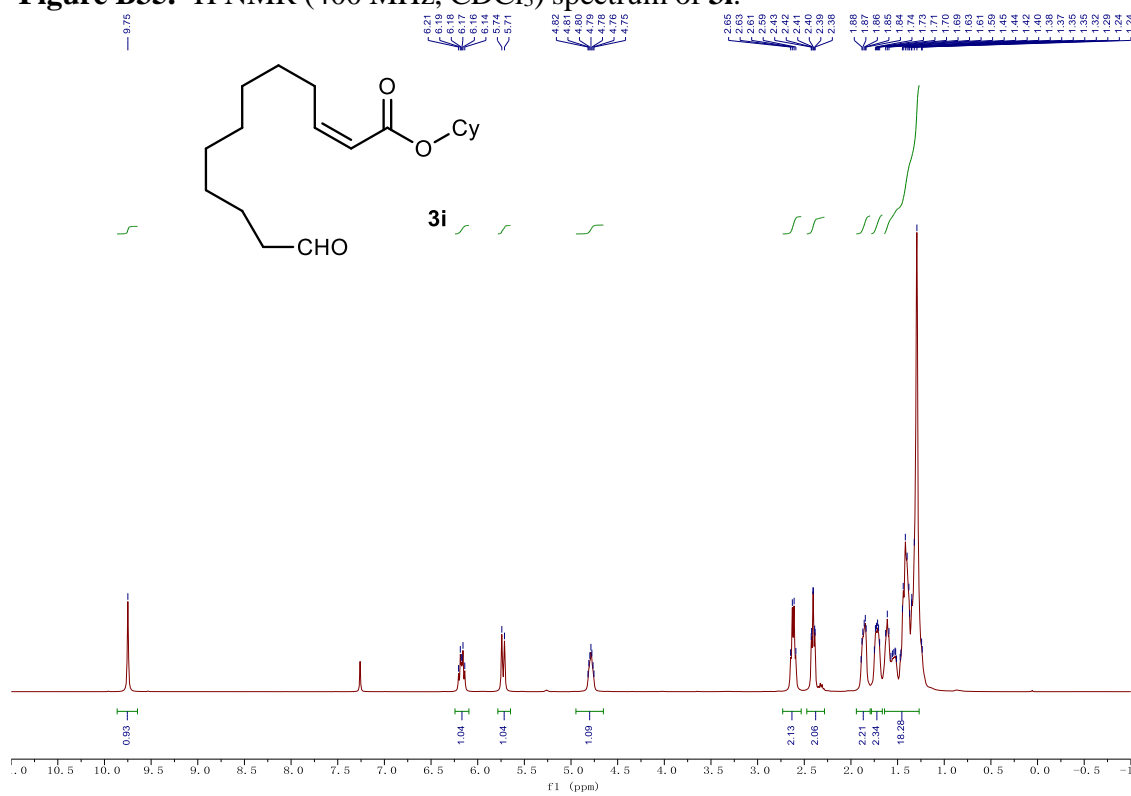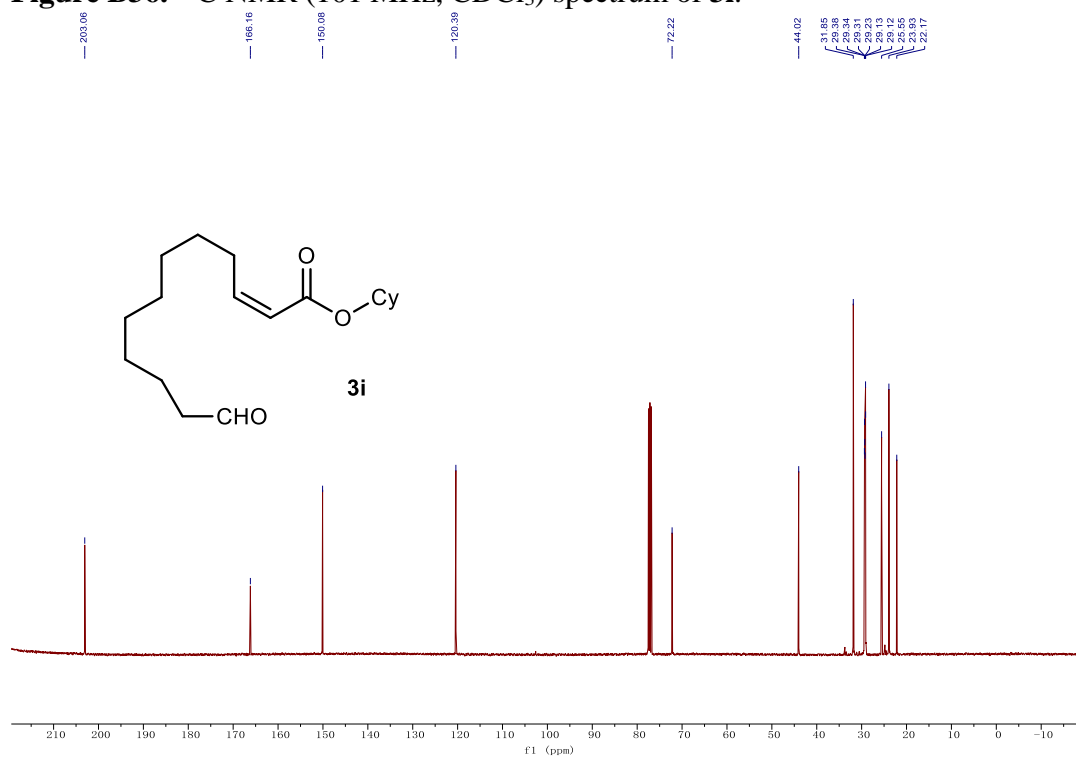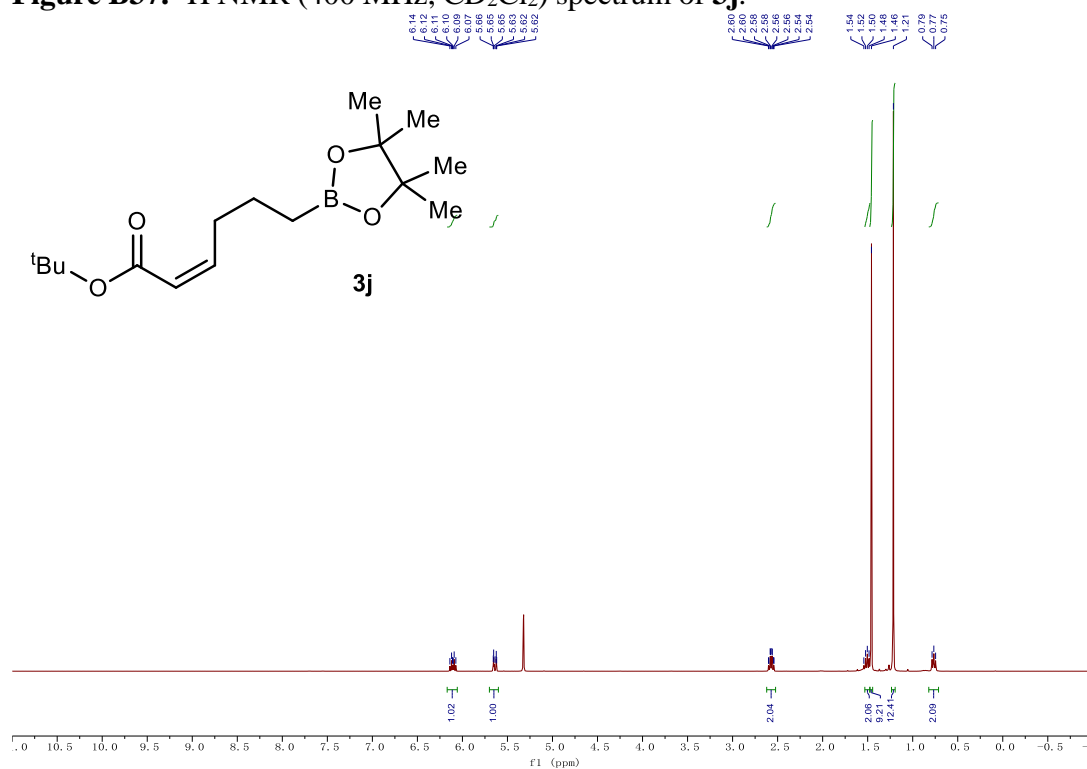**Figure B19.** ^{1}H NMR (400 MHz, CDCl$_3$) spectrum of **3a**.
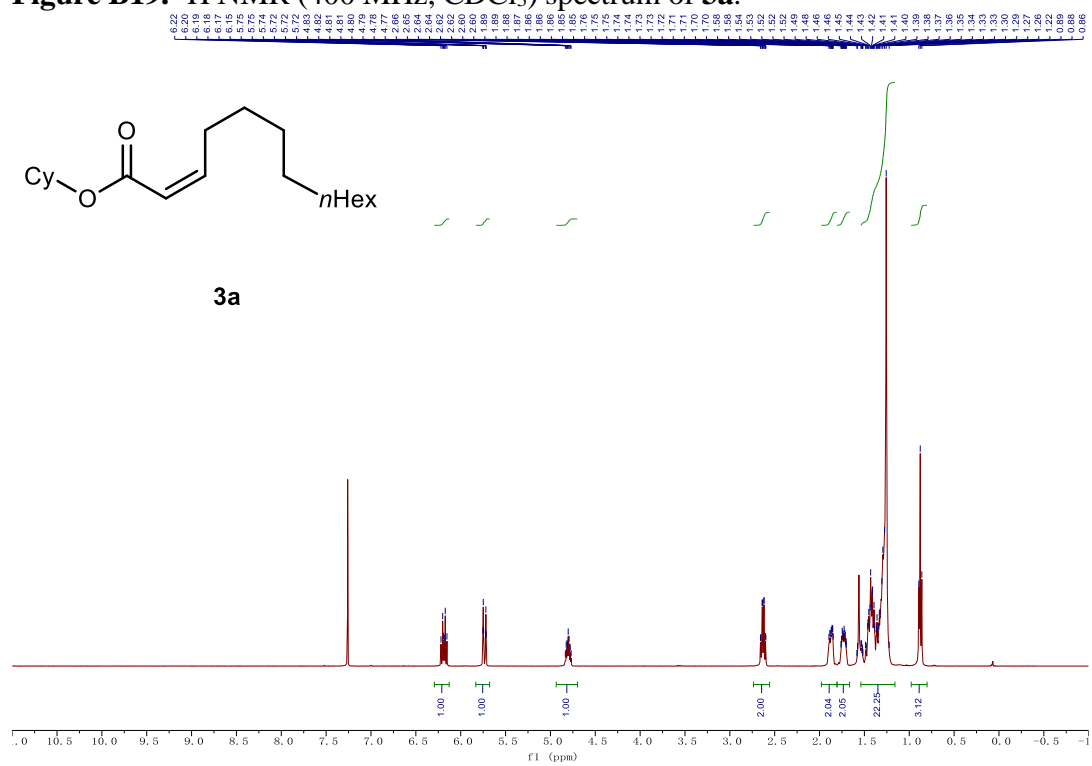
Figure B20. ^{13}C NMR (101 MHz, CDCl$_3$) spectrum of **3a**.
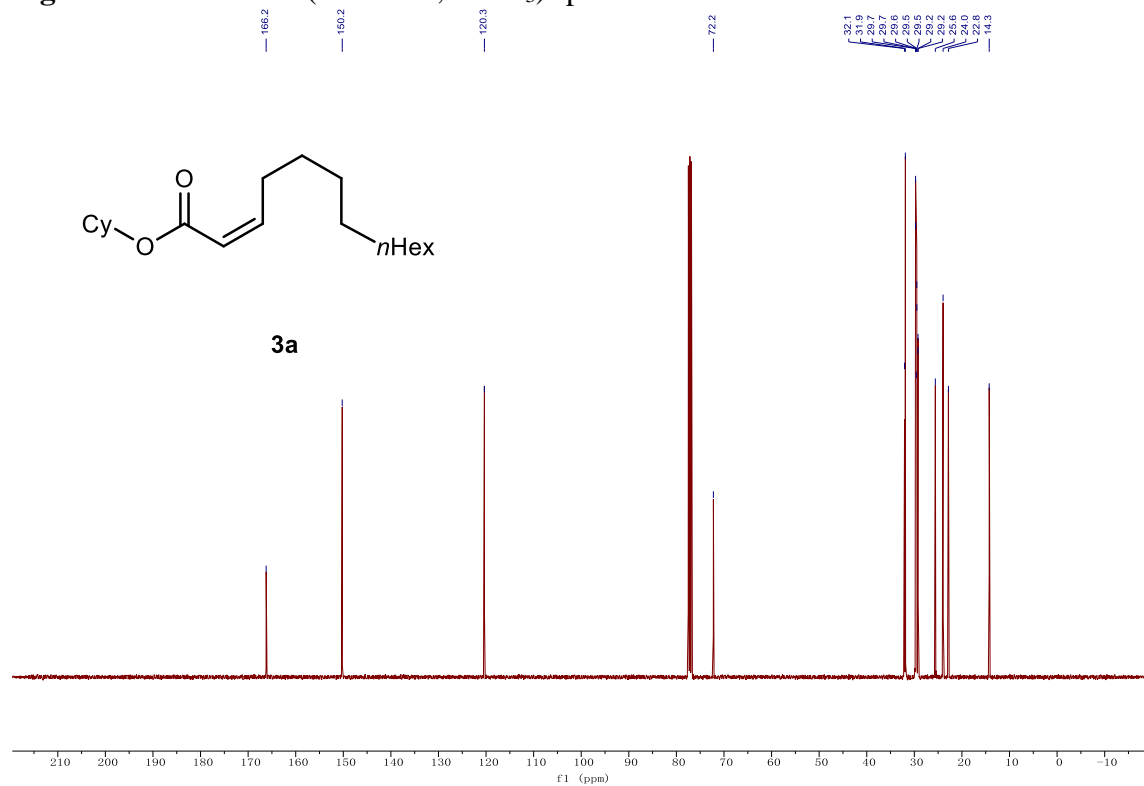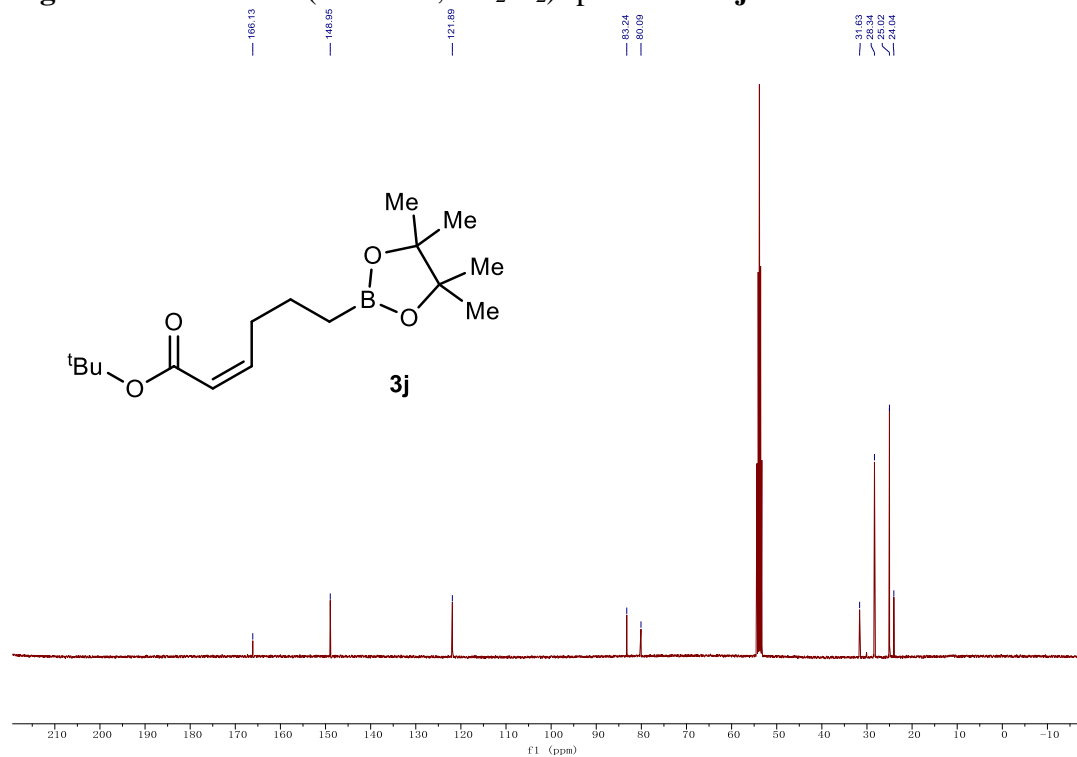
Figure B21. ^{1}H NMR (400 MHz, CDCl$_3$) spectrum of **3b**.
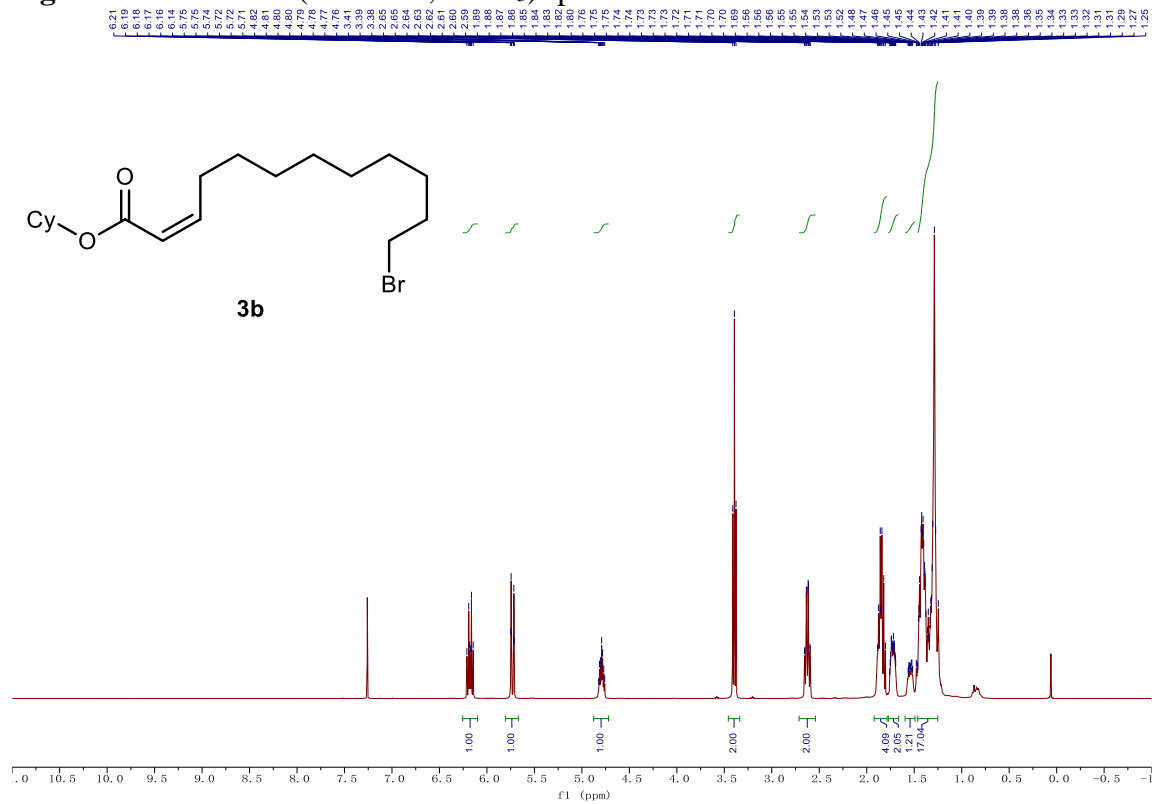
Figure B22. ^{13}C NMR (101 MHz, CDCl$_3$) spectrum of **3b**.
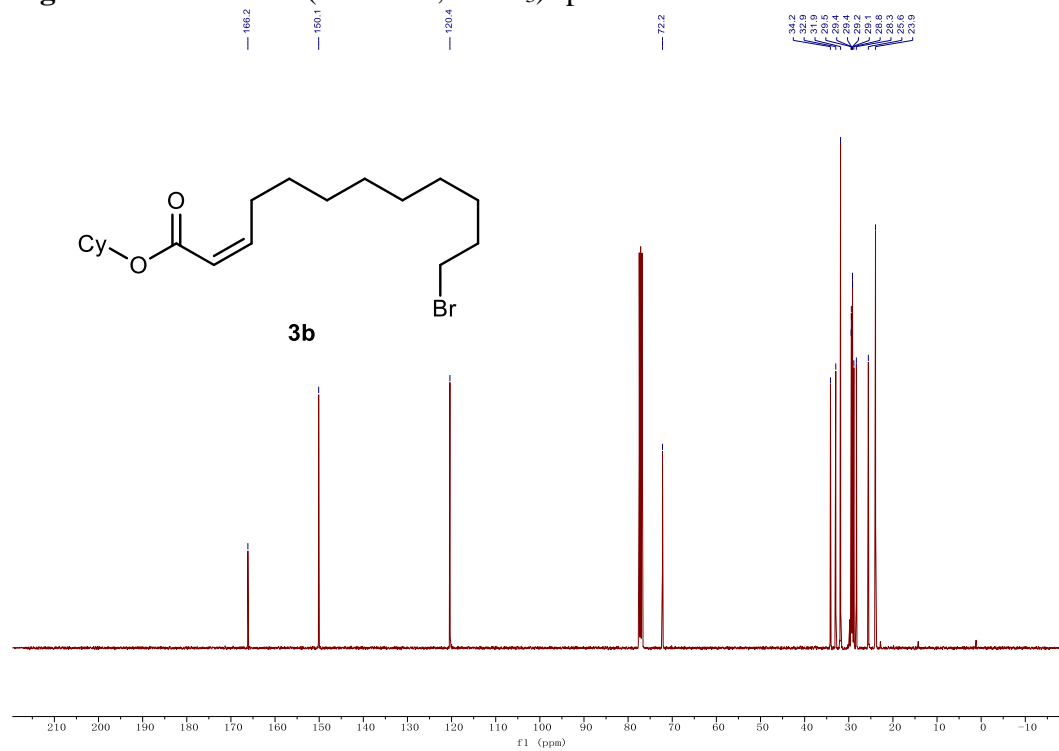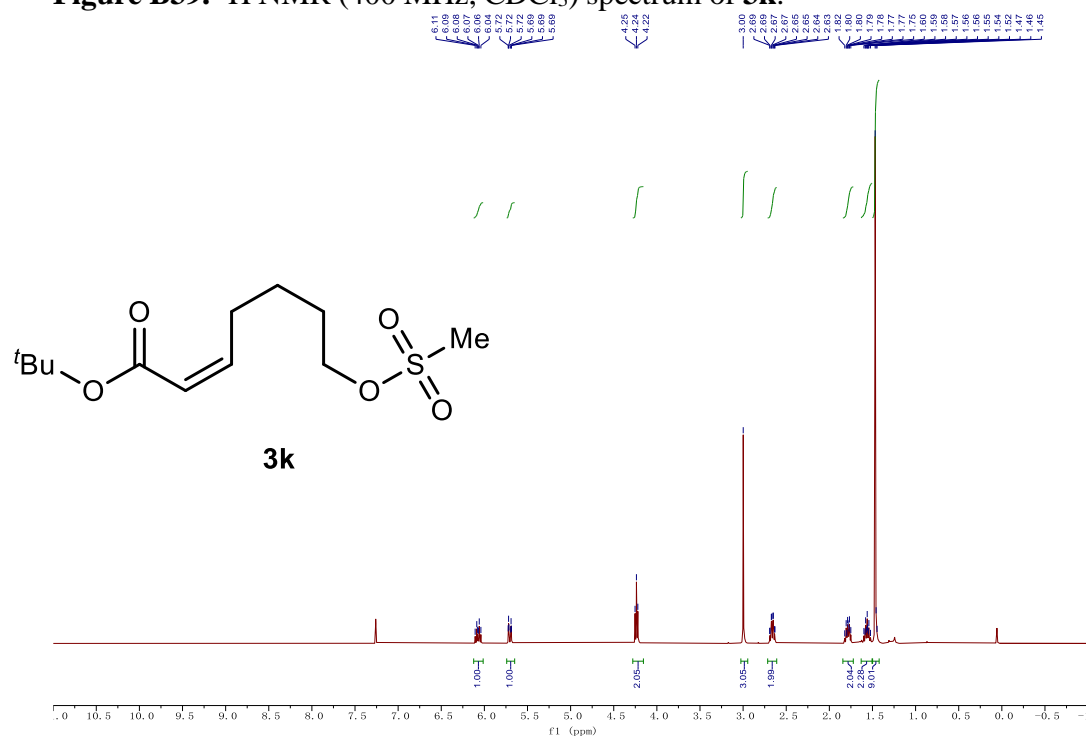
Figure B23. ^{1}H NMR (400 MHz, CDCl$_3$) spectrum of **3c**.
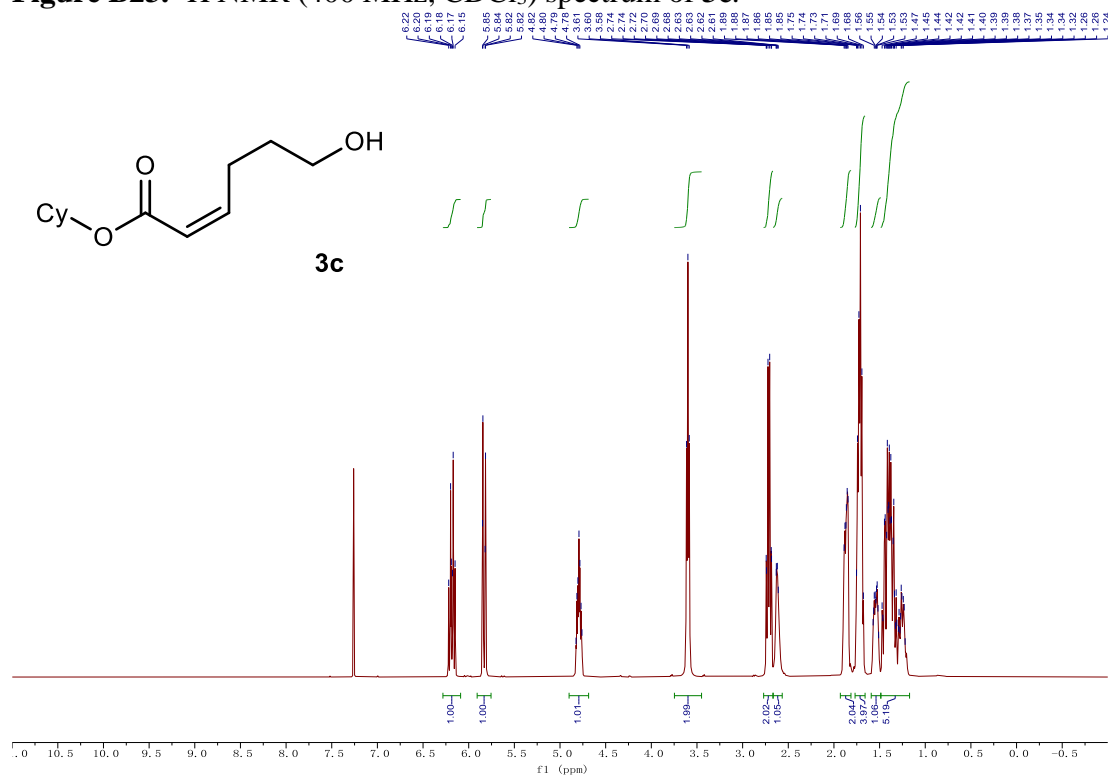
Figure B24. ^{13}C NMR (101 MHz, CDCl$_3$) spectrum of **3c**.
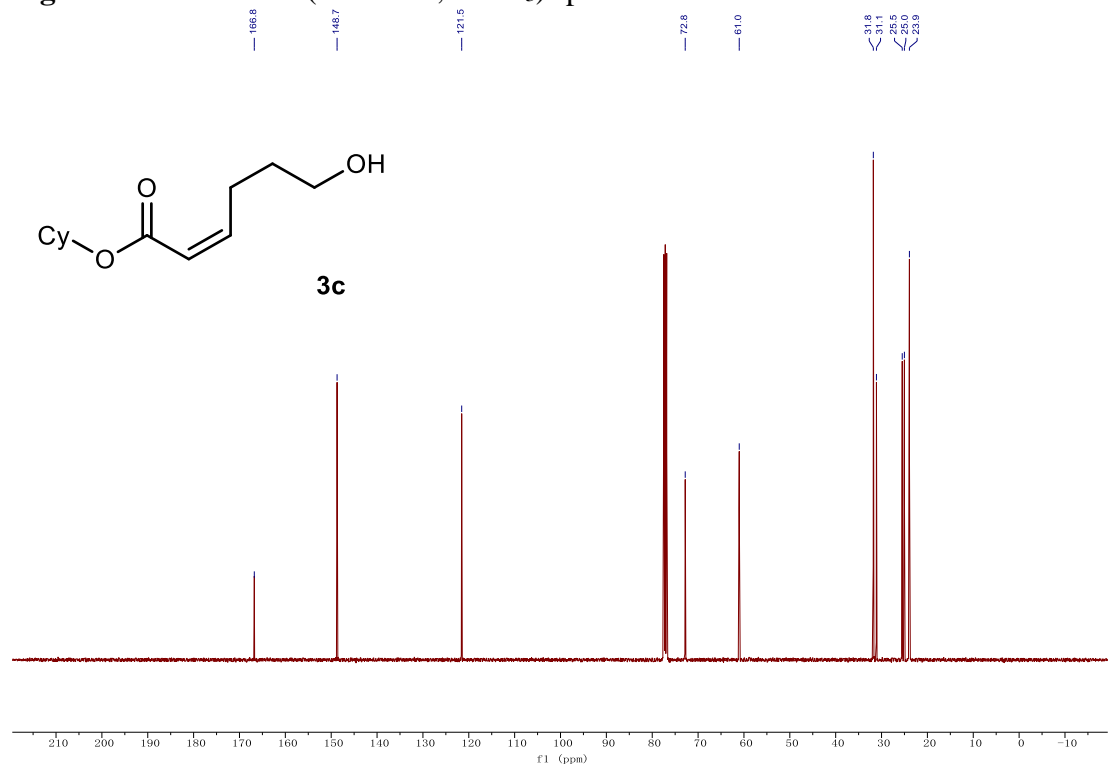
Figure B25. ^{1}H NMR (400 MHz, CDCl$_3$) spectrum of **3d**.
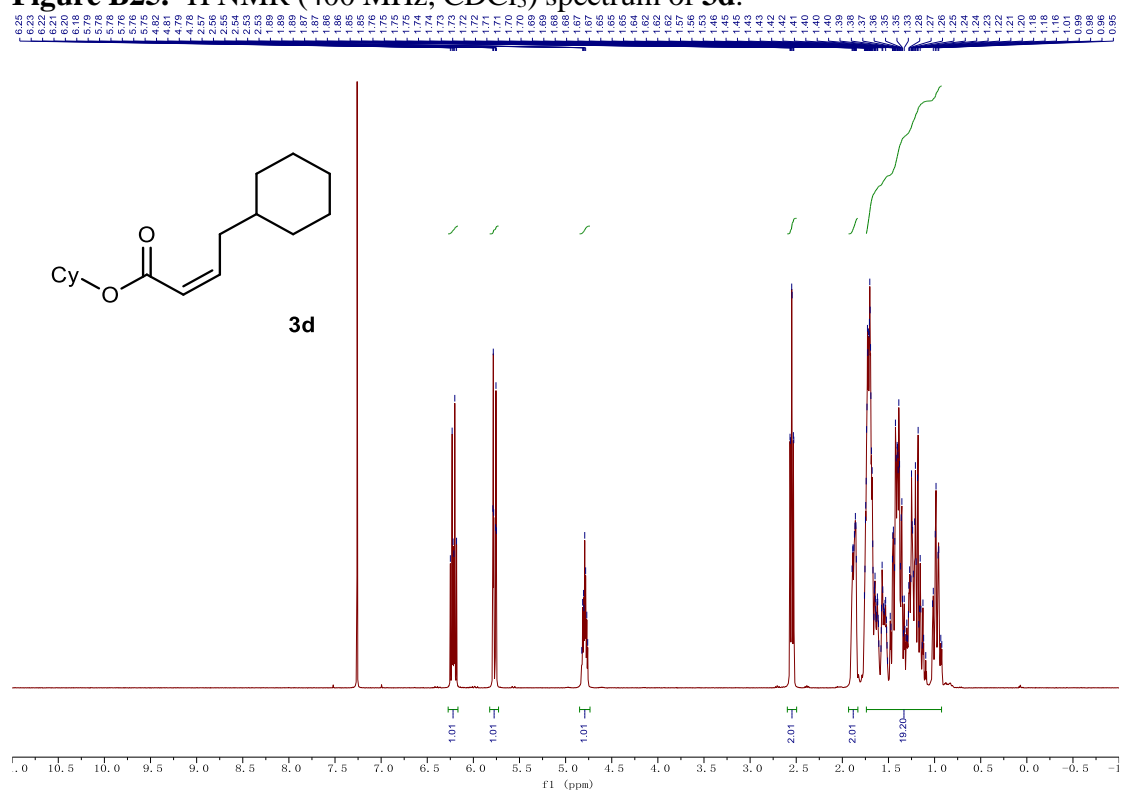
Figure B26. ^{13}C NMR (101 MHz, CDCl$_3$) spectrum of **3d**.
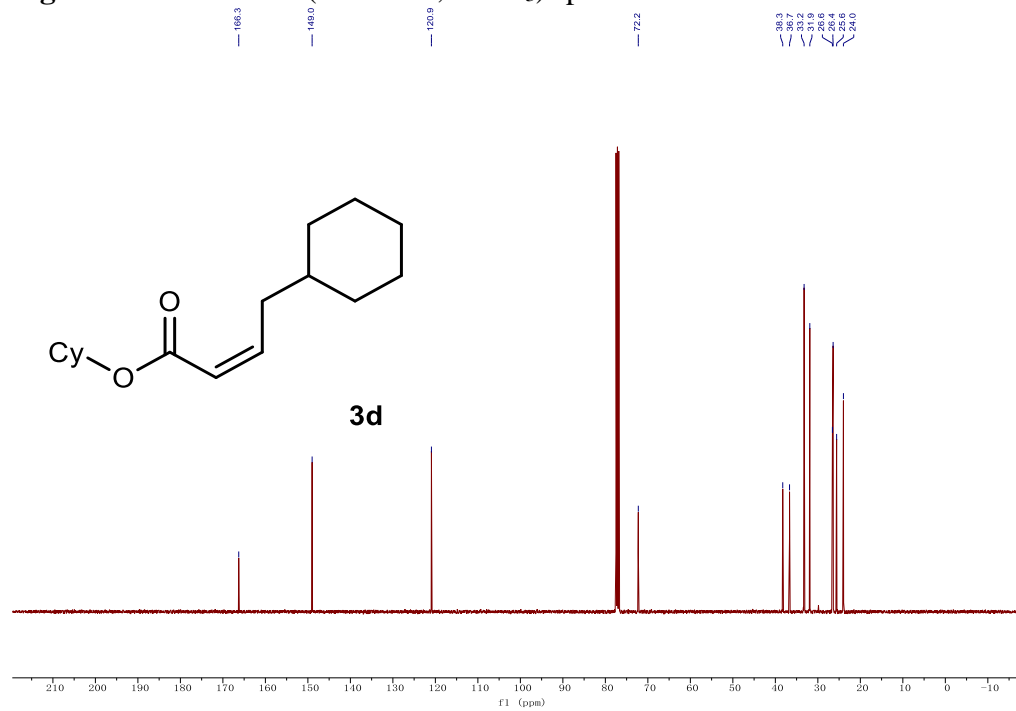
Figure B27. ^{1}H NMR (400 MHz, CD$_2$Cl$_2$) spectrum of **3e**.
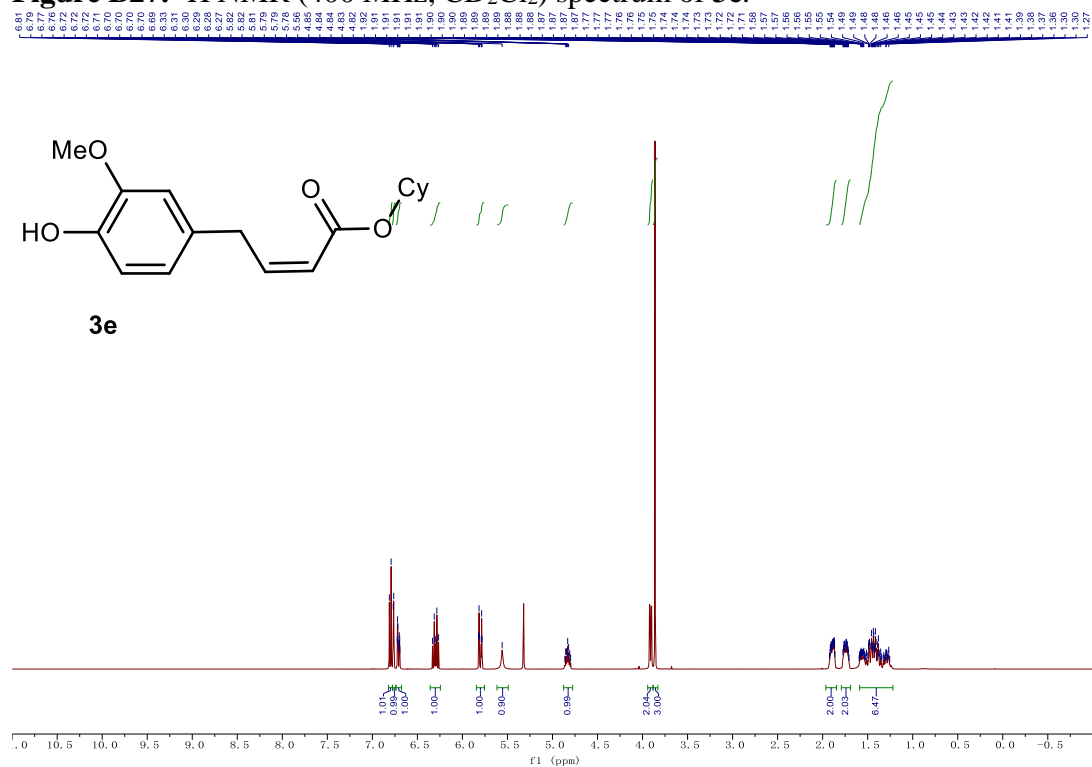
Figure B28. ^{13}C NMR (101 MHz, CD$_2$Cl$_2$) spectrum of **3e**.
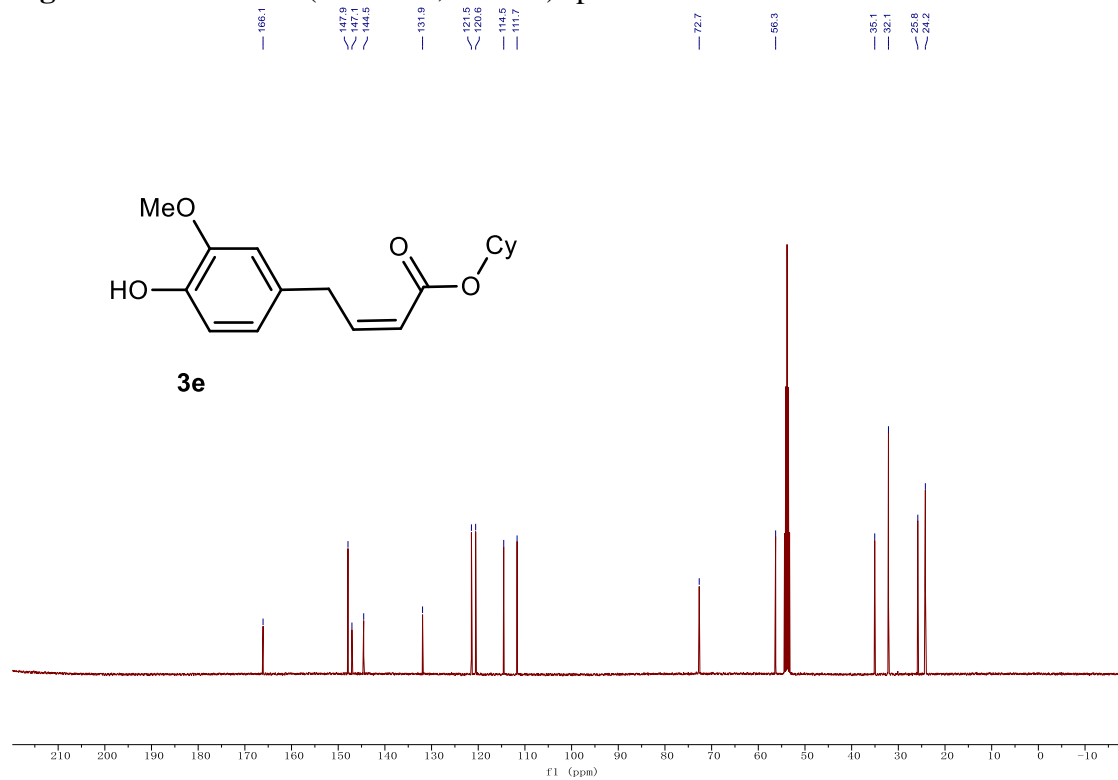
Figure B29. ^{1}H NMR (400 MHz, CDCl$_3$) spectrum of **3f**.

3f

Figure B30. ^{13}C NMR (101 MHz, CDCl$_3$) spectrum of **3f**.
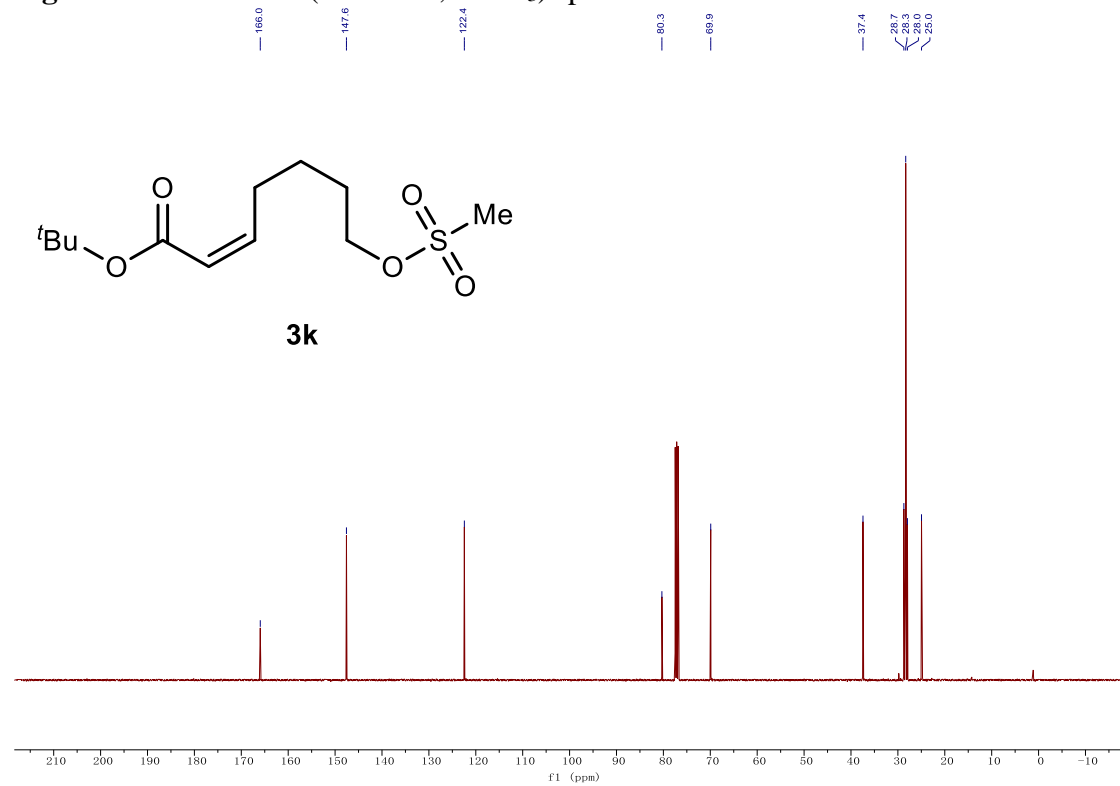

3f

Figure B31. ^{1}H NMR (400 MHz, CDCl$_3$) spectrum of **3g**.
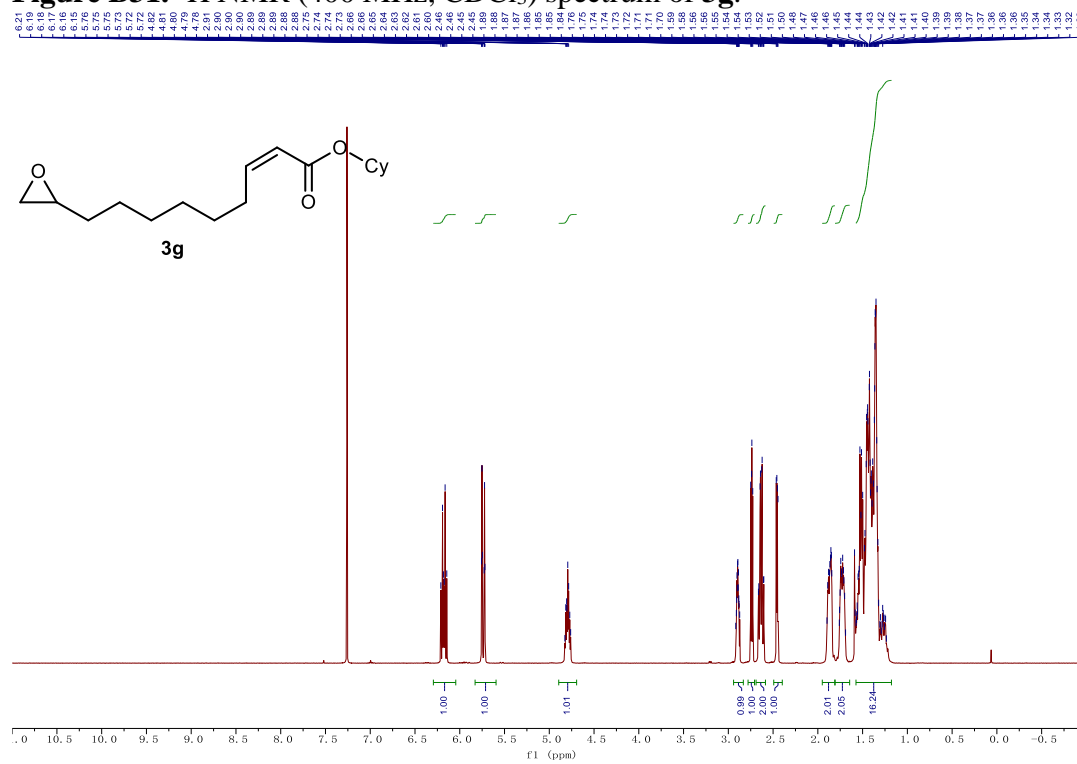
Figure B32. ^{13}C NMR (101 MHz, CDCl$_3$) spectrum of **3g**.
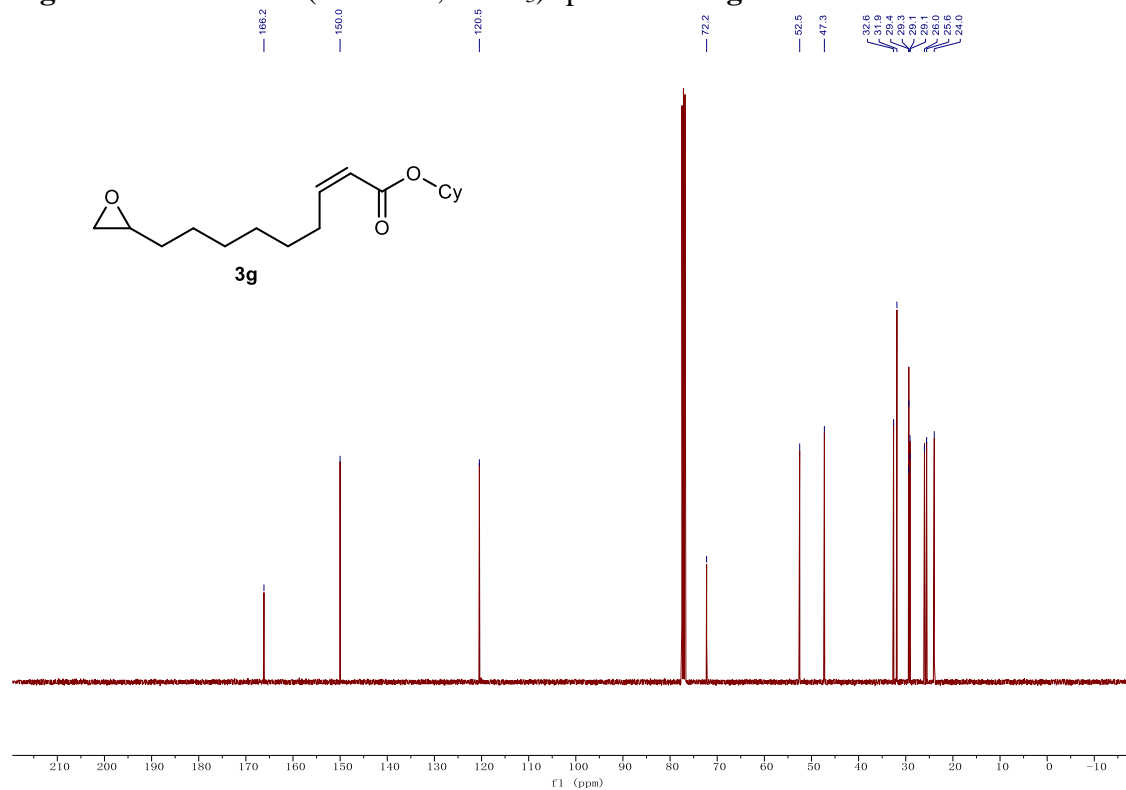
Figure B33. ^{1}H NMR (400 MHz, CDCl$_3$) spectrum of **3h**.
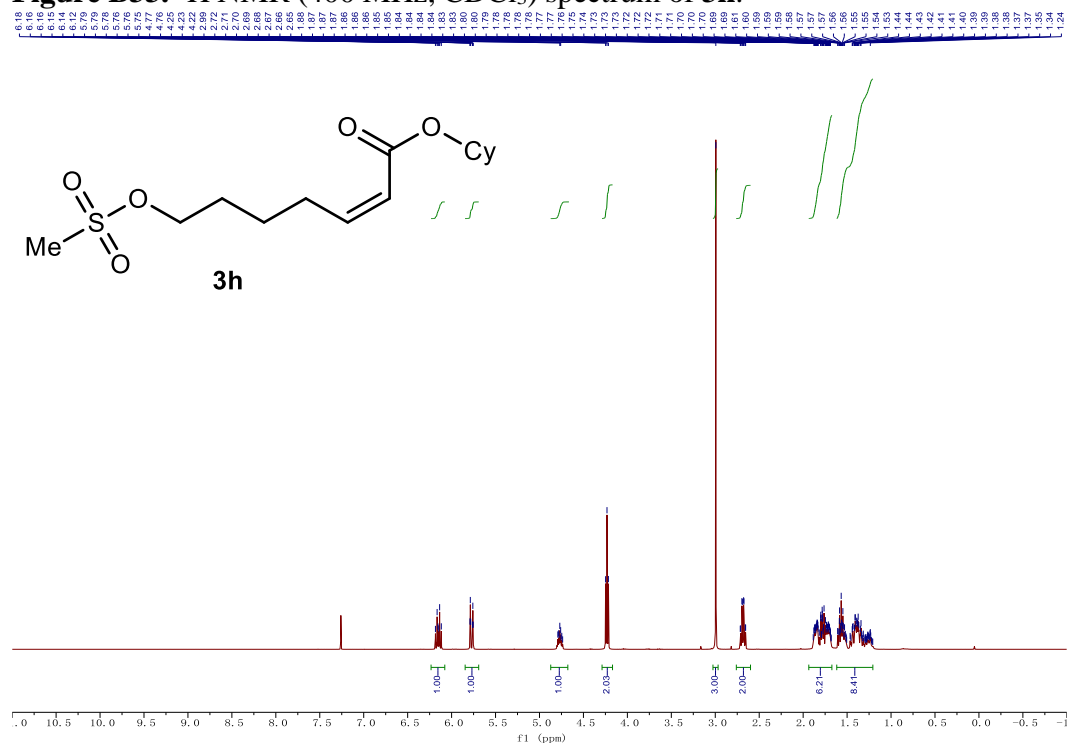
Figure B34. ^{13}C NMR (101 MHz, CDCl$_3$) spectrum of **3h**.
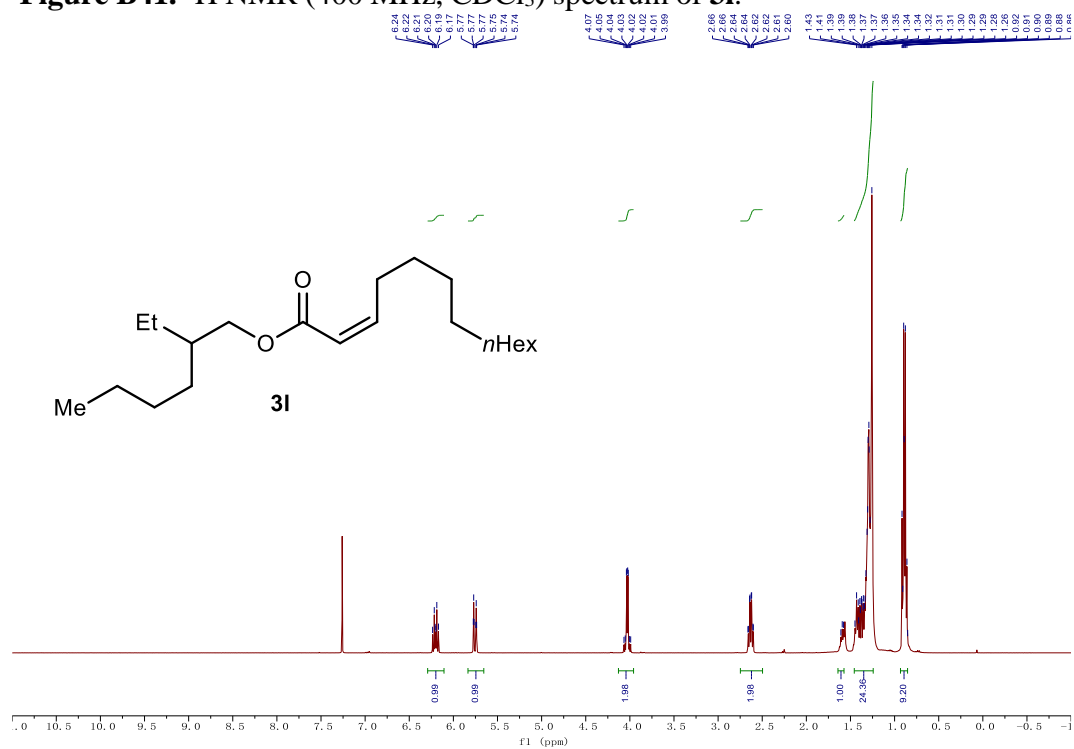
Figure B35. ^{1}H NMR (400 MHz, CDCl3) spectrum of **3i**.

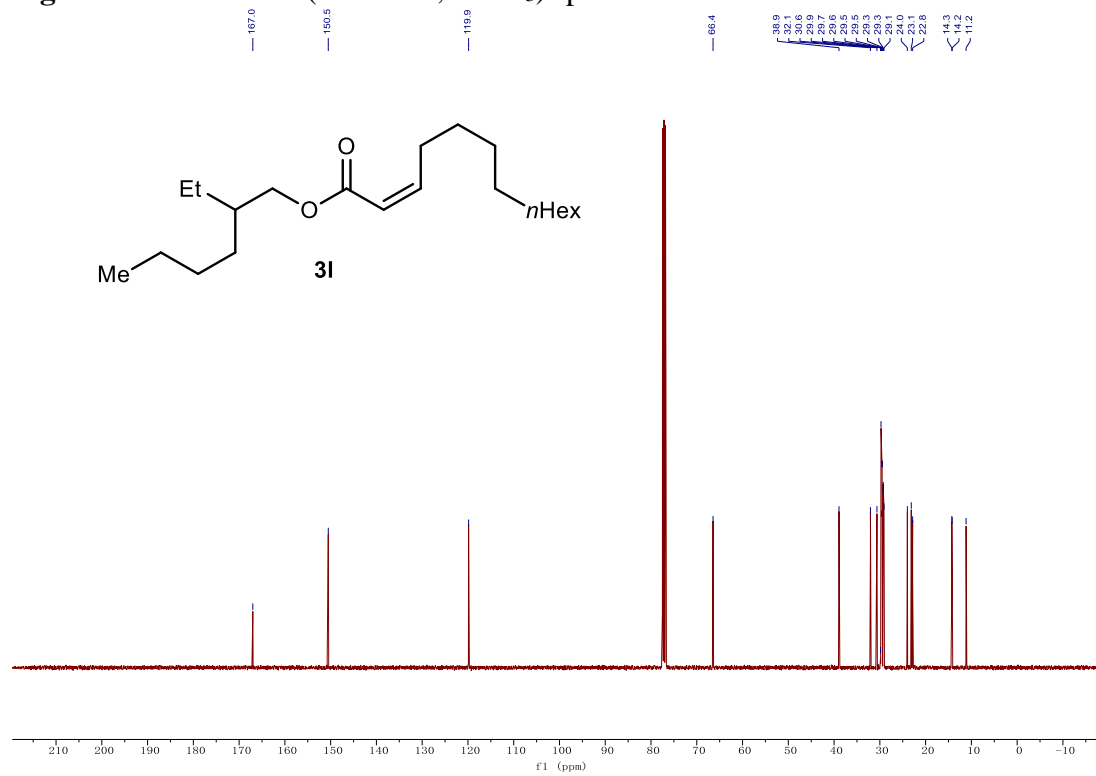**Figure B36.** ^{13}C NMR (101 MHz, CDCl3) spectrum of **3i**.

Figure B37. ^{1}H NMR (400 MHz, CD$_2$Cl$_2$) spectrum of **3j**.

Figure B38. ^{13}C NMR (101 MHz, CD$_2$Cl$_2$) spectrum of **3j**.

Figure B39. ¹H NMR (400 MHz, CDCl₃) spectrum of **3k**.

Figure B40. ¹³C NMR (101 MHz, CDCl₃) spectrum of **3k.**

Figure B41. ^{1}H NMR (400 MHz, CDCl$_3$) spectrum of **3l**.

Figure B42. ^{13}C NMR (101 MHz, CDCl$_3$) spectrum of **3l**.
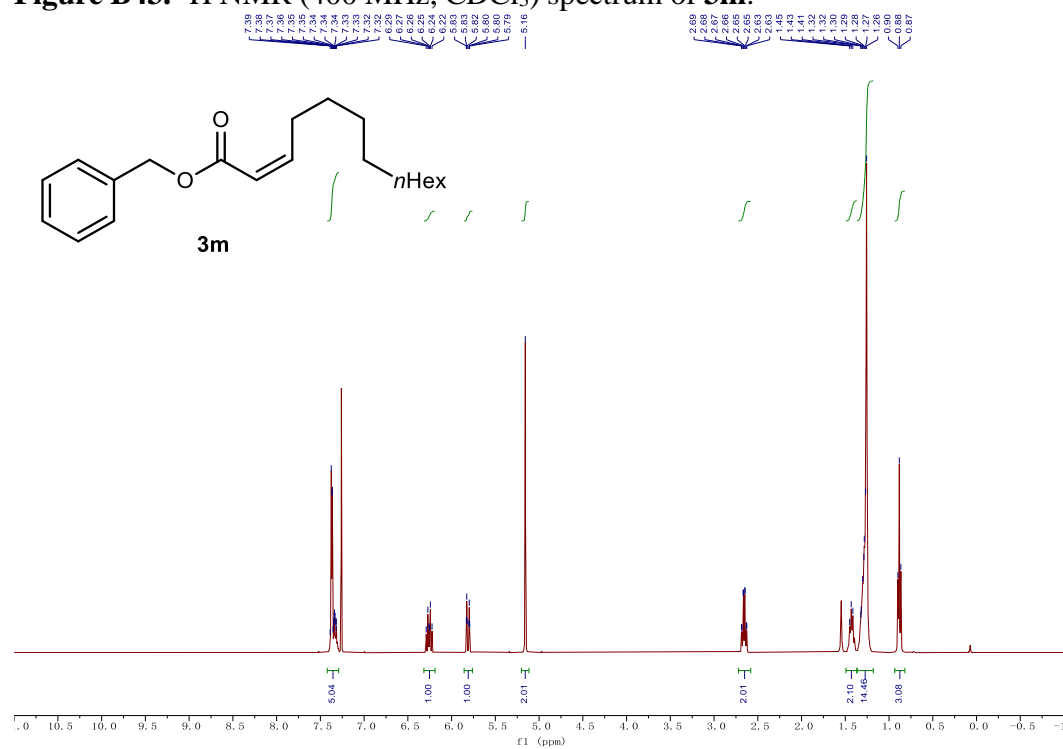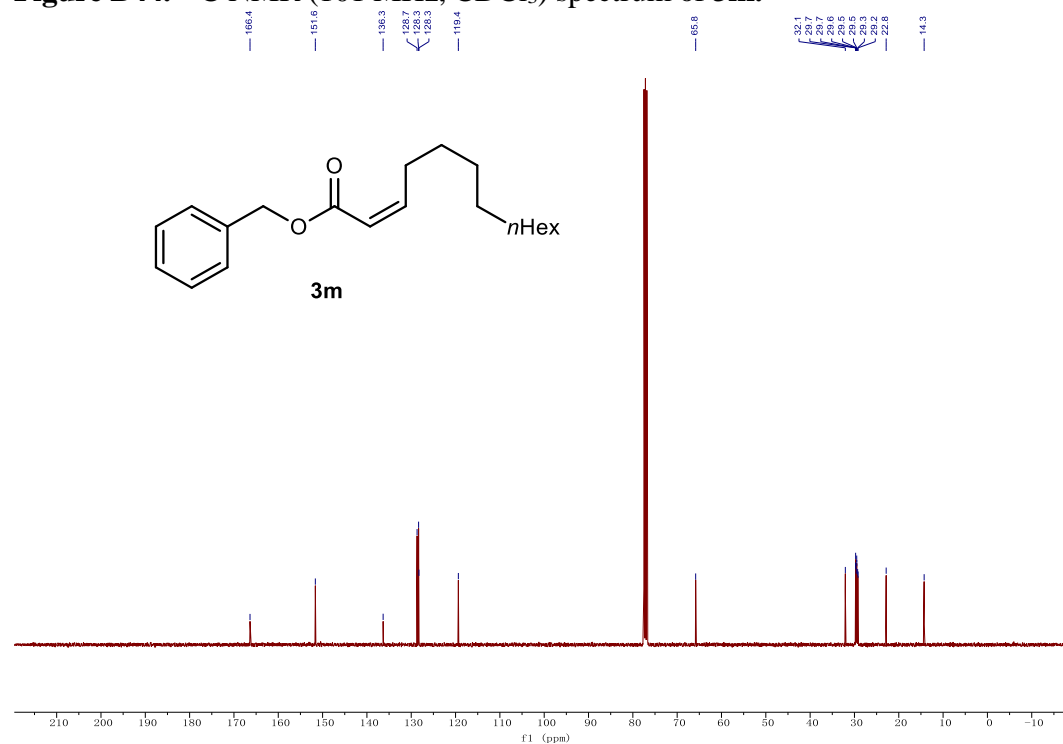
Figure B43. ^{1}H NMR (400 MHz, CDCl$_3$) spectrum of **3m**.

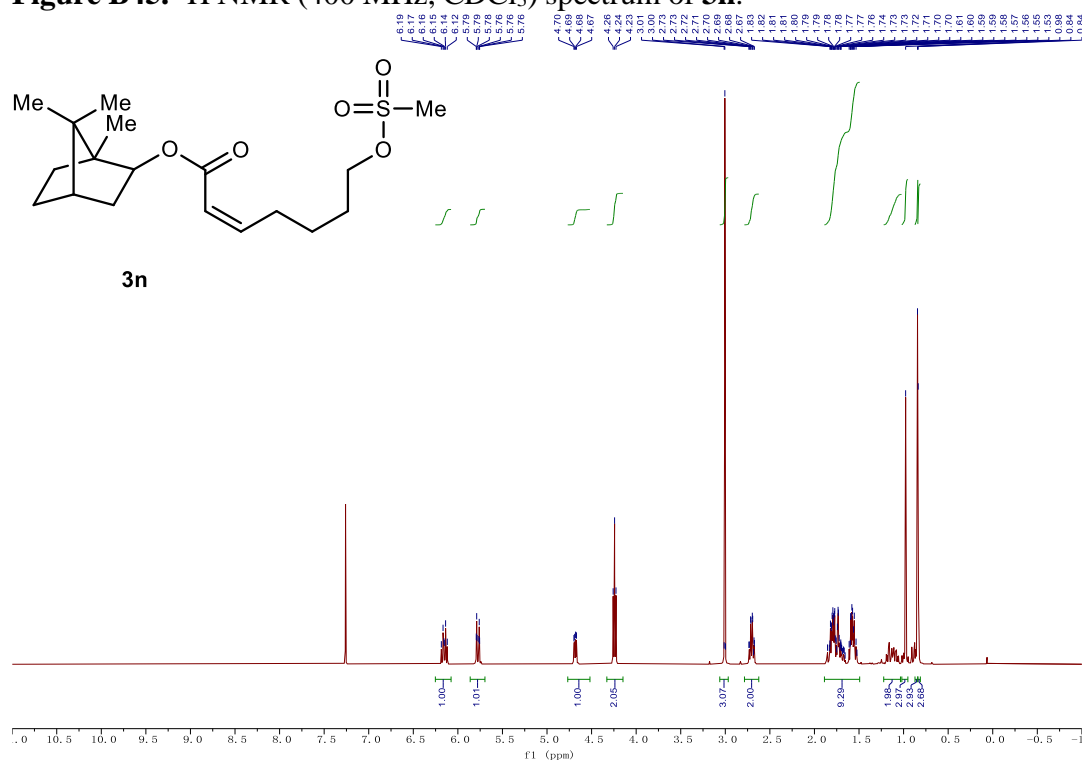**Figure B44.** ^{13}C NMR (101 MHz, CDCl$_3$) spectrum of **3m**.

Figure B45. ^{1}H NMR (400 MHz, CDCl₃) spectrum of **3n**.

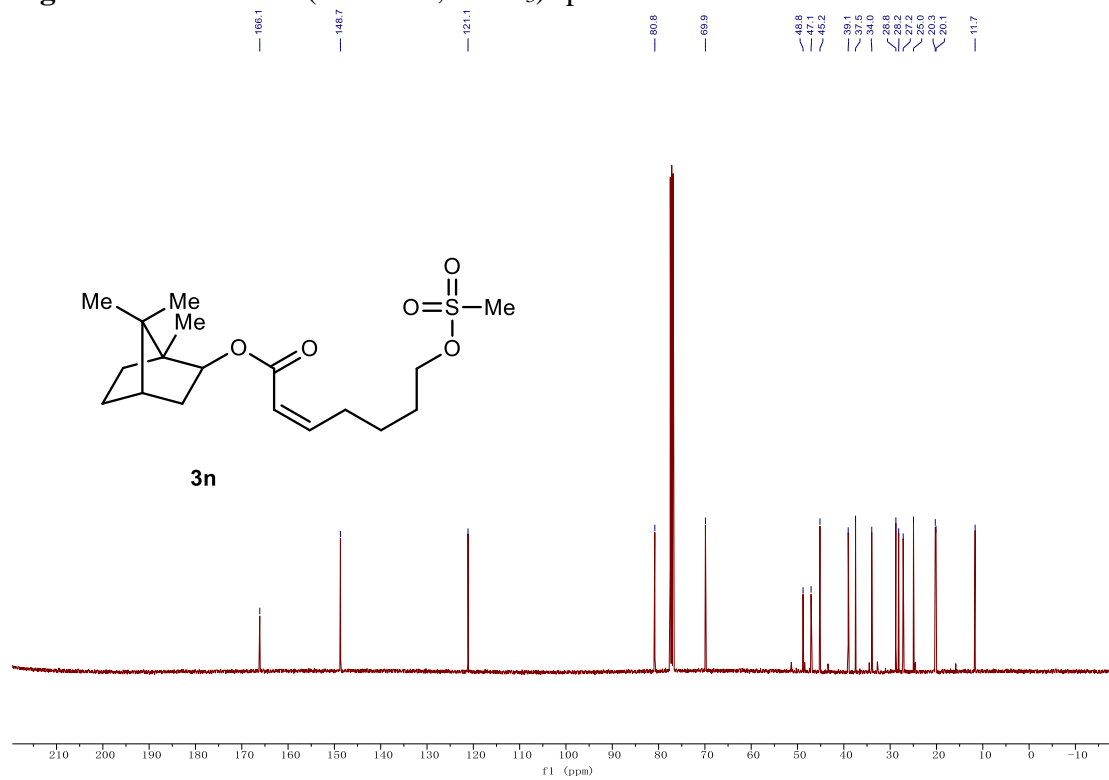**Figure B46.** ^{13}C NMR (101 MHz, CDCl₃) spectrum of **3n.**

Figure B47. ^{1}H NMR (400 MHz, CDCl$_3$) spectrum of **3o**.

Figure B48. ^{13}C NMR (101 MHz, CDCl$_3$) spectrum of **3o**.

Figure B49. ^{1}H NMR (400 MHz, CDCl$_3$) spectrum of **3p**.

Figure B50. ^{13}C NMR (101 MHz, CDCl$_3$) spectrum of **3p.**
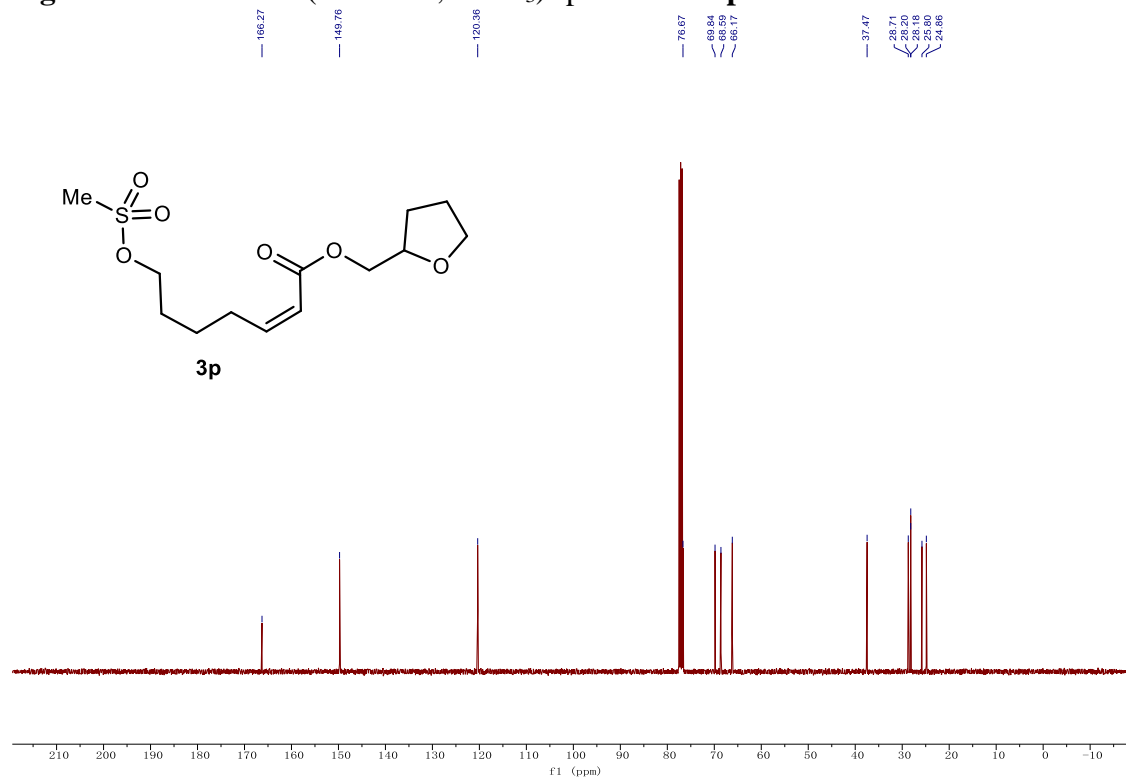
Figure B51. ^{1}H NMR (400 MHz, CDCl$_3$) spectrum of **3q**.

Figure B52. ^{13}C NMR (101 MHz, CDCl$_3$) spectrum of **3q.**
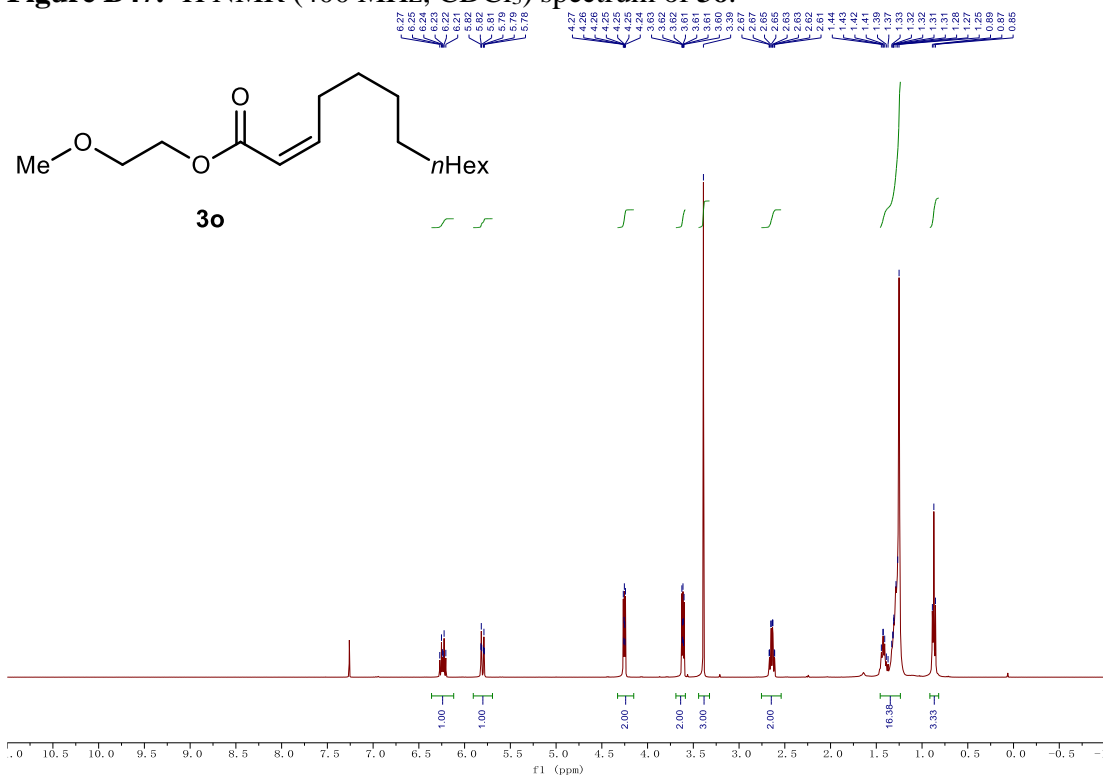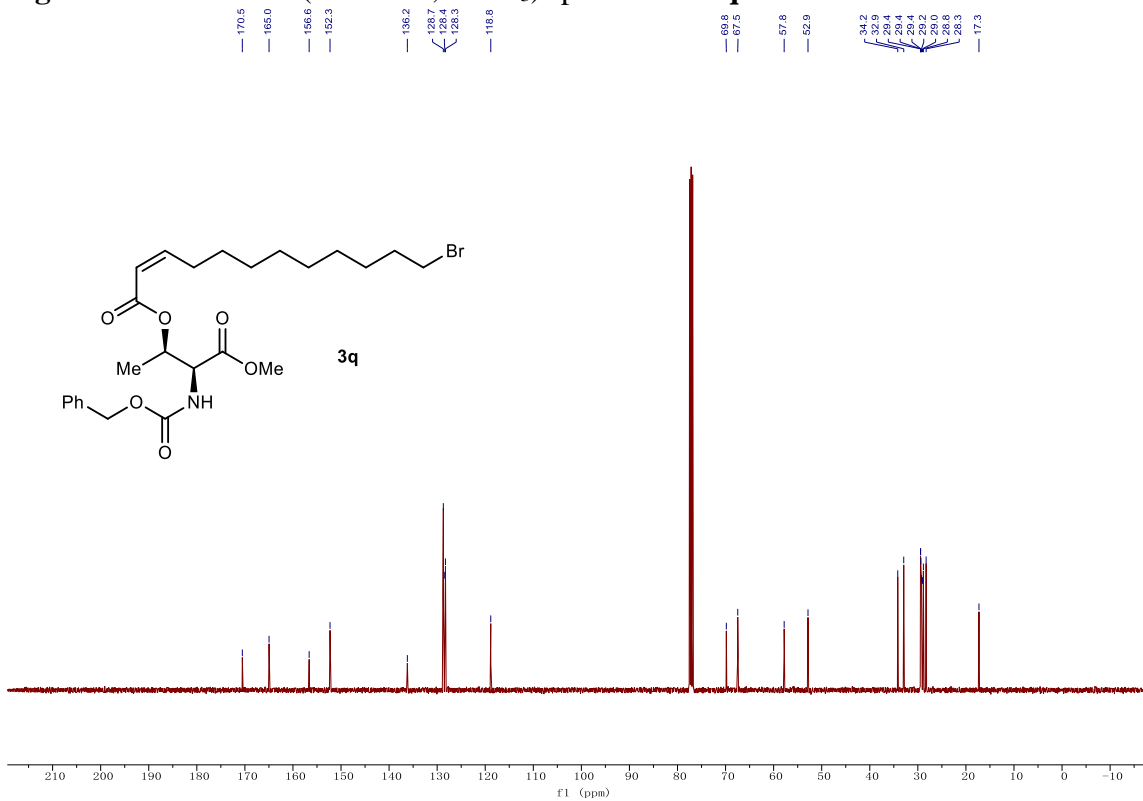
Figure B53. ^{1}H NMR (400 MHz, CDCl$_3$) spectrum of **3r**.
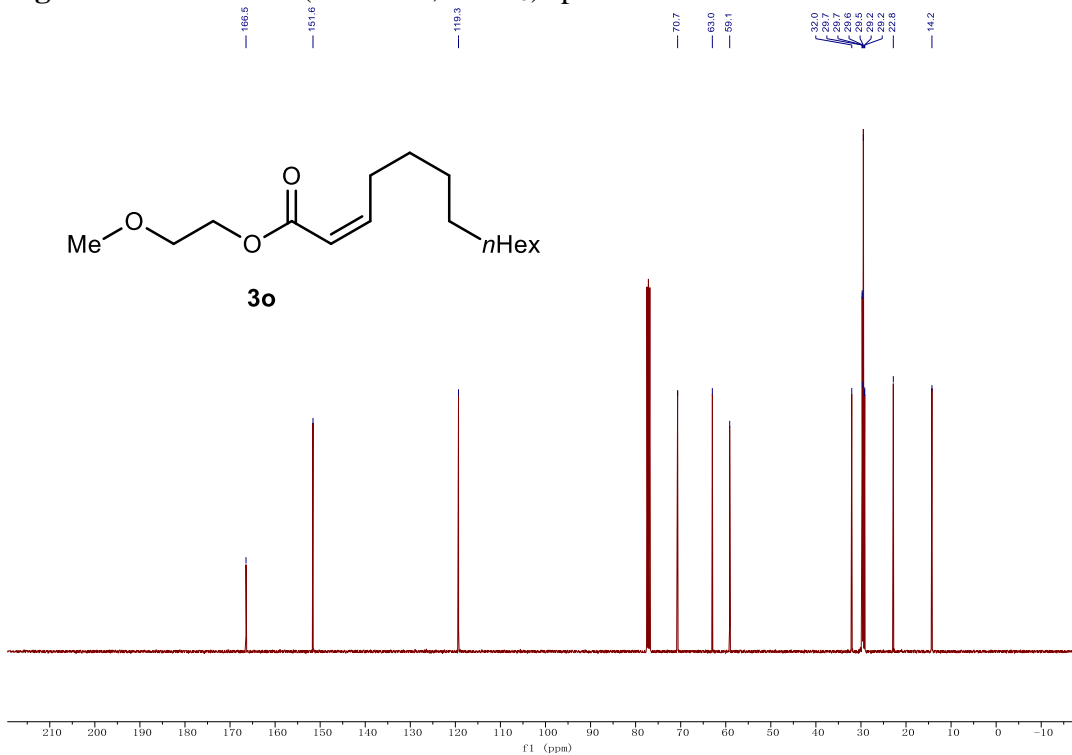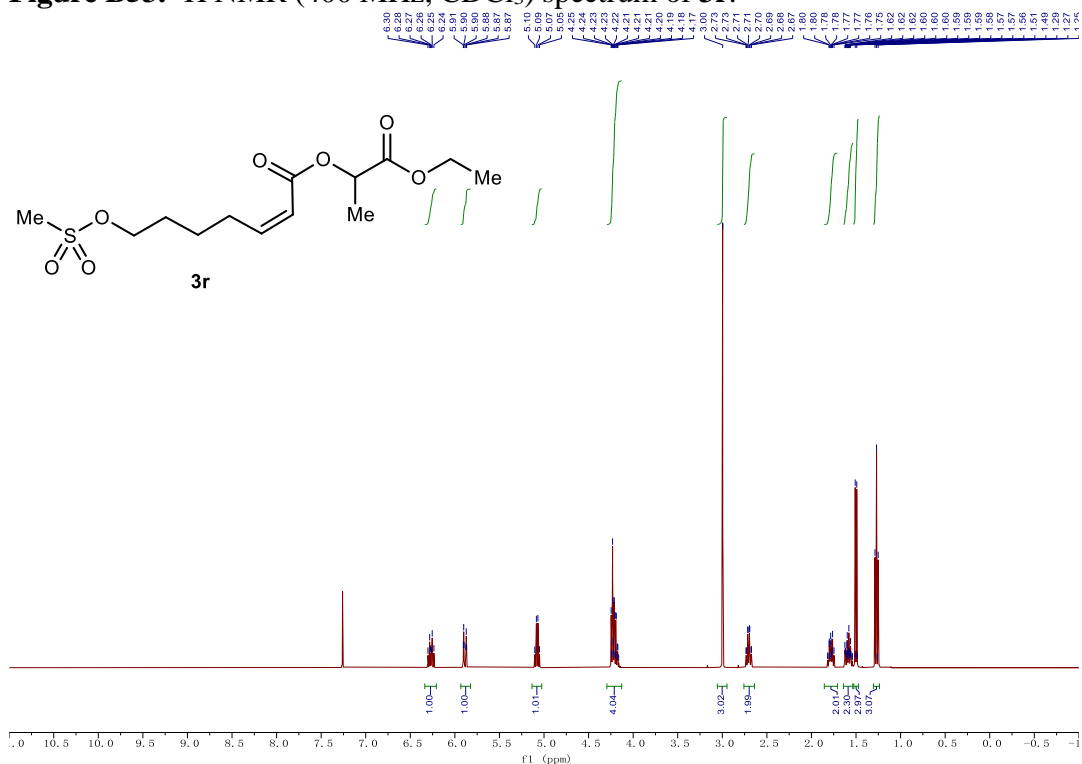

Figure B54. ^{13}C NMR (101 MHz, CDCl$_3$) spectrum of **3r.**
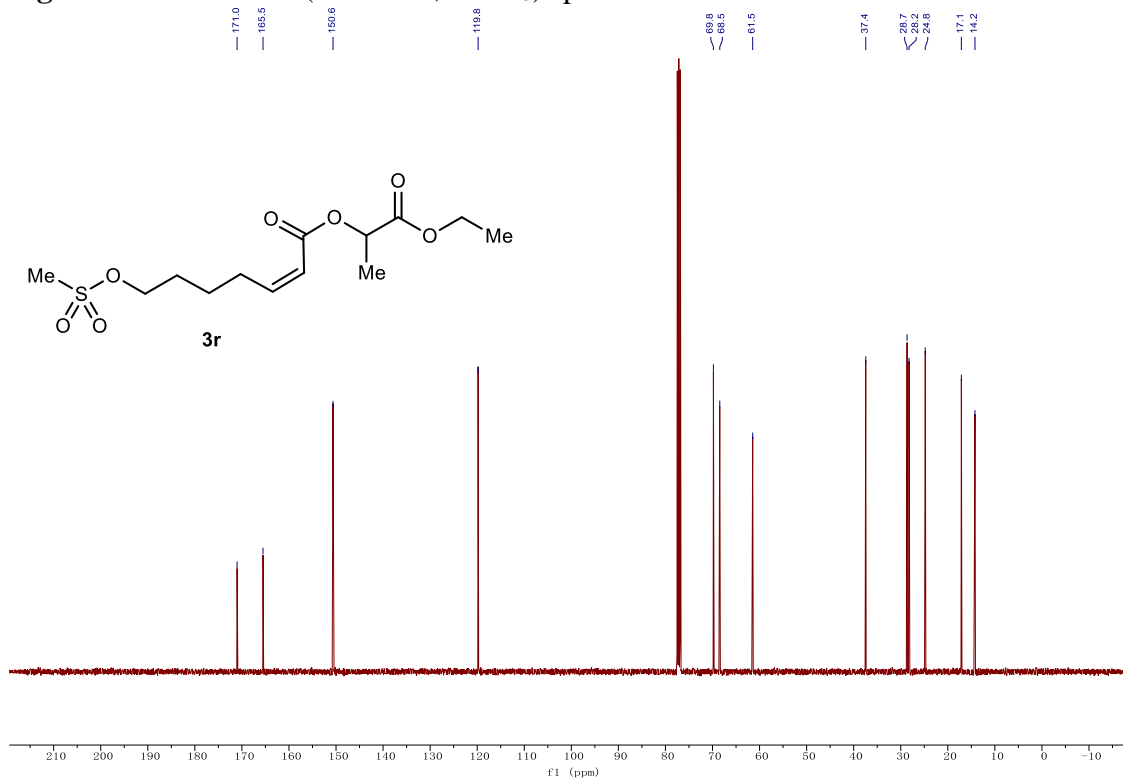
Figure B55. ^{1}H NMR (400 MHz, CDCl$_3$) spectrum of **3t**.
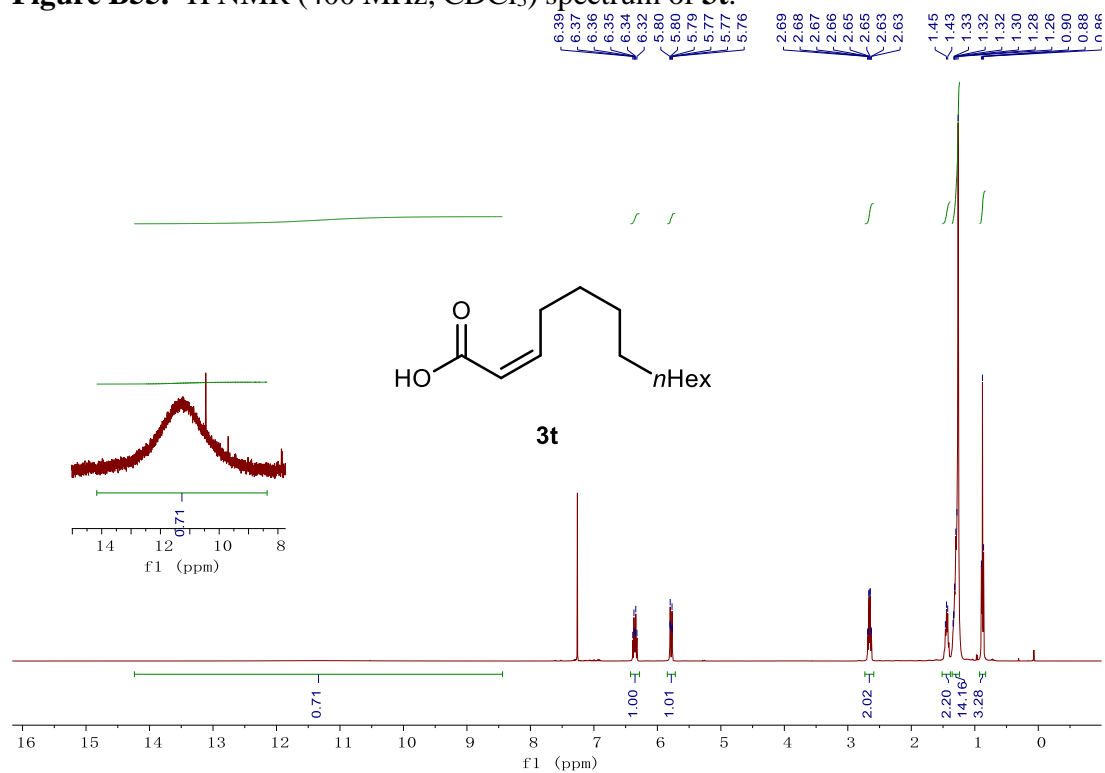
Figure B56. ^{13}C NMR (101 MHz, CDCl$_3$) spectrum of **3t**.
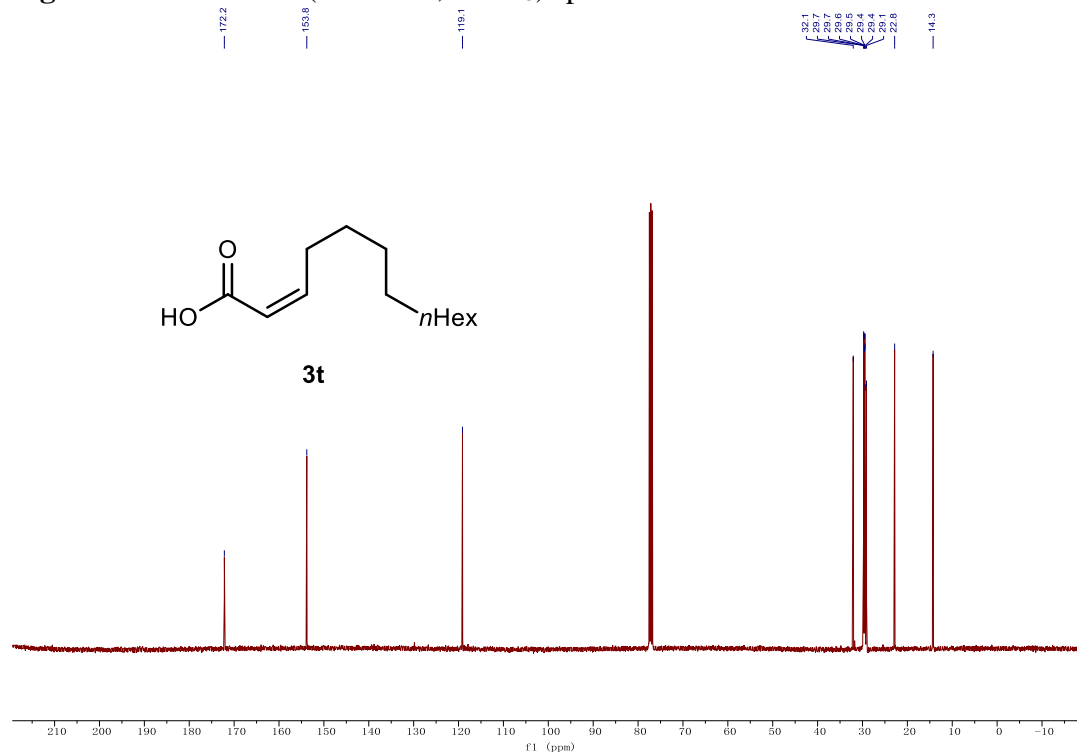
Figure B57. ^{1}H NMR (400 MHz, CDCl$_3$) spectrum of **5a**.

Figure B58. ^{13}C NMR (101 MHz, CDCl$_3$) spectrum of **5a.**
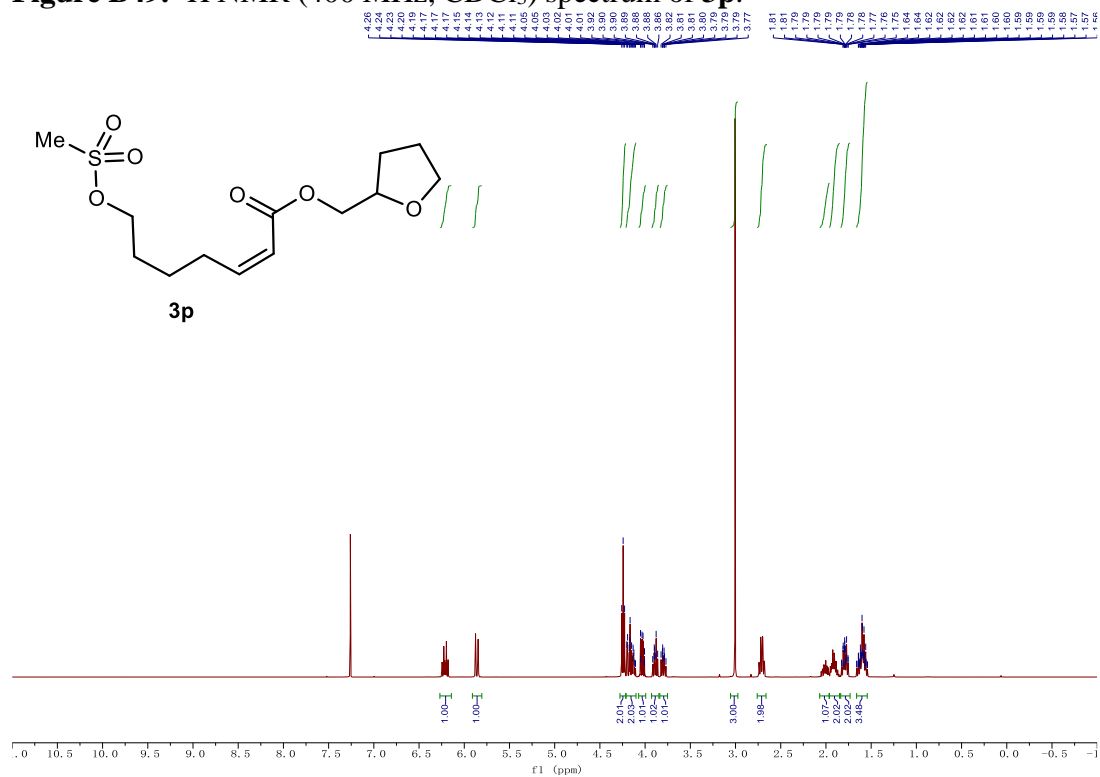
Figure B59. ^{1}H NMR (400 MHz, CDCl$_3$) spectrum of **5b**.

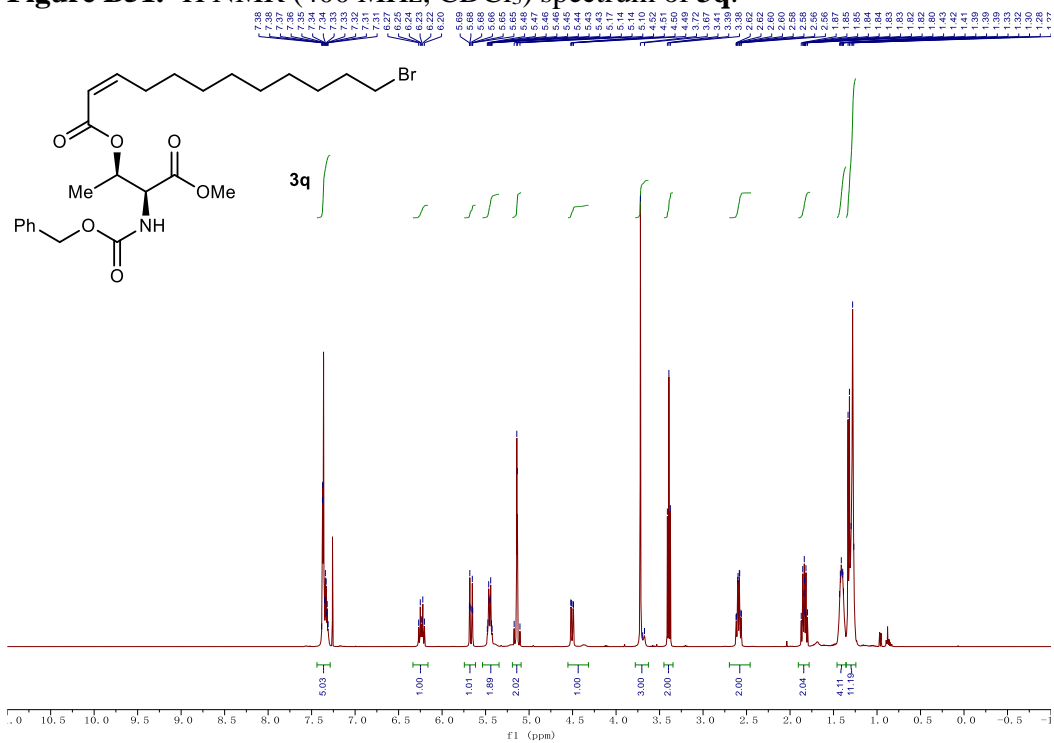**Figure B60.** ^{13}C NMR (101 MHz, CDCl$_3$) spectrum of **5b**.

Figure B61. ^{1}H NMR (400 MHz, CDCl$_3$) spectrum of **5c**.

Figure B62. ^{13}C NMR (101 MHz, CDCl$_3$) spectrum of **5c**.
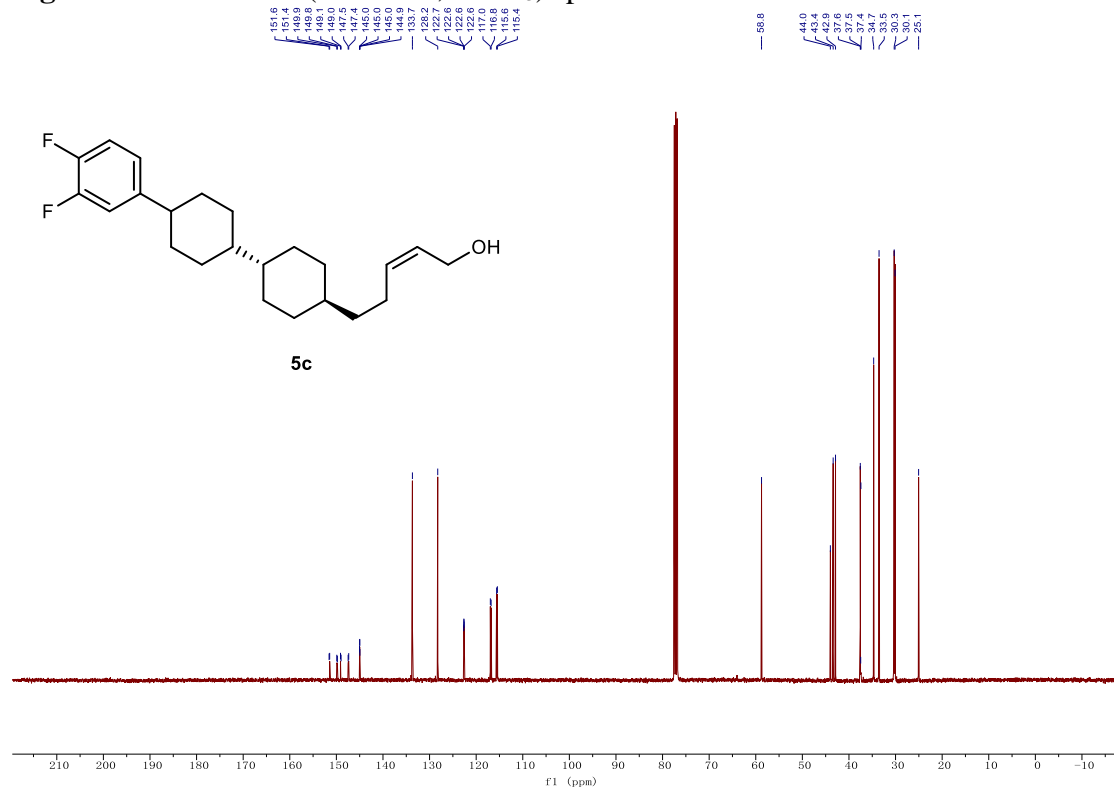
Figure B63. ^{1}H NMR (400 MHz, CDCl$_3$) spectrum of **5d**.
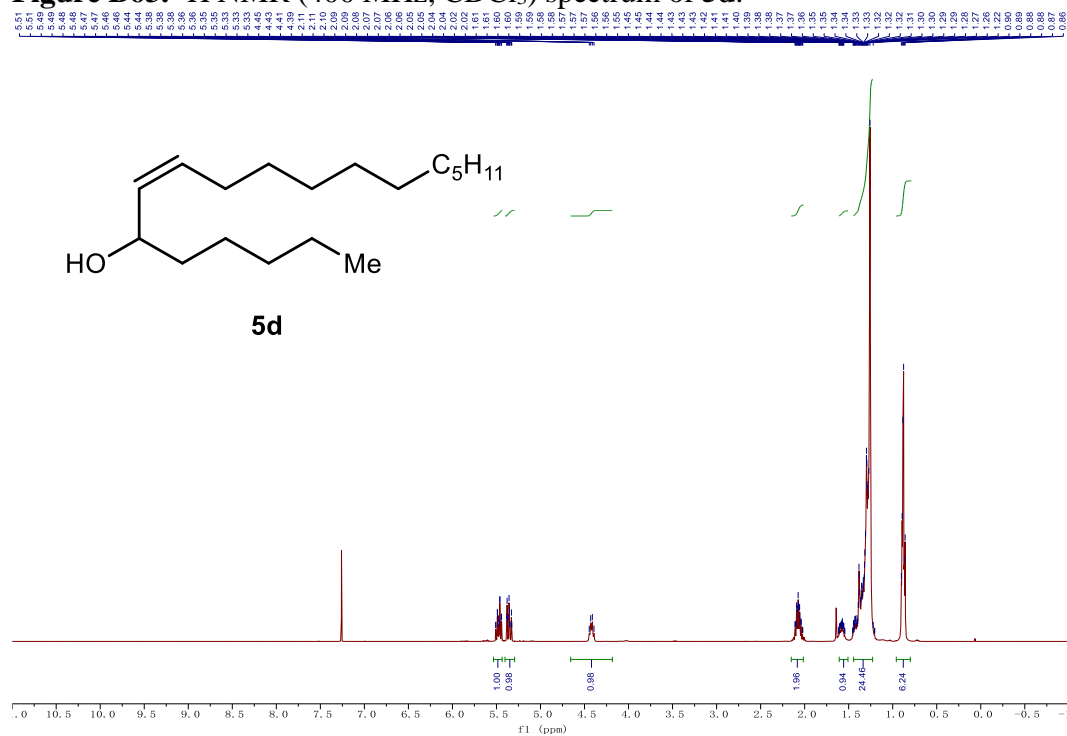
Figure B64. ^{13}C NMR (101 MHz, CDCl$_3$) spectrum of **5d.**
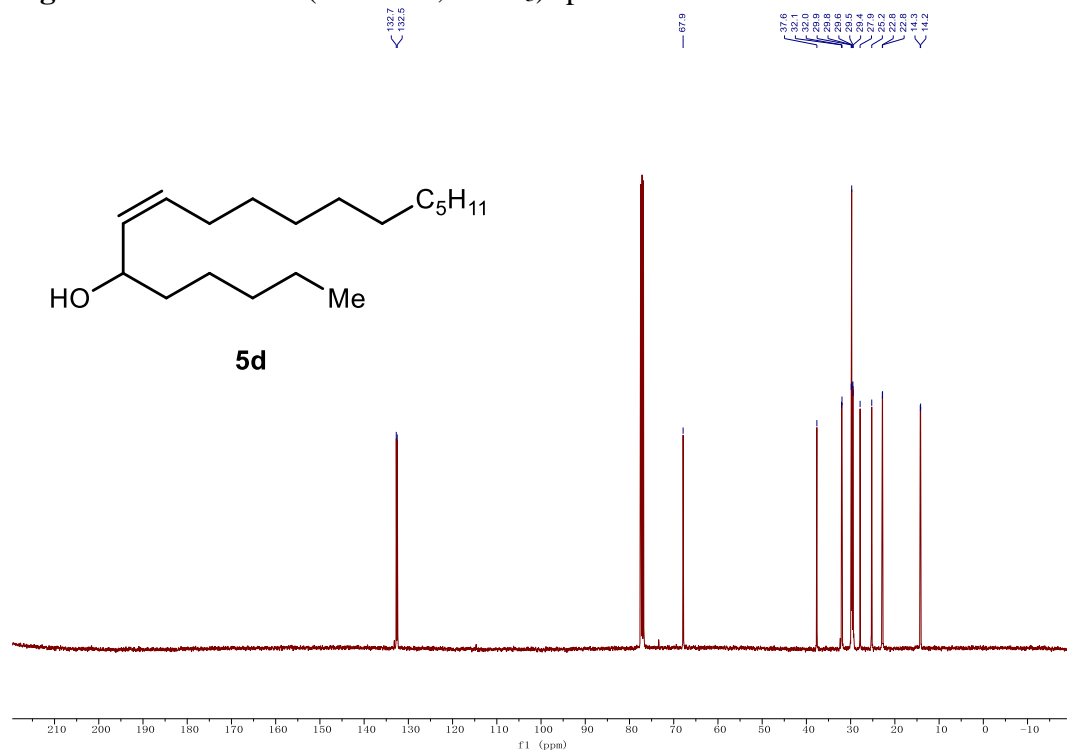
Figure B65. ^{1}H NMR (400 MHz, CDCl$_3$) spectrum of **5e**.
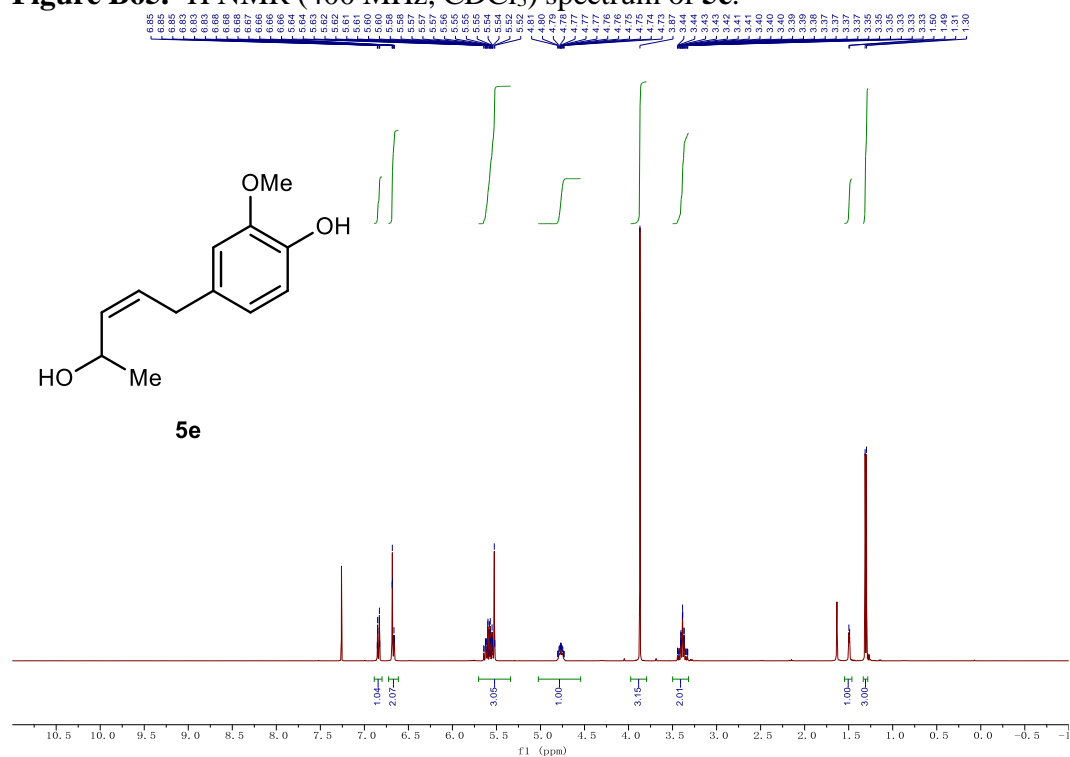
Figure B66. ^{13}C NMR (101 MHz, CDCl$_3$) spectrum of **5e.**
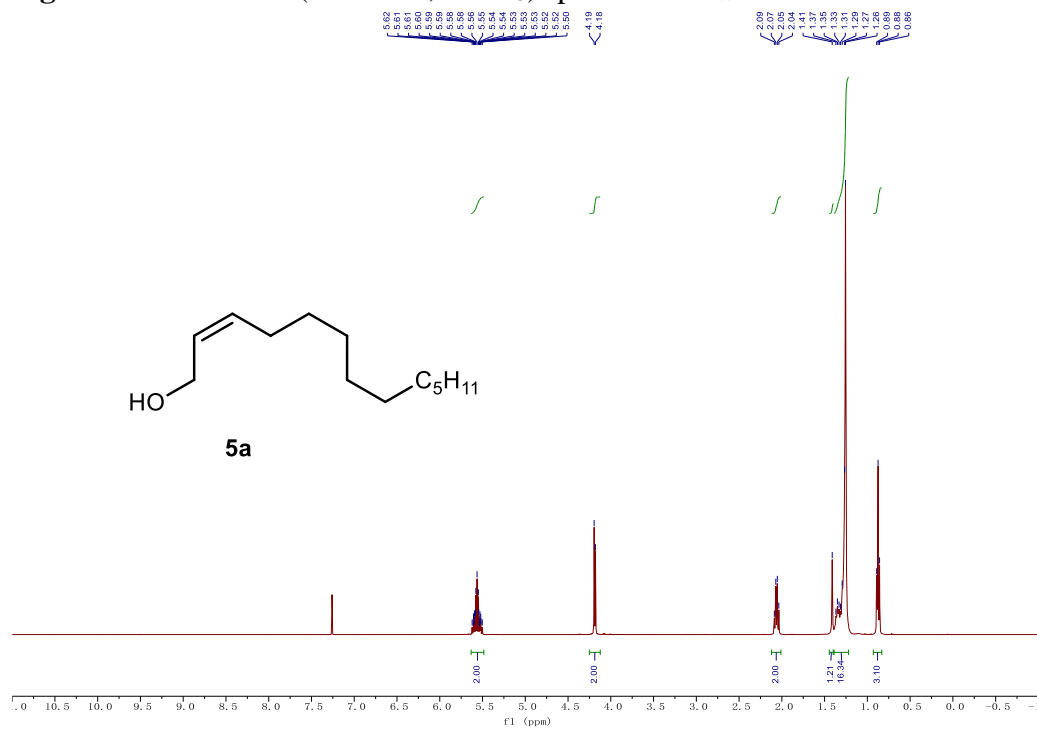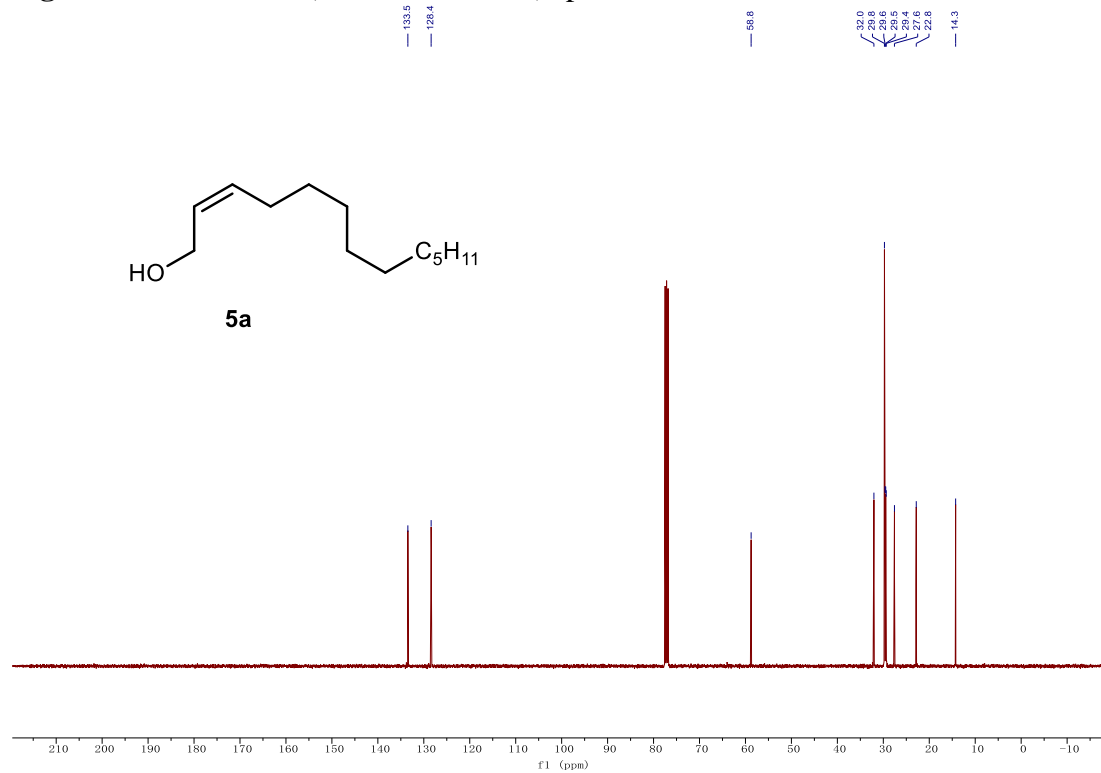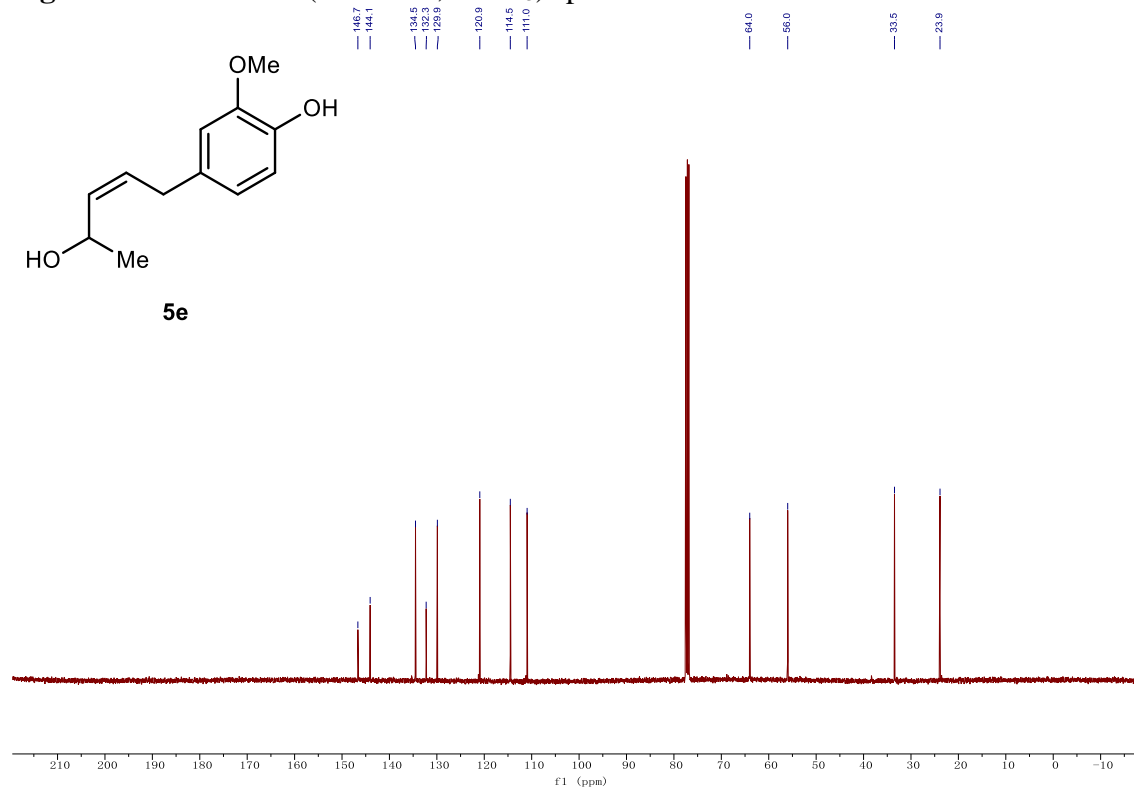
Figure B67. ^{1}H NMR (400 MHz, CDCl$_3$) spectrum of **5f**.
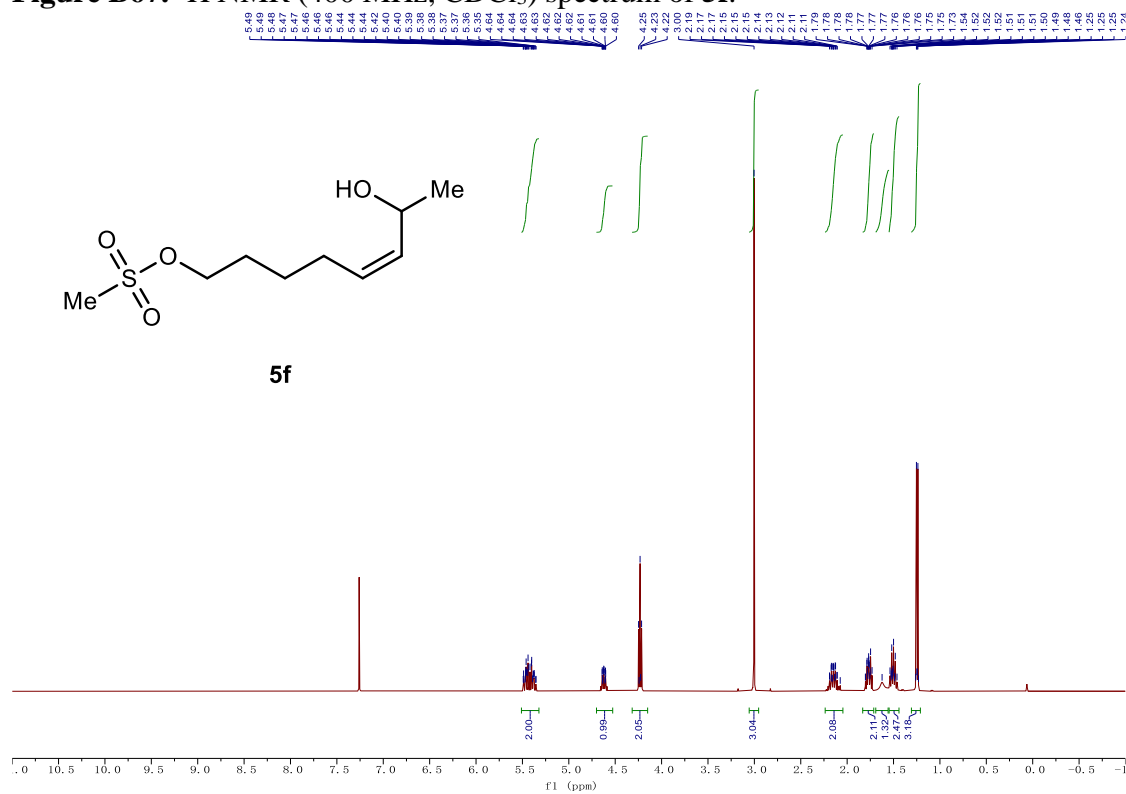
Figure B68. ^{13}C NMR (101 MHz, CDCl$_3$) spectrum of **5f**.
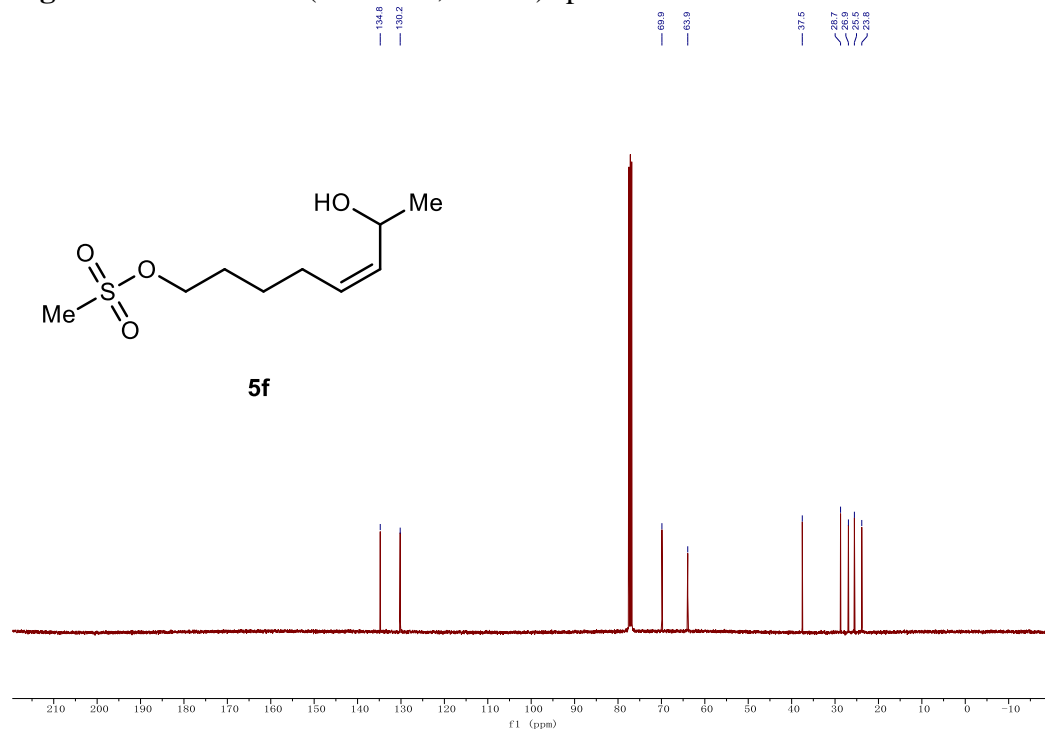
Figure B69. ^{1}H NMR (400 MHz, CDCl$_3$) spectrum of **5g**.

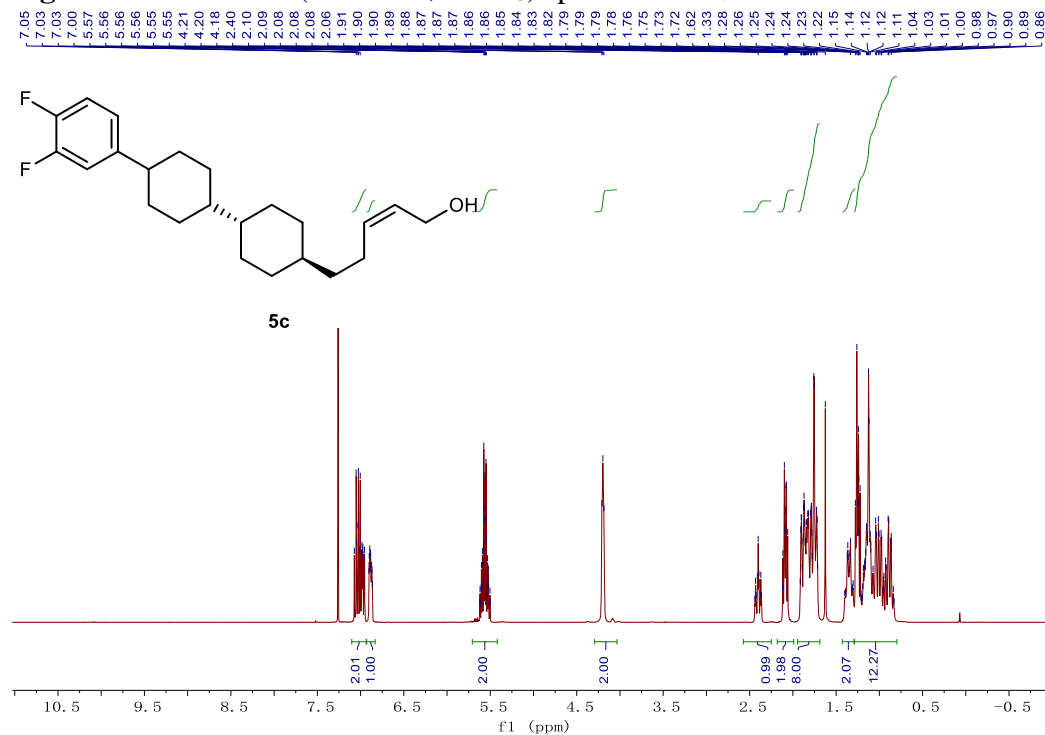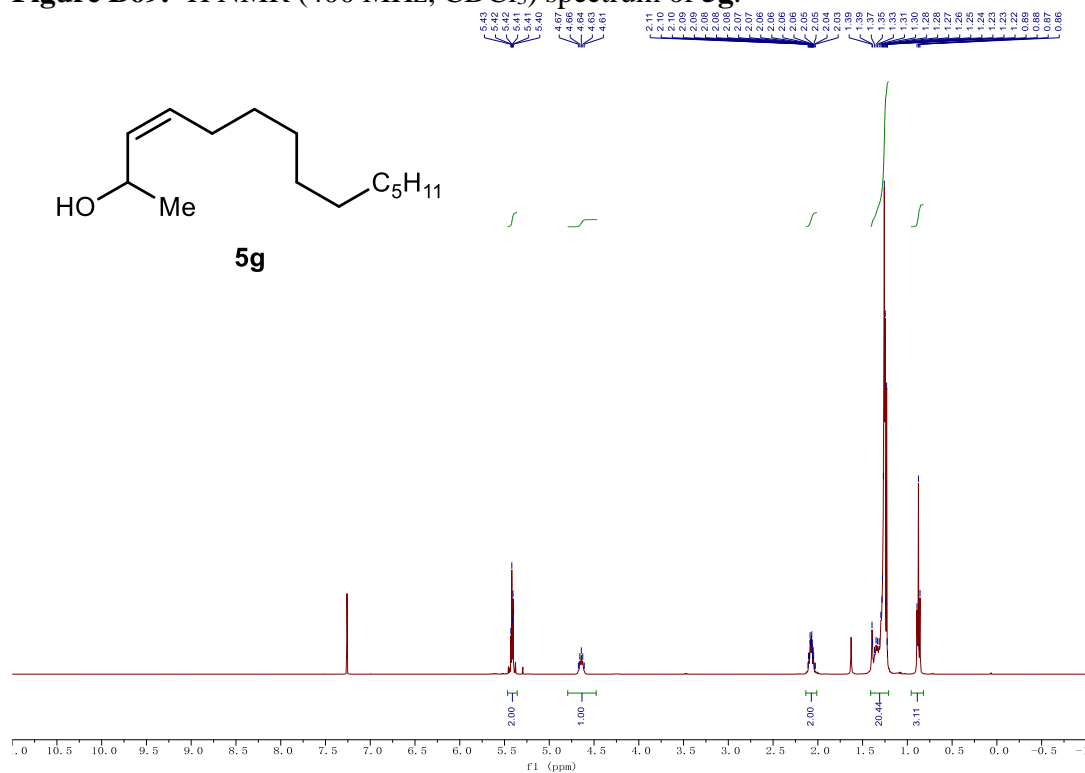**Figure B70.** ^{13}C NMR (101 MHz, CDCl$_3$) spectrum of **5g**.
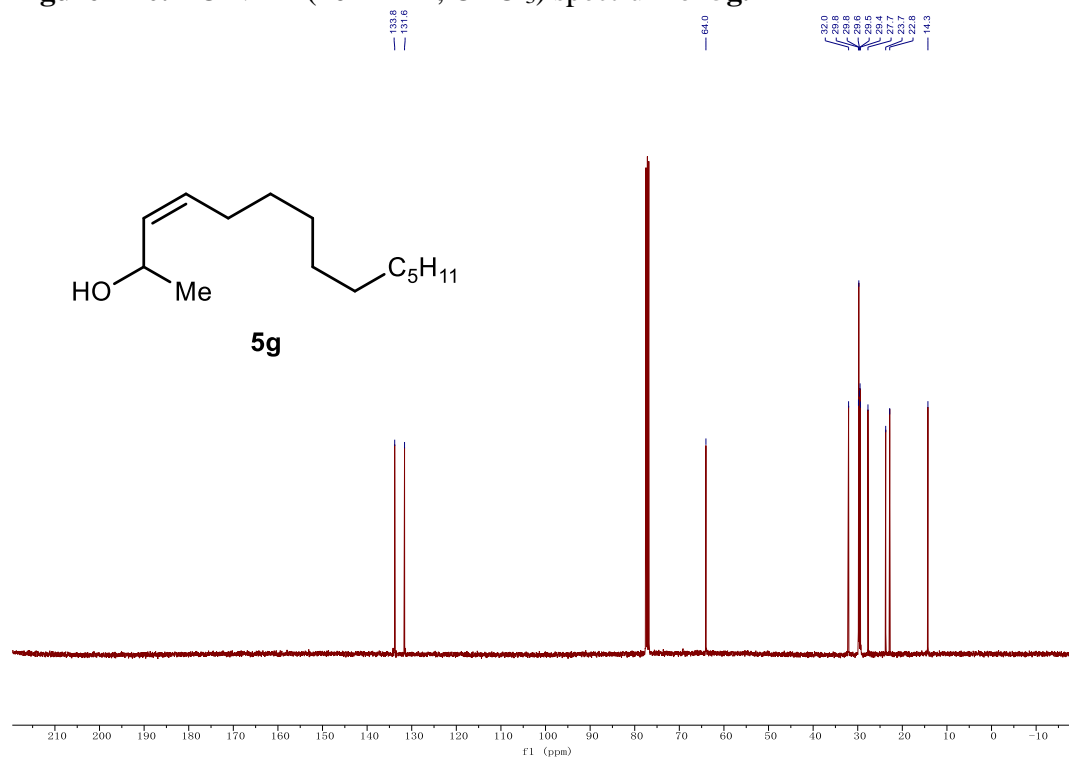
Chapter 3

Synthesis and Separation of Macrocyclic Polyolefins through Polar Monomer Incorporation and Chain-End Modification

3.1 Introduction

Ring opening metathesis polymerization (ROMP) of cycloolefin monomers can lead to secondary metathesis reactions, including intrachain metathesis reactions (or back-biting reactions) and interchain metathesis reactions. These side reactions can broaden the product molecular weight distribution and cause deviations from the target molecular weight.[1,2] However, back-biting can also generate macrocycles (Scheme 3.1), which have unique chemical and physical properties compared to their linear counterparts.[3,4] As the synthesis of macrocycles continues to advance rapidly, there is increasing interest in exploring their potential applications in materials science and drug delivery.[3,5–7] For instance, cyclic polyolefins can serve as additives to linear counterparts to tune their physical properties. In the commercialized polycyclooctene (PCOE) based rubber additive VESTENAMER®, the high percentage of macrocycles is responsible for the lower melting point and viscosity.
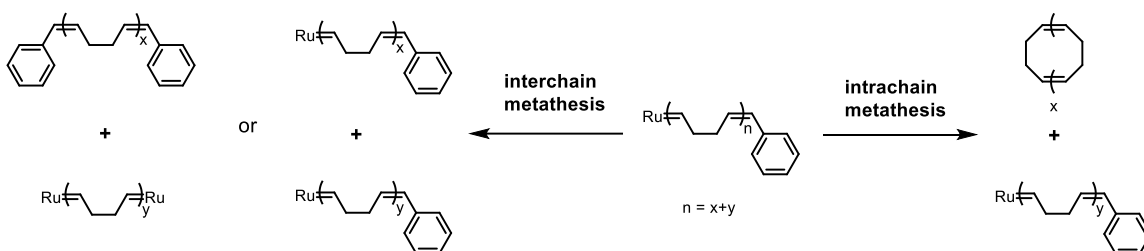
Scheme 3.1. Secondary metathesis reactions for a propagating PBD chain in ROMP initiated by Grubbs catalyst.

By regulating the ring-chain equilibrium, it becomes possible to generate pure macrocycles. Several studies have explored this approach using different catalysts and monomers. For instance, Qiao used a second-generation Hoveyda-Grubbs (**HG2**) catalyst to create functionalized macrocyclic oligo(cyclooctene)s, while Sampson synthesized alternating cyclic polymers using a similar approach.[8,9] Weck also successfully synthesized macrocycles using a third-generation Grubbs (**G3**) catalyst from a cyclooctene derivative.[10,11] In these studies, low monomer concentrations (ranging from 0.1 M to 0.5 M) and high catalyst loadings (ranging from 0.8% to 4%) were utilized. However, producing macrocycles from ROMP under other reaction conditions, such as higher monomer concentrations or lower catalyst loadings, remains challenging due to the difficulty of separating macrocycles from linear components.

In addition, while there has been extensive research on the ring-chain equilibrium, current methods for characterizing macrocycles are limited. Gas chromatography (GC) is commonly used, but it cannot detect macrocycles above certain molecular weight.[12–16] Other methods, such as viscometry, have been employed to estimate macrocycle content in polycyclopentene (PCP), but they do not provide information on the molecular weight of the macrocycles.

To gain a better understanding of macrocycles, it would be useful to isolate them from the reaction mixture and characterize them individually. Liquid chromatography at the critical condition (LCCC) has shown promise in separating linear and cyclic polymers with similar chemical composition, but maintaining the critical conditions can be challenging, and even small changes in mobile phase composition or temperature can disrupt the delicate balance required for LCCC.[17–23]

Alternatively, interaction chromatography can be employed to chemically distinguish the linear and cyclic chains and isolate the macrocycles, providing greater insight into the ring-chain equilibrium.

To address these challenges, we propose a synthetic approach to isolate macrocycles generated in ROMP. We introduce polar functional groups into the linear chains, which facilitates the separation of macrocycles from the reaction mixture using silica gel chromatography. Our study focuses on the ROMP of cyclooctadiene (COD) as a prime example, examining how various reaction factors - such as feed monomer concentration, reaction temperature, reaction time, solvent, catalyst loading, and catalyst structure - affect the molecular weight and yield of macrocycles. We also examine the formation of macrocycles in the ROMP of cyclooctene (COE), cyclopentene (CP), and norbornene (NB).

3.2 Separation of macrocycles through chain-end modification
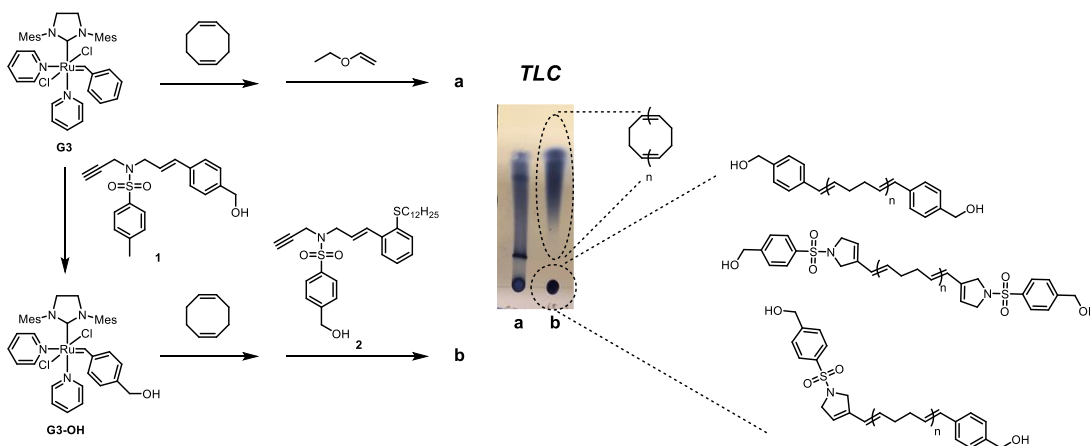
Scheme 3.2. Synthesis of hydroxyl terminated polybutadiene using ROMP and structure of products. TLC analysis of product was developed by 10:3 (v/v) hexanes/dichloromethane and stained by cerium ammonium molybdate stain. **a**: ROMP of COD initiated by **G3** and terminated by ethyl vinyl ether. **b**: ROMP of COD initiated by **G3-OH** and terminated by **2**.

Thin-layer chromatography (TLC) analysis shows that hydroxyl-terminated polystyrene or polybutadiene, within a certain molecular weight range, exhibit stronger interaction with silica gel and have smaller retention factors (R_f) compared to hydrogen-terminated polystyrene (PS) or polybutadiene (PBD). This highlights how a single polar end-group can significantly alter adsorption behavior.[24,25] Introducing polar groups to the linear polymer produced from ROMP can enable easier isolation of less polar macrocycles using silica gel chromatography.

Recently, Gutekunst has developed a series of enyne metathesis reactions to efficiently modify benzylidene initiator of **G3** and terminate ROMP while attaching desired end-groups.[26–28] We used this chemistry to synthesize **G3-OH** and initiate ROMP of COD under standard condition ([COD] = 1.1M in C_6D_6; [COD]/[**G3-OH**] = 100, 30 min, 20 °C). The **G3** was first reacted with 3 equivalents of **1** for 15 minutes. ^{1}H NMR showed >95% conversion from **G3** to **G3-OH**, as determined from the integration of the benzylidene proton to anthracene as an internal standard (Figure C1). Stock solution of **G3-OH** in C_6D_6 was added to COD in C_6D_6, resulting in a COD concentration of 1.1M and a [COD]/[**G3-OH**] molar ratio of 100. The solution was stirred at 20 °C for 30 minutes. **G3-OH** displayed similar activity to **G3**, producing linear PBD with similar molecular weight distribution (M_n = 10.4 kDa, Đ = 1.48, Figure C2). After reaction was completed, 2 equivalents of **2** were added to quench the polymerization. ^{1}H NMR showed full monomer conversion, no catalyst decomposition, and full conversion of catalyst to the inert thioether chelated **G3-thio** (Figure C1). Ideally, all linear species, including the product from interchain metathesis will have hydroxy groups at both chain ends (Scheme 3.2).

The reaction mixture was initially analyzed by TLC. With 10:3 (v/v) hexanes/dichloromethane (DCM) as eluent, two spots are identified – one polar component

tentatively assigned as linear PBD with an R_f close to 0, and one oblong spot with larger R_f as cyclic PBD. Complete separation of two spot without overlapping enabled the chromatographic separation of linear PBD. For comparison, PBD initiated by **G3** under same conditions, without addition of **2**, is developed into a single spot (Scheme 3.2).

	M_n (kDa)	Đ	Yield (%)
F1 (cyclic)	0.7	2.86	16.1
F2 (cyclic)	1.3	1.27	4.3
F3 (cyclic)	1.8	1.04	7.0
F4 (cyclic)	4.0	1.03	2.0
F5 (linear)	14.2	1.33	18.0
F6 (linear)	11.0	1.49	26.8
F7 (linear)	8.9	1.33	24.2
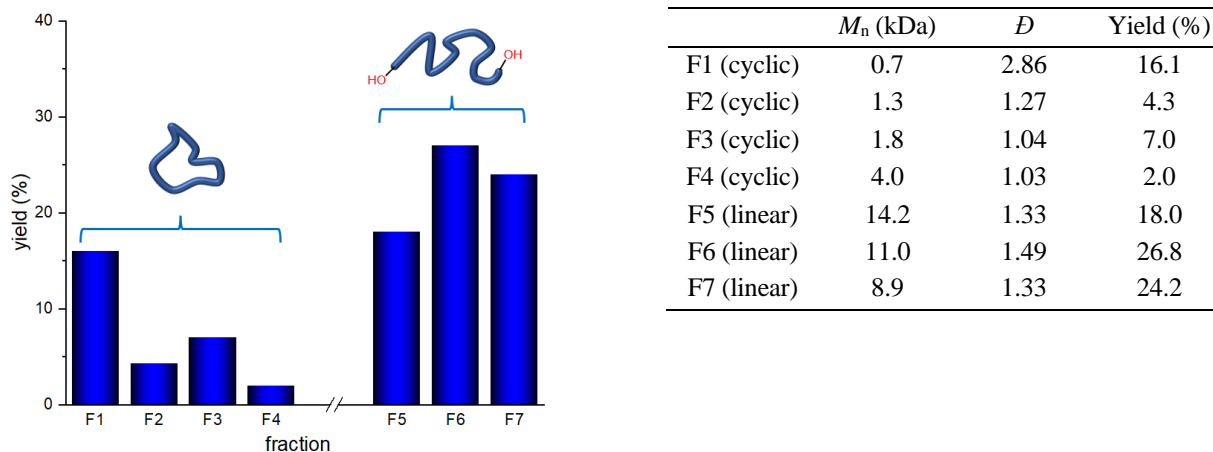
Figure 3.1. Elution order of cyclic and linear PBD. Table shows M_n, Đ and yield of each fraction.

The reaction mixture was loaded onto a silica gel column and eluted with 10:1 to 1:10 (v/v) hexanes/DCM. Notably, the elution order for the product was intriguing, with macrocycles of smaller molecular weight eluting first, followed by macrocycles of larger molecular weight. Subsequently, longer linear chains were eluted, followed by shorter linear chains (see Figure 3.1). Hercules previously observed the reverse elution order of cyclic polymer while separating linear and cyclic polyesters and polyurethanes using specific ethylene bridged hybrid silica particles as the stationary phase and acetonitrile as the mobile phase. They found that linear chain length was inversely proportional to elution time, and suggested that acetonitrile was a good solvent for linear chains but a non-solvent for cyclic chains, tentatively explaining the phenomenon.[29] Weck and Qiao have also reported a similar elution order for macrocycles.[8,11]

In our study, we found that the adsorption of linear chains on the stationary phase was primarily due to the hydroxyl groups. As molecular weight increased, the polarity of the chains was diminished by the hydrocarbon backbones, resulting in larger R_f values for longer chains. Conversely, for cyclic chains, smaller chains eluted earlier due to the absence of polar end-groups, which resulted in weaker interactions. McCarthy has previously reported similar differences in adsorption behavior for hydrogen-terminated PS and hydroxyl-terminated PS.[24]

3.3 Characterization of macrocycles

All four cyclic PBD fractions were combined to form **C1**, with a yield of 29%. GPC analysis of **C1** revealed a high dispersity of 2.75 and a small molecular weight of 0.8 kDa. The DRI trace showed a separated peak at the elution time of *trans,trans,trans*-1,5,9-cyclododecatriene (*ttt*-CDT), followed by a monotonic decrease in RI response with shorter elution times for larger cyclic species (Figure 3.2a). This can be attributed to the decreasing probability of the Ru catalyst reacting with a more distant double bond in the backbone.[30] Attempts to synthesize a linear analogue with similar molecular weight and dispersity to **C1** were unsuccessful, but the retention time of a synthesized linear PBD (M_n = 1.3 kDa, $Đ$ = 1.47) was significantly longer than that of fractioned cyclic PBD (M_n = 1.3 kDa, $Đ$ = 1.27) of similar molecular weight (Figure 3.2b). Another fractioned cyclic PBD with similar retention time to this linear PBD exhibited larger molecular weight (M_n = 2.3 kDa, $Đ$ = 1.15). All fractioned cyclic PBD fractions **F1-F4** from **C1** exhibited longer retention times and thus smaller hydrodynamic volumes than their linear counterparts (Figure C3), indicating the topological purity of **C1**. This purity was further demonstrated by the absence of end-groups in **C1**, as the intensity of the styrenic protons in the 1H NMR spectrum was below the detection limit (Figure 3.2c). End group peak intensity for high molecular weight linear PBD is low, but such impurity was absent given the

large retention time of **C1**. On the other hand, linear PBD with low molecular weight shows stronger

end group signals, so this topological impurity present is likely to be very low.

(a)

(b)

(c)

(d)
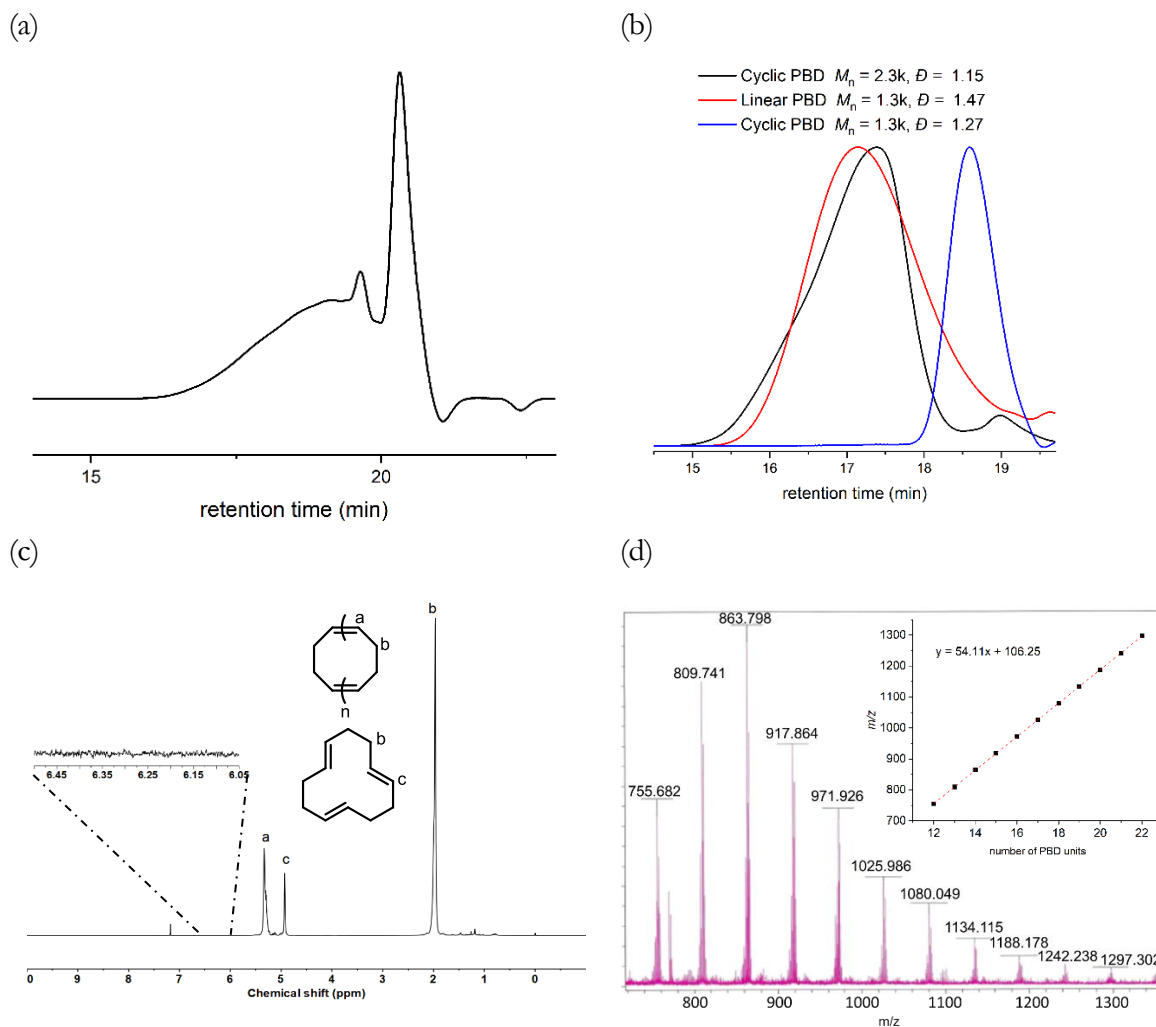
Figure 3.2. (a) GPC differential refractive index (DRI) chromatograms showing product distribution of **C1**. (b) GPC DRI traces comparison between cyclic and linear PBD. (c) ^{1}H NMR spectrum (CDCl$_3$) of **C1** with expansion of the 6.05−6.50 ppm region. Absence of signals for styrenic end-group protons indicates no linear polymer impurity was present. (d) MALDI ToF MS for **F1** obtained in reflection mode. Inset shows the plot of the m/z values (y) versus the number of C$_4$H$_6$ repeat units (x) for the peak series.

The low polarity of the pure hydrocarbon composition resulted in poor ionization and difficulty in measuring the MALDI ToF MS. Only MALDI ToF MS for the lower molecular weight fraction **F1** was obtained, which revealed a single series of peaks corresponding to cyclic PBD (Figure 3.2d, see Figure C4 for MALDI ToF MS obtained in linear mode). Plotting the *m/z* values for the peaks versus the number of PBD repeating units yielded a relationship of $y = 54.11x + 106.25$, corresponding to the structure of $[(C_4H_6)_n + Ag^+]$. Peaks corresponding to linear PBD of different end-groups (Scheme 3.2) with a degree of eight repeating units (1041.19, 910.19, and 779.18) were absent. A peak interval of 54.11 suggests that the cyclic polymers were formed via backbiting rather than cyclooligomerization of COD, which would have resulted in a peak interval of 108.22 or increased intensities for peaks with even numbers of repeating units in the MS.

3.4 Improvement of the separation method by polar monomer incorporation

The results of all the characterization techniques used indicate that the macrocycles were successfully isolated from the reaction mixture. However, there are some significant limitations to this approach. Firstly, if a smaller catalyst loading is used compared to the standard conditions, the polarity of longer linear PBD may not be high enough to allow for their separation from the macrocycles. For instance, when the [COD]/[**G3-OH**] ratio is increased to 1000, higher molecular weight linear PBD is mixed with higher molecular weight cyclic PBD (see Figure C5). Secondly, the efficiency of the enyne metathesis chemistry employed to modify the ruthenium catalyst and quench polymerization is much lower for catalysts other than **G3**.[26,27] To investigate the distribution of cyclic PBD under these conditions, we modified the reaction approach by adding a polar monomer, exo-cis-5-norbornene-2,3-dicarboxylic acid (NDA), after polymerization of the COD and before quenching the reaction with **2** ([COD]/[NDA] = 10). The reaction can be quenched shortly (within

30 seconds) after the addition of NDA because of its fast polymerization, thus minimizing the effect on the reaction equilibrium of ROMP of COD (see Figure C6).[12,31] The resulting PBD-*b*-PNDA copolymer, which has much higher polarity, greatly improves the efficiency of separating cyclic PBD through interaction chromatography.

3.5 Analysis of macrocyclic species in ROMP of cyclooctadiene

Using this improved method, we investigated macrocycle formation during the ROMP of COD under various conditions. We found that decreasing the catalyst loading resulted in an increased molecular weight for linear PBD, but the molecular weight for cyclic PBD did not show a significant variation from the standard condition (Table 3.1, entries 1-1 and 1-2). In order to obtain larger cyclic PBD, the propagating Ru needs to react with a further backbone double bond, but this reactivity is independent of the catalyst loading. We observed a slight decrease in the yield of cyclic PBD, which could be a consequence of the reduced Ru concentration and thus less frequent back-biting events, or a pre-equilibrium state due to a slower reaction rate.[32]

Table 3.1. Molecular weight of crude linear PBD and yield and molecular weight of macrocycles from ROMP of COD.
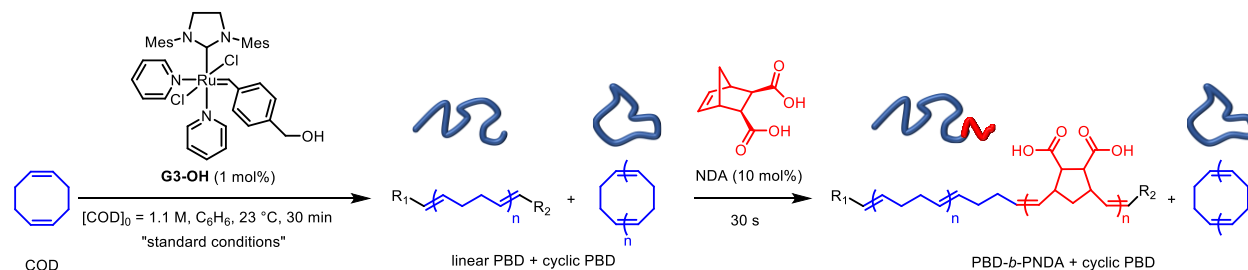
Entry	Change from "standard condition"	Crude PBD $M_n(M_w)$ (kDa)	cPBD yield(%)	cPBD $M_n(M_w)$ (kDa)
1-1	None	10.8(16.0)	29	0.8(2.2)
1-2	[COD]/[Ru] = 400	22.2(35.1)	28	0.9(1.6)
1-3	[COD]/[Ru] = 1000	35.9(63.5)	24	0.7(1.6)
1-4	T = 0 °C	11.8(15.7)	20	0.7(1.0)

1-5	T = 50 °C	10.4(14.1)	34	1.3(3.5)
1-6[a]	T = 70 °C	4.5(5.5)	25	1.6(2.0)
1-7	$[COD]_0 = 0.27M$	3.3(5.3)	64	0.3(1.4)
1-8	$[COD]_0 = 0.1M$	1.2(5.2)	92	0.3(0.8)
1-9	t = 5 minutes	8.3(12.6)	22	1.5(3.0)
1-10[a]	t = 300 minutes	9.2(15.8)	31	2.3(4.1)
1-11	THF instead of benzene	9.5(15.5)	25	0.5(1.0)
1-12	hexanes/benzene (v/v = 1/6) instead of benzene	11.0(16.2)	26	0.7(2.0)
1-13[a]	[Ru] = G1	6.2(9.8)	8	7.2(9.0)
1-14[a]	[Ru] = G2	11.2(18.0)	26	2.0(4.2)
1-15	[Ru] = HG2	17.4(27.1)	37	0.4(1.2)
1-16[a]	[Ru] = G3	10.9(16.2)	42	0.6(2.9)
1-17	$[COD]/[Ru] = 1000, [COD]_0 = 0.27M$	1.1(7.0)	34	0.5(1.2)
1-18[b]	$[COD]/[Ru] = 1000, [COD]_0 = 0.27M$	1.8(8.9)	29	0.4(1.6)
1-19[c]	[COD]/[Ru] = 1000, [COD]/[MA] = 10, THF instead of benzene	2.3(3.8)	21	0.4(1.5)

[a] Styrenic protons (ca. δ_H 6.15 and 6.32 ppm) are identified in the ^{1}H NMR spectra of separated cPBD products.
[b] Reaction was first equilibrated at 1.1 M for 15 minutes, then diluted to 0.27 M and equilibrated for another 15 minutes.
[c] NDA is not added.

The reaction temperature is a complex factor. In the metathesis reaction equilibrium of PBD, *ttt*-CDT is favored over larger oligomers or *ctt*-CDT/*cct*-CDT because of its higher enthalpic loss in the back-biting process, and only the formation of *ttt*-CDT is significantly affected by temperature among all macrocycles.[14] At 50 °C, the formation of *ttt*-CDT is suppressed and an elevated temperature promotes the formation of larger macrocycles, which are entropy-driven.[2,33,34] As a result, cyclic PBD (cPBD) was produced with a larger molecular weight and the yield of cPBD increased to 34% (Table 3.1, entry 1-5). At a decreased reaction temperature of 0 °C, molecular weight and yield of cPBD decreased (Table 3.1, entry 1-4). When the temperature was further increased to 70 °C, **G3-OH** degraded during polymerization, resulting in smaller linear PBD and linear impurities in separated cPBD according to characteristic signals of styrenic protons (ca. δ_H

6.25 and 6.40 ppm) identified on ^{1}H NMR of the product (Table 3.1, entry 1-6, see Figure C7 for ^{1}H NMR spectrum).

The feed monomer concentration is a crucial factor that determines the ring-chain equilibrium. According to the Jacobson−Stockmayer theory, a critical monomer concentration $[M]_c$ can be established below which only cyclic oligomers are formed. When the monomer concentration is larger than $[M]_c$, the equilibrium concentration of cyclic fraction remains constant, and linear polymer chains start to grow.[35,36] When $[COD]_0$ was decreased to 0.27 M and 0.1 M, only oligomeric PBD were identified on GPC, and the yield of cPBD was increased to 64% and 92%, respectively. Since there was not sufficiently long linear PBD to release larger cPBD from back-biting, the molecular weight of cPBD decreased (Table 3.1, entries 1-7 and 1-8).

For the ROMP of COD, a prolonged reaction time of up to 8 hours is required to reach the thermodynamic equilibrium, during which the yield of macrocycles, especially *ttt*-CDT, gradually increases.[12,37,38] When reaction time was shortened to 5 minutes, molecular weight of cPBD increased due to lower yield of *ttt*-CDT, and yield of cPBD decreased (Table 3.1, entry 1-9). However, if the reaction is run for 300 minutes, linear impurities are identified in separated cPBD due to catalyst decomposition (Table 3.1, entry 1-10).

Previous reports suggested the solvent quality has a negligible influence on the kinetic and thermodynamic distribution of macrocycles by comparing toluene, DCM, chloroform and a theta solvent (3-pentanone/2-pentanone).[12,39] However, ROMP of COD and COE yielded a slightly larger fraction of cyclic oligomers in heptane than in benzene, according to some earlier reports.[39,40] Theoretical models also suggest a decreased yield of cyclics in good solvents, particularly in a diluted solution, because the expanded chains would impede chain-end encounter.[41] In our study, when

hexanes/benzene (v/v = 1/6) was selected as the solvent, precipitated PBD was observed during polymerization, which redissolved after addition of NDA solution, but molecular weight and yield of cPBD did not change much compared to the standard conditions (Table 3.1, entry 1-12). However, when THF was used instead of benzene, a decreased molecular weight and yield for cPBD were observed. This can be rationalized by the coordinating ability of THF, which can suppress secondary metathesis including back-biting, instead of solvent quality difference, as both benzene and THF are considered good solvents for PBD isopropyloxyaryl.[42,43]

The structure of the catalyst can significantly affect the reaction equilibrium in ROMP. For instance, **G1** is shown to initiate ROMP with minimal secondary metathesis.[33,42] When **G1** is used in place of **G3-OH**, the yield of cPBD decreased to 8%, and product distribution of cPBD largely differed from standard conditions (Figure C8) with minimal *ttt*-CDT formation (Table 3.1, entry 1-13). It indicates a kinetic product distribution was obtained instead of the thermodynamic equilibrium, which may be explained by **G1**'s inability to polymerize *ttt*-CDT.[12,38] However, ^{1}H NMR analysis showed the presence of linear contaminants eluting with cBPD, which are attributed to products from interchain metathesis containing two styrene end groups that could not be separated from cPBD. When **G2** is used, ROMP yields cPBD with a higher molecular weight than the standard condition, but the product also contained this linear impurity (Table 3.1, entry 1-14). When **G3** is used instead of **G3-OH**, yield of non-polar species increased to 42%, with 13% attributed to the styrene terminated linear PBD (Table 3.1, entry 1-16). Yield of this linear PBD component decreases with a lower catalyst loading or feed monomer concentration. **HG2** has a coordinating isopropyloxyaryl group, which led to a stronger tendency for back-biting, resulting in macrocycles with a higher yield but lower molecular weight.[8] Different from **G1**, **G2**, and **G3**, interchain
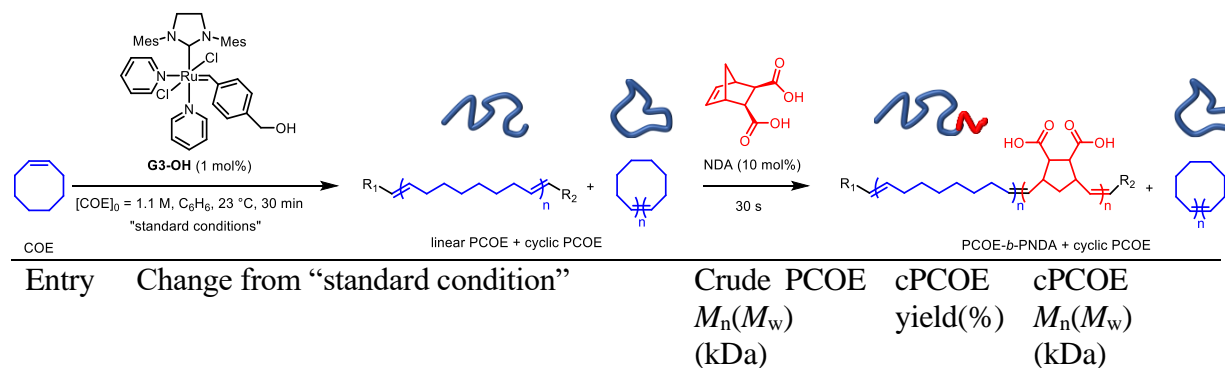
metathesis reactions were absent, as shown by the clean ^{1}H NMR of the separated nonpolar product (Table 3.1, entry 1-15).

The yields and molecular weights of cyclic PBD in entries 1-17 and 1-18 are similar, despite different reaction conditions. Entry 1-17 was performed with reduced catalyst loading ([COD]/[Ru] = 1000) and concentration ([COD]$_0$ = 0.27 M), while entry 1-18 began with the same catalyst loading at a higher concentration (1.1 M) for 15 minutes before being diluted to 0.27 M to reach equilibrium. These experiments demonstrate that ROMP of COD is an equilibrium-controlled polymerization and that the product distribution is determined by the final reaction conditions.[2,34,44,45]

One way to achieve molecular control in the ROMP of medium ring strain monomers is by using acyclic internal olefin moieties as chain-transfer agents (CTAs).[46–48] We utilized maleic acid (MA) as a CTA ([COD]/[MA] = 10) to end-cap linear PBD with carboxylic acid groups. Linear PBD was synthesized with low molecular weight, and cyclic PBD was still separated with a yield of 21% (Table 3.1, entry 1-19). It indicates the introduction of CTAs cannot eliminate the formation of macrocycles.

3.6 Analysis of macrocyclic species in ROMP of cyclooctene, cyclopentene, and norbornene

Table 3.2. Molecular weight of crude linear PCOE and yield and molecular weight of macrocycles from ROMP of COE.

Entry	Change from "standard condition"	Crude PCOE $M_n(M_w)$ (kDa)	cPCOE yield(%)	cPCOE $M_n(M_w)$ (kDa)

2-1	None	12.4(16.8)	12	1.4(3.1)
2-2	[COE]: [Ru] = 1000	78.5(108.5)	8	2.0(2.7)
2-3	T = 50 °C	12.4(17.0)	11	1.4(4.6)
2-4	$[COE]_0 = 0.27M$	6.3(8.8)	42	1.6(2.8)
2-5	$[COE]_0 = 0.1M$	4.7 (5.5)	81	1.5(1.8)
2-6	$t = 5$ minutes	12.6(15.4)	12	1.6(3.2)
2-7[a]	[Ru] = G2, $[COE]_0 = 0.1M$	2.1(3.2)	92	2.5(3.9)
2-8	[Ru] = HG2, $[COE]_0 = 0.1M$	0.6(1.5)	99	0.8(2.0)
2-9[a]	[Ru] = G3	10.9(16.0)	19	2.0(3.8)

[a] Styrenic protons (ca. δ_H 6.23 and 6.37 ppm) are identified in the ^1H NMR spectra of separated cPCOE products.
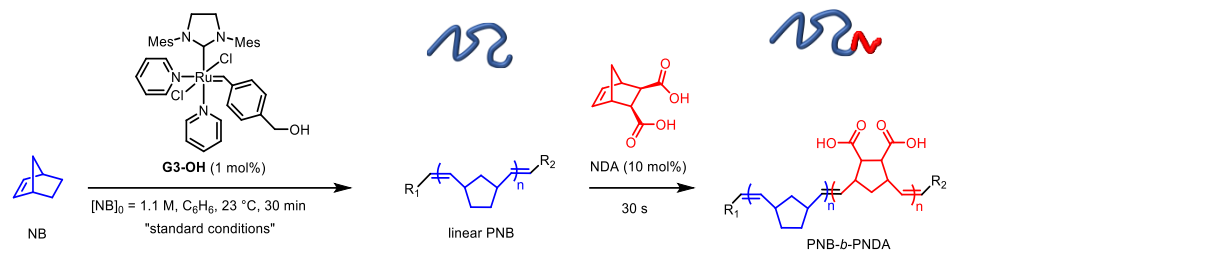
Compared to the ROMP of COD, less is known about the product distribution of COE.[13] In general, the yield of cyclic PCOE is lower than that of PBD, which can be attributed to the lower density of backbone double bonds in COE, providing fewer sites for back-biting reactions. Since the ROMP of COE does not produce a specific thermodynamically favored product like *ttt*-CDT, the reaction quickly reaches equilibrium in as little as 5 minutes, resulting in macrocycles with larger molecular weight compared to COD (Table 3.2, entries 2-1 and 2-6). Increasing temperature has minimal influence on the formation of cyclic POE due to the same reason (Table 3.2, entry 2-3). When **G3-OH** was substituted with **G2** or **HG2**, the solution quickly gelled due to slow initiation, leading to high-molecular weight linear PCOE that was unable to dissolve even after prolonged equilibration. As a result, reactions using **G2** and **HG2** were conducted at a diluted solution. Table 3.2, entry 2-8 shows near full conversion to cyclic PCOE, consistent with the findings of Qiao.[8] The comparison between Table 3.2, entries 2-1 and 2-9 revealed that the yield of linear PCOE resulting from interchain metathesis reaction was calculated to be 7% (Table 3.2, entry 2-9).

Table 3.3. Molecular weight of crude linear PCP and yield and molecular weight of macrocycles from ROMP of CP.

Entry	Change from "standard condition"	Crude PCP $M_n(M_w)$ (kDa)	cPCP yield(%)	cPCP $M_n(M_w)$ (kDa)
3-2	None	5.3(6.7)	11	1.4(1.7)
3-1	$[CP]_0 = 2.8M$	17.1(27.2)	5	1.2(1.6)
3-3	$[CP]_0 = 0.27M$	-	-	-
3-4	$[Ru] = HG2, [CP]_0 = 0.27M$	-	-	-

Cyclopentene (CP) has a low ring strain of 28.4 kJ mol^{-1} and entropic penalty for its polymerization is large $(-\Delta S_p \approx 70 \pm 6$ J K^{-1} mol$^{-1})$.[49,50] At a $[CP]_0$ of 0.27 M, no polymerization occurred at 23°C (Table 3.3, entries 3-3 and 3-4). Increasing $[CP]_0$ to 2.8 M resulted in a 5% yield of cPCP with Mn of 1.2 kDa (Table 3.3, entry 3-2). The yield of cPCP was improved to 11% when $[CP]_0$ was decreased to 1.1 M, with a comparable M_n (Table 3.3, entry 3-1). Using a more reactive Mo-based catalyst, Register reported the synthesis of higher molecular weight cyclic PCP at smaller catalyst loading.[51] In an attempt to produce higher molecular weight cPCP, we used a high $[CP]_0$ of 2.8 M and a [CP]/[**G3-OH**] of 10000, but the resulting gelled solution made it impossible to introduce the NDA block into the linear chain, preventing the separation of the product.

Table 3.4. Molecular weight of crude linear PNB and yield and molecular weight of macrocycles from ROMP of NB.

Entry	Change from "standard condition"	Crude PNB $M_n(M_w)$ (kDa)	cPNB yield(%)	cPNB $M_n(M_w)$ (kDa)
4-1	None	10.3(14.7)	-	-
4-2	[NB]: [G3-OH] = 1000, $[NB]_0$ = 0.27M	70.5(110.1)	-	-
4-3	[NB]: [HG2] = 1000, $[NB]_0$ = 0.27M, t = 360 minutes	57.0(137.0)	-	-

In terms of ROMP for NB – a high ring strain monomer, macrocycles are not formed even with lower initial monomer concentration, longer reaction time and **HG2** as the catalyst (Table 3.4, entry 4-3). The steric bulkiness of the PNB backbone results in a decreased reactivity towards back-biting. Cyclic PNB obtained through ROMP was only reported using $WCl_6/Sn(CH_3)_4$ or more active Mo based catalyst.[52–55] In other cases, a tether structure in the catalyst is required to synthesize cyclic PNB via ring-expansion metathesis polymerization.[56–59] In our study, PNB is proven to resist back-biting in ROMP using Grubbs catalyst.

3.7 Conclusions

In conclusion, our study has shown that the introduction of polar functional groups to linear polymer products enables the facile separation of macrocycles from ROMP reaction mixtures. This approach offers several advantages, including the ability to prepare macrocycles under different reaction conditions and improved characterization of macrocyclic species compared to traditional methods such as GC or viscometry. Furthermore, the method can be extended to the study of

macrocycle formation in other metathesis reactions, such as acyclic diene metathesis and ring-closing metathesis. The potential for more efficient screening of macrocyclic species can also be realized by combining the synthetic approach with advanced liquid chromatography to analyze the aliquot from crude reaction mixture, eliminating the need for manual column separation.

Through investigation of the reaction factors affecting the yield and molecular weight of macrocycles during ROMP of COD, we found that cyclic PBD with higher molecular weight can be obtained by increasing the reaction temperature below the catalyst degradation temperature or by decreasing the reaction time. We also observed that higher yields can be achieved by diluting the solution or using **HG2** as the catalyst. Furthermore, we demonstrated the synthesis of cyclic PCOE and PCP using this approach. However, we acknowledge that there are limitations to this method, such as the inability to separate macrocycles from gelled solutions and the presence of linear impurities in cases of catalyst decomposition or interchain metathesis for **G1** and **G2**. Thus, future research should focus on developing more universal methods to overcome these challenges.

3.8 Experimental section

3.8.1 General materials information

Without additional notes, all reagents which were commercially available from Sigma-Aldrich, Combi-Blocks, Tokyo Chemical Industry Co. Ltd., and Alfa Aesar were used without further purification. Linear PBD **L1** and **L4** were purchased from Scientific Polymer Products, Inc. Linear PBD **L2** and **L3** were prepared according to reported procedures using *cis*-4-octene as chain transfer agent.[46] The first generation Grubbs catalyst **G1**, the second generation Grubbs catalyst **G2**, and the second generation Hoveyda-Grubbs catalyst **HG2** were generously provided by Materia Inc. The third generation Grubbs catalyst **G3** was prepared according to reported procedures.[60]

Cyclopentene, cis-cyclooctene and cyclooctadiene were purchased from Sigma Aldrich and purified according to reported procedures.[61] Solvents used for polymerization were degassed by freeze-pump-thaw and stored over activated molecular sieves in the glovebox. In other cases when dry solvents were needed, solvents were purified by passing through the solvent purification system (SPS). Deuterated solvents were purchased from Cambridge Isotopes Laboratories, Inc. and used as received. Compounds **S1**, **2** and exo-cis-5-norbornene-2,3-dicarboxylic acid were synthesized according to reported procedures.[26,27,31]

3.8.2 General experimental information

The standard Schlenk techniques were used for all reactions carried out under an argon atmosphere. The retention factor (Rf) of thin-layer chromatography (TLC) was recorded using E. Merck silica gel 60 F254 precoated plates (0.25 mm) and visualized by cerium ammonium molybdate or potassium permanganate staining. ^{1}H and ^{13}C NMR spectra were recorded on either Bruker Ascend 400 MHz or Varian Inova 500 MHz spectrometer. High resolution mass spectra (HRMS) were provided by the California Institute of Technology Mass Spectrometry Facility using a JEOL JMS-600H High-Resolution Mass Spectrometer. Gel permeation chromatography (GPC) data were collected in tetrahydrofuran (THF) at 25 °C using two Agilent PLgel MIXED-B 300×7.5 mm columns with 10 μm beads, connected to an Agilent 1260 Series pump, a Wyatt 18-angle DAWN HELEOS light scattering detector, and an Optilab rEX differential refractive index detector. Molar masses were determined from light scattering. Dn/dc values were used for PBD (0.13), PCOE (0.11), PCP (0.12), and PNB (0.17). Samples were filtered through a 0.20 mm PTFE filter before injection. MALDI ToF MS was obtained using Autoflex from Bruker. Sample preparation was

adopted from previous reports, using silver trifluoroacetate as ionization reagent and anthracene as matrices.[62]

All polymerization reactions are carried out under nitrogen atmosphere inside a glove box. To a scintillation 20 mL equipped with a stir bar, 2.45 mmol monomer and solvent were added, then catalyst stock solution was added rapidly using syringe into stirring monomer solution. After reaction is complete, 5% of the solution by volume is extracted and terminated by ethyl vinyl ether (EVE) to characterize molecular weight. 1mL THF solution of 3 is added to the remaining stirring polymer solution and stirred for 0.5 minute (vial would be shaken rigorously when solution is too viscous to stir well). Afterwards, 1mL benzene solution of 2 is added to quench the reaction when **G3** or **G3-OH** is used. After 3 minutes, 100 μL EVE is added to quench any residue active catalyst. When **G1**, **G2**, or **HG2** are used, 1mL methanol solution of potassium 2-isocyanoacetate (PICA) and 500 μL EVE are added and stirred for 30 minutes to quench the reaction. 3 g silica gel is added to the solution, and solvent is carefully removed by rotovap. The residue solid is further dried on vacuum line, and then loaded on a silica gel column and eluted with 20% DCM in hexanes. Collected fractions are combined, concentrated, and characterized by NMR and GPC.

3.8.3 Synthetic details
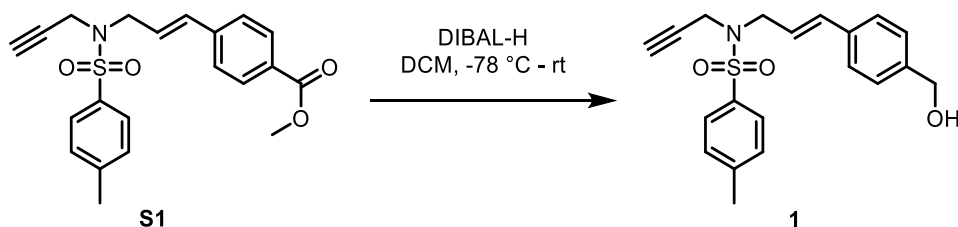
1: In a 250 mL Schlenk flask, S1 (6.1 g, 16 mmol, 1 eq) was dissolved in 150 mL of degassed dry DCM under argon atmosphere. The solution was cooled to -78 °C, followed by dropwise addition

of DIBAL-H solution (1.1 M in cyclohexane, 36 mL, 40 mmol, 2.5 eq) using syringe. The reaction was warmed to room temperature slowly. After 30 minutes, TLC showed completion of the reaction, and the reaction was quenched by Rochelle's salt (saturated aqueous sodium potassium tartrate solution) and stirred for 10 hours. The reaction mixture was diluted with 100 mL of DCM, washed with brine, dried over Na_2SO_4, and concentrated in vacuo. Purification of the crude mixture by column chromatography (33% EtOAc in hexanes), isolating the desired product as a yellow oil (5.15 g, 91%).

calcd. $[M]^+$ 355.1242 Found: 355.1237.

^{1}H NMR (400 MHz, CDCl$_3$) δ 7.80 – 7.73 (m, 2H), 7.37 – 7.24 (m, 6H), 6.57 (d, J = 15.8 Hz, 1H), 6.08 (dt, J = 15.1, 6.8 Hz, 1H), 4.68 (s, 2H), 4.20 – 4.10 (m, 2H), 3.99 (d, J = 6.8 Hz, 2H), 2.44 (s, 3H), 2.05 (q, J = 2.1 Hz, 1H).

^{13}C NMR (101 MHz, CDCl$_3$) δ 143.8, 140.9, 136.0, 135.5, 134.6, 129.6, 127.8, 127.3, 126.8, 123.0, 76.6, 74.0, 64.9, 48.6, 36.0, 21.6.

3.9 References

(1)   Bielawski, C. W.; Grubbs, R. H. Highly Efficient Ring-Opening Metathesis Polymerization (ROMP) Using New Ruthenium Catalysts Containing N-Heterocyclic Carbene Ligands. *Angewandte Chemie International Edition* **2000**, *39* (16), 2903–2906.

(2)   Bielawski, C. W.; Grubbs, R. H. Living Ring-Opening Metathesis Polymerization. *Progress in Polymer Science* **2007**, *32* (1), 1–29.

(3)   Haque, F. M.; Grayson, S. M. The Synthesis, Properties and Potential Applications of Cyclic Polymers. *Nat. Chem.* **2020**, *12* (5), 433–444.

(4)   *Cyclic Polymers*; Semlyen, J. A., Ed.; Kluwer Academic Publishers: Dordrecht, 2002.

(5)   Chen, C.; Weil, T. Cyclic Polymers: Synthesis, Characteristics, and Emerging Applications. *Nanoscale Horizons* **2022**, *7* (10), 1121–1135.

(6)   Golba, B.; Benetti, E. M.; De Geest, B. G. Biomaterials Applications of Cyclic Polymers. *Biomaterials* **2021**, *267*, 120468.

(7)   Liénard, R.; De Winter, J.; Coulembier, O. Cyclic Polymers: Advances in Their Synthesis, Properties, and Biomedical Applications. *Journal of Polymer Science* **2020**, *58* (11), 1481–1502.

(8)   Blencowe, A.; Qiao, G. G. Ring-Opening Metathesis Polymerization with the Second Generation Hoveyda–Grubbs Catalyst: An Efficient Approach toward High-Purity Functionalized Macrocyclic Oligo(Cyclooctene)s. *J. Am. Chem. Soc.* **2013**, *135* (15), 5717–5725.

(9) Song, A.; Parker, K. A.; Sampson, N. S. Cyclic Alternating Ring-Opening Metathesis Polymerization (CAROMP). Rapid Access to Functionalized Cyclic Polymers. *Org. Lett.* **2010**, *12* (17), 3729–3731.

(10) Zheng, X.; Jones, C. W.; Weck, M. Ring-Expanding Olefin Metathesis: A Route to Highly Active Unsymmetrical Macrocyclic Oligomeric Co-Salen Catalysts for the Hydrolytic Kinetic Resolution of Epoxides. *J. Am. Chem. Soc.* **2007**, *129* (5), 1105–1112.

(11) Liu, Y.; Rawlston, J.; Swann, A. T.; Takatani, T.; Sherrill, C. D.; Ludovice, P. J.; Weck, M. The Bigger, the Better: Ring-Size Effects of Macrocyclic Oligomeric Co(III)-Salen Catalysts. *Chem. Sci.* **2011**, *2* (3), 429–438.

(12) Dewaele, A.; Renders, T.; Yu, B.; Verpoort, F.; Sels, B. F. Depolymerization of 1,4-Polybutadiene by Metathesis: High Yield of Large Macrocyclic Oligo(Butadiene)s by Ligand Selectivity Control. *Catal. Sci. Technol.* **2016**, *6* (21), 7708–7717.

(13) Dewaele, A.; Berlo, B. V.; Dijkmans, J.; Jacobs, P. A.; Sels, B. F. Immobilized Grubbs Catalysts on Mesoporous Silica Materials: Insight into Support Characteristics and Their Impact on Catalytic Activity and Product Selectivity. *Catal. Sci. Technol.* **2016**, *6* (8), 2580–2597.

(14) Thorn-Csányi, E.; Ruhland, K. Quantitative Description of the Metathesis Polymerization/Depolymerization Equilibrium in the 1,4-Polybutadiene System, 1. Influence of Feed Concentration and Temperature. *Macromolecular Chemistry and Physics* **1999**, *200* (7), 1662–1671.

(15) Ahuja, R.; Kundu, S.; Goldman, A. S.; Brookhart, M.; Vicente, B. C.; Scott, S. L. Catalytic Ring Expansion, Contraction, and Metathesis-Polymerization of Cycloalkanes. *Chem. Commun.* **2007**, No. 2, 253–255.

(16) Sato, H.; Tanaka, Y.; Taketomi, T. Microstructure of 1,5-Cyclooctadiene Oligomers. *Die Makromolekulare Chemie* **1977**, *178* (7), 1993–1999.

(17) Olesik, S. V. Liquid Chromatography at the Critical Condition. *Anal Bioanal Chem* **2004**, *378* (1), 43–45.

(18) Lee, W.; Park, S.; Chang, T. Liquid Chromatography at the Critical Condition for Polyisoprene Using a Single Solvent. *Anal. Chem.* **2001**, *73* (16), 3884–3889.

(19) Doi, Y.; Ohta, Y.; Nakamura, M.; Takano, A.; Takahashi, Y.; Matsushita, Y. Precise Synthesis and Characterization of Tadpole-Shaped Polystyrenes with High Purity. *Macromolecules* **2013**, *46* (3), 1075–1081.

(20) Yan, Z.-C.; Costanzo, S.; Jeong, Y.; Chang, T.; Vlassopoulos, D. Linear and Nonlinear Shear Rheology of a Marginally Entangled Ring Polymer. *Macromolecules* **2016**, *49* (4), 1444–1453.

(21) *Fractionation of Cyclic Polystyrene from Linear Precursor by HPLC at the Chromatographic Critical Condition | Macromolecules*. https://pubs.acs.org/doi/10.1021/ma000807b (accessed 2023-01-24).

(22) Gao, L.; Oh, J.; Tu, Y.; Chang, T. Preparation of Low Molecular Weight Cyclic Polystyrenes with High Purity via Liquid Chromatography at the Critical Condition. *Polymer* **2018**, *135*, 279–284.

(23) Cho, D.; Park, S.; Kwon, K.; Chang, T.; Roovers, J. Structural Characterization of Ring Polystyrene by Liquid Chromatography at the Critical Condition and MALDI−TOF Mass Spectrometry. *Macromolecules* **2001**, *34* (21), 7570–7572.

(24) Iyengar, D. R.; McCarthy, T. J. Trends in Adsorption of End-Functionalized Polystyrenes by Thin-Layer Chromatography. *Macromolecules* **1990**, *23* (20), 4344–4346.

(25) Ji, H.; Sato, N.; Nonidez, W. K.; Mays, J. W. Characterization of Hydroxyl-End-Capped Polybutadiene and Polystyrene Produced by Anionic Polymerization Technique via TLC/MALDI TOF Mass Spectrometry. *Polymer* **2002**, *43* (25), 7119–7123.

(26) Fu, L.; Zhang, T.; Fu, G.; Gutekunst, W. R. Relay Conjugation of Living Metathesis Polymers. *J. Am. Chem. Soc.* **2018**, *140* (38), 12181–12188.

(27) Zhang, T.; Fu, L.; Gutekunst, W. R. Practical Synthesis of Functional Metathesis Initiators Using Enynes. *Macromolecules* **2018**, *51* (16), 6497–6503.

(28) Zhang, T.; Gutekunst, W. R. Pulsed-Addition Ring-Opening Metathesis Polymerization with Functional Enyne Reagents. *Polym. Chem.* **2020**, *11* (2), 259–264.

(29) Montenegro-Burke, J. R.; Bennett, J. M.; McLean, J. A.; Hercules, D. M. Novel Behavior of the Chromatographic Separation of Linear and Cyclic Polymers. *Anal Bioanal Chem* **2016**, *408* (3), 677–681.

(30) Halverson, J. D.; Lee, W. B.; Grest, G. S.; Grosberg, A. Y.; Kremer, K. Molecular Dynamics Simulation Study of Nonconcatenated Ring Polymers in a Melt. I. Statics. *J. Chem. Phys.* **2011**, *134* (20), 204904.

(31) Foster, J. C.; Varlas, S.; Blackman, L. D.; Arkinstall, L. A.; O'Reilly, R. K. Ring-Opening Metathesis Polymerization in Aqueous Media Using a Macroinitiator Approach. *Angewandte Chemie* **2018**, *130* (33), 10832–10836.

(32) Höcker, H.; Reimann, W.; Reif, L.; Riebel, K. Kinetics and Thermodynamic Aspects of the Metathesis Reaction of Cycloolefins Considering Particularly the Molecular Weight Distribution of the Products. *Journal of Molecular Catalysis* **1980**, *8* (1), 191–202.

(33) Neary, W. J.; Kennemur, J. G. Variable Temperature ROMP: Leveraging Low Ring Strain Thermodynamics To Achieve Well-Defined Polypentenamers. *Macromolecules* **2017**, *50* (13), 4935–4941.

(34) Monfette, S.; Fogg, D. E. Equilibrium Ring-Closing Metathesis. *Chem. Rev.* **2009**, *109* (8), 3783–3816.

(35) Jacobson, H.; Stockmayer, W. H. Intramolecular Reaction in Polycondensations. I. The Theory of Linear Systems. *J. Chem. Phys.* **1950**, *18* (12), 1600–1606.

(36) Suter, U. W.; Höcker, H. Macrocyclization Equilibria in Polycycloolefins. *Die Makromolekulare Chemie* **1988**, *189* (7), 1603–1612.

(37) Thorn-Csányi, E.; Hammer, J.; Pflug, K. P.; Zilles, J. U. Formation and Degradation of 1,4-Polybutadiene via Metathesis: New Results Concerning Cyclic Oligomers. *Macromolecular Chemistry and Physics* **1995**, *196* (4), 1043–1050.

(38) Allaert, B.; Ledoux, N.; Dieltiens, N.; Mierde, H. V.; Stevens, C. V.; Van Der Voort, P.; Verpoort, F. Secondary Metathesis with Grubbs Catalysts in the 1,4-Polybutadiene System. *Catalysis Communications* **2008**, *9* (6), 1054–1059.

(39) Chauvin, Y.; Commereuc, D.; Zaborowski, G. Catalysis of Olefin Transformation by Tungsten Complexes, 6. Equilibrium Oligomer Concentration in the Polymerization of 1,5-Cyclooctadiene. *Die Makromolekulare Chemie* **1978**, *179* (5), 1285–1290.

(40) Höcker, H.; Reimann, W.; Riebel, K.; Szentivanyi, Z. Ring-Chain Equilibria in the Metathesis Reaction of Cycloolefines. *Die Makromolekulare Chemie* **1976**, *177* (6), 1707–1715.

(41) Chen, Z.-R.; Claverie, J. P.; Grubbs, R. H.; Kornfield, J. A. Modeling Ring-Chain Equilibria in Ring-Opening Polymerization of Cycloolefins. *Macromolecules* **1995**, *28* (7), 2147–2154.

(42) Walker, R.; Conrad, R. M.; Grubbs, R. H. The Living ROMP of Trans-Cyclooctene. *Macromolecules* **2009**, *42* (3), 599–605.

(43) Myers, S. B.; Register, R. A. Crystalline−Crystalline Diblock Copolymers of Linear Polyethylene and Hydrogenated Polynorbornene. *Macromolecules* **2008**, *41* (18), 6773–6779.

(44) Thorn-Csányi, E.; Ruhland, K. ROMP of COD under Equilibrium Conditions: The Turning Point Concept. *Macromolecular Symposia* **2000**, *153* (1), 145–150.

(45) Tuba, R.; Grubbs, R. H. Ruthenium Catalyzed Equilibrium Ring-Opening Metathesis Polymerization of Cyclopentene. *Polymer Chemistry* **2013**, *4* (14), 3959.

(46) Ji, S.; Hoye, T. R.; Macosko, C. W. Controlled Synthesis of High Molecular Weight Telechelic Polybutadienes by Ring-Opening Metathesis Polymerization. *Macromolecules* **2004**, *37* (15), 5485–5489.

(47) Pitet, L. M.; Hillmyer, M. A. Carboxy-Telechelic Polyolefins by ROMP Using Maleic Acid as a Chain Transfer Agent. *Macromolecules* **2011**, *44* (7), 2378–2381.

(48) Morita, T.; Maughon, B. R.; Bielawski, C. W.; Grubbs, R. H. A Ring-Opening Metathesis Polymerization (ROMP) Approach to Carboxyl- and Amino-Terminated Telechelic Poly(Butadiene)s. *Macromolecules* **2000**, *33* (17), 6621–6623.

(49) Neary, W. J.; Kennemur, J. G. Polypentenamer Renaissance: Challenges and Opportunities. *ACS Macro Lett.* **2019**, *8* (1), 46–56.

(50) Kobayashi, S. Ring-Opening Metathesis Polymerization. In *Encyclopedia of Polymeric Nanomaterials*; Kobayashi, S., Müllen, K., Eds.; Springer: Berlin, Heidelberg, 2015; pp 2154–2164.

(51) Mulhearn, W. D.; Register, R. A. Synthesis of Narrow-Distribution, High-Molecular-Weight ROMP Polycyclopentene via Suppression of Acyclic Metathesis Side Reactions. *ACS Macro Lett.* **2017**, *6* (2), 112–116.

(52) Reif, L.; Höcker, H. Oligomer Distribution in the Polymerization of 2-Norbornene via Metathesis. *Die Makromolekulare Chemie, Rapid Communications* **1981**, *2* (2), 183–185.

(53) Reif, L.; Höcker, H. The Influence of Conjugated Dienes on the Metathetical Polymerization of Cycloolefins. *Die Makromolekulare Chemie, Rapid Communications* **1983**, *4* (10), 693–695.

(54) Reif, L.; Hoecker, H. Kinetics and Thermodynamics of the Metathesis Reaction of Cycloolefins. 2. Molecular Weight Distribution. *Macromolecules* **1984**, *17* (4), 952–956.

(55) Saf, R.; Schitter, R.; Mirtl, C.; Stelzer, F.; Hummel, K. Electrospray Ionization Mass Spectrometry Investigation of Oligomers Prepared by Ring-Opening Metathesis Polymerization of Methyl N-(1-Phenylethyl)-2-Azabicyclo[2.2.1]Hept-5-Ene-3-Carboxylate. *Macromolecules* **1996**, *29* (24), 7651–7656.

(56) Wang, T.-W.; Huang, P.-R.; Chow, J. L.; Kaminsky, W.; Golder, M. R. A Cyclic Ruthenium Benzylidene Initiator Platform Enhances Reactivity for Ring-Expansion Metathesis Polymerization. *J. Am. Chem. Soc.* **2021**, *143* (19), 7314–7319.

(57) Xia, Y.; Boydston, A. J.; Grubbs, R. H. Synthesis and Direct Imaging of Ultrahigh Molecular Weight Cyclic Brush Polymers. *Angewandte Chemie International Edition* **2011**, *50* (26), 5882–5885.

(58) Gonsales, S. A.; Kubo, T.; Flint, M. K.; Abboud, K. A.; Sumerlin, B. S.; Veige, A. S. Highly Tactic Cyclic Polynorbornene: Stereoselective Ring Expansion Metathesis Polymerization of Norbornene Catalyzed by a New Tethered Tungsten-Alkylidene Catalyst. *J. Am. Chem. Soc.* **2016**, *138* (15), 4996–4999.

(59) Hou, X.; Chen, X.; Gao, X.; Xu, L.; Zou, H.; Zhou, L.; Wu, Z.-Q. Synthesis of Cyclic Polyolefin: Ring-Opening Metathesis Polymerization by Binuclear Vanadium Complexes†. *Chinese Journal of Chemistry* **2021**, *39* (5), 1181–1187.

(60) Love, J. A.; Morgan, J. P.; Trnka, T. M.; Grubbs, R. H. A Practical and Highly Active Ruthenium-Based Catalyst That Effects the Cross Metathesis of Acrylonitrile. *Angewandte Chemie* **2002**, *114* (21), 4207–4209.

(61) Yoon, K.-Y.; Noh, J.; Gan, Q.; Edwards, J. P.; Tuba, R.; Choi, T.-L.; Grubbs, R. H. Scalable and Continuous Access to Pure Cyclic Polymers Enabled by 'Quarantined'Heterogeneous Catalysts. *Nature Chemistry* **2022**, *14* (11), 1242–1248.

(62) Macha, S. F.; Limbach, P. A.; Savickas, P. J. Application of Nonpolar Matrices for the Analysis of Low Molecular Weight Nonpolar Synthetic Polymers by Matrix-Assisted Laser

Desorption/Ionization Time-of-Flight Mass Spectrometry. *J. Am. Soc. Spectrom.* **2000**, *11* (8), 731–737.

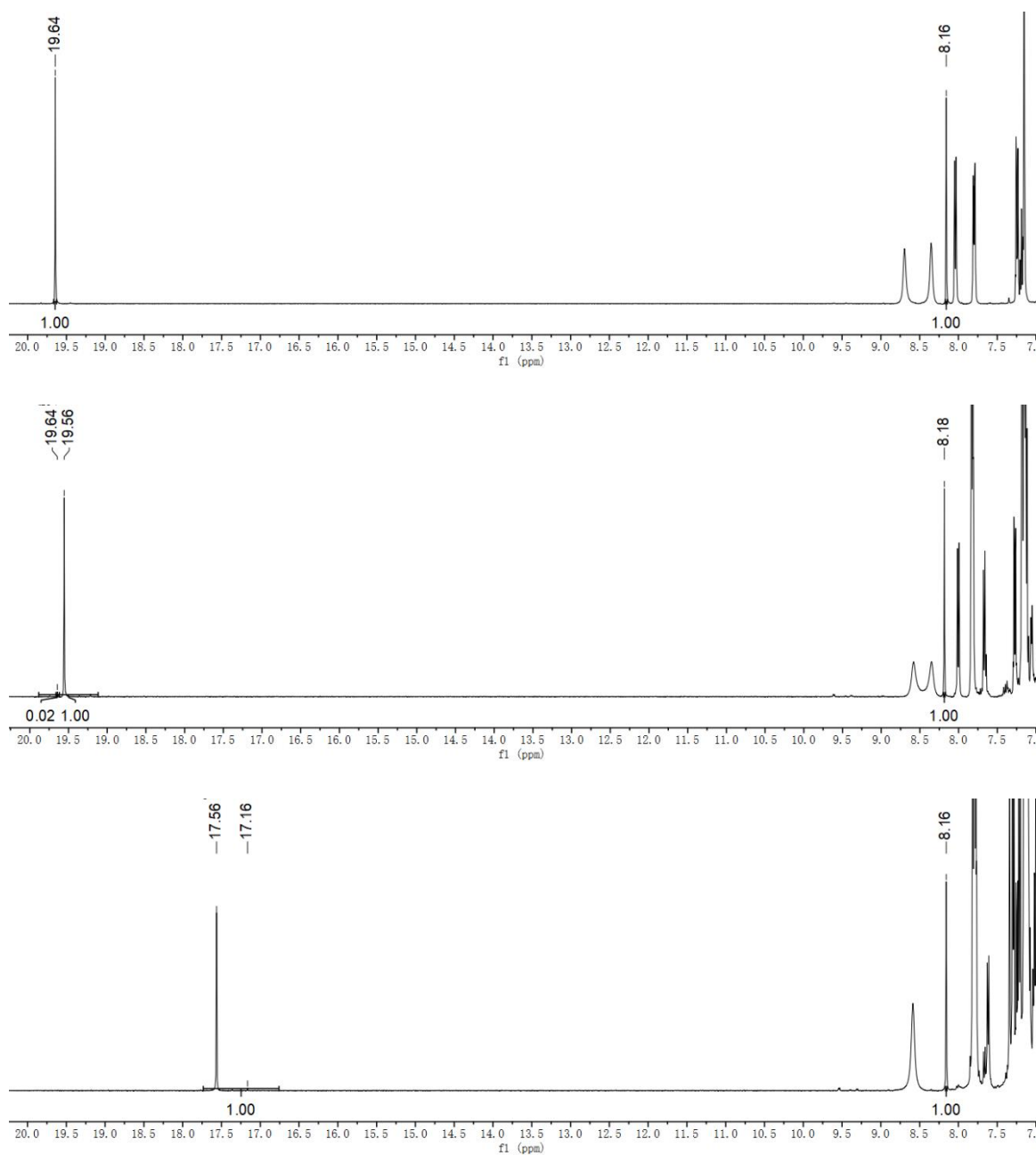# Appendix 3. Spectra Relevant to Chapter 3

Figure C1. ^{1}H NMR sepctra (C$_6$D$_6$) of **G3** (top), **G3-OH** (middle), and **G3-thio** (bottom). Peak at 8.16 ppm is from anthracene internal standard.
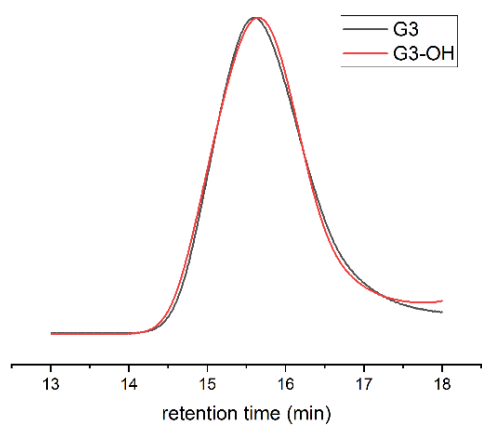
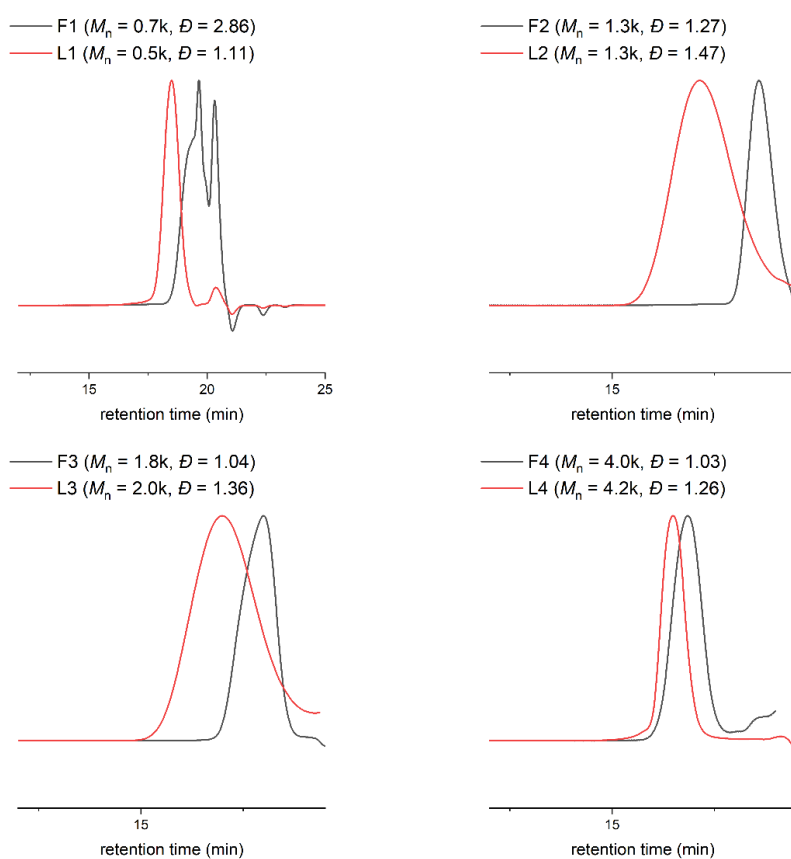**Figure C2.** GPC traces of linear PBD initiated by G3 and G3-OH.

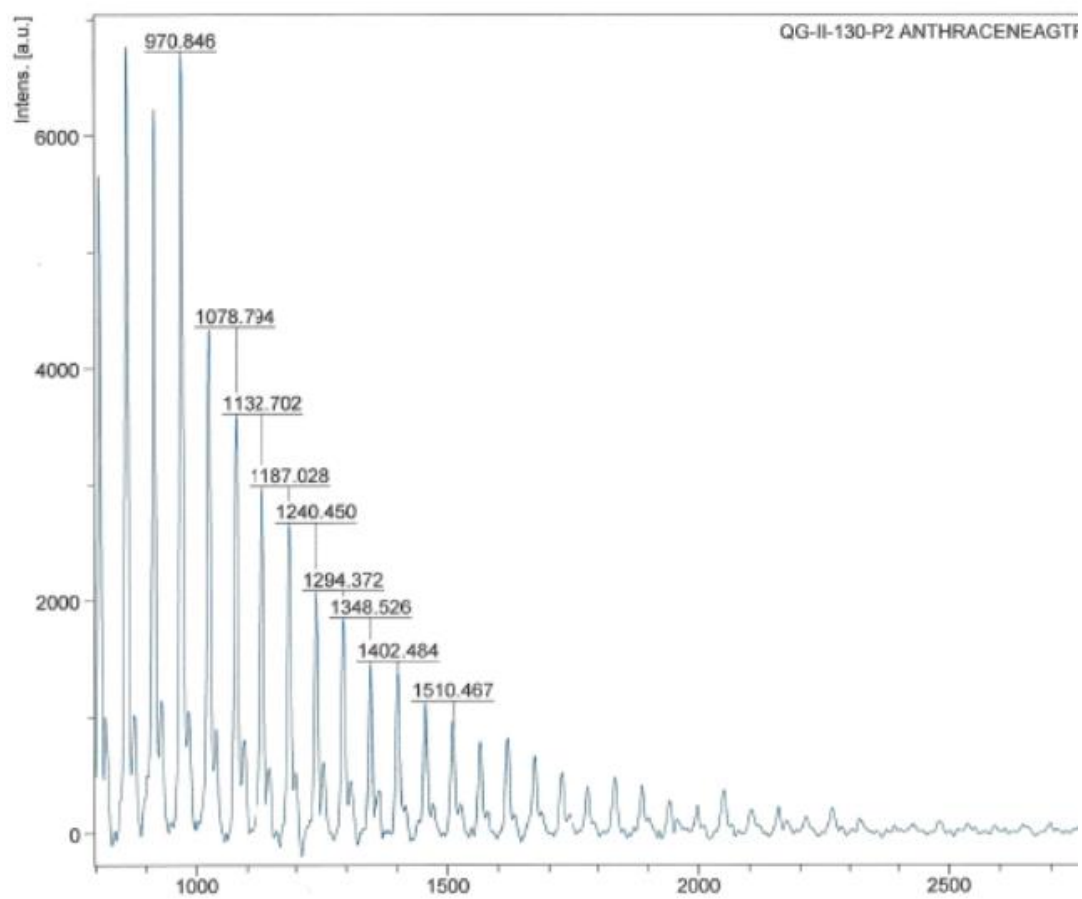**Figure C3.** GPC dRI traces comparison between cyclic fractions **F1-F4** and corresponding linear PBD.

Figure C4. MALDI ToF MS for cyclic fraction **F1** obtained in linear mode.
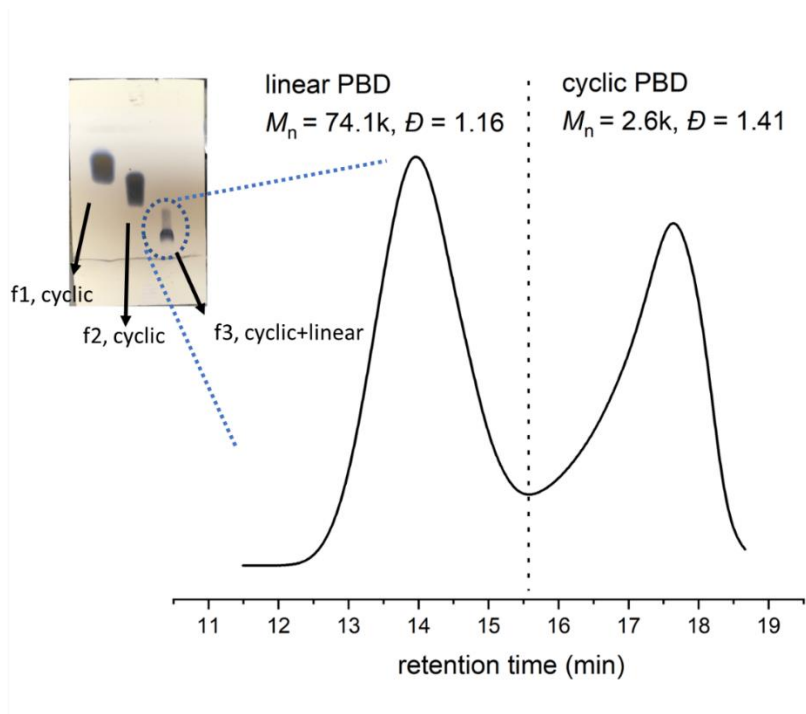
Figure C5. After the column separation of reaction mixture with decreased catalyst loading ($[COD]_0/[G3\text{-}OH] = 1000{:}1$), first two fractions (f1 and f2) were cyclic PBD. Fraction f3 was inseparable linear and cyclic PBD. TLC and GPC dRI traces for the f3 is shown above.
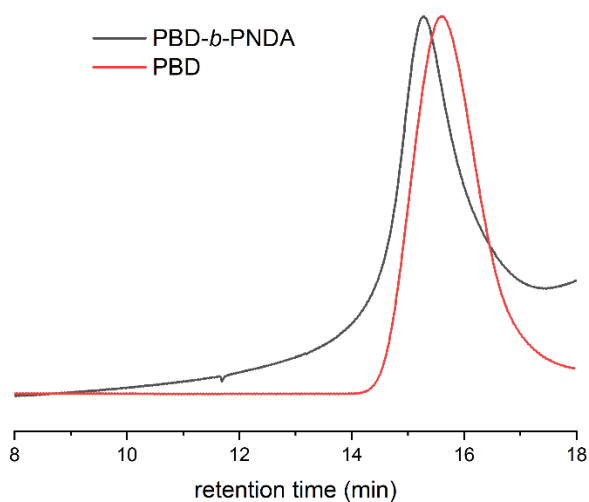
Figure C6. GPC dRI traces of linear PBD from Table 1, entry 1-1 and corresponding PBD-*b*-PNDA block copolymer.
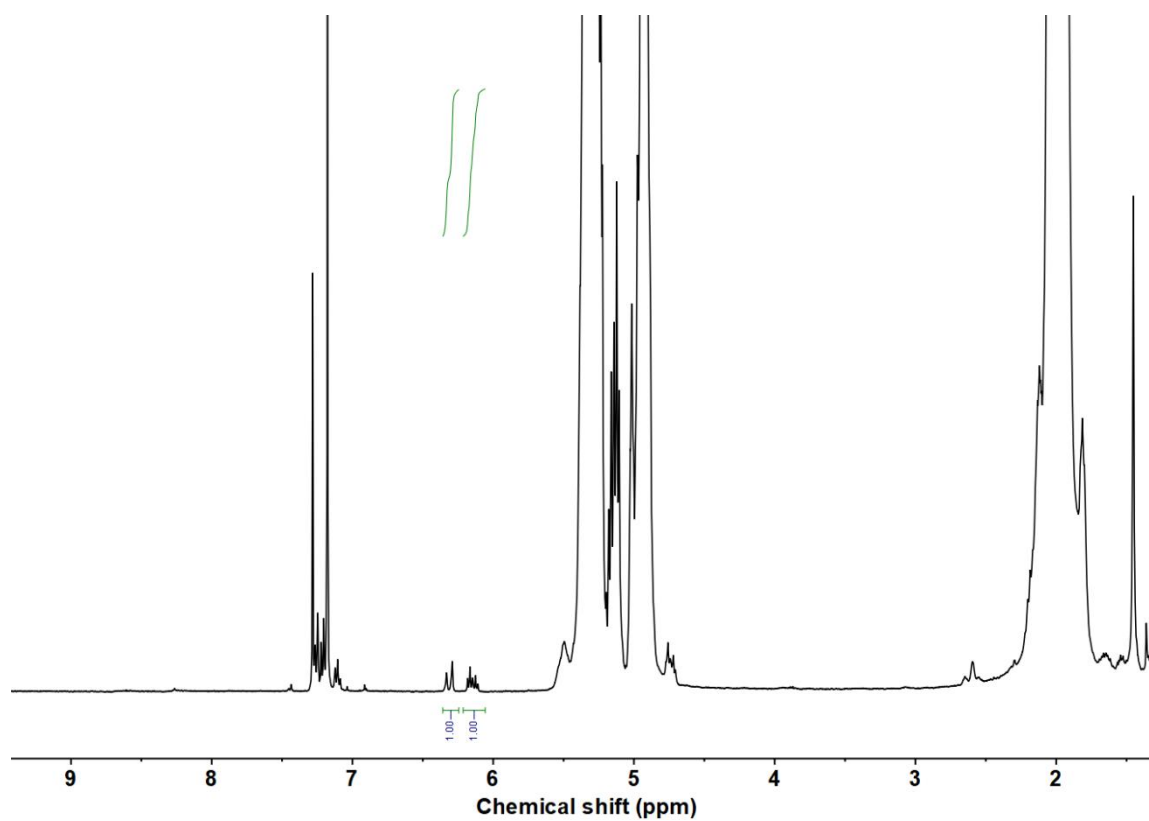
Figure C7. ¹H NMR sepctrum (CDCl₃) of cyclic PBD obtained in Table 1, entry 1-6.
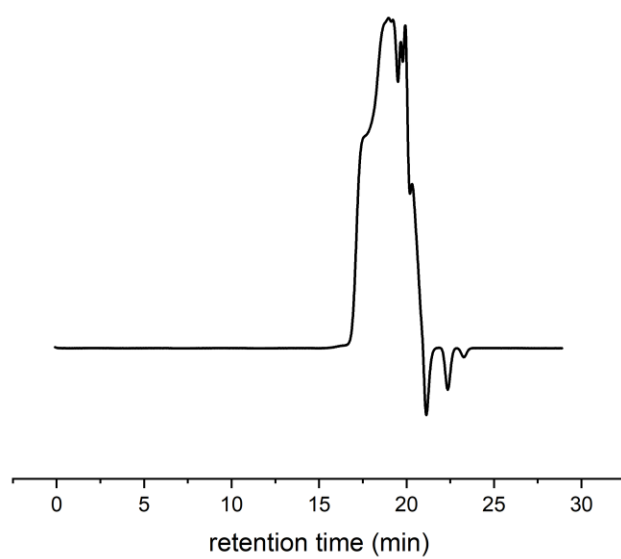
Figure C8. GPC DRI trace of cyclic PBD obtained in Table 1, entry 1-13.
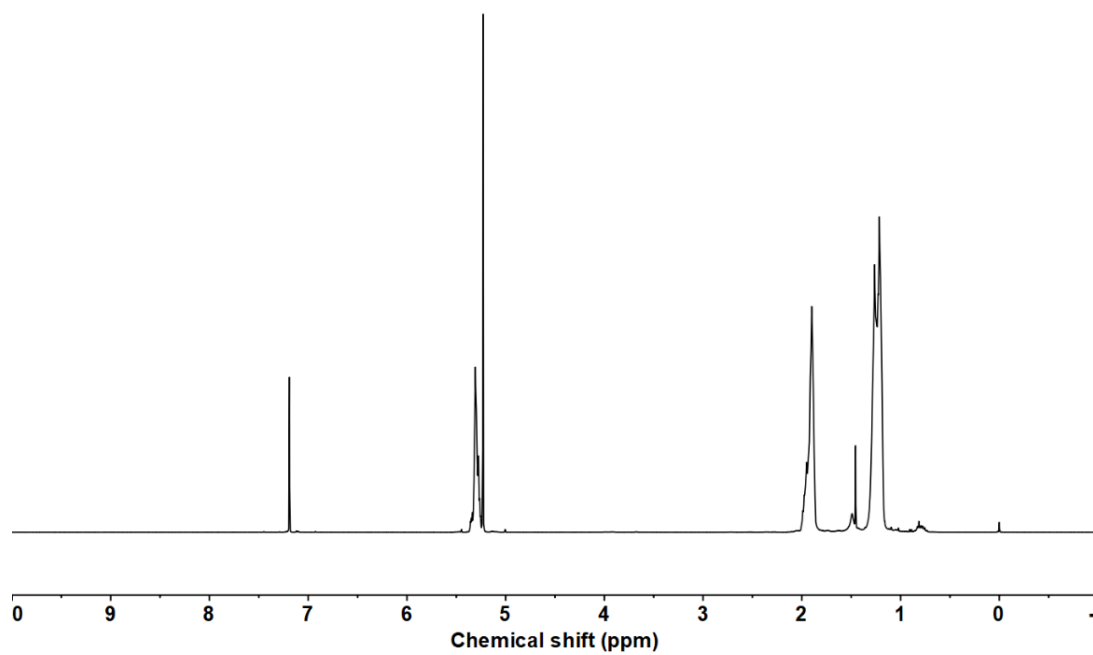
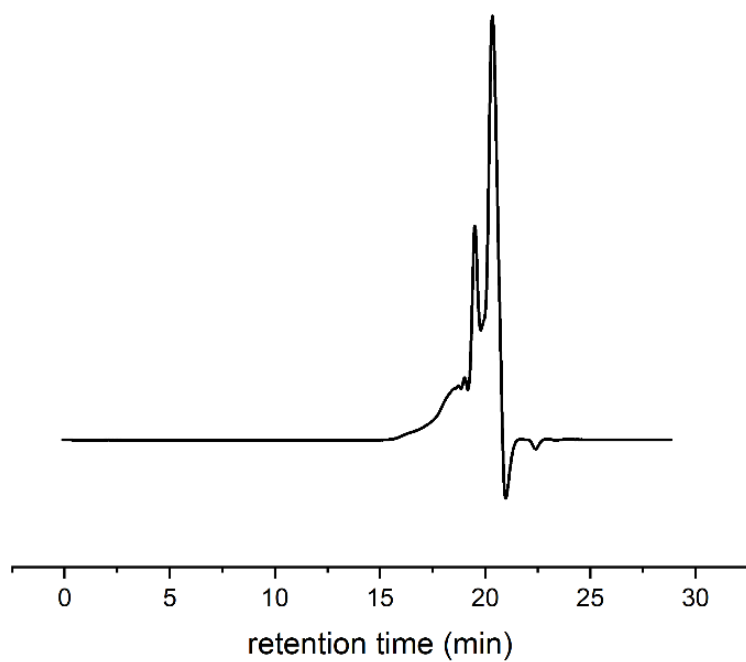**Figure C9.** ¹H NMR sepctrum (CDCl₃) of cyclic PCOE from Table 2, entry 2-1.

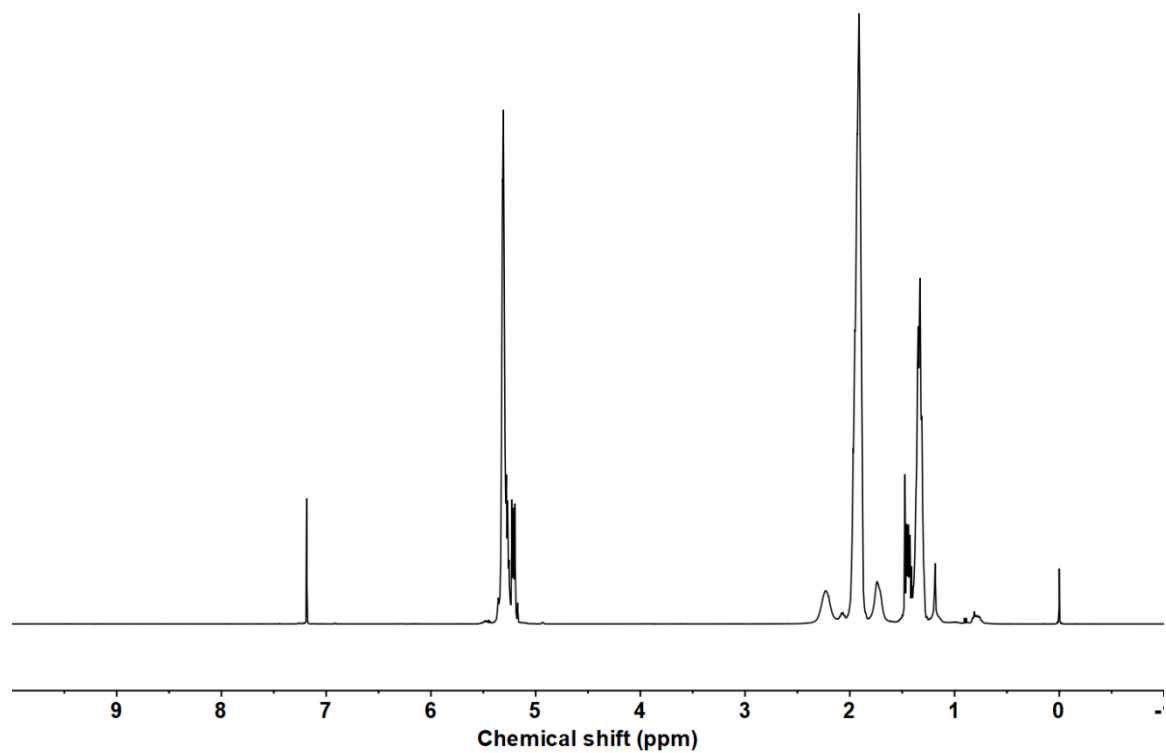**Figure C10.** GPC DRI trace of cyclic PCOE obtained in Table 2, entry 2-1.

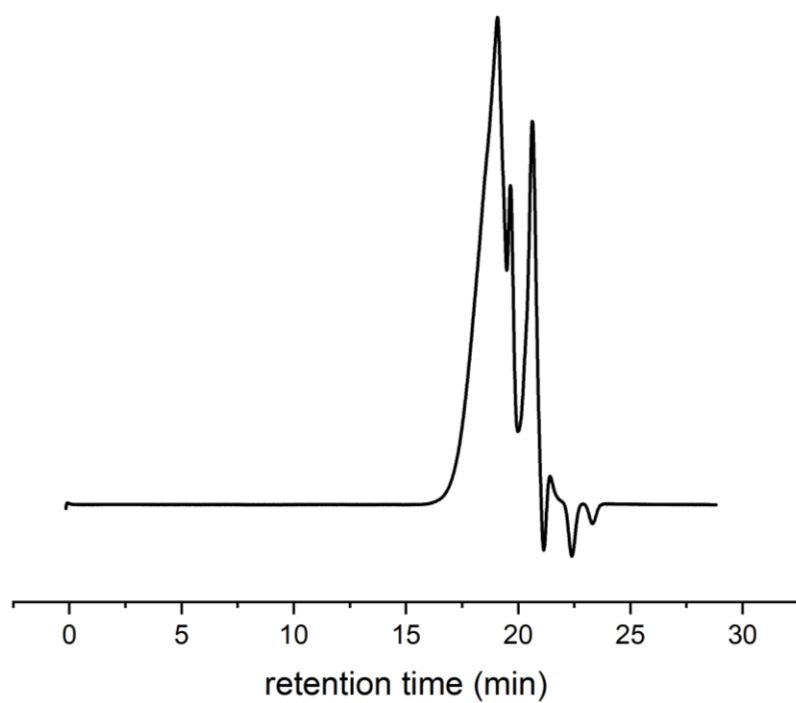**Figure C11.** ^{1}H NMR sepctrum (CDCl$_3$) of cyclic PCP from Table 3, entry 3-1.

Figure C12. GPC DRI trace of cyclic PCOE obtained in Table 3, entry 3-1.

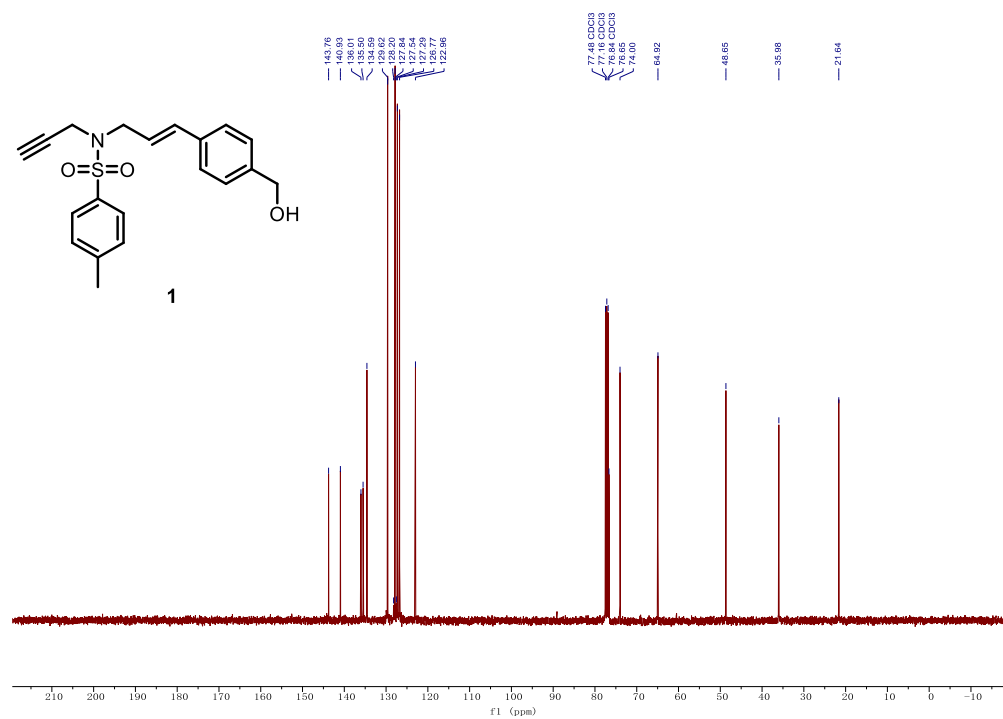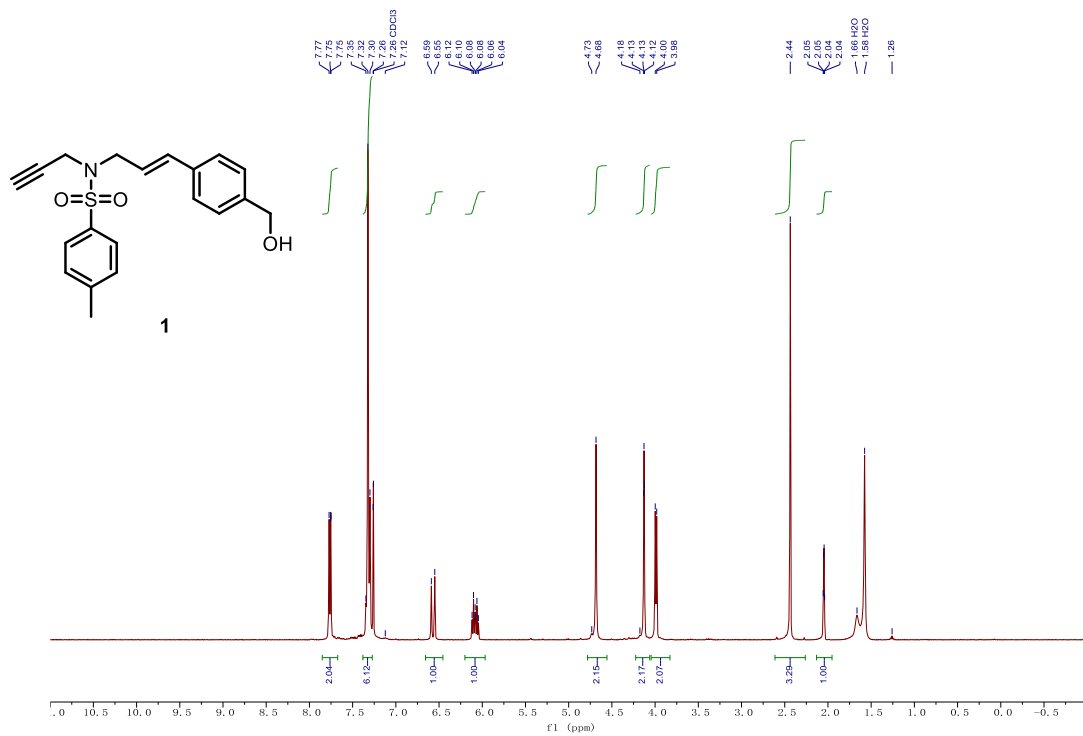**Figure C13.** ^{1}H NMR (400 MHz, CDCl$_3$) spectrum of **1**.

Figure C14. ^{13}C NMR (101 MHz, CDCl$_3$) spectrum of **1**.

About the author

Quan Gan was born on August 26th, 1994, to Hengzhi Gan and Hongxia Ma. He grew up in Baoding, a city in Hebei Province in northern China. Quan developed a keen interest in natural science, especially biology and chemistry, under the guidance of his father during his childhood.

He moved to Tianjin in 2013 to pursue his undergraduate studies at Nankai University, where he joined the research group of Prof. Yijing Wang to study electrochemistry and Prof. Zhen Xi's Laboratory to study chemical biology. Quan spent nine months as a visiting undergraduate researcher in the research group of Prof. Hailiang Wang at Yale University during his fourth year of undergraduate studies, where he conducted his thesis research on the development of electrocatalysts for hydrogen evolution reaction.

Quan learned about Caltech from the famous TV series "The Big Bang Theory". He was very surprised when he found out he was admitted to Caltech to pursue his graduate studies and was even more surprised when Prof. Bob Grubbs kindly accepted him into the Grubbs group. Organic chemistry was a relatively new area for Quan, so he had a hard time in the beginning. However, with the guidance of Bob and colleagues in the Grubbs group, he contributed to the development of cyclic polymer synthesis and characterization. He also gained some experience in organic synthesis, organometallic chemistry, and polymer physics. After Prof. Grubbs passed away in 2021, Prof. Max Robb generously offered Quan to join the Robb group, where Quan spent his last year and learned about interesting mechanochemistry. Following the completion of his Ph.D., Quan will join the Central Research Institute of Huawei Technologies in Shenzhen, China, and continue his adventure in polymer chemistry.

In his spare time, Quan enjoys playing guitar and table tennis. He spent much of his time watching movies and animes and playing hardcore video games. He also loves cooking for his friends.